Krzysztof Szade

Protection of hematopoietic stem cells
from premature aging – the role of heme oxygenase-1

Ochrona hematopoetycznych komórek macierzystych przed
przedwczesnym starzeniem – rola oksygenazy hemowej-1

Kraków 2015

ACKNOWLEDGMENTS

CONTENT:

6

ABBREVIATIONS

Abbreviation	Full description
ABC	ATP-Binding Cassette
ARC	adventitial reticular cells
ATP	Adenosine triphosphate
CAR	CXCL12-abudant reticular cells
CaR	calcium-sensing receptor
CLL	chronic lymphocytic leukemia
CLP	common lymphoid progenitor
CMP	common myeloid progenitors
ECM	extracellular matrix
EPCR	endothelial protein C receptor
GMP	granulocyte-myeloid progenitors
HSC	hematopoietic stem cells
HSPC	hematopoietic stem and progenitor cells
iPS	induce pluripotent stem cells
LT-HSC	long-term hematopoietic stem cells
MEP	megakaryocyte-erythroid precursors
MPP	multipotent progenitor
mTOR	mammalian target of rapamicin
PGJ_2	prostaglandin-J_2
PrC	polycomb repressive complexes
PαS	PDGFR and Sca-1 expressing mesenchymal stem cells
SnPP IX	tin protoporphyrin IX
SP	side population
ST-HSC	short-term hematopoietic stem cells
Tie-2	TEK tyrosine kinase
VSEL	very small embryonic-like stem cells
vWF	von Willebrand Factor

ABSTRACT

Protection of hematopoietic stem cells from premature aging - the role of heme oxygenase-1.

Hematopoietic stem cells (HSC) support the production of all blood cells throughout a lifetime, but during aging they gradually lose their regenerative potential. Changes in the HSC associated with aging are well known, but the mechanisms responsible for protection of the HSC from age-related decline remain largely unexplained. Heme oxygenase-1 (HO-1) is an important anti-inflammatory and anti-apoptotic protein involved in the protection of mature hematopoietic cells. However, little is known how this enzyme affects the functioning of the HSC.

Moreover, in recent years there have been reports suggesting that non- hematopoietic cells preserve the potential for hematopoietic differentiation in postnatal organism. One of these populations called VSEL (Very Small Embryonic-Like cells) was defined as adult stem cells that have potential of pluripotent stem cells. They were characterized by small size, lack of mature blood cells markers (called lineage markers, Lin) and hematopoietic marker CD45 expression, but having expression of Sca-1 (Lin$^-$Sca-1$^+$CD45$^-$ phenotype). The proposed VSEL properties have not been verified functionally at the single cell level, what is necessary to confirm their multidirectional hematopoietic differentiation.

The aim of this study was to investigate whether blood cells in the postnatal organism can be derived from non-hematopoietic Lin$^-$Sca-1$^+$CD45$^-$ fraction or only from the defined HSC. After checking this possibility, the next step was to verify the hypothesis that the activity of HO-1 protects the stem cells from premature aging and exhaustion of hematopoietic regenerative potential.

In the first step of the study we demonstrated that the expression of c-Kit and KDR markers distinguished from Lin$^-$Sca-1$^+$CD45$^-$ fraction three distinct subpopulations: c-Kit$^+$KDR$^-$, c-Kit$^-$KDR$^+$, c-Kit$^-$KDR$^-$. Flow cytometry and imaging cytometry (ImageStream) showed that the subpopulation of c-Kit$^+$KDR$^-$ contains only small cells (FSC^{low}) satisfying the criterion of cell size VSEL. The subpopulation of c-Kit$^-$KDR$^+$ contains only larger cells, and a subpopulation of c-Kit$^-$KDR$^-$ is enriched with apoptotic cells that bind annexin V. RT-PCR analysis showed no expression of pluripotent marker Oct-4A in whole bone marrow, Lin$^-$Sca-1$^+$CD45$^-$FSC^{low} population as well as in single sorted Lin$^-$Sca-1$^+$CD45$^-$FSC^{low} cells.

Single sorted Lin⁻Sca-1⁺CD45⁻c-Kit⁺ did not form hematopoietic colonies, even after co-culture with OP9 cells, in contrast to hematopoietic progenitor cells Lin⁻Sca-1⁺CD45⁺c-Kit⁺. Further experiments showed that the population of Lin⁻Sca-1⁺CD45⁻c-kit⁺ cells is enriched with early apoptotic cells, characterized by chromatin fragmentation. It can also be contaminated with nuclei expelled from erythroblasts during erythropoiesis.

The first step of our research demonstrated that the population of murine bone marrow cells with Lin⁻Sca-1⁺CD45⁻FSC^{low} phenotype is heterogeneous and does not have expression of the transcription factor Oct4 that characterizes pluripotent cells. Most importantly, this population does not show hematopoietic potential and is enriched with early apoptotic cells. Therefore, in the next steps we focused on determining the role of HO-1 in aging of well-defined HSC.

We have shown that young mice lacking the HO-1 gene (HO-1$^{-/-}$) are characterized by the expansion of the long-term repopulating hematopoietic stem cells in bone marrow (called long-term HSC, LT-HSC) defined as Lin⁻c-Kit⁺Sca-1⁺CD150⁺CD48⁻CD34⁻ and a predominance of myeloid over lymphoid cells in peripheral blood. LT-HSC from HO-1$^{-/-}$ mice demonstrated higher signal of phosphorylated form of histone γH2aX, which is a marker of DNA damage. Finally, HO-1$^{-/-}$ LT-HSC transplanted into irradiated wild-type (HO-1$^{+/+}$) provides lower donor-derived chimerism than the wild-type control cells. All of the above disorders/disturbances observed in LT-HSC from young HO-1$^{-/-}$ mice appeared in the LT-HSC from old HO-1$^{+/+}$.

These results evidenced that the lack of heme oxygenase-1 causes premature aging of LT-HSC. This is linked with their increased activation and proliferation. We observed that in young HO-1$^{-/-}$ mice more LT-HSC are in G1 cell cycle phase and in G2/S/M phases, and less in the G0 phase when compared to the HO-1$^{+/+}$ mouse. LT-HSC from HO-1$^{-/-}$ mice show also lower ATP levels, what may indicate a disturbed metabolism.

The proper functioning of LT-HSC cells is guaranteed by specialized stem cell niche. Further experiments were designed to clarify whether the premature aging of LT-HSCs in the HO-1$^{-/-}$ mice is associated with lack of HO-1 in the LT-HSC themselves or in the cells composing the niche. We observed that highest expression of HO-1 in the bone marrow characterizes CD31^{high}Sca-1^{high} endothelial cells and reticular mesenchymal cells (called CXCL12-abudant reticular cells, CAR), which form the HSC niche. In contrast, in hematopoietic stem and progenitor cells HO-1 expression is low.

To determine whether the activity of HO-1 in the bone marrow niche is essential for protection of LT-HSC we transplanted HO-1$^{+/+}$ LT-HSC to HO-1$^{+/+}$ or HO-1$^{-/-}$ recipient mice. After 32 weeks, the HO-1$^{-/-}$ recipient mice showed worse chimerism in the peripheral blood and bone marrow. Then, the donor-derived bone marrow cells from primary HO-1$^{-/-}$ or HO-1$^{+/+}$ recipients were transplanted into secondary HO-1$^{+/+}$ recipients. Only the cells that were initially transplanted into HO-1$^{+/+}$ mice reconstituted hematopoietic system in secondary recipients in contrast to the cells primary transplanted into HO-1$^{-/-}$ recipients, which did not contribute to chimerism in secondary recipients.

In summary, the HO-1 suppresses proliferation and activation of hematopoietic stem cells and reduces level of DNA damage. HO-1 is also essential for the proper functioning of the bone marrow niche, and its absence in the hematopoietic niche causes premature aging of LT-HSC and decreases their regenerative potential.

STRESZCZENIE

Ochrona hematopoetycznych komórek macierzystych przed przedwczesnym starzeniem – rola oksygenazy hemowej-1.

Hematopoetyczne komórki macierzyste (HSC) podtrzymują produkcję wszystkich komórek krwi przez okres całego życia, jednakże wraz ze starzeniem się organizmu stopniowo tracą swój potencjał regeneracyjny. Zmiany w HSC związane ze starzeniem się są dobrze poznane, ale mechanizmy odpowiadające za ochronę komórek HSC przed tymi zmianami pozostają w dużej mierze niewyjaśnione. Ważnym białkiem cytoprotekcyjnym i antyapoptotycznym biorącym udział w ochronie dojrzałych komórek hematopoetycznych jest oksygenaza hemowa-1 (HO-1). Nie wiadomo jednak, czy enzym ten wpływa na funkcjonowanie HSC.

Ponadto, w ostatnich latach pojawiły się doniesienia sugerujące, że potencjał do różnicowania hematopoetycznego w postnatalnym organizmie posiadają także komórki spoza linii hematopoetycznej. Jedną z takich domniemanych populacji, nazwaną VSEL (*ang. very small embryonic-like cells*), zdefiniowano jako komórki macierzyste o właściwościach pluripotencjalnych, charakteryzujące się małymi rozmiarami, niewykazujące ekspresji markerów dojrzałych komórek krwi (*ang. lineage markers, Lin*) oraz hematopoetycznego markera CD45, ale posiadające ekspresję Sca-1 (czyli: $Lin^-Sca-1^+CD45^-$). Postulowane właściwości VSEL nie zostały jednak zweryfikowane na poziomie pojedynczej komórki, co jest niezbędne do potwierdzenia ich wielokierunkowego różnicowania hematopoetycznego

Celem niniejszej pracy było zbadanie, czy komórki krwi w organizmie postnatalnym mogą wywodzić się z niehematopoetycznej frakcji $Lin^-Sca-1^+CD45^-$, czy też wyłącznie ze zdefiniowanych HSC. Po sprawdzeniu tej możliwości, kolejnym krokiem było zweryfikowanie hipotezy, że aktywność HO-1 chroni komórki macierzyste przed przedwczesnym starzeniem się i wyczerpaniem hematopoetycznego potencjału regeneracyjnego.

W pierwszym etapie badań wykazaliśmy, że ekspresja markerów c-Kit i KDR wyróżniła spośród komórek o fenotypie $Lin^-Sca-1^+CD45^-$ trzy subpopulacje: $c-Kit^+KDR^-$, $c-Kit^-KDR^+$, $c-Kit^-KDR^-$. Analiza z wykorzystaniem cytometrii przepływowej i obrazowej (ImageStream) wykazała, że subpopulacja $c-Kit^+KDR^-$ zawiera wyłącznie małe komórki (FSC^{low}), spełniające kryterium wielkości komórek VSEL. Subpopulacja $c-Kit^-KDR^+$ zawierała wyłącznie większe

komórki, natomiast subpopulacja c-Kit⁻KDR⁻ była wzbogacona w komórki apoptotyczne wiążące anneksynę V. Analizy RT-PCR nie wykazały ekspresji pluripotencjalnego markera Oct-4A w całym szpiku, subpopulacji Lin⁻Sca-1⁺CD45⁻FSC^low, jak również w sortowanych, pojedynczych komórkach Lin⁻Sca-1⁺CD45⁻FSC^low.

Pojedynczo sortowane komórki Lin⁻Sca-1⁺CD45⁻c-Kit⁺ nie tworzyły kolonii hematopoetycznych, nawet w kokulturze z komórkami OP9, w przeciwieństwie do hematopoetycznych komórek progenitorowych Lin⁻Sca-1⁺CD45⁺c-Kit⁺. Dalsze badania wykazały, że populacja Lin⁻Sca-1⁺CD45⁻c-Kit⁺ jest wzbogacona w komórki wczesnoapoptotyczne charakteryzujące się fragmentacją chromatyny. Może być również zanieczyszczona jądrami usuwanymi z erytroblastów podczas erytropoezy.

Pierwszy etap naszych doświadczeń wykazał więc, że mysia populacja komórek szpiku kostnego o fenotypie Lin⁻Sca-1⁺CD45⁻FSC^low jest heterogenna i nie ma ekspresji czynnika transkrypcyjnego Oct4A, charakterystycznego dla komórek pluripotencjalnych. Co najważniejsze, populacja ta nie wykazuje potencjału hematopoetycznego i jest wzbogacona w komórki wczesnoapoptotyczne. Dlatego w dalszym etapie badań skoncentrowaliśmy się na określeniu roli HO-1 w starzeniu się ściśle zdefiniowanych komórek HSC.

Wykazaliśmy, że młode myszy pozbawione genu HO-1 (HO-1⁻ᐟ⁻) charakteryzują się ekspansją długoterminowo odnawiających się hematopoetycznych komórek macierzystych w szpiku kostnym (*ang. long term HSC, LT-HSC*) zdefiniowanych jako Lin⁻c-Kit⁺Sca-1⁺CD150⁺CD48⁺CD34⁻ oraz przewagą komórek linii mieloidalnej nad linią limfoidalną wśród komórek krwi. Komórki LT-HSC z myszy HO-1⁻ᐟ⁻ wykazywały również wyższy sygnał fosforylowanej formy histonu γH2aX, który jest markerem uszkodzeń DNA. Komórki LT-HSC z myszy HO-1⁻ᐟ⁻ przeszczepione do naświetlonych myszy typu dzikiego (HO-1⁺ᐟ⁺) rekonstytuowały hematopoezę w mniejszym stopniu, niż kontrolne komórki typu dzikiego. Wszystkie powyższe zaburzenia komórek LT-HSC obserwowane u młodych myszy HO-1⁻ᐟ⁻ pojawiały się w komórkach LT-HSC u starych HO-1⁺ᐟ⁺.

Otrzymane wyniki wskazują, że brak oksygenazy hemowej-1 powoduje przedwczesne starzenie się komórek LT-HSC. Jest ono związane z ich wzmożoną aktywacją i proliferacją. Zaobserwowaliśmy, że u młodych myszy HO-1⁻ᐟ⁻ więcej komórek LT-HSC jest w fazach G1 i G2/S/M cyklu komórkowego, a mniej w fazie G0 w porównaniu do myszy HO-1⁺ᐟ⁺. LT-HSC z

myszy HO-1$^{-/-}$ wykazują także niższy poziom ATP, co może świadczyć o zaburzonym metabolizmie.

Dla prawidłowego funkcjonowania komórek LT-HSC niezbędna jest wyspecjalizowana nisza szpikowa. Kolejne doświadczenia miały na celu wyjaśnienie, czy przedwczesne starzenie się LT-HSC u myszy HO-1$^{-/-}$ jest związane z brakiem HO-1 w samych komórkach LT-HSC, czy w komórkach niszy. Wykazaliśmy, że najwyższa ekspresja HO-1 w szpiku kostnym charakteryzuje komórki śródbłonka oraz siateczkowate komórki mezenchymalne (*ang. CXCL12-abudant reticular cells, CAR*), które tworzą niszę HSC. Natomiast w samych hematopoetycznych komórkach macierzystych i progenitorowych ekspresja HO-1 była niska.

W celu sprawdzenia, czy aktywność HO-1 w niszy szpikowej jest kluczowa dla ochrony komórek LT-HSC, przeszczepiliśmy komórki LT-HSC z myszy HO-1$^{+/+}$ do myszy-biorców HO-1$^{+/+}$ lub HO-1$^{-/-}$. Po 32 tygodniach myszy-biorcy o genotypie HO-1$^{-/-}$ wykazywały mniejszy chimeryzm we krwi obwodowej, a także posiadały w szpiku kostnym mniej LT-HSC pochodzących od przeszczepionych komórek. Następnie, komórki pochodzące od dawcy ze szpiku kostnego pierwszych biorców HO-1$^{+/+}$ lub HO-1$^{-/-}$ zostały przeszczepione do kolejnych biorców drugorzędowych, wyłącznie o genotypie HO-1$^{+/+}$. Jedynie komórki, które pierwotnie przeszczepione były do myszy HO-1$^{+/+}$ rekonstytuowały układ hematopoetyczny u biorców drugorzędowych, w przeciwieństwie do komórek przeszczepionych pierwotnie do biorców HO-1$^{-/-}$, które nie przyczyniały się do chimeryzmu u biorców drugorzędowych.

Podsumowując, HO-1 zmniejsza proliferację i aktywację hematopoetycznych komórek macierzystych, oraz zmniejsza w nich poziom uszkodzeń DNA. HO-1 jest również niezbędna do prawidłowego funkcjonowania niszy szpikowej, a jej brak w niszy hematopoetycznej powoduje przedwczesne starzenie i wyczerpywanie się potencjału regeneracyjnego komórek LT-HSC.

INTRODUCTION

Hierarchy of postnatal hematopoiesis

Discovery and identification of hematopoietic stem and progenitor cells

The hematopoiesis refers to a process of new blood cells production. Mature blood cells are short lived and up to 10^6 new blood cells have to be produced each second to sustain hematological homeostasis in human organism [1]. Such continuous production of high number of cells needs to be well controlled to avoid exhaustion of hematological system and to provide proper cellular composition of blood throughout organism's lifespan.

Studies began in 1960's revealed how the hematopoietic system is organized and maintained. The pioneering experiments by Till and McCulloch indicated that different kinds of mature blood cells originate from common clonal precursor cells [2, 3]. The establishment of methods allowing prospective isolation of mouse hematopoietic stem cells (HSC) combined with their transplantation to irradiated hosts allowed revealing hematopoietic hierarchy in details [4] (Fig. 1.1). Transplantation of purified and strictly defined murine populations revealed that HSC are on the top of hematopoietic hierarchy and represent the only population that give rise to all kinds? of blood cells and simultaneously could self-renew their own reservoir (reviewed and summarized in [5]).

Among cells referred to as HSC, two different subsets were further distinguished. The so called long-term HSC (LT-HSC) owe their name to potential to reconstitute irradiated mice in serial transplantations [6]. Short term (ST-HSC) also reconstitute all blood cells of irradiated host, but their self-renewal is limited as they do not provide reconstitution in serial transplantation model [6]. Therefore only the LT-HSC entirely fulfill the definition of stem cells.

In mouse, both LT-HSC and ST-HSC lack expression of mature lineage blood cells (Lin⁻) and express Sca-1, c-Kit, CD150 [4, 6, 7]. But upon LT-HSC differentiation toward ST-HSC, the CD34 antigen appears on cell surface, what allows distinguishing these two cell subsets [8]. Expression of next antigens, Flk-2 [9] and CD48 [7], characterizes the multipotent progenitor (MPP) fraction which can differentiate to all blood cells, but does not self-renew their own population. Other markers that are used to distinguish LT-HSC include endothelial protein C receptor (EPCR) [10], TEK tyrosine kinase (Tie-2) [11] and endoglin (CD105) [12].
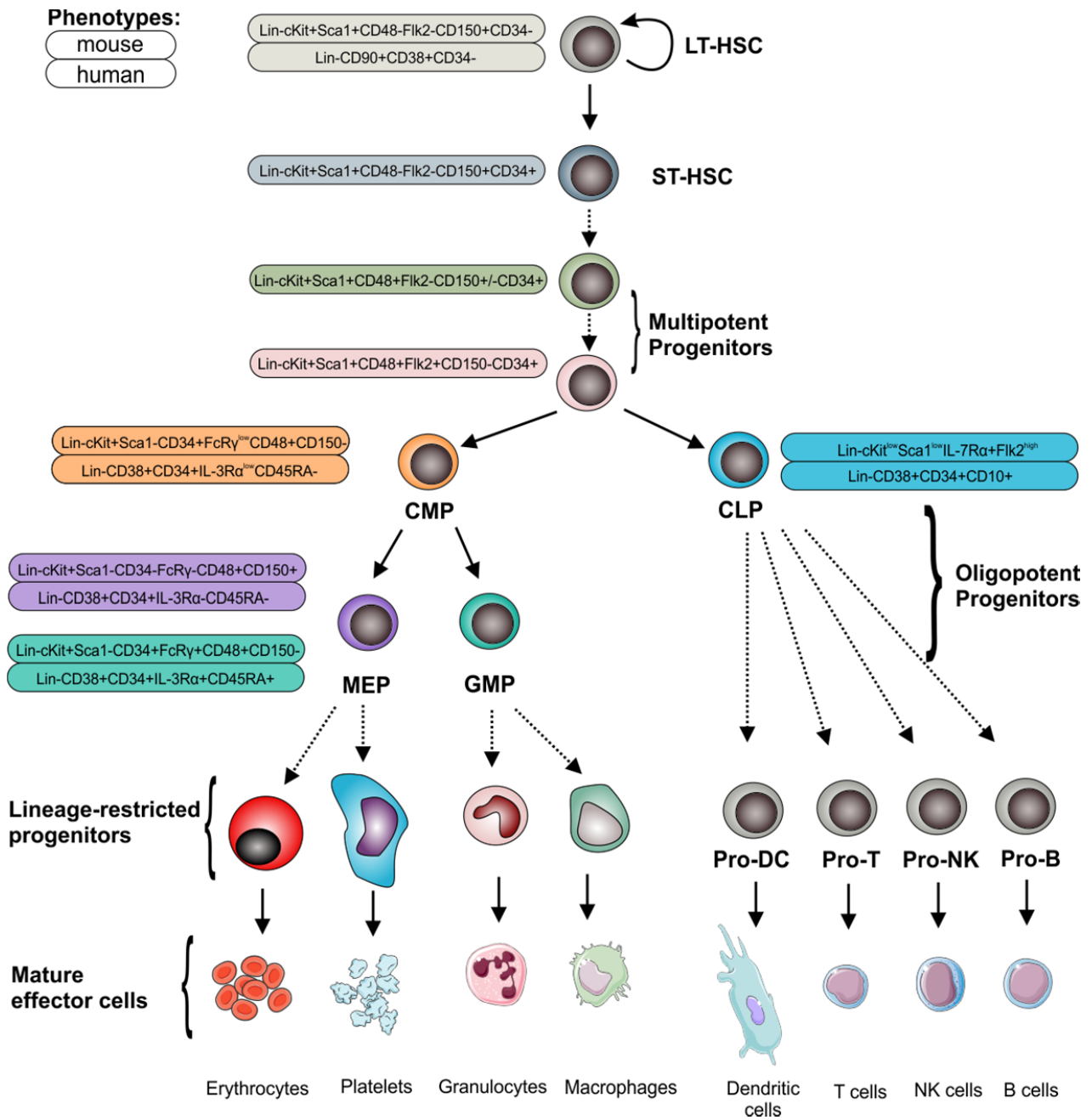
Fig. 1.1 *The hierarchical organization of hematopoiesis. Based on [1] and modified.*

The next descending populations in hematopoietic hierarchy are already committed to myeloid/erythroid or lymphoid lineage (Fig. 1.1). The common myeloid progenitors (CMP, Lin$^-$c-Kit$^+$Sca-1$^-$CD34$^+$FcRγ^{low}CD48$^+$CD150$^-$) give rise to megakaryocyte-erythroid precursors (MEP, Lin$^-$c-Kit$^+$Sca-1$^-$CD34$^-$FcRγ^{low}CD48$^+$CD150$^+$) and granulocyte-myeloid progenitors (GMP, Lin$^-$c-Kit$^+$Sca-1$^-$CD34$^+$FcRγ^+CD48$^+$CD150$^-$) (Fig. 1.1) [13]. The lymphocytes are derived from common lymphoid progenitor (CLP) which could be distinguished by analysis of IL7Rα expression (Lin-c-Kit^{low}Sca-1^{low}IL7Rα^+Flt-3^{high}) [14]. Further lineage differentiation of committed progenitor cells leads to production of mature blood cells (Fig. 1.1).

Not only can the cell surface markers be used to identify HSC. It was proposed that HSC, but not progenitor and mature cells could efflux fluorescent dye Hoechst 33342. This feature of HSC could be distinguished by flow cytometry and allow efficient purification of engraftable and blood-reconstituting cells in mouse model [15]. Due to the characteristic flow cytometry profile, this population was called "side population" (SP). The rationale behind the "side population" as criterion of HSC isolation is linked with multidrug-resistant ATP-Binding Cassette (ABC) transporters such as MDR-2 and ABCG2, that can efflux also the lipophilic fluorescent dyes [16]. High expression of ABC transporters in HSC could be explained as one of the evolutionary conserved mechanism that protects lifelong-lived HSC from toxic compounds. The majority of SP$^+$ bone marrow cells show phenotype consistent with main surface markers of HSC: Lin$^-$c-Kit$^+$Sca-1$^+$CD48$^-$CD34$^-$, however controversy exists about contribution of long-term reconstituting CD150$^+$ and CD150$^-$ fractions that are present among the SP$^+$ [17, 18].

The advances in identification and purification of mouse stem and progenitor cells were fundamental for deciphering how the hematopoietic system is organized. However, it turned out that human hematopoietic compartment cannot be characterized and classified by the same markers that were found in mouse, what hindered translation to clinical settings. In case of human HSC, the phenotype Lin$^-$CD90$^+$CD38$^-$CD34$^+$ was proposed [19], however it is likely that this phenotype is still not unique for HSC and includes also multipotent progenitors [1]. Recently, the CD49f expression was showed to discriminate the human HSC from MPP [20].

The techniques used for prospective isolation of HSC triggered the studies that clarify the postnatal hematopoiesis. Nevertheless, it is the biological function: self-renewal, long-term reconstitution of all blood cells and engraftibility in in-vivo assays, that defines the HSC and not the phenotype alone. Although the isolation methods based on phenotype are so efficient that

few or even one single transplanted cell provide long-term reconstitution [8, 21, 22], the phenotype of cells with HSC potential could be altered upon stress conditions or in genetically modified mouse models [23]. Therefore, characterization of HSC by phenotype cannot exclude in-vivo assays [23].

Different function of HSC and MPP: quiescence versus proliferation

Despite the close relationship of HSC and MPP fractions, these two different populations play exclusively different biological functions (discussed in [24]) (Fig. 1.2). The HSC present quiescent character. Analysis of cell cycle revealed that HSC divide extremely rarely – only ~2% of HSC are in G2/M/S phase [25]. Not only HSC infrequently enter HSC proliferation phase, but majority of them are in G0 phase and only small part in G1 phase [25]. These quiescent properties of HSC could be interpreted as evolutionary conserved function to constitute reservoir providing new blood cell production for whole lifespan. The low proliferation rate and exit from cell cycle allow avoiding proliferation-induced damage of DNA. The quiescent character is connected with low metabolic activity [26]. HSC produce adenosine-5'-triphosphate (ATP) via glycolysis and reduce oxidative phosphorylation by pyruvate dehydrogenase kinase (Pdk)-dependent mechanism [27]. Suppressed oxidative metabolism protects HSC from generation of reactive oxygen species (ROS). The MPP represents opposite characteristics. They actively proliferate, what results in expansion of cells which than follow the lineage specifications [24].

The differences in quiescence and proliferation state between HSC and MPP could be understood in the light of their self-renewal potential. Only the HSC can self-renew and the next differentiation step toward MPP is connected with loss of the self-renewal capabilities [24]. The self-renewal of HSC sustains the stem cell reserve, but is inevitable connected with accumulation of acquired DNA damages. Therefore, from evolutionary point of view, the low proliferation rate of the self-renewing HSC is beneficial [24, 28]. Oppositely, all MPP cells differentiate to functional, mostly short-lived blood cells (apart from long-lived memory lymphocytes), and potential proliferation-induced damages would not be accumulated in the hematopoietic system [28].
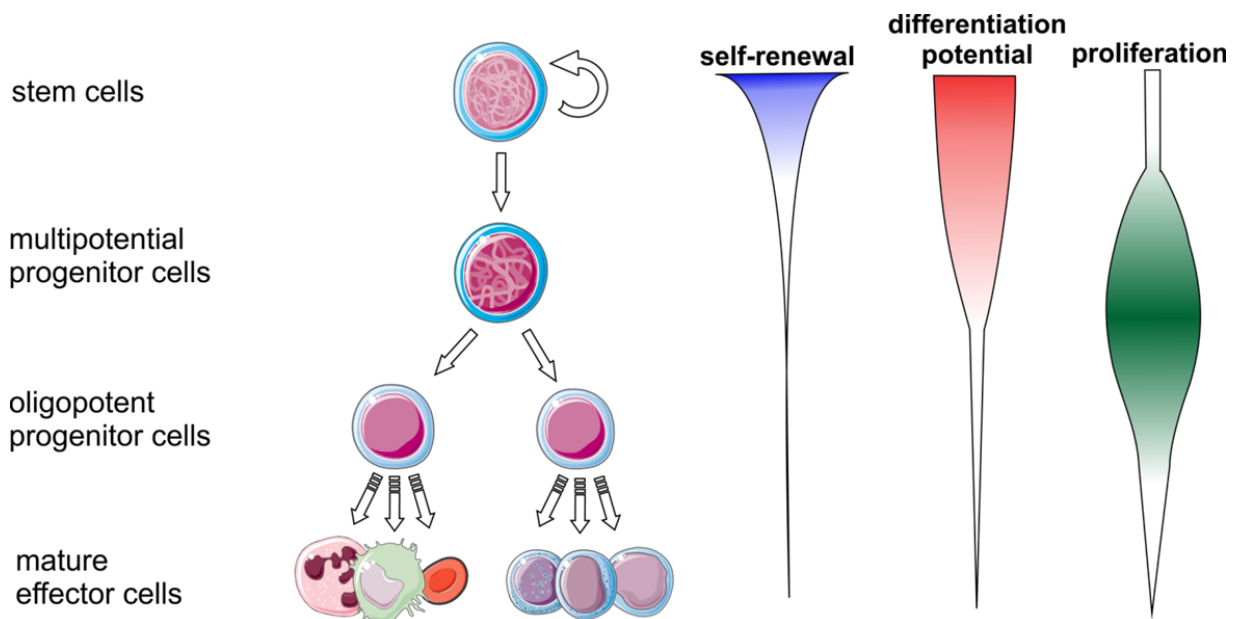
Fig. 1.2 *Different biological functions of HSC and MPP.*

Heterogeneity of HSC

The progress in identification and sorting of rare cells allows to isolate highly purified population of hematopoietic stem cells. Although the methodology gives the possibility to isolate almost homogenous population in term of potential to reconstitute sublethally irradiated mouse, purified HSC are still heterogeneous regarding their differentiation pattern, proliferation and self-renewal (reviewed in [29]).

The best method to analyze heterogeneity of HSC is transplantation of single HSC and tracking its progeny. Using this strategy, Dykstra and co-workers found four (α, β, γ, δ) functionally different subsets of HSC among murine CD45^{mid}Lin^{-}Rhodamie123^{-}SP^{+} bone marrow fraction [30]. The four fractions could be separated by the type of the blood cells they produce. The α subset differentiates almost exclusively to myeloid cells, while the β subset gives balanced reconstitution of myeloid, T cells, and B-cells [30]. The γ and δ are myeloid-deficient clones, with γ subsets produce both T and B cells whereas δ differentiate preferentially to T-cells [30] (Fig. 1.3). The distinct HSC subset with preferential differentiation towards platelets was also described and could be prospectively isolated by von Willebrand Factor (vWF) expression

(Lin⁻c-Kit$^+$Sca-1$^-$CD150$^+$CD48$^-$vWF$^+$) [31]. However, in long-term experiments the platelets-primed HSC also gave rise to myeloid and lymphoid biased HSC [31]. This observation suggested that vWF$^+$ HSC may be at the apex of HSC hierarchy.

Another Other technique that can be applied to study HSC heterogeneity is based on lentiviral barcoding and high-throughput sequencing. This approach revealed presence of two subsets of HSC: one with B- and T- cell biased differentiation and the second with B- cell and granulocyte biased differentiation [32].

Not only the differentiation biases can discriminate distinct subsets of HSC, but their self-renewal capability also differs. The α and β subset were the only ones that reconstituted secondary and tertiary recipient mice, what indicated their self-renewal [30]. The γ and δ HSC were not able to produce blood cells in any of secondary recipients [30]. The study on vWF$^+$ HSC also revealed their self-renewal activity [31].

Finally, there is also a study showing two differently proliferating subsets among HSC with mean turn-over rates 4 and 21 weeks [25]. However, it is still unclear if this observation represents different state of HSC (activated and dormant) or rather represents separate subpopulations with distinct differentiation potential.

The heterogeneity of HSC clones could be the result of random stochastic commitment, or intrinsic, preprogrammed feature of a given clone or alternatively depends on extrinsic factors regulating their fate. When α and β HSC subsets were transplanted to secondary and tertiary recipients, their commitment to given subtype was highly inheritable, indicating that the intrinsic factors are crucial. This was also in accordance with previous study [33]. But the transitions between α and β states, as well as transition of platelets-primed HSC toward myeloid and lymphoid biased HSC were also observed, what points to possible extrinsic regulation. The extrinsic influence on HSC heterogeneity was evidenced by the changes between α, β, γ, δ states caused by 4 day in vitro culture [30]. Therefore, the observed heterogeneity results both from intrinsic programs and extrinsic factors.
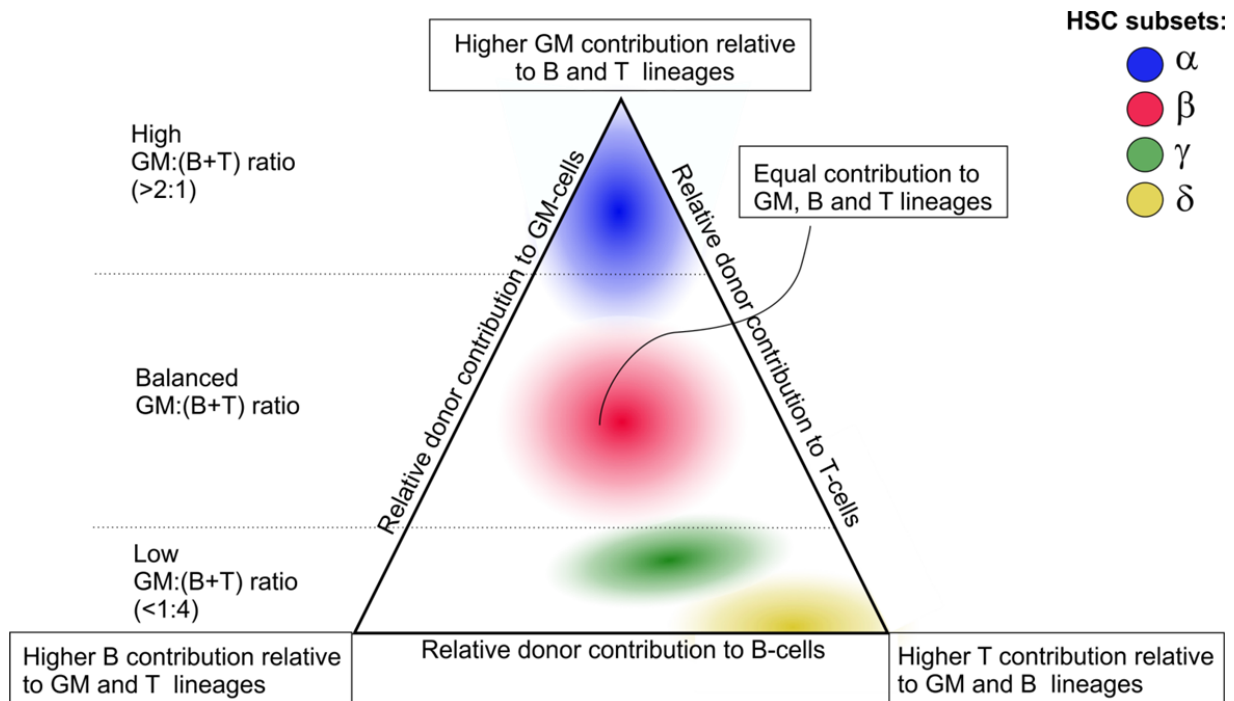
Fig. 1.3 *Graph representing heterogeneity among HSC. Based on [30] and modified.*

Molecular mechanisms shaping the hematopoietic fate

Identification of cell's phenotype at given differentiation stage allows more detailed studies on molecular mechanisms responsible for lineage commitment. The main attention was put on transcription factors (TFs) that can modulate expression of gene networks. The majority of important TFs were found by using mouse gene knockout models. Identified TFs, including GATA-1, GATA-2, GATA-3, FOG-1, Gfi-1b, EKLF, PU.1, C/EBPα, C/EBPε, PU-1, Ikaros, Notch, TCF-1, represent different families of DNA-binding proteins (reviewed in [34]). Changes in expression of some of these TFs were also observed in hematological malignancies (eg. GATA-1 in megakaryocytic leukemia [35], C/EBPα [36] and PU.1 [37] in myeloid leukemia, while Pax5 in B-lymphoid leukemia [38], what confirmed their crucial role in regulation of hematopoietic differentiation.

Initially, these studies linked deficiency of a given TFs with differentiation block at specified stage of hematopoietic hierarchical tree [34], however later studies on single hematopoietic stem and progenitor cells revealed that the interactions between many detected

TFs constitute very complex network of dynamic regulatory relationships [39]. Thus, the role of TFs in hematopoietic differentiation could not be understand understood as simplified notion that activation of given TF drives the commitment to specified lineage. Oppositely, the TFs with antagonistic roles are simultaneously active in the same cell. Even the direct physical interaction of TFs was evidenced that led to block of each other's activity, like in case of GATA-1 and PU.1 in promoting erythroid and megakaryocytic fate vs. myeloid fate [40], EKLF and Fli-1 for erythroid vs. megakaryocytic fate [41], GATA-3 and T-bet for TH1 vs. TH2 differentiation [42]. Therefore, not only the given TF induce the commitment to specified lineage, but also counteracts the differentiation to alternative fate. Such mechanism is believed to provide efficient way for dynamic regulation of numerous possible hematopoietic fate choices [34].

The high expression of TFs was mainly observed in more committed progenitors and their activity was linked with restriction to defined hematopoietic fate (eg. GATA-1 in megakaryocyte-erythroid differentiation and PU.1 in granulocyte-monocyte differentiation [40]). However, the same TFs that drive the differentiation of committed progenitors are simultaneously expressed in HSC and MPP, albeit at significantly lower levels [34]. Nevertheless, the expression of lineage-affiliated genes in HSC does not imply the lineage specification of HSC. This was proved by elegant study where Cre-Lox and YFP system in mouse was used to follow fate of cells expressing lysosome – a myeloid marker [43]. It turned out that part of HSC became YFP$^+$, what meant they had to express lysozyme at some time point. When the YFP$^+$ HSC were transplanted to irradiated mice they were able to reconstitute not only the myeloid cells, but all kinds of blood cells [43]. Thus, the expression of low levels of lineage-affiliated genes in HSC does not restrict the multipotency of HSC. It is was proposed that the expression of different lineage-restricted TFs and genes within the same HSC or MPP cell reflects the open chromatin state of hematopoietic gene regions [44]. This phenomenon is referred to as "lineage priming" [45]. During the differentiation to more specified lineages more regions of chromatin become restricted, but expression of lineage-specific TFs and genes is enhanced, what finally results in lineage commitment [44].

Hematopoiesis after transplantation and native hematopoiesis

The current knowledge of postnatal hematopoiesis would not be gained without experimental bone marrow transplantation (BMT) in mouse model [5]. In this assay, the recipient animals are myeloablated to clear and prepare the bone marrow niche for the engraftment of transplanted HSC [46]. Among myeloablation methods, the sublethal dose of ionizing radiation is most commonly used [46], but also high dose of chemotherapeutics [47] or even antibody-based methods to condition recipients could be applied [48]. Although, BMT or transplantation of purified populations of cells is still fundamental method in current research on hematopoietic processes, one could ask if hematopoietic recovery after transplantation reflects the native hematopoiesis in non-transplantation settings.

Until recently, it remained hard to address this question due to lack of proper experimental models. There were several studies showing transplantation in non-myeloablative conditions, but still the transplantation itself was not excluded from the experimental scheme [49]. The progresses has been made recently by two independent groups that developed mouse models to study native hematopoiesis [50, 51].

Work of Sun and colleagues for the first time indicated that native hematopoiesis might significantly differ from the hematopoiesis observed after the transplantation [50]. They developed a mouse model that allows following clonal tracking of HSC and MPP progeny without transplantation. The model uses the inducible transposon element, that is mobilized and randomly incorporated into other genome locus. The mobilization is linked with DsRed expression, and the unique integration site could be distinguished by whole genome amplification, PCR and sequencing. The random integration sites enable differentiating cells that origin from distinct clones [50].

These clonal tracing technique revealed that these are MPPs (defined as $Lin^-c\text{-}Kit^+Sca\text{-}1^-CD48^+CD150^-$) that drive native hematopoiesis rather than classically defined LT-HSC ($Lin^-c\text{-}Kit^+Sca\text{-}1^-CD48^-CD150^+$) [50]. Moreover, high number of different MPP clones are active at given time (estimated to be at least 831 active clones) that are quickly exchanged by successive ones (estimated half-life of active granulocytic clone is 3.3 week) [50]. This is clearly in contrast to numerous transplantation studies, where mature PB cells are derived from limited number of LT-HSC. What can explain this difference is that donor MPP do not engraft after transplantation.

The second study by Bunsch and coworkers took advantage of genetic labelling of LT-HSC using Tie-2 promotor and quantify the contribution of stem and progenitor fractions by limiting dilution assay and modelling [51]. They evidenced that LT-HSC (defined as Lin$^-$c-Kit$^+$Sca-1$^+$CD150$^+$CD48$^-$) contribution to native hematopoiesis is minimal in comparison to ST-HSC (defined as Lin$^-$c-Kit$^+$Sca-1$^+$CD150$^-$CD48$^-$), that mainly drive blood cell production [51]. The results indicated also that ST-HSC possessed significant self-renewal potential [51]. The significant LT-HSC contribution to native blood cell production was observed only during fetal development and early postnatal life, while in adult mice was increased by 5-fluoruracil induced leukopenia [51].

Concluding, these two studies on clonality of native hematopoiesis suggest that current view on hematopoietic hierarchy has to be modified. They rise many new questions concerning the developmental origin of the MPP/ST-HSC, aging of hematopoietic system and origin of hematological malignancies. However, these are the first studies about native hematopoiesis using the non-transplantation based methods, thus next independent verification, including different experimental approaches, are needed to fully confirm the conclusions. Finally, the important question is if these experiments done on mice cultured in sterile specific pathogen free (SPF) conditions could be translated to humans, who do not live in sterile conditions but encounter many environmental hematopoietic stress conditions throughout their lifespan.

Pluripotent adult stem cell as possible hematopoietic precursors

The potential of HSC to provide lifelong production of blood cells is well proven [5]. However, some hypotheses proposed that postnatal organism possesses also stem cells that have pluripotent capabilities and under appropriate conditions give rise to blood cells. This implies that such cells would be the precursors of HSC and of all other tissue resident stem cells (Fig. 1.4).

Multipotent adult progenitor cells

The multipotent adult progenitor cells (MAPC) were described by Catherine Verfaillie group in 2002 and proposed to be adult stem cells with broad plasticity [52]. These bone-marrow derived
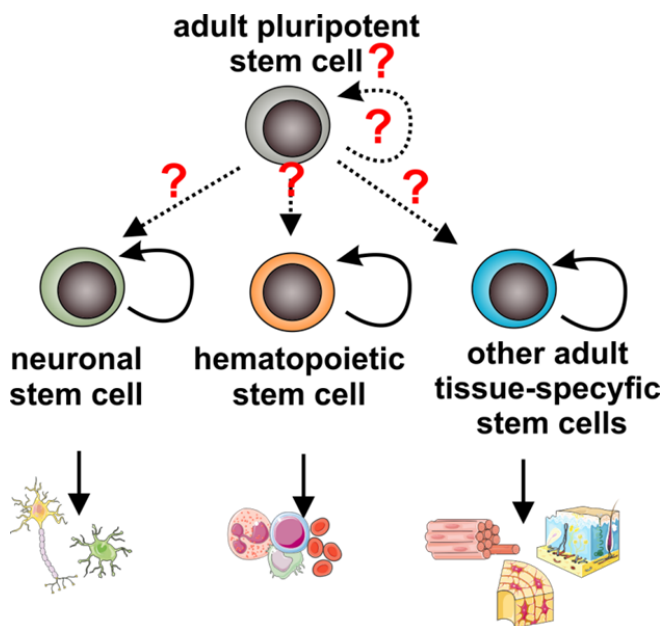
Fig. 1.4 *The hypothesis of adult pluripotent stem cells as the source of other tissue-specific stem cells, including HSC.*

cells isolated by long-term in vitro culture were able to differentiate to all three embryonic lineages and were even shown to complement blastocyst, what indicated their pluripotency [52]. Nevertheless, these results could not be confirmed by other independent groups [53, 54]. Their hematopoietic potential is also doubtful. Although the MAPC cells provide the reconstitution of hematopoietic system, the number of the cells required to be transplanted in order to observe the reconstitution is 3 order of magnitude higher comparing to classically defined hematopoietic stem and progenitor cells $(Lin^-Sca-1^+c-Kit^+Thy-1^{low})$ [55].

Very small embryonic like stem cells

Very small embryonic like stem cells (VSELs) described by Mariusz Ratajczak group in 2006 are another adult cells claimed to be pluripotent [56]. VSELs, similarly to MAPC, were initially isolated from murine bone marrow and were shown to express embryonic markers (Oct-4, Nanog). Differentiation to cells of all three embryonic lineages was also presented [56]. The suggested phenotype of VSELs was $Lin^-Sca-1^+CD45^-$, but the proposed unique feature characterizing these cells was their small size [56]. Murine VSELs had a diameter of 3.6 μm (exact size varies between publications),what is much smaller than HSC and even smaller than erythrocytes [56]. Next studies from the same group claimed that VSELs can be isolated from different organs (brain, kidney, heart, cord blood) both from mouse and humans. In contrast to MAPC, VSELs did not complement blastocyst [57] or reconstitute the hematopoietic system upon transplantation to irradiated hosts, what was explained by their quiescent character [58]. However, Ratajczak's group showed that if VSELs are predifferentiated into hematopoietic cells

by co-culture with OP9 stromal cells they can contribute to blood cells in transplantation model [58].

Verification of pluripotent adult stem cell hypothesis

The potential of these claimed adult stem cells populations lacks confirmation by independent studies [54]. The presented data indicating their hematopoietic potential is not verified by experiments on single cell level, which are necessary to prove the stemness potential and exclude possible artifacts connected with the contamination with other cells [54]. Other studies questioned the presence of Oct-4^{+} pluripotent stem cells, such as MAPCs and VSELs, in adult organism. One of these studies used mice where Oct-4 gene was knockdown in adult mice by inducible Cre-loxP system [59]. The knockdown of the Oct-4 gene neither affects hematopoietic reconstitution nor regeneration of any other tissues [59]. This indicates that even if Oct4^{+} pluripotent stem cells exist in postnatal organism they do not play a role in tissue regeneration. Other studies reported no Oct-4^{+} cells in adult bone marrow in Oct4-GFP mice model [60]. Finally, the VSELs population isolated from human cord blood were shown to lack embryonic, hematopoietic, neural, and mesenchymal markers [61]. Their transcriptome was also very different from embryonic and adult stem cells [61]. Importantly this population did not proliferate in any tested conditions and was enriched for aneuploid cells [61].

Therefore, the presence of pluripotent precursors of HSC in postnatal organism is doubtful and needs further independent verification.

Aging of HSC

HSC acquire changes during aging

Functioning of hematopoietic system changes with aging of an organism (reviewed in [62], Fig. 1.5A). One of the most evident age-related changes is a phenomenon referred to as myeloid bias. Myeloid bias is manifested by increased frequency of myeloid cells among peripheral blood cells and decreased abundance of lymphoid fraction, including lymphoid progenitors and naïve B and T lymphocytes [30, 63–65]. This is connected with higher incidence of myeloid disorders, like myeloid dysplastic syndrome and myeloid leukemia in elderly individuals, while the lymphoid malignances prevail in younger age [62]. It is also well

documented that elderly patients mount adaptive immune response with much smaller efficiency comparing to younger ones, what could be explained as a consequence of observed decreased T lymphopoiesis and reduced repertoire of B cells (reviewed in [66–68]). Accordingly, vaccination effects in elderly patients are weak [66]. Other dysfunction of hematopoietic system aging is increased incidence of anemia [69].

All of these age-associated dysfunctions of hematopoietic systems may be the result of alterations on different steps of hematopoiesis. The decreased lymphoid potential is linked with comprised function of lymphoid progenitors, as well as with extrinsic factors: bone marrow microenvironment in case of B cells [70] and thymus atrophy in case of T cells [71].

However, there are several evidences that age-related alterations could be explained not only by dysfunction of effectors cells or committed progenitors, but originate already in stem cell compartment [72]. When murine HSC from aged donors are transplanted to the syngeneic young recipients, the reconstituted hematopoietic system showed typical age-related features, with relative dominance of myeloid fraction over lymphoid fraction [30, 63]. The old murine HSC produced B-cells demonstrating age-related changes within B-cell repertoire [73].

The findings on aging of hematopoietic system revealed by studies on mouse models could be, at least partially, translated to humans. The aged human HSC showed the same myeloid biased as murine HSC [74]. Also age-related hematopoietic malignances in humans, like chronic lymphocytic leukemia (CLL) connected with oligoclonal and restricted B-cell development, originate in HSC populations as evidenced by xeno-transplantation into immunocompromised mice [75]. Therefore, the aging mechanisms of hematopoietic systems are likely to be evolutionary conserved and studies on model organisms with shorter lifespan, like mouse, may contribute to understand aging of human hematopoiesis.

Frequency and regenerative potential of aged HSC

Given that several evidences indicted that aging of hematopoietic system originates already in stem cell compartment, many studies concentrated on age impact directly on HSC. Paradoxically, strictly defined HSC are more frequent in bone marrow of older mice as well as in eldery patients [74, 76]. Additionally, the differences in HSC frequency among older mice are

much higher than in young individuals, what indicates that older mice lost the potential to control size of stem cell pool [77].

Although the HSC pool expands with aging, the regenerative potential of HSC deteriorates as shown by both in vitro and in vivo models (reviewed in [78]). In experiments using in vitro co-cultures with stromal cells, old HSC formed two times less colonies that young ones [77]. Not only, the efficiency of colony formation was impaired, but also the colony growth was delayed in old HSC [77].

The in vivo experiments involving HSC transplantation confirmed the reduced regenerative potential of aged HSC. Among transplanted purified $Lin^-c\text{-}Kit^+Sca\text{-}1^+CD48^-CD34^-E^+CD150^+$ population, there were 2.2 fold lower number of functional HSC in older mice compared to young ones (26% vs 12% respectively). The old HSC did not self-renew their pool as efficiently as young HSC in serial transplantation tests [77].

For successful reconstitution of irradiated host, the systematically injected HSC have to home and engraft into bone marrow niches. The old HSC had impaired short-term (16-21 hours) homing ability in direct competitive comparison with young HSC, what additionally reduced their regenerative potential [77].

Finally, the clonal analysis of HSC pool in older mice revealed more myeloid-dominant stem cell clones among $Lin^-c\text{-}Kit^+Sca\text{-}1^+CD48^-CD34^-E^+CD150^+$ fraction, what is in accordance with observed myeloid-biased hematopoiesis in older individuals.

These studies on regenerative potential of HSC in mice model are in line with clinical observations. Some clinical studies showed negative correlation of donor age with allogenic transplant outcome [79, 80]. However, it has to be stated that in clinical settings many factors apart from age influence the transplant outcome. This makes the analysis of age impact on transplant success difficult and studies reporting no correlation between donor age and transplantation also exist [81].

Models of HSC aging

Different models aim to explain changes among hematopoietic stem cell pool during aging [82] (Fig. 1.5B,C,D). Originally, it was proposed that all HSC gradually lose their function

28
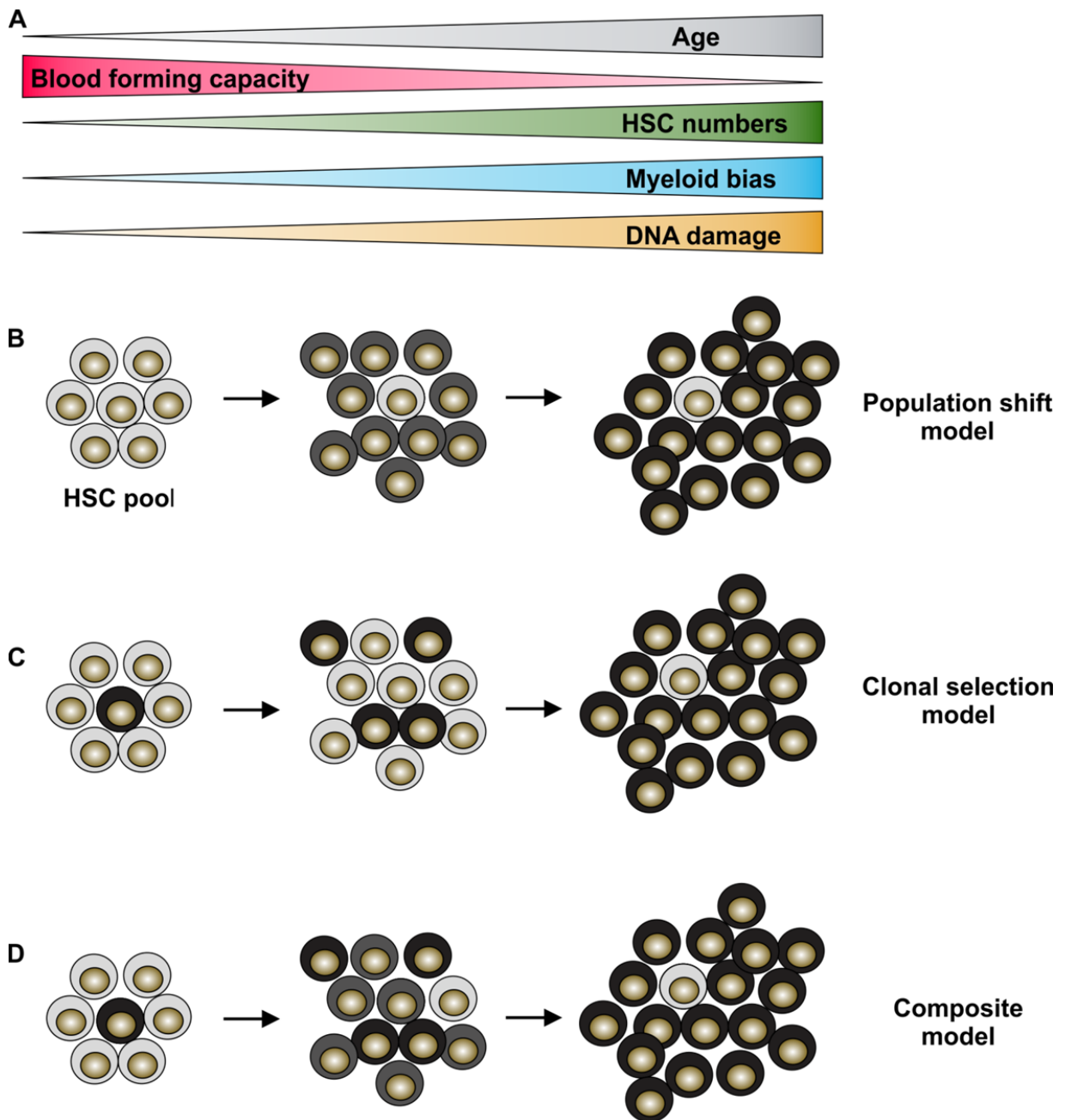
Fig. 1.5 *(A) Main changes acquired by HSC during aging and proposed models describing the observed age-related changes among HSC pool. (B) Population shift model implies that all HSC gradually changes during aging. (C) The clonal selection model proposes expansion of myeloid biased HSC clones (depicted as black cell) with time. (D) The composite model suggests that both models contribute to aging of HSC. Based on [82] and modified.*

29

with time – the model referred to as "population shift" [82]. However, it became evident that hematopoietic stem cell pool is heterogeneous and some HSC clones preferentially differentiate toward myeloid fraction while others toward lymphoid cells (described in more details in "*Heterogeneity of HSC*" section).

In the light of this phenomenon, the age-related changes such as myeloid bias may be the result of clonal selection and domination of myeloid-based HSC clones that extensively self-renew. The Beerman and co-workers confirmed this hypothesis by prospective identification and isolation of myeloid-biased HSC clones (Lin$^-$c-Kit$^+$Sca-1$^+$CD34$^-$Flt3$^-$**CD150^{high}**) and more balanced between myeloid and lymphoid output HSC clones (Lin$^-$c-Kit$^+$Sca-1$^+$CD34$^-$Flt3$^-$ **CD150^{low}**) [83]. They showed that it is myeloid biased CD150^{high} fraction of HSC that mostly expanded during aging, while the balanced CD150^{low} HSC subpopulation increased to lesser extent [83]. Moreover, the CD150^{low} HSC isolated from old animals sustained their potential to provide balanced reconstitution of myeloid and lymphoid fraction [83]. But despite producing balanced progeny, the old CD150^{low} HSC repopulated the recipients significantly worse per cell basis than in case of control young HSC [83]. This data demonstrated that aging of HSC pool could be described by composite model that implies both gradual loss of HSC potential as well as clonal selection. The composite model is further confirmed by clinical case of 115-year old healthy women evidencing that all her blood cells were derived from only two HSC clones [84].

Therefore the models of population shift and clonal selection are not mutually exclusive. Oppositely, combined together they reflect our understanding of HSC aging most accurately [82].

Link between proliferation and aging of HSC

It was proposed that the decline of HSC with aging is a direct result of underwent cell divisions. This view was confirmed by experiments involving serial transplantation, in which HSC are forced to extensive proliferation and reconstitution of irradiated host [77, 85]. After tertiary serial transplantation HSC already showed myeloid-biased output typical for aged animals [77, 85].

There are also more direct proofs demonstrating that HSC entering cell cycle gradually lose their stem cell potential. The research strategy to follow dividing HSC in vivo employs a

pulse labeling by inducible fusion histone 2B (H2B) and GFP and then tracking label dilution or retention among stem cells and their progeny [86]. Wilson and colleagues showed that robust regeneration potential sustained among Lin⁻c-Kit⁺Sca-1⁺CD150⁺CD48⁻CD34⁻ cells that retain the label for longer time period (70-306 days). Label retention implied that they did not proliferate [25]. In contrast, cells from the HSC fraction that lost label - so underwent cell divisions - were significantly less functional [25]. However, authors suggested that HSC can change their state from dormant non-cycling to active cycling states [25].

Other group using similar model (H2B-GFP under promotor of human CD34 gene [87]) presented partially opposite data [88]. They confirmed that proliferating HSC have decreased stem cell ability, but showed data indicating that activation of HSC and entering into cell cycle is irreversible: once HSC starts to proliferate it is "slaved for extinction" [88]. It is worth noticing, that such interpretation would undermine the common notion on self-renewal as the crucial determinant of HSC. To address this issue, authors showed that even if the cells self-renew phenotypically (sustained surface stem cell markers and are in G0 phase) they have already lost stem cell functionality due to previous entrance into cycling phase. Importantly, they emphasized the importance of activated HSC in steady-state, non-transplantation setting and argued that the previously observed extensive self-renewal is typical for high stress conditions observed after transplantation [88].

Concluding, the divisional history of HSC seemed to be inseparably connected with their decline with age. However, while some of the age-related changes could be explained by divisional history, such us myeloid biased and loss of regenerative potential, others like expansion of stem cell pool are harder to interpret as direct consequence of the proliferation-induced impairment.

Mechanism of HSC aging: role of DNA damage

Although, the age-associated changes in HSC are quite well described, the underlying mechanism of aging process of HSC remains not fully understood. Some studies indicate that HSC-intrinsic mechanisms may explain hematopoietic disorders observed during aging [63].

The accumulating DNA damage was proposed as one of the triggers of HSC aging [89]. The HSC self-renew their own population and are long lived population to provide blood

production throughout lifespan. These features predispose them to accumulate DNA damage in contrast to short lived progenitor cells. Indeed, both old mouse and human HSC possessed increased number of double break DNA strands [89, 90] as revealed by measuring γH2aX foci – a marker of DNA damage response. However, only few of the DNA repair pathways were altered in aged HSC, like X-ray repair cross-complementing protein (*Xrcc1*), Bloom syndrome protein (*Blm*), and XPA binding protein (*Xab2*) [91]. Additionally, mice deficient in some DNA damage response mechanisms, like xeroderma pigementosum D or Ku80 autoantigen, did not have altered HSC pool [89]. Other mice strain with compromised DNA damage pathways had altered function of HSC and showed premature aging phenotypes, but only upon challenge and not in steady-state conditions (reviewed in [72]). In accordance with these observations, it was shown that quiescent HSC do not actively repair DNA damage, but instead accumulate DNA damage [92]. However, upon the entry into cell cycle the DNA repair processes are reactivated and progenitor populations show reduced DNA strand breaks [92].

It was also proposed that not the DNA response machinery itself, but the signaling pathways activated by DNA damage: cell cycle checkpoints , apoptosis or differentiation might be responsible for age-related phenotypes. This was confirmed by some studies indicating the p16^{INK4A} [93] and p53 [94] were changed in aged HSC. However, the reported effects were weak and were not confirmed by other studies [95]. Therefore, the activity of DNA repair processes among HSC as well as their causative role in HSC aging is still matter of debate.

Given that HSC express high levels of telomerase, it was suspected that not only DNA strand breaks, but also the telomeres erosion might lie behind the HSC aging. HSC isolated from third generation of telomerase-deficient mice exhibited premature aging. Forcing HSC to proliferation by serial transplantation shortened their telomeres and was linked with aged-like phenotypes [96]. But, overexpressing telomerase did not protect HSC in serial transplantation assays [97]. Also the HSC from old mice did not have significantly shorter telomeres when compared to young HSC [98]. This indicates that both DNA strand breaks as well as telomere erosion may be markers of aging, rather than causative triggers of HSC dysfunctions acquired during aging.

Mechanism of HSC aging: epigenetic drift

The crucial feature of stem cells is their ability to self-renew their own pool. Proper self-renewal requires not only the error-free DNA replication during cell division but also precise transfer of epigenetic signature to a daughter cell. As aging disturbs self-renewal, the epigenetic machinery was thought to be responsible for the age-related changes.

Epigenetic information relies on processes such as DNA methylation as well as histone methylation, acetylation and ubiquitination status (reviewed in [99]). Specific deletion of DNA methyltransferase Dnmt3 in HSC expanded the stem cell pool but impaired their differentiation – changes observed also during HSC aging [100]. The genome wide comparison of DNA methylome of young and old HSC confirmed that altered DNA methylation is linked with HSC aging [101]. It showed hypermethylation of regulatory regions of gens involved in differentiation and hypomethylation of genes responsible for the stem cell functions [101].

The histone modifications and chromatin organization were also affected in aged HSC. Several genes implicated in regulation of chromatin structure, like histone deacetylases (Hdacs) and sirtuins, were downregulated with age [91]. The sirtuin-deficient HSC presented an aged-like phenotype [102]. Much attention was also paid to the role of polycomb repressive complexes (PrC) that are responsible for the various modification of histones (reviewed in [103]). Several target genes of PrC had altered H3K4 (lysine 4 in histone H3) and H3K27 (lysine 27 in histone H3) trimethylation status [101]. Apart from these changes the global acetylation of H4K16 (lysine 16 on histone H4) was reduced in aged HSC [104].

There are no doubts that epigenetic drift may be responsible for transcriptional alterations observed in aged HSC. However, the question remains if the changes in epigenetic information are one of the direct drivers of HSC aging or just the consequence of this process.

The perspective of reversing HSC aging

While our knowledge about aging of hematopoietic system is increasing, the tempting question appears: is it possible to reverse the aging of HSC? The possibility of inducing pluripotency from differentiated cells by transcription factors gives hopes that similar reversal of aging state could be obtained. The proof-of-concept showing that old HSC could be transformed to HSC with young state properties was provided by Wahlestedt and co-workers [98]. They

reprogramed hematopoietic stem and progenitor cells from old animals into induce pluripotent stem cells (iPS) and then used them in blastocyst complementation assay [98]. The HSC from the derived mice resembled young HSC [98]. It was proposed that epigenome erasure was responsible for the reversal of old HSC state.

However, from the therapeutic point of view, it would be hard to rearrange whole epigenome. Therefore the experiments showing that modification of even one gene can reverse some of the age-related declines are of great interest. One of the examples is *Satb1*, which is a chromatin organizer and was found to be downregulated in old HSC [105]. The overexpression of *Satb1* in old HSC increases their lymphoid output, at least in vitro [105]. Overexpression of other gene, a mitochondrial deacetylase Sirt3, increased the reconstitution potential of aged HSC, but did not reverse their myeloid bias [102]. This indicated that age-related changes in HSC result from several intrinsic factors that independently contribute to the age-related alterations.

Oppositely to *Satb1* and *Sirt3* which are downregulated in aged HSC, other potential targets are upregulated, among them mammalian target of rapamicin (mTOR) pathway [106, 107] and Rho GTPase *Cdc42* [104]. Administration of rapamicin – a mTOR inhibitor – reduced the numbers of HSC, restored the lymphoid differentiation capabilities and reconstitution potential in old individuals [107]. Also, the inhibitor of *Cdc42* called Casin reversed myeloid bias and some features of old HSC phenotype [104]. Importantly, apart from inhibiting Cdc42, Casin modifies also epigenetic information, what may underlie the observe effects.

Rapamacin and Casin are examples evidencing that administration of single drug can at least partially reverse age-related decline of hematopoiesis. Of course, administration of such drugs may potentially lead to serious side effects, but nevertheless this is the proof-of-concept that changes among HSC caused by age are not irreversible and developing strategies to overcome them is worth effort.

HSC-extrinsic aging factors

Most of the known factors affecting HSC aging are intrinsic to stem cells. The question how important are extrinsic factors for HSC aging remains mainly unaddressed. One of few studies on extrinsic factors showed that increased concentrations of pro-inflammatory cytokine RANTES skew HSC toward myeloid differentiation [108]. Also the increased fat content in bone

marrow microenvironment observed in elderly individuals is correlated with decreased SDF-1, which is crucial regulator of HSC function and therefore may contribute to exhaustion of HSC with age [109]. Other extrinsic mechanism that were shown to be implicated to HSC aging are gap junctions mediated by CXN43 channels [110]. These gap junctions transfer ROS produced in HSC to adjacent stromal cells, and by this mechanism protect HSC from ROS-induced damage [111].

As described in next chapter *"The bone marrow niche of hematopoietic stem cells"*, stem cell niche is crucial for maintenance of HSC. Given that niche protects HSC from environmental stress as well as regulates proliferation, self-renewal and differentiation of HSC it is likely that alterations of niche functioning may be implicated in aging of HSC. However, up to date only few studies focused on aging of HSC niche, showing impairment of bone formation, increased adipogenesis and decomposition of extracellular matrix (ECM) [112–114]. Therefore, next studies on how the niche impacts aging of HSC are required to fully understand mechanisms of age-related decline of hematopoiesis.

The bone marrow niche of hematopoietic stem cells

The concept of stem cell niche

The term "stem cell niche", referred to as local microenvironment where stem cells reside (Fig. 1.6). While it is now well evidenced, that niche is specialized region of tissue that is indispensable for controlling the stem cell fate, the cell compartments and molecular mechanism underlying the concept of the stem cell niche remains a matter of debate (reviewed in [115, 116]).

The first hypothesis, implying that HSC requires a specialized bone marrow microenvironment for proper functioning, was proposed by Ray Schofield in 1978 [117]. Then, the Dexter and co-workers confirmed in in vitro model that bone marrow derived-stromal cells are crucial for maintenance of hematopoiesis [118]. The development of genetic mouse models as well as high-resolution imaging techniques enabled to address more specific questions about the localization and components of stem cells niche. The studies using engineered mouse strains, in which the osteoblasts were targeted by overexpression of parathyroid hormone expression [119] or by deletion of BMPr1α gene [120], evidenced that the increased number of osteoblasts correlates with higher number of HSC. This indicated that it is the osteoblastic lineage localized in endosteal region that governs stem cell potential of HSC. However, it could not be stated if the

observed effect is due to direct interaction of osteoblasts and HSC or there are indirect mechanism involved. Next studies refined the notion of periendosteal osteoblastic niche of HSC and pointed to perivascular space as crucial region for regulation of HSC. The microscopic analysis revealed that most of Lin⁻CD41⁻CD150⁺CD48⁻ murine HSC resides not further then 5 cell diameters from bone marrow sinusoids [7, 121]. In contrast, only 20% of detected HSC were close to endosteal region [7, 121–123]. Also the in vivo imaging revealed, that systematically injected HSC homed to perivascular region where resides at least for several months [124].

But the endosteal and perivascular niche are not mutually exclusive. Oppositely, this two bone marrow compartments partially overlap [115]. The endosteal region is highly vascularized with many vessels linking the bone with the bone marrow [115]. Furthermore more HSC preferentially resides near trabecular bone region indicating that the role of bone proximity in stem cell niche cannot be omitted [125].
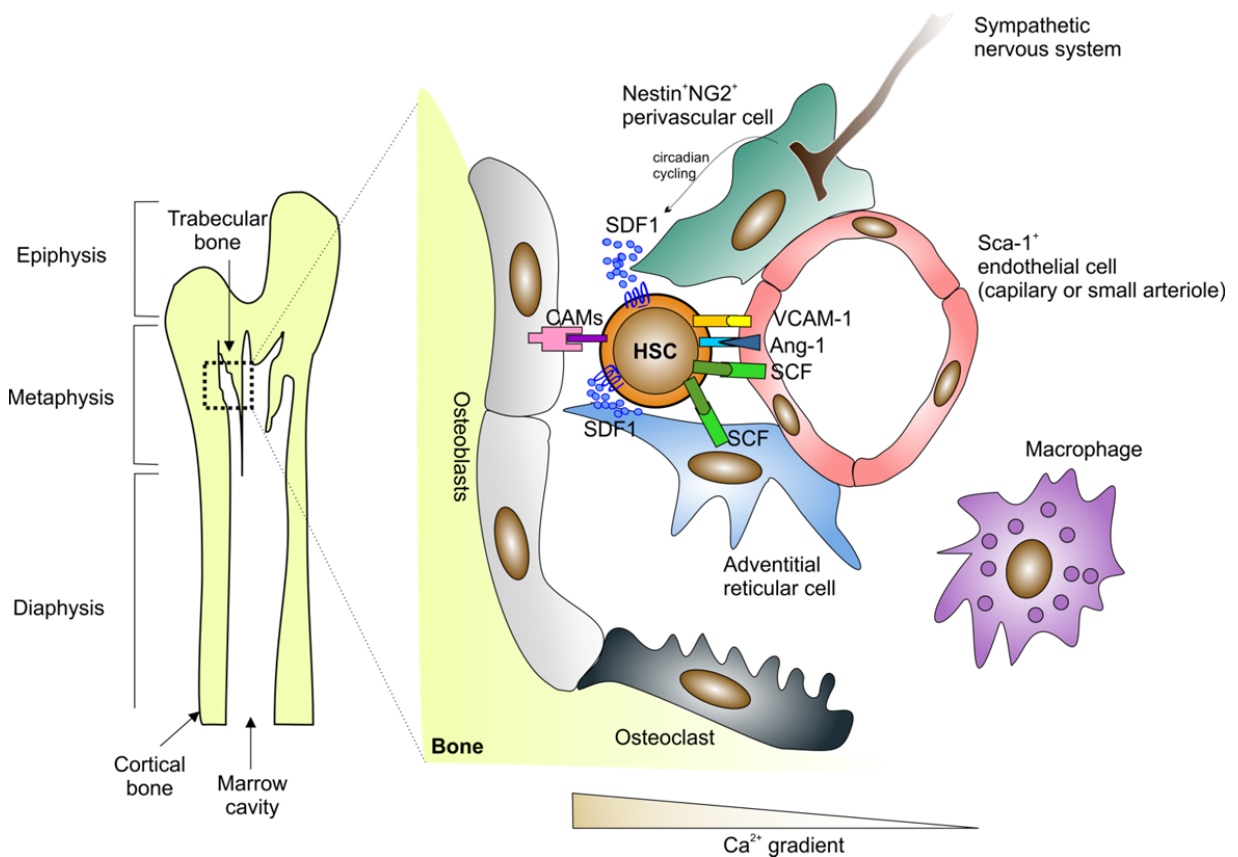
Fig.1.6 *Representation of cellular architecture of bone marrow niche of HSC and main molecular mechanisms involved in niche-dependent regulation of HSC. Based on [126] and [116] and modified.*

Endothelial and reticular cells in perivascular HSC niche

The two main cell types building the bone marrow perivascular niche of HSC are endothelial cells and adventitial reticular cells (ARC) (Fig. 1.6).

The prevailing type of bone marrow vasculature are large (> 50um diameter), fenestrated sinusoids with thin wall that consists of single layer of endothelial cells [115]. The fenestrated nature of endothelial cells allows cellular and molecular exchange between bone marrow and blood that is crucial for proper hematopoiesis. The importance of sinusoids for maintenance of hematopoiesis could be deduced from developmental observations: the prior formation of sinusoids is prerequisite to establish new sites of hematopoiesis [127].

For long time aspect of the heterogeneity of bone marrow endothelium was not addressed. Recently, the bone marrow endothelial cells were divided into two distinct subtypes based on expression of CD31, endomucin and Sca-1 as well as spatial localization and phenotypic features [128]. The predominat type of endothelial cells in bone marrow express CD31 weakly and showed only moderate expression of endomucin [128]. These cells localize in diaphysis region of bone marrow and form sinusoids – the prevailing type of vasculature in the bone marrow. Due to forming many branches this type of cells was called L-type bone marrow endothelium [128]. In contrast, the second fraction of endothelial cells exhibits high expression of CD31, endomucin and Sca-1, localizes mainly in metaphysis region of the bone where forms long column-like tubes that are interconnected by vessel loops[128]. Based on this phenotype, the fraction was called H-type endothelial cells. The H-type capillaries are placed where αSMA bone marrow arterioles terminates [128]. The H-type and L-type endothelial cells interconnects on the boundary of diaphysis and metaphysis and near endosteal region [128].

The H-type endothelial cells are minority of all endothelial cells in bone marrow (~2%), but are hierarchically upstream of L-type endothelium. The lineage tracing techniques evidenced that the H-type endothelium can generate L-type endothelium upon irradiation [128]. It was also shown that H-type endothelial cells are dependent on HIF-1a pathway [128].

Another study underlines the importance of Sca-1^{+} small arterioles for maintenance of quiescent HSC [129]. These Sca-1^{+} arterioles express also VEGFR2, VEGFR3 and Tie2 antigenes [129]. The whole-mount imaging of bone marrow revealed that quiescent HSC preferentially localized to the Sca-1 arterioles [129].

Although the relationship between H-type endothelium and Sca-1 arterioles was not directly studied, the comparison of these two studies indicates that these two populations may represent spatially neighboring niche in the bone marrow that is close to endosteal region.

The endothelial cells in bone marrow are covered by adventitial reticular cells (ARC) and together compose the basic "unit" of perivascular HSC niche [130]. ARC represents population harboring functional potential of skeletal stem cells – they can differentiate in vivo to osteoblastic cells and their progeny(osteocytes and bone-lining cells), chondrocytes, adipocytes and fibroblasts (reviewed in [131]). The ability to self-renew their own population fulfills the criterion of stem cells [131].

The unique feature of the ARC cells is their ability to reconstruct hematopoietic niche upon heterotopic transplantation [127]. ARC injected subcutaneously within a scaffold formed ossicle, that is then invaded by host vasculature and subsequently colonized by hematopoietic stem and progenitor cells [127].

Various isolation methods and nomenclature issues make difficult to compile numerous studies on skeletal stem cells (reviewed in [131, 132]. Different names were ascribed to this population in the literature: multipotent stromal cell, mesenchymal stem cell or CXCL12-abudant reticular cells (CAR). Identification of several cell surface markers allows prospective isolation of ARC, however there was no one widely accepted and used phenotype. In mouse models some used expression of PDGFR, CD105, CD90 or VCAM-1 [132]. Additionally expression of Sca-1 among with PDGFR distinguished another skeletal stem cell subpopulation called PαS [133]. Several different transgenic mouse models were used to target skeletal stem cells by using promotors of Nestin [129, 134], Leptin-receptor [135] and Prx1 [136]. Finally, two laboratories propose broad panel of markers to describe developmental hierarchy of skeletal stem cell lineage [137, 138]. Generally, many cell populations studied based on different phenotypes and models overlapped with each other but the functional criterion remains the gold standard to identify HSC-supportive skeletal stem cells [115].

The high resolution immunochemistry studies of mouse tibia revealed, that the ARC cell (defined as $PDGFR^+$ or $Runx2^+$) preferentially covered H-type endothelial cells near metaphysis and endosteal region [128]. The $Sca-1^+$ arterioles are also specifically covered by perivascular cells expressing Nestin and NG2, however without leptin receptor expression. The depletion of these $Nestin^+NG2^+$ cells reduced the pool of quiescent HSC[129].

These observations may indicate that these are not abundant bone marrow sinusoids that compose the HSC niche, but rather the two rare kinds of Sca-1^{+} endothelial cells together with the adjacent reticular cells. The data showing presence of HSC nearby sinusoids does not have to be contradictory with this hypothesis. Given the dense and regular sinusoid network observations of colocalization of HSC and sinusoids may result not from the preferential interaction between these two cell types but solely from random HSC distribution [129]. Indeed, the detailed statistical analysis demonstrated that HSC are significantly and preferentially associated with Sca-1^{+} arterioles, but not with sinusoids [129].

Cellular architecture of perivascular niche

Not only the endothelial and reticular cells regulate perivascular niche, but several other cell types also participates in this process (Fig. 1.6). The sympathetic nerves interacts with perivascular cells and control the Cxcl12 expression [139]. This regulation is responsible for circadian oscillations of Cxcl12 levels and subsequent daily fluctuations of HSC numbers mobilized into peripheral circulation [140]. Other regulation of HSC niche governs by neuronal system is the activation of TGF-β by nonmyelinating Schwann cells [141].

The other hematopoietic cells also contribute to HSC niche. Among them the bone marrow macrophages emerge as crucial population that shapes HSC niche. The fraction of CD169^{+} macrophages were essential for retention of HSC in the niche [142]. Depletion of CD169^{+} macrophages mobilized HSC into a blood stream in steady-state conditions and further augmented the pharmacological mobilization by G-CSF or CXCR4 antagonists [142]. The osteoclasts responsible for the bone resorption derive from macrophages and caused egress of HSC into circulation [143]. However, the role of macrophages is not clear, as other study identified macrophage population called "osteomacs" which revealed opposite activity – their loss increased HSC egress [144]. Nevertheless, the macrophages are important cellular element of the HSC niche.

Another population of hematopoietic cells, megakaryocytes, also control the HSC niche [145, 146]. When the megakaryocytes were depleted from the bone marrow the HSC numbers increased [145, 146]. The megakaryocytes restrict proliferation of HSC possibly by two

mechanisms. First, they produce CXCL4 chemokine that regulates HSC proliferation [145]. Secondly, they are source of TGF-β, which also governs the HSC quiescence [146].

The bone marrow niche provides an immune-suppressive environment that protects HSC from immune attack. The immune privilege of HSC niche is provided by T regulatory cells (T$_{regs}$) [147]. In vivo imaging revealed colocalization of FoxP3-positive Tregs with HSC [147]. The presence of Tregs enabled survival of HSC from allogenic donor in IL-10-dependent fashion [147].

The molecular mechanism of HSC niche

The functioning of HSC niche depends on several interacting biological mechanisms, including secreted factors and their signaling pathways, adhesion molecules, extracellular matrix and chemical gradients (reviewed in [148, 149], Fig. 6).

SDF-1 and stem cell factor (SCF) are niche-derived factors which necessity for HSC function is well documented [135, 136, 150, 151]. The SDF-1 and SCF are produced mainly by perivascular reticular cells and endothelial cells [135, 136]. SDF-1 acts on CXCR4 receptor present on HSC and other hematopoietic cells [151]. The SDF-1-CXCR4 axis is fundamental for homing and mobilization: blocking the CXCR4 receptor cause rapid egress of HSC to the circulation [151].

The receptor for stem cell factor expressed by HSC is c-kit [152, 153]. Blocking interactions of SCF with c-kit results in HSC clearance from bone marrow [48, 154]. Oppositely, over-activity of c-kit promotes myeloproliferative disorders [155].

The crucial role of niche in production of SDF-1 and SCF was evidenced by studies selectively deleting their expression in stromal and endothelial cells [135, 136]. The conditional ablation of SDF-1 in Prx-1$^+$ stromal cells decreased HSC numbers in bone marrow and promoted their mobilization [136]. The increased mobilization was also observed when SDF-1 was deleted in leptin receptor-expressing cells [135]. While the SDF-1 deletion in endothelial cells also affected HSC, the observed alterations were modest, indicating that rather stromal cells and not the endothelial cells are main source of SDF-1 in HSC niche [136].

However, deletion of SCF in Tie-2$^+$ endothelial cells caused massive HSC depletion and significantly impaired their reconstitution potential [135]. Similarly, the SCF deletion in

perivascular leptin receptor-expressing cells also decreased HSC numbers in bone marrow, what demonstrated that HSC require SCF from both endothelial and perivascular cells [135]. Apart from SCF and SDF, endothelial cells express also angiopoetin 1 [11] and angiopoetin-like 3 [156], that are important for HSC quiescence.

Several studies focused on WNT signaling pathway as potential niche-dependent mechanism of HSC control. Altering several factors involved in canonical WNT pathway, such as dickkopf homolog 1 (Dkk1), secreted frizzled-related protein 1 (Sfrp1) and early B-cell factor 2 (Ebf2) affected the HSC self-renewal and caused their premature exhaustion [157–159]. However, the role of the canonical WNT pathway in HSC regulation remains controversial, as the simultaneous ablation of β- and γ-catenin did not affect HSC homeostasis [160]. The possible explanation of this discrepancies may be connected with presence of unknown compensatory β-catenin homolog [161]. The involvement of the non-canonical WNT pathway was also reported [162, 163]. It was suggested that non-canonical WNT pathway inhibits the canonical pathway [164]. This is important as the low activity of canonical WNT pathway sustained HSC quiescence, while high activation or complete ablation of this signaling pushed HSC into proliferative state [165]. Thus, next studies are required, to clarify role of this complex signaling network in HSC homeostasis.

Other factors produced by niche act on Notch signaling in HSC – pathway regulating fate of different adult stem cell populations. The Jagged 1(Jag1) Notch ligand is produced by perivascular cells and endothelial cells [127, 166]. The conditional deletion of Jag1 in endothelial cells impaired the numbers and reconstitution potential of HSC indicating its role in regulation of self-renewal of LT-HSC [166]. In contrast, the endothelial Jagged 2 (Jag2) regulated expansion of ST-HSC [167]. Notwithstanding, the approach using the dominant negative form of Notch did not confirm role of Notch for maintenance of HSC [168]. Therefore, the role of Notch in HSC niche is still under debate. The complexity of Notch signaling and potential compensatory effects have to be addressed to resolve observed inconsistences.

The direct interaction of niche with HSC is mediated by adhesion molecules. Among them, the role of β1 integrins in crosstalk between HSC and niche was highlighted by several reports. The α4β1 integrin were essential for HSC for both short-term homing upon transplantations as well as for maintenance of long-term repopulating potential [169]. The α4β1 binds to vascular cell adhesion molecule 1 (V-CAM1) that is present on the surface of niche

41

composing endothelial cells and osteoblasts [170, 171]. Other integrins α1β1 and α5β1 mediated the adhesion of HSC to osteoblasts by binding to osteopontin [172]. Intrestingly, osteopintin binds also CD44 that is expressed by HSC [173]. The bone marrow endothelial cells express also the Robo4 receptor that was shown to guide HSC to translocate from blood vessels into bone marrow niche [174].

Apart from protein factors, the chemical gradients of Ca^{2+} and oxygen are crucial for biology of HSC niche. Osteoclasts resorb bone what results in release of Ca^{2+} ions [175]. This creates Ca^{2+} gradient, with highest concentrations near endosteal region and lower concentration near center of metaphysis [175]. The HSC express calcium-sensing receptor (CaR), which activation enhanced signaling of CXCR4 and adhesion of collagen I [176]. This mechanism was believed to take part in preferential homing of HSC near endosteal regions [176].

It is thought that multiply types of quiescent adult stem cells resides in low oxygen conditions (reviewed in [26, 177]). Despite being well vascularized, bone marrow is generally hypoxic tissue due to high cellular density and oxygen consumption [178]. Indirect evidences such like the constant activity of HIF1α pathway [179], low staining by perfusion dyes [180] and analysis with pimonidazol hypoxic marker [181], suggested that HSC occupy the low oxygen niche. However, the direct in vivo measurements of oxygen tension within the bone marrow made this hypothesis controversial [178]. Oppositely, to the previous concepts, the highest oxygen tension was found close to the bone near endosteal region, while lower oxygen concentration was detected deeper in to center of the marrow [178]. The especially high oxygenated regions were near endosteal arterioles covered by nestin-expressing perivascular cells [178]. Given that other reports showed that HSC reside near endosteal regions and close to nestin^{+} stromal cells, the HSC niche may be higher oxygenated than the rest of the bone marrow.

Role of HO-1 in hematopoiesis
part of this chapter was published in:
Kozakowska M, Szade K, Dulak J, Jozkowicz A
"Role of heme oxygenase-1 in postnatal differentiation of stem cells: a possible cross-talk with microRNAs"
Antioxid Redox Signal. 2014 Apr 10;20(11):1827-50) [182]

Enzymatic activity of HO-1

HO-1 is an enzyme that degrades free heme into carbon monoxide (CO), biliverdin, that is subsequently converted to bilirubin by biliverdin reductase and ferrous iron (Fe^{2+}) [183] (reviewed in [184, 185], Fig. 1.7). Free heme is prooxidative molecule, while the enzymatic products of HO-1 activity, CO and bilirubin, are
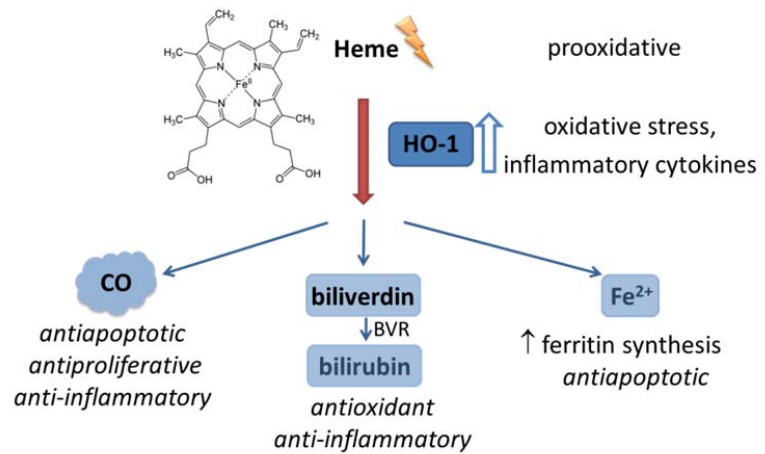
Fig. 1.7 *Enzymatic reaction catalyzed by HO-1 and properties of its products*

anti-apoptotic, anti-oxidative and anti-inflammatory mediators [184, 185]. The conversion of prooxidative heme into anti-inflammatory products makes HO-1 an important cell protective enzyme. HO-1 is highly inducible by many stress factors, such us oxidative stress or inflammation as well as by several growth factors like VEGF, SDF-1, TGFβ and PDGF (reviewed in [186]). Oppositely to HO-1, the other isoform heme oxygenase 2 (HO-2) is non-inducible, constitutively active protein expressed in variety of tissues [187].

Not only is the HO-1 crucial in acute stress connected with massive heme release, eg. in hemorrhages, but it also sustains homeostasis of several biological processes in steady state conditions. Till now, HO-1 role in cardiovascular biology is best recognized [185]. Several studies confirmed proangiogenic properties of HO-1 [188–190]. The HO-1 is a downstream mediator of crucial angiogenic factors VEGF [189] and SDF-1 [191]. Moreover the HO-1 activity itself can induce expression of VEGF [188].

In vivo and preclinical models confirmed the HO-1 involvement in angiogenic processes. The HO-1 overexpression by viral vectors was beneficial in model of rat hind limb ischemia [192], rabbit model of denuded arteries [193] and in attempts using bone-marrow derived cells in treatment of ischemic pig hearts [194].

Complex role of HO-1 in maintaining homeostasis includes also modulation of immune response (reviewed in [195]) and regulation of cancerogenesis and tumor growth (reviewed in [196]).

Nuclear localization of HO-1

The HO-1 was known to be localized in endoplasmic reticulum, but recently the nuclear localization of HO-1 was also evidenced [197]. It was proposed that HO-1 translocates to nucleus when the C-terminus of the protein is cut [197]. While it is thought that HO-1 did not reveal enzymatic activity in nucleus [198], it could modulate binding of NFkB and SP-1 transcription factors [197]. Furthermore, the non-enzymatically active HO-1 mutant protein was at least as effective in cytoprotection against oxidative stress as the native protein [199].

Based on these evidence, the role of HO-1 in the cell is not only restricted to its enzymatic activity and its non-enzymatic role of nuclear form should be also considered [200]. Though, the exact mechanism of HO-1 action in the nucleus has to be further elucidated.

HO-1 and hematopoietic differentiation

As the HSC stand at the top of hematopoietic hierarchy and their function is critical to maintain hematological homeostasis, it is understandable that during evolution HSC have been equipped in many mechanisms that protect them from stress conditions. Cao and co-workers evidenced that HO-1 is one of these crucial protective factors upon induction of acute stress [201]. Paradoxically, HO-1$^{+/-}$ heterozygous mice showed more rapid recovery in the model of 5-fluorouracil myelotoxic injury or better reconstitution at initial time points after bone marrow transplantation. However, when the HO-1$^{+/-}$ animals were exposed to chronic stress or HO-1$^{+/-}$ HSC were serially transplanted, significant decrease of hematopoietic recovery and exhaustion of HSC reserve was finally observed [201]. These results suggest an important role of HO-1 in regulating the balance between self-renewal and differentiation of HSPC under environmental stress. It was proposed that reported HO-1-dependent inhibition of stress-induced HSC proliferation is reliant on CO. Reduced HO-1 expression and lowered CO concentration led to a decreased activation of p38-MAPK pathway and, consequently, to low levels of p21 in cycling cells [201] (Fig. 1.8).
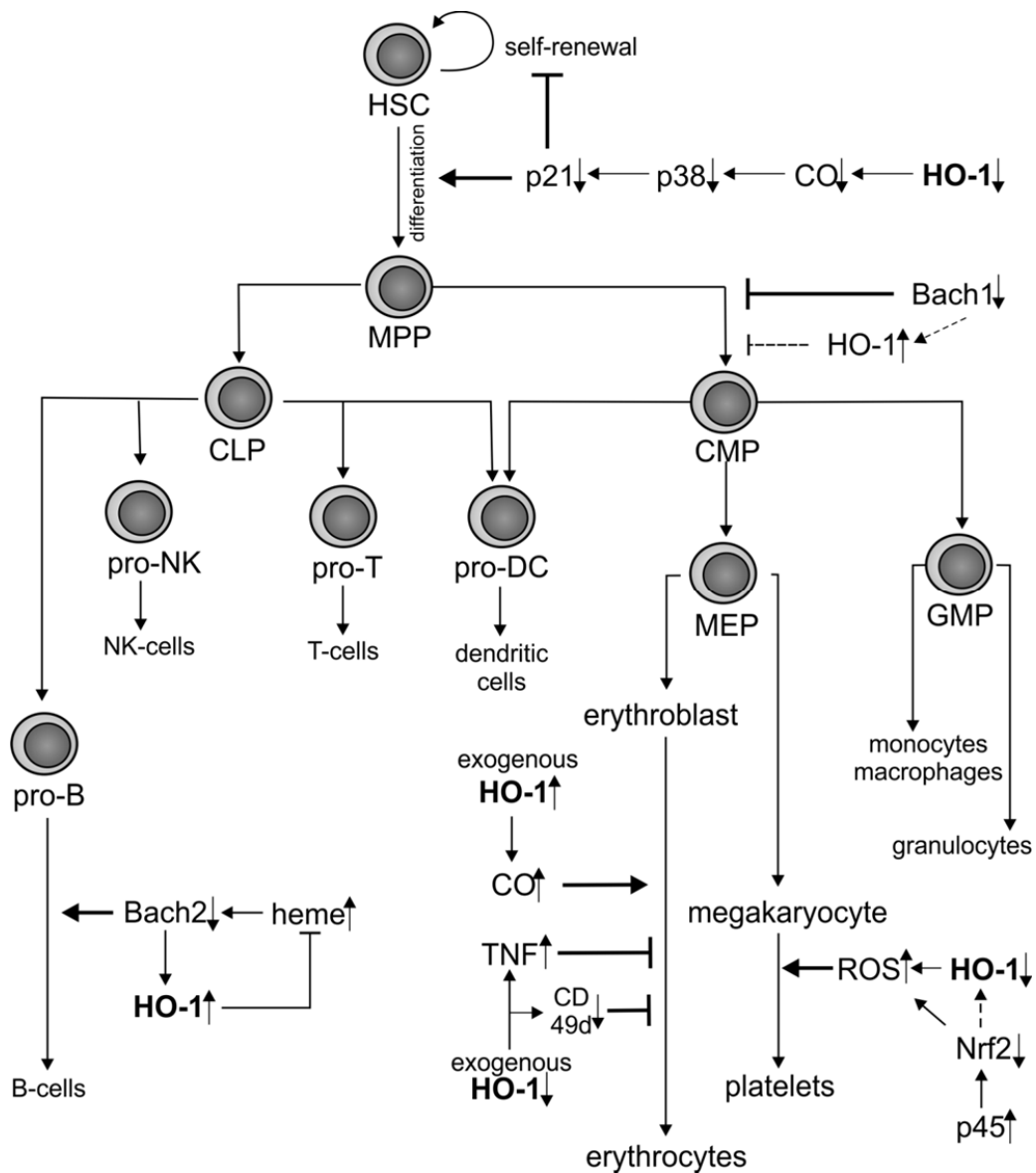
Fig. 1.8 *Role of HO-1 in hematopoiesis. From Kozakowska M, Szade K, Dulak J, Jozkowicz Antioxid Redox Signal. 2014 Apr 10;20(11):1827-50) [182]*

Similarly, decrease in a long-term blood chimerism was observed after bone marrow transplantation from Nrf2$^{-/-}$ mice [202]. Although Nrf2 is one of the main transcription factors driving expression of HO-1, the HO-1 mRNA levels in HSC from Nrf2$^{-/-}$ mice were not altered, suggesting that mechanism of this effect is independent of HO-1 activity [202]. However, the effect of Nrf2 may be similar, as recent study demonstrated that HSC and progenitor cell

compartment was expanded in Nrf2$^{-/-}$ mice at the expense of HSC quiescence and self-renewal [203].

In next stage of hematopoiesis HSC differentiate to multipotent progenitors (MPP) and subsequently to common myeloid progenitors (CMP) or common lymphoid progenitors (CLP) (Fig. 1, described in details in chapter *"Hierarchy of postnatal hematopoiesis"*). The transition to CLP might be affected by HO-1 as indicated by studies done in Bach1$^{-/-}$HO-1$^{-/-}$ mice [204]. Bach1 is transcriptional repressor of HO-1, but oxidative stress abolishes its repressive activity and leads to upregulation of HO-1 [205]. The Bach2, specifically expressed in B-cells, also might regulate HO-1 expression in similar manner [206]. Bach1$^{-/-}$HO-1$^{-/-}$ mice exhibited higher numbers of HSC and MPP fractions in bone marrow, but lower numbers of CMPs and, consequently, CMP-derived progeny, including dendritic cell-restricted progenitors, common dendritic cell progenitors, monocytes, macrophages, and dendritic cells. It suggests that Bach1/HO-1 pathway may be important in committing HSC to CMP [204]. Nevertheless, the discussed event in Bach1$^{-/-}$HO-1$^{-/-}$ mice is, at least to some extent, HO-1-independent, as Bach1$^{-/-}$HO-1$^{+/+}$ mice show similar decrease in macrophage and dendritic cells as Bach1$^{-/-}$HO-1$^{-/-}$ phenotype. Therefore, the exact role of HO-1 in HSC/CMP transition has to be clarified in a model of Bach$^{+/+}$HO-1$^{-/-}$ mice. Other pathways dependent on Bach-1/Nrf2 may play a role [203].

Several reports evidenced the involvement of HO-1 in differentiation of lineage committed progenitors (Fig. 1.8). The first studies regarding its role in maturation of hematopoietic progenitors concerned erythropoiesis [207, 208]. Erythroblasts differentiate in the bone marrow and spleen within the defined niches called erythroblastic islands [209] (reviewed in [210]) These structures were characterized as a central macrophage with many surrounding and interacting erythroid cells at different stages of maturation. Interestingly, the lack of HO-1 expression in erythroblasts is well-described in both K562 erythroid cell line [211] as well as in primary human bone marrow-derived erythroid progenitors [211]. Oppositely, HO-1 is constitutively expressed in macrophages therefore it has been suggested that HO-1 activity in these cells is crucial to regulate erythropoiesis [212]. Indeed, exogenous CO accelerated the differentiation of K562 cells *in vitro* [212]. Moreover, in the *in vivo* model of HO-1$^{+/-}$ bone marrow transplantation the differentiation of erythroblasts was impaired [213]. This effect was mostly visible in the spleen as a prevailing site of erythropoiesis under stress conditions and to lesser extent in the bone marrow. Interestingly, higher percentage of TNFα-expressing

macrophages was found in the spleen of HO-1$^{+/-}$ mice. As TNFα inhibits erythropoiesis, this may explain the erythropoietic defect in HO-1$^{+/-}$ individuals [213]. Furthermore, HO-1 deficient proerythroblasts displayed a decreased surface expression of α-subunit of α4β1 integrin (CD49d) which is crucial for adhesion to central macrophages, what might contribute to alterations of erythropoiesis [213].

HO-1 may also regulate thrombopoiesis (Fig. 1.8) [214, 215]. Treatment of Meg-01 human megakaryoblastic cell line or primary human cord blood-derived megakaryocytes with prostaglandin-J$_2$ (PGJ$_2$) led to the platelet release and concomitantly upregulated HO-1 expression [214]. However, when HO-1 activity was inhibited by SnPP IX (tin protoporphyrin IX) before PGJ$_2$ stimulation, the release of platelets was further increased. Additionally, PGJ$_2$-induced platelet production was accompanied by elevation of oxidative stress. Hence, it is likely that the well-known anti-oxidant properties of HO-1 may inhibit the platelet production [214]. Similar effect may be exerted by Nrf2 which shares DNA binding specificities with NF-E2 p45, an essential regulator of megakaryopoiesis [215]. Accordingly, it has been demonstrated that p45 through competing with Nrf2 promotes increased oxidative status what enhances platelet gene expression and megakaryocytic maturation [215].

Contribution of HO-1 to development of murine lymphoid lineages has been suggested in case of B-cell maturation (Fig. 1.8). Accordingly, HO-1 expression increases with stages of B-cell differentiation, being the lowest in pre-B, moderate in immature-B, higher in mature-B and highest in plasma cells [206]. As proposed, HO-1 regulates intracellular heme levels that affect the humoral immunity in Bach1 and Bach2-dependent mechanism. In turn, Bach1 and Bach2 modulate expression of HO-1 indicating a presence of negative feedback loop [206].

Despite increasing number of studies, many aspects of how HO-1 influences hematopoiesis needs to be further elucidated. Growing body of evidence underlines the crucial role of stromal cells within HSC niche in controlling the HSC self-renewal and quiescence (described in details in chapter *"The bone marrow niche of hematopoietic stem cells"*). It remains unclear if HO-1 modulates HSC potential by regulating the niche components. Moreover, the nuclear form of HO-1 that lacks an enzymatic activity has been recently described [197]. That raises a question if the involvement of HO-1 in hematopoiesis described till now is solely dependent on its enzymatic activity or to some extent also on its not well-characterized non-enzymatic functions.

AIMS OF THE STUDY

The presented study aimed to verify two hypotheses:

1) The non-hematopoietic fraction of Lin⁻Sca-1⁺CD45⁻ adult bone marrow gives rise to blood cells

Rationale:

The role of defined HSC in sustaining blood production through lifetime is well evidenced. However, some recent reports claimed that non-hematopoietic, Lin⁻Sca-1⁺CD45⁻ fraction of bone marrow cells is pluripotent, hierarchically upstream of HSC and possesses potential to differentiate into hematopoietic lineage in postnatal organism. If this hypothesis is true, the Lin⁻Sca-1⁺CD45⁻ population would be the most crucial for maintaining blood production during aging. Nevertheless, the heterogeneity and potential of these cells was not verified in stringent single-cell assays that are required to proof their multipotent hematopoietic potential.

The presented work aimed to characterize bone marrow Lin⁻Sca-1⁺CD45⁻ population and address their hematopoietic potential in stringent single-cell assays.

2) HO-1 protects HSC from premature aging

Rationale:

HO-1 is an important cytoprotective and anti-apoptotic protein that protects mature hematopoietic cells. However its role in steady-state functioning and aging of HSC remains unaddressed. Given the known properties of HO-1, we proposed research strategy intended to verify if HO-1 is a factor that governs protection of HSC from age-related changes

Till now majority of studies concentrate on HSC-intrinsic mechanisms of aging. Despite the data supporting the crucial role of niche as extrinsic regulator of HSC self-renewal and differentiation, the impact of niche on HSC ageing was overlooked (5). Therefore in the presented research strategy, we especially focused on potential role of HO-1 in niche-dependent mechanisms of aging.

MATERIALS AND METHODS

Animal experiments and ethics statement

All animal procedures and experiments were performed in accordance with national and European legislations, after approval by the First Local Ethical Committee on Animal Testing at the Jagiellonian University in Krakow (approval number: 56/2009 and 113/2014). In the study following mice strains were used: mixed background strain C57Bl/6×FVB (HO-1$^{-/-}$ or HO-1$^{+/+}$), as well as C57Bl/6×FVB×C57BL/6-Tg(UBC-GFP)30Scha/J (HO-1$^{-/-}$ or HO-1$^{+/+}$, GFP$^+$), kindly obtained from Dr Anupam Agarwal. C57BL/6-Tg(UBC-GFP)30Scha/J used in the study were bought from Jackson Laboratories.

BM isolation and staining

Bone marrow cells were isolated by cutting the ends of tibias and femurs and flushing the bone marrow cavity with PBS (Lonza) without calcium and magnesium ions and supplemented with 2% fetal bovine serum (FBS) (Lonza). In case of analysis of VSELs the bone marrow was flushed with RPMI medium with 10% FBS.

For analysis of bone marrow niche cells (endothelial cells, CAR cells and other mesenchymal populations) the flushed bones and the previously cut ends of bones were chopped and digested in 0.2% collagenase type I (Gibco) dissolved in αMEM medium with 10% FBS for 1 hour in 37°C in shaker (230 rpm).

The cell suspensions were filtered with 70 µm strainer, depleted of erythrocytes by use of a hypotonic solution, centrifuged (600g, 10 minutes, 4 ºC), resuspended in PBS (Lonza) with 2% FBS, and stained for 20 minutes on ice. When required the fluorescence-minus-one controls were performed.

Antibodies used to analyze cell surface antigens by flow cytometry are summarized in Tab. 2.1. The stained cells were analyzed using LSRII flow cytometer (BD Biosciences) or LSR Fortessa cytometer (BD Biosciences), with FACSDiva (BD Biosciences) and FlowJo (TreeStar) software.

Antibody/dye		Clone	Company
CD34-FITC		RAM34	BD Biosciences
CD-34-Alexa700		RAM34	BD Biosciences
Sca-1-PE-Cy7		D7	BD Biosciences
Sca-1-PE-Cy5		D7	Biolegend
c-Kit-APC-eFluor780		2B8	eBioscience
KDR-FITC		Avas12alpha1	BD Biosciences
KDR-APC		Avas12alpha1	BD Biosciences
CD45-V450		30F-11	BD Biosciences
CD45-FITC		30F-11	BD Biosciences
CD45-APC		30F-11	BD Biosciences
CD45-APC-Cy7		30F-11	BD Biosciences
CD105-PE-Cy7		MJ7/18	Biolegend
CD3-APC		17A2	BD Biosciences
CD11b-V450		M1/70	BD Bioscience
Gr-1-PE-Cy7		RB6-8C5	BD Bioscience
CD150-APC		TC15-12F12.2	Biolegend
CD48-PerCP-Cy5.5		HM-48-1	Biolegend
CD49f-APC		GoH3	Biolegend
CD90.2-APC		30-H12	Biolegend
CD71-FITC		RI7217	Biolegend
CD31-FITC		MEC13.3	BD Bioscience
CD31-PE		MEC13.3	BD Bioscience
Annexin V-FITC		cat.4830-01-K	Trevigen
CD45R-PE	Lineage panel	RA3-6B2	BD Biosciences
Ly6G and Ly6C-PE		RB6-8C5	BD Biosciences
TCRγδ-PE		GL3	BD Biosciences
TCRβ-PE		H57-597	BD Biosciences
CD11b-PE		M1/70	BD Biosciences
Ter119-PE		TER119	BD Biosciences

Tab. 2.1 *Antibodies for cell surface antigens used in flow cytometry analysis.*

Flow cytometric analysis

All the hematopoietic stem and progenitor populations were analyzed in similar manner as shown in Fig. 2.1. If not stated otherwise, the LT-HSC are defined as Lin⁻c-Kit⁺Sca-1⁺CD48-CD150⁺CD34⁻, ST-HSC as Lin⁻c-Kit⁺Sca-1⁺CD48-CD150^{mid}CD34⁺ and MPP as Lin⁻c-Kit⁺Sca-1⁺CD48⁺CD150⁻CD34⁺.

The analysis of the niche populations was done according to gating presented in Fig. 2.1.

Analysis of heterogeneity of Lin⁻Sca-1⁺CD45⁻ fraction with the corresponding gating is presented in the Result section.

Analysis of cell cycle status, γH2aX and HO-1 expression by flow cytometry

The cells were firstly stained for cell surface antigens as described. Then the cells were fixed and permeabilized with by Transcription Factor Buffer Set or IntraSure Kit (both BD Biosciences) according to the manufacture's protocol.

After this step cells were stained with next antibodies. For cell cycle analysis the Ki67-FITC antibody was used together with DAPI or 7-ADD. Gating analysis of cell cycle status is shown in Fig. For the γH2aX staining we used antibody recognizing form that is phosphorylated at serine 139 (Millipore, clone JBW301, dil. 1/500, 45 min. at room temperature) and secondary goat anti-mouse antibody conjugated with Alexa488 dye (Abcam, ab150113, dil. 1/400, 30 min. room at room temperature).

To analyze HO-1 expression in the bone marrow SPA-894 rabbit antibody was used (Enzo Life Sciences, dil. 1/200, 45 min. room at room temperature) followed by staining with goat anti-rabbit antibody conjugated with Alexa 488 or Alexa 594 dye (Abcam, ab150077 and ab150080, dil. 1/400, 30 min. room at room temperature). To all two-steps staining, samples stained with secondary but without primary antibody were used as controls.
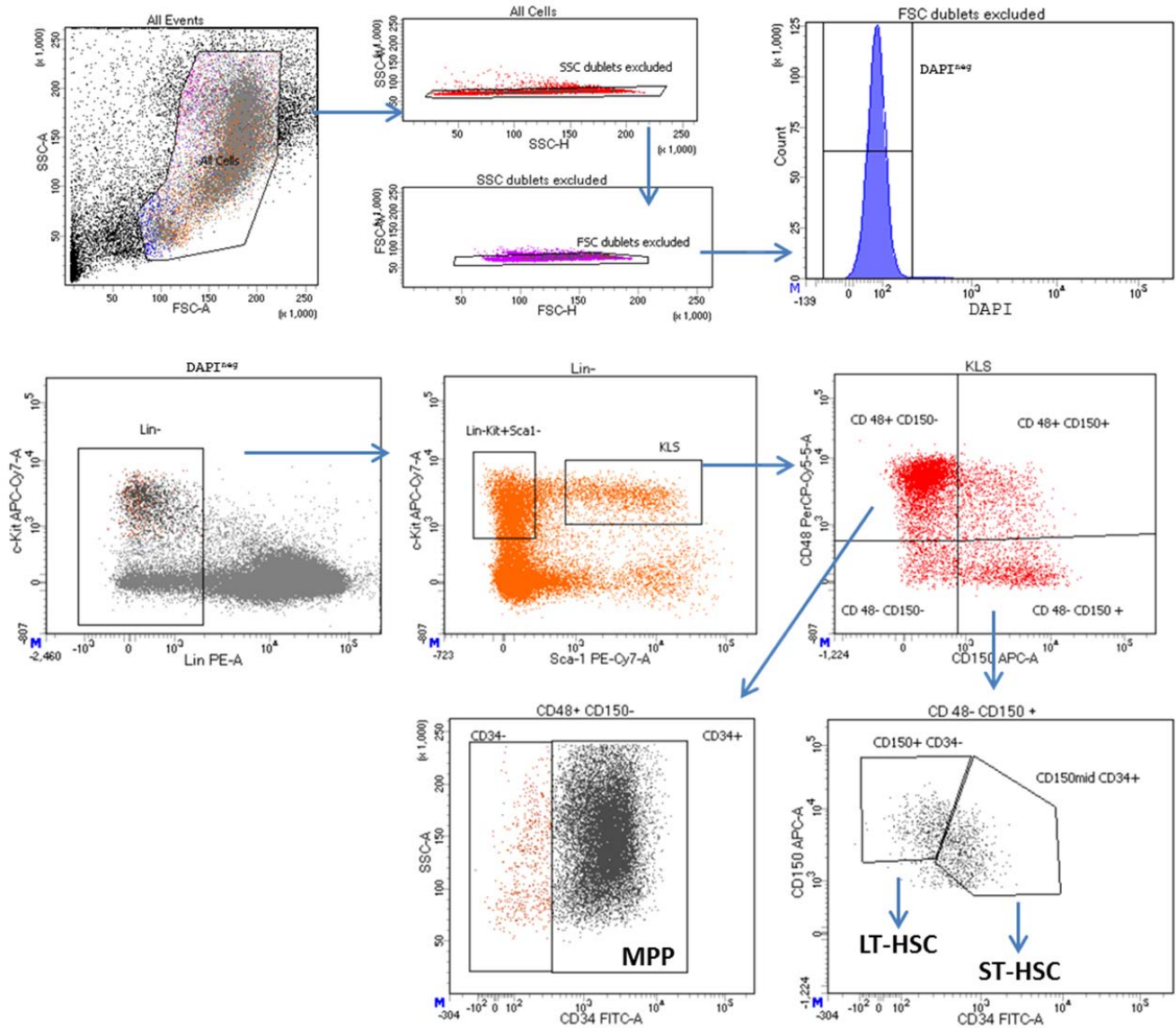
Fig. 2.1 *Gating strategy of hematopoietic stem and progenitor cells.*

Cell sorting

For functional test requiring separation of given population we used MoFlo XDP cell sorter. Cells were stained as described above and gating strategy was the same as on flow cytometry analysis (Fig. 2.1).
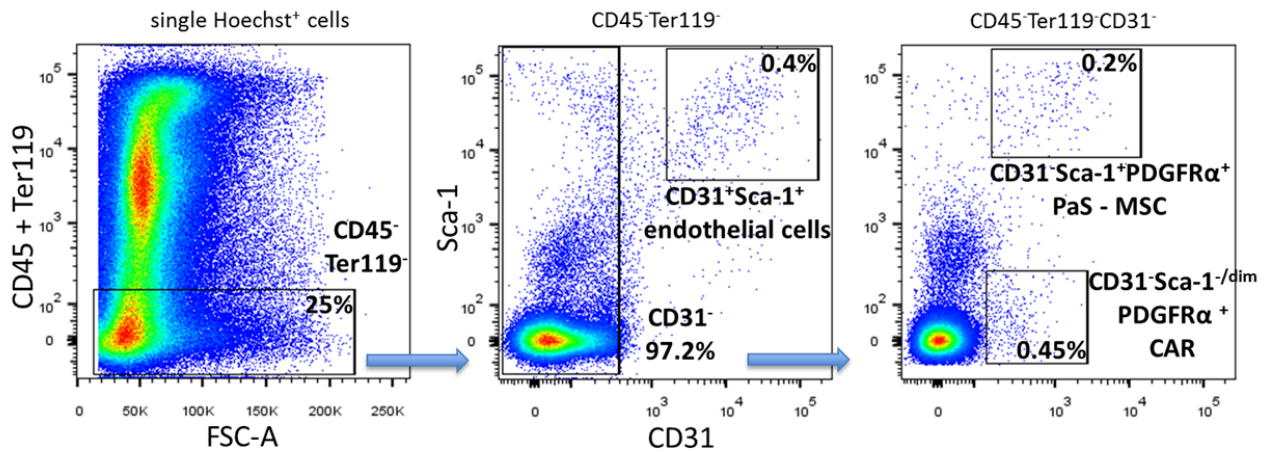
Fig. 2.2 *Gating strategy of cells composing stem cell niche with representative percentage of cells in given gate.*

ImageStream analysis of Lin$^+$Sca-1$^+$CD45$^-$ BM fraction

The bone marrow cells were isolated and labeled as described above, with combination of CD45-FITC, Lin-PE, Sca-1-PE-Cy5, and c-Kit-APC-Cy7 antibodies, and analyzed by ImageStream X system (Amnis) with 40x and 60x objectives, using Inspire and Ideas software (Amnis). The single cells were gated by analyzing Aspect Ratio Intensity vs. Area parameters, calculated on the brightfield channel. The cells that were in focus were selected by analyzing the Gradient RMS parameter calculated on brightfield channel. Further gating strategy was done in a similar way to flow cytometric analyses (Fig. 2.3). The diameter of the cells (Fig. 2.4) was calculated using Ideas 4.0 software, by given formula: $2 \times (Area/\pi)^{0.5}$.

Single cell hematopoietic colony forming *in vitro* assay

BM-derived cells were isolated, stained as described above using combination of CD45-FITC, Lin-PE, Sca-1-PE-Cy5, CD105-PE-Cy7 or c-Kit-APC-Cy7 antibodies, and sorted with MoFlo XPD (Beckman Coulter) cell sorter. Only DAPI-negative cells with integral membrane were chosen, using gating strategy presented in Fig. S3. Cells were sorted to non-adherent round-bottom 96-well plates (Greiner Bio-One), with a single cell per well, into 150 µl of serum-free expansion medium (StemSpan® SFEM, Stem Cell Technologies), supplemented with 20% of BIT 9500 Serum Substitute (Stem Cell Technologies), 0.1% of Ex-Cyte supplement (Millipore),

and cytokine mix: murine stem cell factor (mSCF, Peprotech), human thrombopoietin (hTPO, Peprotech), murine interleukin-3 (mIL-3, Peprotech), and human erythropoietin (hEPO, Sigma-Aldrich), all at the concentration of 20 ng/ml. Cells were cultured for 10 days (37 ºC, 5% CO_2), then wells with colonies were counted, the colonies were harvested, diluted with PBS to final volume of 250 μl, cytospined (1,000 rpm, 10 minutes, room temperature), air-dried, and stained using Wright's method with Hemacolor Kit (Merck).
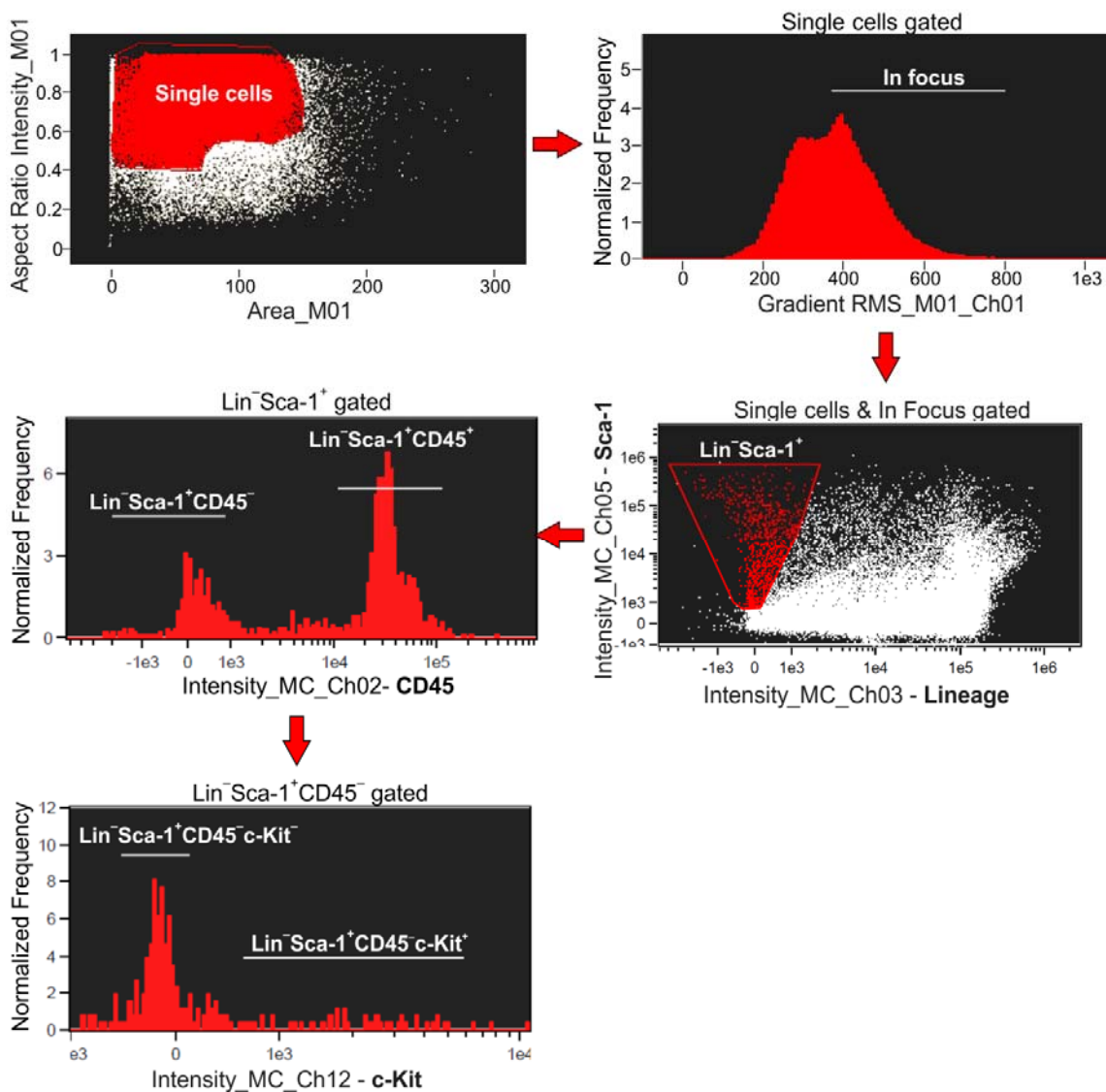
Fig. 2.3 *Gating strategy of of Lin⁺Sca-1⁺CD45⁻ BM fraction using Image Stream fraction.*
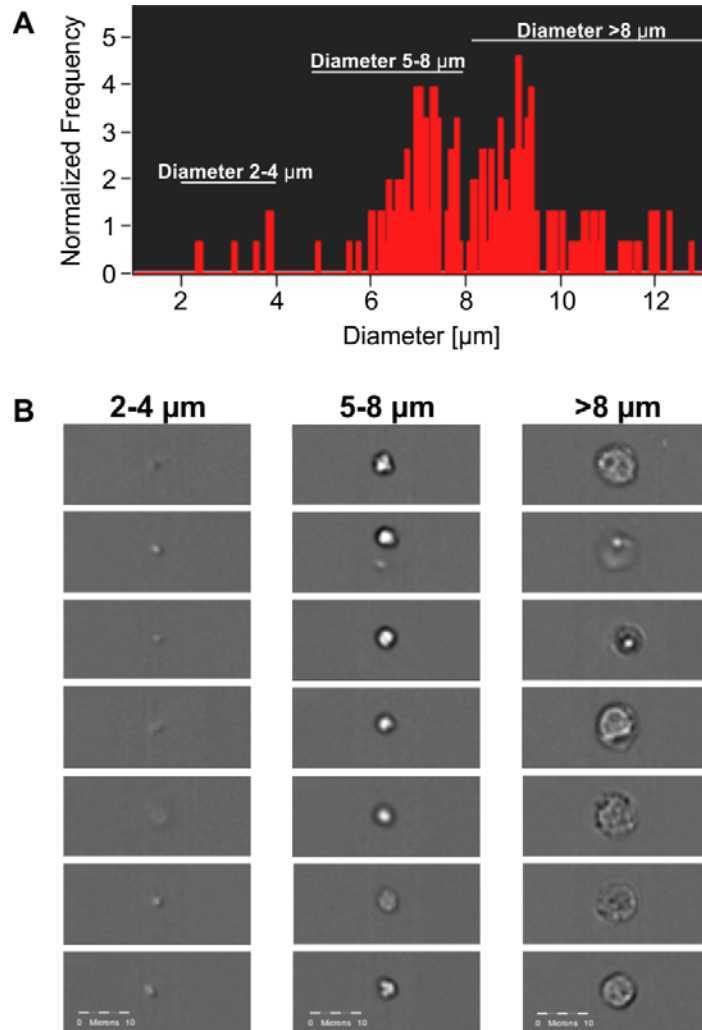
Fig. 2.4 *Analysis of cell diameter with corresponding photos of analyzed events with Image Stream system.*

Hematopoietic differentiation with OP9 co-culture

The OP9 cells were kindly provided by Dr Justyna Drukała. 2,500 OP9 cells per well of 96-well plate were seeded in αMEM medium supplemented with 20% FBS (Lonza), sodium bicarbonate (2.2 g/L, Sigma), β-mercaptoethanol (55 μM), penicillin (100 U/ml, Sigma) and streptomycin (100 μg/ml streptomycin, Sigma). After 3 days, when they reached confluence, medium was changed and Lin⁻CD45⁻Sca-1⁺FSC^low or SKL CD45⁺ populations were directly sorted over the OP9 feeder layer.

First strategy implied sorting Lin$^-$Sca-1$^+$CD45$^-$FSC^{low} or SKL CD45$^+$ cells from the BM of C57BL/6-Tg(UBC-GFP)30Scha/J mice ubiquitously expressing green fluorescent protein (GFP) reporter transgene (1,000 cells per well with confluent OP9 layer). After 4 days of co-culture, medium and trypsinized cells were collected, washed with PBS containing 2% FBS, and the GFP$^+$ cells were sorted on non-adherent round-bottom 96-well plates, with a single cell per well, into 150 µl of serum-free expansion medium, supplemented with 20% of BIT 9500 serum substitute, mSCF, mIL-3, hEPO and hTPO as described above. After 14 days wells with GFP$^+$ colonies were counted.

In the second strategy, we sorted aliquots of 1, 25, 50, 75 and 100 Lin$^-$ Sca-1$^+$CD45$^-$ FSC^{low} or SKL CD45$^+$ cells per well with confluent OP9 layer. After 5 days of co-culture, medium and trypsinized cells from a well were washed, centrifuged, suspended in 150 µl of serum-free expansion medium, supplemented with 20% of BIT 9500 serum substitute, mSCF, mIL-3, hEPO and hTPO as described above and seeded in well on non-adherent round-bottom 96-well plates. After 14 days wells with colonies were counted. Frequency of cells with clonogenic potential within studied population was estimated using the limiting dilution method. Log$_{10}$ of percentage of negative wells in given sorted cell concentration was plotted against sorted cell concentration. Next, by using linear regression and Poisson distribution statistics, the number of cells in a given population consisting of one clonogenic cell was calculated as that corresponding to value of 37% negative wells.

TUNEL assay on sorted cells

Cells were sorted on poli-L-lysine coated slides according to protocol proposed by Ema and co-workers [22]. Chromatin fragmentation was examined with TUNEL assay (FragEL™ DNA Fragmentation Detection Kit, Calbiochem) according to the manufacturer's instruction. The cells were analyzed using Nikon Eclipse Ti (Nikon) fluorescence microscope.

Erythroblast *in-vitro* enucleation

Process of erythroblast enucleation was studied *ex vivo* following the method described by Yoshida and co-workers [216]. Bone marrow cells were isolated and stained using CD45-FITC and Ter119-PE antibodies. The 225,000 of CD45$^-$Ter119$^+$ erythroblasts were sorted per well of 24-well plate by means of MoFlo XPD cell sorter. Part of sorted population was stained

immediately after sort (with Lineage, CD45, Sca-1, c-Kit, CD105 antibodies, and Hoechst; CD45 and Ter119 antigens were labeled with the antibodies used for erythroblasts sorting) and analyzed by flow cytometry (LSR-II). Remaining sorted cells were incubated in αMEM medium (Lonza) with 10% FBS (37 ºC, 5% CO_2). After 1 h, 2.5 h and 6 h cells were collected, stained as described above and analyzed by flow cytometry. Additionally, cells from the whole bone marrow were stained directly after isolation and analyzed in the same way.

RNA isolation, RT-PCR and real–time PCR

Total cellular RNA was purified by phenol/chloroform extraction. Reverse transcription was performed with M-MuLV Reverse Transcriptase (Finnzymes) and oligo(dT) primers (Promega). When indicated, the DNase I treatment of RNA prior to reverse transcription was performed using the RNase-Free DNase Set (Qiagen) for 15 minutes in room temperature, followed by heat-inactivation.

PCR reaction was conducted with Taq polymerase (Promega) using the following conditions: 95°C for 5 minutes, 40 cycles of 95°C for 30 seconds, annealing temperature for 30 seconds, and 72°C for 45 seconds, with final elongation at 72°C for 5 minutes. Following primers were used in the study: Oct-4A Forward – 5'-CCC CAA TGC CGT GAA GTT GGA GAA GGT-3', Oct4B Forward – 5'-ATG AAA GCC CTG CAG AAG GAG CTA GAA CA-3', Oct4A and Oct4B Reverse – 5'-TCT CTA GCC CAA GCT GAT GGC GAT GTG T-3', according to Mizuno and Kosaka [217], EF-2 Forward – 5'-GCG GTC AGC ACA CTG GCA TA-3' Reverse – 5'-GAC ATC ACC AAG GGT GTG CAG-3' acted as endogenous control. Additionally, set of primers designed by Kucia et al. [56] was used: Oct-4 Forward – 5'-ACC TTC AGG AGA TAT GCA AAT CG-3', Oct-4 Reverse – 5'-TTC TCA ATG CTA GTT CGC TTT CTC T-3'. Agarose gel electrophoresis (3% agarose in TAE buffer) of the PCR products was performed according to standard laboratory protocols.

Quantitative real-time PCR (qPCR) with melt curve analysis of the amplified products was carried out using the StepOne Plus cycler (Applied Biosystems) and SYBR® Green JumpStart™ Taq ReadyMix™ (Sigma-Aldrich).

Single cell qPCR or analysis of HO-1 mRNA expression in bone marrow was performed with AmpliSpeed system (Beckman Coulter Biomedical, Germany). The single cells per fields, or 50 cells per field in case of HO-1 analysis in bone marrow, were sorted on AmpliGrid slides

and dried overnight in 4 ºC. Then, a reverse transcription reaction was carried out with NCode™ VILO™ miRNA cDNA Synthesis Kit (Life Technlogies, USA) directly on the slide on AmpliSpeed cycler. The obtained cDNA was used for qPCR reaction.

Next generation sequencing (NGS) and transcriptome analysis

For transcriptome analysis material from 2 mice was pooled and treated as one independent sample to increase amount of starting input. For NGS experiments RNA was isolated with Single Cell RNA Purification Kit (Norgen, Biotek) according to manufacturer's protocol, with the difference, that final elution was done 4 additional times with the same elution buffer (14 μl). Cells were sorted directly to 100 μl of lysing buffer.

After the isolation of RNA, the quality of the isolated material was checked by capillary electrophoresis using Bioanalyzer system and PicoRNA Kit (Agilent). Although, we observed contamination with DNA, the RNA was intact with no signs of degradation (Fig. 2.5A). As the following protocol is not sensitive for DNA contamination and the RNA amounts were very low, we did not treat the samples with DNAse.

To prepare libraries for NGS we applied protocol based on SMARTer technology and followed the protocol explained in details in work by Picelli et al. [218]. In general, the strategy is based on reverse transcription with simultaneous template switching be means of locked nucleic acid (LNA) primers. The LNA primers are complementary to the 2-5 untemplated nucleotides introduced by the Moloney murine leukemia (M-MLV) reverse transcriptase at the end of 3' cDNA transcript. In the next step the obtained cDNA is amplified by PCR. Number of PCR cycles depended on the initial amount of RNA in input material and varied between 16 to 20 cycles. The product was cleaned up by Ampure XP beads (Beckman Coulter) with 1:0.6 (DNA/beads) ratio and checked by capillary electrophoresis using High Sensitivity DNA Chip (Agilent) (Fig. 2.5B). The tagmentation, adapter ligation including indexing and final enrichment PCR was done using Nextera XT Kit using ~200 pg of amplified DNA for tagmentation. The final bead clean up was done using 1:0.6 (DNA/beads) ratio. The quality and concentration analysis of prepared libraries were checked by High Sensitivity DNA Chip (Fig. 2.5C).
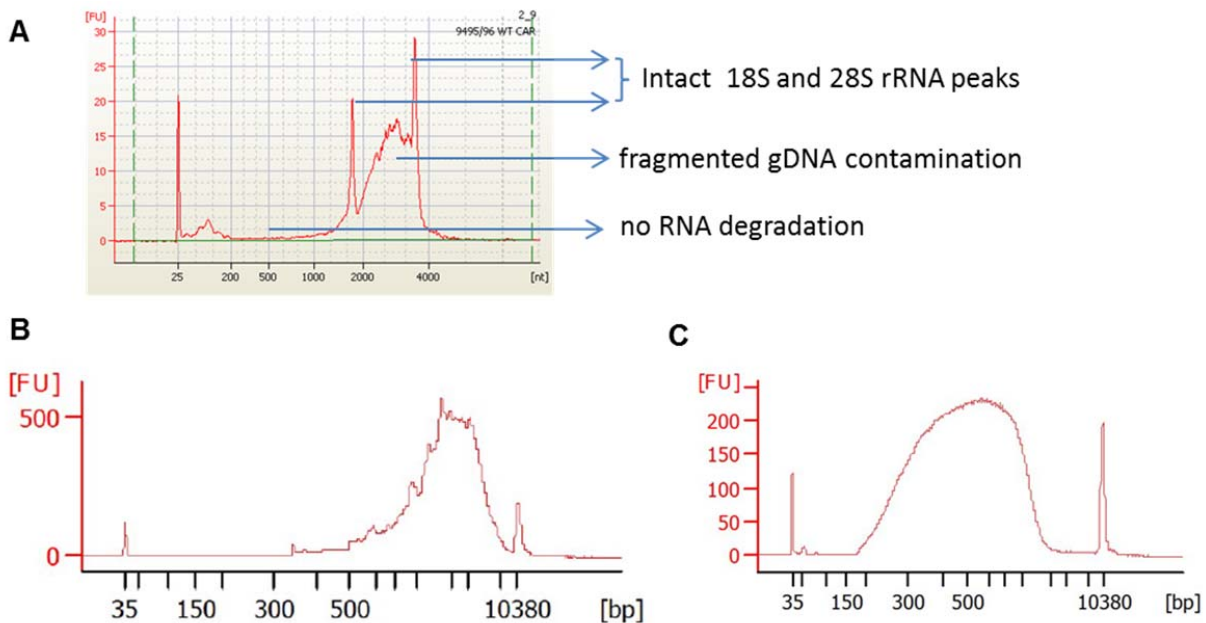
Fig, 2.5 *Preparation of libraries from RNA for NGS. (A) Quality check of isolated RNA showing intact RNA, with some gDNA contamination. (B) cDNA after reverse transcription and PCR preamplification. (C) Final libraries after tagmentation and enrichment PCR.*

The 32 samples were pooled and sequenced on 2 lines of NextSeq500 instrument (Illumina).with 75 bp single-end reads by EMBL Gene Core (Heidelberg, Germany). The average number of reads was ~20 milions/sample. The reads were aligned to mm10 reference mouse genome by BWA mapping software [219] and lead to average ~10 milions of uniquely mapped reads/sample.

The analysis of differential gene expression was performed using DESeq2 method with default settings [220] in R programming environment. The expression results were further used for gene set enrichment analysis (GSEA) and pathway enrichment analysis. The GSEA was done using Reactome database [221] and ReactomePA package (Yu G. ReactomePA: Reactome Pathway Analysis. R package version 1.12.3.). For the pathway enrichment analysis we used Gene Ontology Biological Process [222] database and classical hypergeometric test on first 1000 genes with the lowest p-value using GOStats package [223]. Enrichment analysis based on KEEG database [224] was done using GAGE package [225].

All the R-scripts used to analyze data are in the Supplementary Data attached on separate DVD.

Production of lentiviral vectors and transduction of HSC

LeGO-G2 vectors were used to transduce sorted HSC [226]. Plasmids required for vector production were kindly provided by Dr Boris Fehse. The lentiviral vectors were produced by transfection of HEK293T cells with LeGO-G2 vectors together with psPax2 and PMD2G packaging plasmids using addition of polyethylenimine. After 48 hours supernatant with viral vectors was collected, filtered through 0.8 μm low binding filter (Cornig) and centrifuged 23000g for 3 hours in 4^0C. The supernatant was discarded, pelleted vectors were suspended in ~70 ul of remaining volume, aliquoted and freezed -80^0C. The titer of the vectors was estimated by transduction of known number of HEK293 cells and evaluation of GFP$^+$ transduced cells by flow cytometry.

For HSC transduction, 540 cells were sorted per 96-well plate into 150 μl of serum free medium (StemSpan SFEM, Stem Cell Technologies), supplemented with 20% of BIT 9500 Serum Substitute (Stem Cell Technologies), 100 ng/ml mSCF and hTPO (Peprotech), 5 μg/ml polybrene and lentiviral vectors at 100 MOI, according to the protocol proposed by Mostoslavsky et al. [227]. After 12 hours of transduction all sorted 540 cells were collected, mixed with bone marrow rescue cells and transplanted to one recipient mice.

HSC and bone marrow transplantation

For transplantation of HO-1$^{+/+}$ and HO-1$^{-/-}$ LT-HSC to HO-1$^{+/+}$ mice we used mice that were generated by crossing of HO-1$^{-/-}$ mice on mixed Bl6/FVB background with C57BL/6-Tg(UBC-GFP)30Scha/J strain. The derived littermates were used for transplantation studies. Each mice received 1000 GFP$^+$ LT-HSC defined as Lin$^-$c-Kit$^+$Sca-1$^+$CD48$^-$CD150$^+$ together $2x10^5$ HO-1$^{+/+}$ GFP$^-$ bone marrow competitor cells. After 16 weeks we transplanted $1x10^6$ donor-derived (GFP$^+$) bone marrow cells to secondary recipients.

For transplantation of HO-1$^{+/+}$ LT-HSC to HO-1$^{+/+}$ and HO-1$^{-/-}$ mice we did not have strain matched GFP$^+$ mice. Instead, we transduced the LT-HSC with LeGO-G2 lentiviral vector coding GFP as described above and transplanted 540 cells mixed with $2x10^5$ HO-1$^{+/+}$ GFP$^-$ bone marrow rescue cells to one recipient mice. After 32 weeks we transplanted $6x10^4$ donor-derived (GFP$^+$) bone marrow cells to secondary recipients (summarized on Fig. 3.23).

To verify influence of CO on LT-HSC function we sorted 950 HO-1$^{+/+}$ GFP$^+$ LT-HSC cells (defined as Lin$^-$c-Kit$^+$Sca-1$^+$CD48$^-$CD150$^+$) per well into 150 μl of serum free medium

(StemSpan SFEM, Stem Cell Technologies), supplemented with 20% of BIT 9500 Serum Substitute (Stem Cell Technologies), 100 ng/ml mSCF and hTPO (Peprotech). We kept LT-HSC ex-vivo in this medium for 36 hours in 3% O_2, 5% CO_2, 92% N_2 atmosphere or at the same condition but supplemented with 250 ppm CO. After 36 hours cells were collected and 950 LT-HSC mixed with HO-1$^{+/+}$ GFP$^-$ 2×10^5 rescue bone marrow cells were transplanted into one recipient mice.

Mice were irradiated in University Children's Hospital of Cracow with help of Dr Jacek Kijowski. All recipient mice were myeloablated by whole body irradiation with ^{137}Cs γ source at 110 cGy/min. Mice received total dose of 900 cGy divided in two parts given within 4 hours. The transplanted cells were delivered by tail vein injection 24 hours after last dose.

The peripheral blood chimerism was checked by submandibular bleeding from the mouse cheek and analyzed in B cells, T cells and granulocytes as shown on Fig. 2.6. The chimerism in bone marrow was checked after scarifying recipients at last time-point.
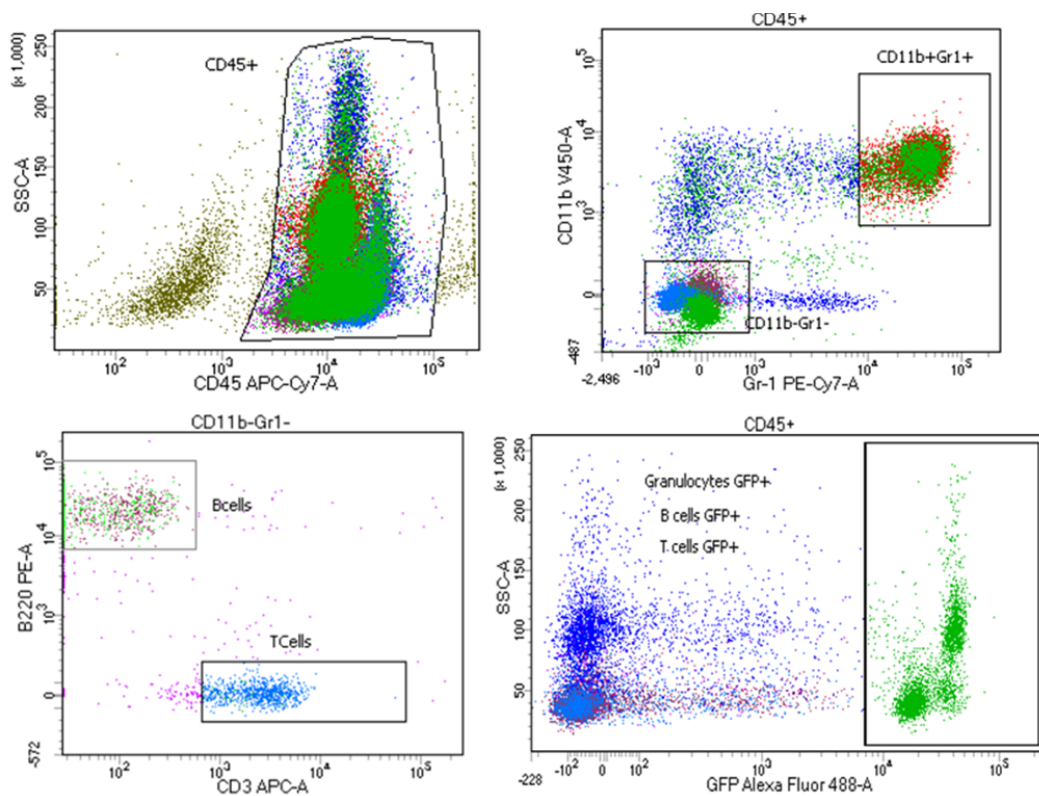
Fig. 2.6 *Analysis of chimerism in peripheral blood after LT-HSC transplantation.*

Immunochemistry of the tibias

Both decalcified and non-decalcified femurs were analyzed. In the decalcification protocol bones were fixed in 4% PFA overnight at room temperature. Bones were washed with PBS for 15 minutes, decalcified in 8% HCl for 2 hours and suspended in 30% sucrose overnight in 4°C.

In the non-decalcification protocol bones were fixed in 4% PFA for 4 hours at at room temperature, washed 10 minutes in PBS, put to 12% sucrose for 10 minutes and then in 25% sucrose overnight at room temperature.

The bones were frozen in Tissue-Tek OCT medium (Sakura) in liquid nitrogen-cooled isopentan and 10 μm thick sections were cut on cryostat (Leica). The sections were post-fixed with 2% PFA for 15 min. To analyze HO-1 expression on the sections SPA-894 rabbit antibody was used (Enzo Life Sciences, dil. 1/200, overnight at room temperature) followed by staining with goat anti-rabbit antibody conjugated with Alexa 488 dye (Abcam, ab150077, dil. 1/400, 30 min. room at room temperature). Sections stained with secondary, but without primary antibody were used as controls. Goat serum was used to block unspecific binding of secondary antibody. Sections were analyzed using Nikon Eclipse Ti (Nikon) fluorescence microscope.

Measurement of CO concentration and heme oxygenase activity in bone marrow

Bone marrow was flushed with 5 ml of PBS within ~5 minutes as described above. The cell suspension was directly centrifuged (600g, 5 min, 4°C), and supernatant were carefully removed. The remaining pellets were frozen in -80°C and CO concentration and heme oxygenase activity was analyzed in a blinded manner by gas chromatography by Dr Luci Muchova (Charles University in Prague). The activity of heme oxygenase was evaluated as CO produced within 20 minutes after adding the reaction substrate NADPH. The obtained results were normalized to protein content in samples.

Measuring ATP concentration in sorted cells

To measure ATP in sorted hematopoietic stem and progenitor cells we applied ATP Bioluminescence Assay Kit HS II (Roche) based on light generation that is proportional to

amounts of ATP in the sample. 1000 cells were sorted to 20 μl of Dilution Buffer and ATP was extracted by adding the same volume of the provided Cell Lysis Buffer. The luciferase substrate was added by automatic injection station of the plate reader (Tecan), and signal was measured 2 seconds after adding the substrate and integrated for 10 seconds. The quantitative analysis of ATP content in the cells was done based on the ATP standard curve.

Statistical analysis

Data are presented as mean ± standard deviation. Unpaired t-test was used to analyze differences when two groups were compared. One-way ANOVA with Bonferroni post-test was applied when more than two groups were compared. When experimental scheme included two variables eg. time and genotype, two-way Anova test was performed. In this case, statistical significance of a given variable was shown only when no significant interaction between variables was detected. Otherwise, only the Bonferroni post-test was performed to analyze of the differences in a given condition are statistical significant. When the data showed non-normal distribution, eg. in case of some transplants, logarithmic normalizations was performed to visualize and analyze data. Significance of proportions was assessed using Fisher exact test. Results were considered as significant when p<0.05. The graphs design and statistical analysis were done using GraphPad Prism 4 and 6 software (GraphPad Software).

RESULTS

PART I – Verification if the non-hematopoietic fraction of Lin⁻Sca-1⁺CD45⁻ from adult bone marrow give rise to blood cells

This part of results was already published in [228]:

Szade et al. Murine Bone Marrow Lin−Sca-1+CD45− Very Small Embryonic-Like (VSEL) Cells Are Heterogeneous Population Lacking Oct-4A Expression. (2013) PLoS ONE 8(5): e63329.

Expression of c-Kit and KDR distinguishes three subpopulations among Lin⁻Sca-1⁺CD45⁻ cells in murine BM

The murine VSELs, claimed to be pluripotent, were originally defined by the Lin⁻Sca-1⁺CD45⁻ phenotype and small size [56]. Here, we investigated if additional markers can be used to select more homogenous population with better stemness characteristics.

Flow cytometry analysis revealed that within the Lin⁻Sca-1⁺CD45⁻ population, the c-Kit and KDR (Flk-1) surface expression can be used to recognize three distinct subsets: c-Kit⁻KDR⁺, c-Kit⁺KDR⁻ and c-Kit⁻KDR⁻ (Fig. 1A). A few c-Kit⁺KDR⁺ events were also detectable, but their number was too low to reliably confirm the presence of a distinct subpopulation. The frequency of total Lin⁻Sca-1⁺CD45⁻ cells in murine BM equaled 0.0316% ± 0.0179% of all nucleated cells (Fig. 1A). Within Lin⁻Sca-1⁺CD45⁻ subsets, the c-Kit⁻KDR⁺ was the rarest subpopulation (0.0039% ± 0.00014%), while c-Kit⁺KDR⁻ and c-Kit⁻KDR⁻ were more frequent (0.0132% ± 0.0094% and 0.0156% ± 0.0106%, respectively) (Fig. 3.1A).

Backgating of each Lin⁻Sca-1⁺CD45⁻ subset showed that c-Kit⁻KDR⁺ cells possessed higher Sca-1 expression comparing to c-Kit⁺KDR⁻ and c-Kit⁻KDR⁻ subpopulations (Fig. 3.1B). Importantly, according to FSC/SSC values, all cells characterized as c-Kit⁻KDR⁺ within Lin⁻Sca-1⁺CD45⁻ population were relatively big (Fig. 1C) and thus, could not be classified as VSELs. In contrast, entire population of c-Kit⁺KDR⁻ cells showed uniform low FSC/SSC values (Fig. 3.1C), whereas c-Kit⁻KDR⁻ cells did not exhibit homogenous FSC/SSC characteristics, being dispersed from very small to relatively big cells. The results indicated that within Lin⁻Sca-1⁺CD45⁻ subpopulation only the c-Kit positive fraction, and part of double negative subset, with its restricted FSC^low SSC^low characteristic, fulfills size criterion of VSEL cells.

Next, the absolute size of the Lin⁻Sca-1⁺CD45⁻c-Kit⁺ was measured using the ImageStream system, as done previously for VSELs [229]. This method allowed gating of cells in similar

64

manner to that presented for flow cytometric analysis (Fig. 2.3). The diameter of unfixed Lin$^-$Sca-1$^+$CD45$^-$c-Kit$^+$ was assessed as 6.8 ± 2.4 µm and was significantly smaller (p<0.001) when compared to the diameter of hematopoietic progenitors (11.4 ± 0.7 µm), defined as Lin$^-$Sca-1$^+$CD45$^+$c-Kit$^+$ (Fig. 1D). The diameter of red blood cells was 6.2 ± 0.6 µm and did not differ significantly from Lin$^-$Sca-1$^+$CD45$^-$c-Kit$^+$ subpopulation (Fig. 3.1D). The size distribution of Lin$^-$Sca-1$^+$CD45$^-$c-Kit$^+$ clustered around the measured mean (44.2% of cells were included within 5-8 µm range), but events with diameter of 2-4 µm or bigger than 8 µm could be also detected (Fig. 2.4). We found that the outliers were enriched in debris as visualized with Image Stream. Moreover, those with diameter between 2-4 µm were too small to confirm reliably their cellular morphology by Image Stream examination (Fig. 2.4).

Additionally, the size of Lin$^-$Sca-1$^+$CD45$^-$c-Kit$^-$ subpopulation was assessed. Consistent with flow cytometry analysis (Fig. 3.1C), bimodal size distribution of this subset could be visualized by Image Stream (Fig. 2.4). Cells with diameter within 5-8 µm range accounted for 41.83%, while cells larger than 8 µm accounted for 52.29% of events, with means of 7.06 µm $\pm$ 0.48 µm and 9.27 µm $\pm$ 1.14 µm, respectively. Events with diameter within 2-4 µm range were hardly detectable (3.27%) (Fig. 2.4).

The cell shrinkage resulting in a lower FSC values is the feature typical for cells undergoing apoptosis [230]. We tested all three Lin$^-$Sca-1$^+$CD45$^-$ subsets for the presence of an apoptotic marker, phosphatidylserine on a cell surface, labeling them with annexin V. The c-Kit$^-$KDR$^+$ and c-Kit$^+$KDR$^-$ subsets hardly presented annexin V binding, while more than half of c-Kit$^-$KDR$^-$ cells were annexin V positive, showing also predominantly lower FSC values (Fig. 3.2).

Adult murine BM and Lin$^-$Sca-1$^+$CD45$^-$ FSC^{low} cells lack expression of Oct-4 mRNA

Expression of Oct-4 was demonstrated as one of molecular hallmarks of pluripotency in VSELs [56]. Given that Lin$^-$Sca-1$^+$CD45$^-$ population is heterogeneous, we wanted to evaluate the level of Oct-4 mRNA expression in each subset.

We used 2 sets of primers proposed by Mizuno and Kosaka [217] to examine Oct-4 expression. One set detects only longer isoform (Oct-4A) and second set detects also shorter (Oct-4B) splicing isoform of murine Oct-4 mRNA. Unexpectedly, qRT-PCR revealed that there is neither Oct-4A nor Oct-4B expression in sorted Lin$^-$Sca-1$^+$CD45$^-$FSC^{low} subpopulation, despite a strong positive signal obtained from ESD3, mouse embryonic stem cell line (Fig. 3.3A). Accordingly, we did not detect Oct-4A and Oct-4B expression in whole murine BM (Fig. 3.3A).
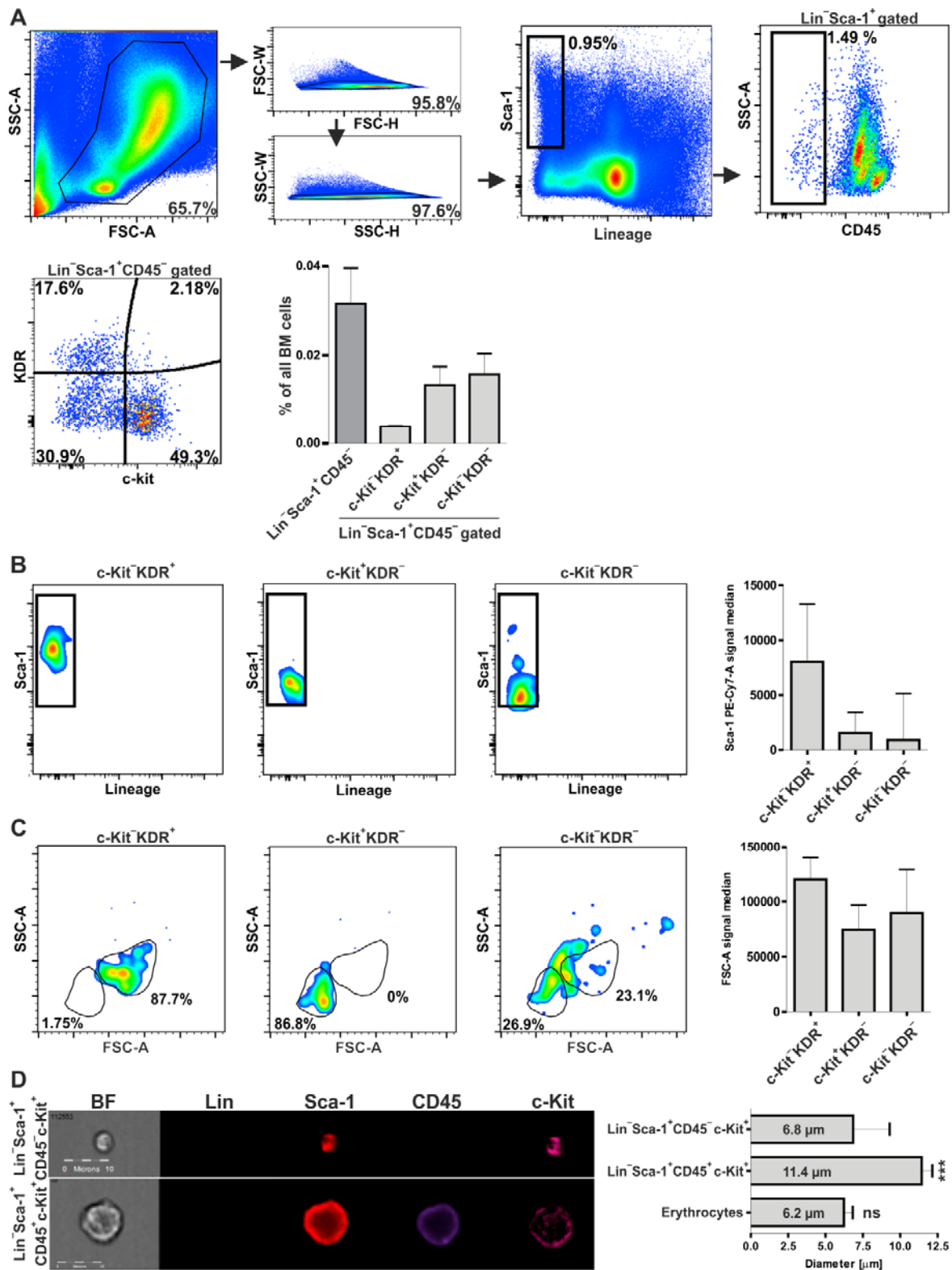
Fig. 3.1 Heterogeneity of BM-derived Lin⁻Sca-1⁺CD45⁻ population. (**A**) c-Kit and KDR distinguished subpopulations within Lin⁻Sca-1⁺CD45⁻ population. (**B**) c-Kit⁻KDR⁺ subpopulation showed higher Sca-1 expression comparing to c-Kit⁺KDR⁻ and c-Kit⁻KDR⁻ subpopulations. (**C**) Backgating of analyzed subpopulation on FSC/SSC dot plot (**D**) Analysis of diameter of non-fixed cells by Image Stream. *** - p<0.001 vs. Lin⁻Sca-1⁺CD45⁻c-Kit⁺.
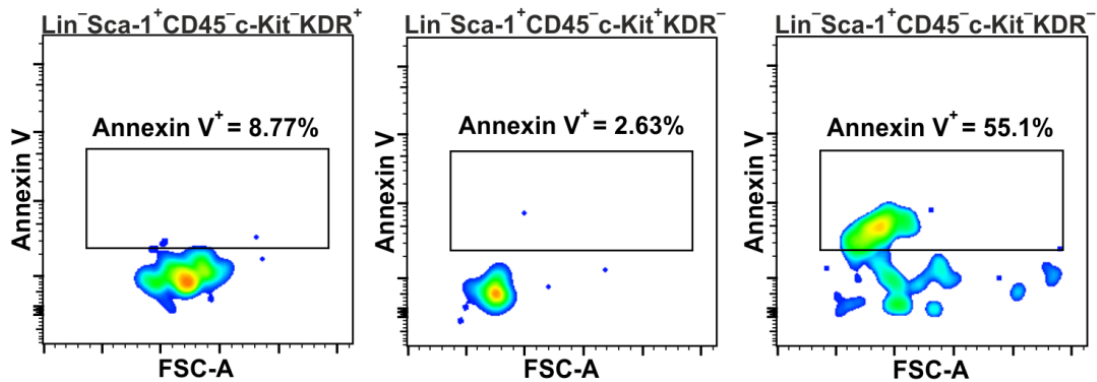
Fig. 3.2 *Binding of annexin V on Lin⁻Sca-1⁺CD45⁻ subpopulations*.

To exclude the possibility that among tested populations there were only few cells that expressed Oct-4A, what could be masked by majority of Oct-4 negative cells, we performed also a single cell RT-PCR analysis of Oct-4A and Oct-4B expression in the Lin⁻Sca-1⁺CD45⁻FSC^low VSELs sorted on the AmpliSpeed grid slides (Fig. 3.3B,C). No specific signal was detected in the no-RT and no-template controls (Fig. 3B). Oct-4A and Oct-4B mRNA was found in 38.1% (16/42) and 52.4% (22/42) of sorted ESD3 cells, respectively, while no positive cells (0/44) were detected in single-sorted Lin⁻Sca-1⁺CD45⁻FSC^low population (Fig. 3.3C).

Because our results were inconsistent with those published by Kucia and colleagues, who had demonstrated the presence of Oct-4 mRNA in BM-derived or liver-derived VSELs [56, 231, 232], we carried out an additional analysis employing primers described in the previous reports [56, 231, 232]. In this case, we were able to detect the product of expected length (70 bp) both in whole BM and in sorted VSEL population (Fig. 3.3D). However the same product was present in samples where no reverse transcription (RT) reaction was performed (Fig 3.3D), indicating a false positive result caused by possible detection of pseudogenes. Indeed, blasting the sequences of primers with mouse genomic DNA (Primer Blast global alignment algorithm [233]) evidenced that while primers proposed by Mizuno and Kosaka [217] did not show any complementarity to genomic Oct-4 pseudogenes, those used in reports by Kucia and colleagues [56, 231, 232] bound to genomic sequence on chromosome 3, which contains Oct-4 pseudogenes [217, 234]. Moreover, they may amplify also the genomic sequence on chromosome 17 corresponding to functional Oct-4 gene. The detected few mismatches are not located within 3' end of the primers and are unlikely to completely prevent amplification of described products on genomic DNA (gDNA). Importantly, the predicted length of product for those primers on Oct-4A cDNA is the same as for products amplified on genomic sequence.

To verify if amplification of genomic sequences may explain the false positive results, we performed the real-time PCR for Oct-4 gene on the gDNA, coupled with melt curve analysis. Melt curves for any of trace products that appeared when using Mizuno and Kosaka primers [217] were considerably different than that from positive control of ESD3-derived cDNA (Fig. 3.4). In contrast, primers applied by Kucia and colleagues [56, 231, 232] led to amplification of products both on gDNA template and in no-RT control, with melt curve highly similar to that from BM cDNA or from positive control (Fig. 3.4). Treatment of total RNA with DNase I prior to reverse transcription clearly affected the amplification of Oct-4 (Fig. 3.4), while did not change the generation of product from control EF-2 gene. This confirms that primers used by Kucia and co-workers [56, 231, 232] can amplify Oct-4 pseudogenes sequences carried over with genomic DNA contamination.
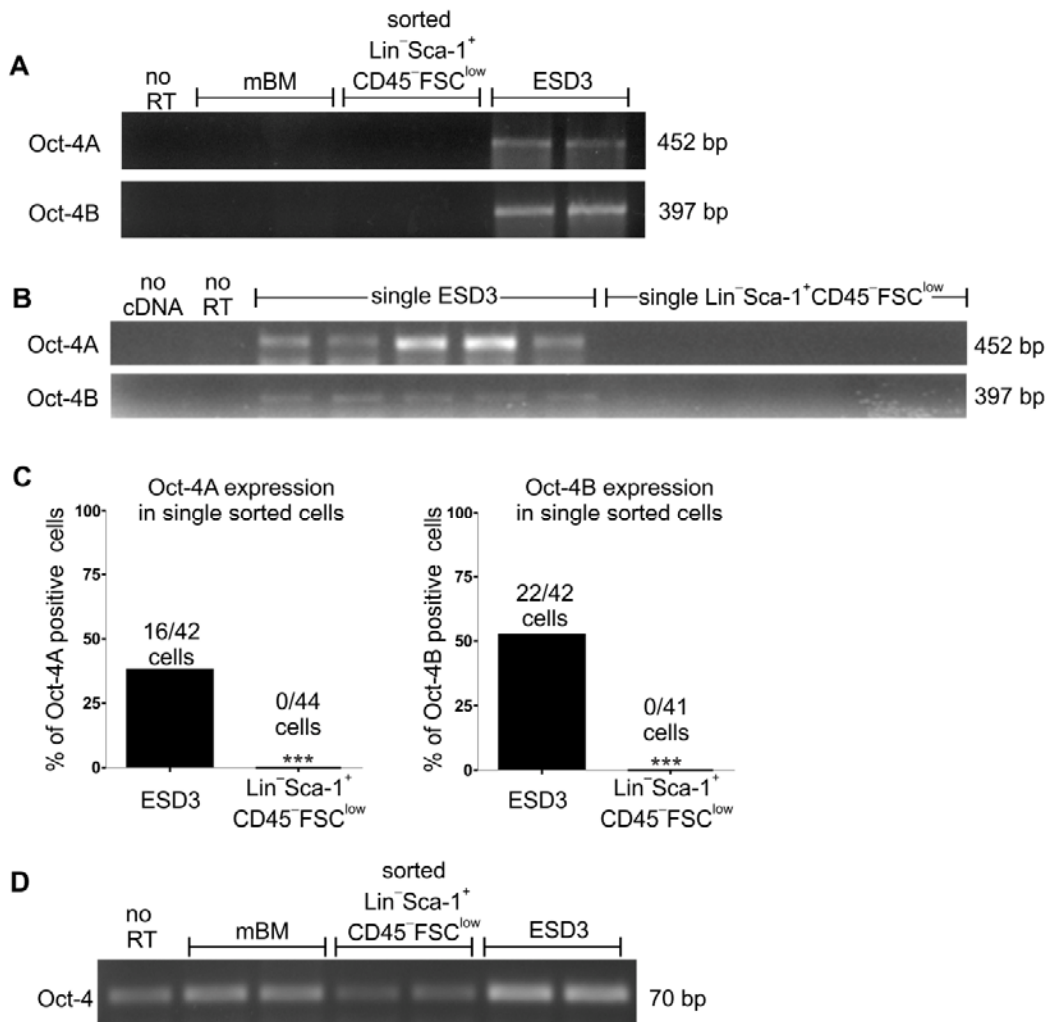
Fig. 3.3 *RT-PCR for Oct-4A and Oct-4B with primers proposed by Mizuno and Kosaka [216] in* **(A)** *bone marrow and sorted Lin$^-$Sca-1$^+$CD45$^-$ FSC^{low}cells and in* **(B,C)** *single sorted cells.* **(D)** *RT-PCR for Oct-4 with primers proposed in earlier studies by Kucia et al. cytacja*
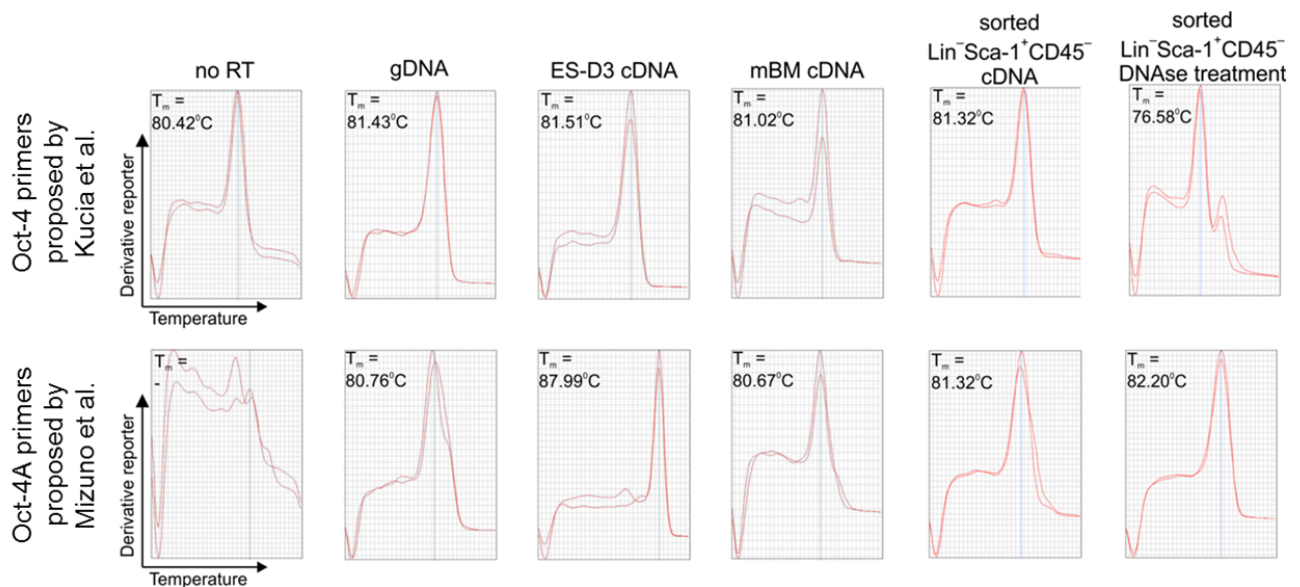
Fig. 3.4 *Analysis of melt curves of products amplified with primers for Oct-4A proposed by Mizuno et al. [217] and for Oct-4 proposed by Kucia et al. [56]. Additionally, part of the material from sorted Lin⁻Sca-1⁺CD45⁻ cells was treated with DNAse to distinguish if potential gDNA contamination affects detection of Oct-4 product when using both set of primers.*

Lin⁻Sca-1⁺CD45⁻ cells do not form single cell-derived hematopoietic colonies *in vitro* assay

Lin⁻Sca-1⁺CD45⁻ cells were reported to give rise to hematopoietic colonies *in vitro* in OP-9 co-culture assay, although hematopoietic potential of freshly isolated VSELs has not been observed [235]. Lin⁻Sca-1⁺CD45⁻c-Kit⁺KDR⁻ subpopulation, being positive for Sca-1 and c-Kit while negative for lineage markers (LKS phenotype – Lin⁻c-Kit⁺Sca-1⁺), overlaps with classically defined hematopoietic stem cells (HSC). Therefore we used a single cell-derived hematopoietic colony test to check whether Lin⁻Sca-1⁺CD45⁻c-Kit⁺FSC^low subset may contain the clonogenic hematopoietic cells. Sorted cells were cultured in a chemically-defined serum-free medium to exclude the possibility of blocking the colony growth by unknown serum factors. The Lin⁻Sca-1⁺CD45⁺c-Kit⁺ population was used in parallel as a positive control. Doublets and DAPI⁺ cells were excluded in sorting strategy.

Colonies were formed in 51.4% (38/74) of wells with single Lin⁻Sca-1⁺CD45⁺c-Kit⁺ cells (Fig. 3.5A). The Wright's staining revealed the presence of progeny derived from different

hematopoietic lineages within a single colony (Fig. 3.5B), proving the multipotency of sorted cell, although the contribution of particular cell lineages varied between the wells. There were also some colonies formed by morphologically homogenous cells, originating possibly from a more differentiated progenitor (Fig. 3.5C). In contrast, none of Lin$^-$Sca-1$^+$CD45$^-$c-Kit$^+$ FSC^{low} (0/76) gave rise to a colony (Fig. 3.5A).
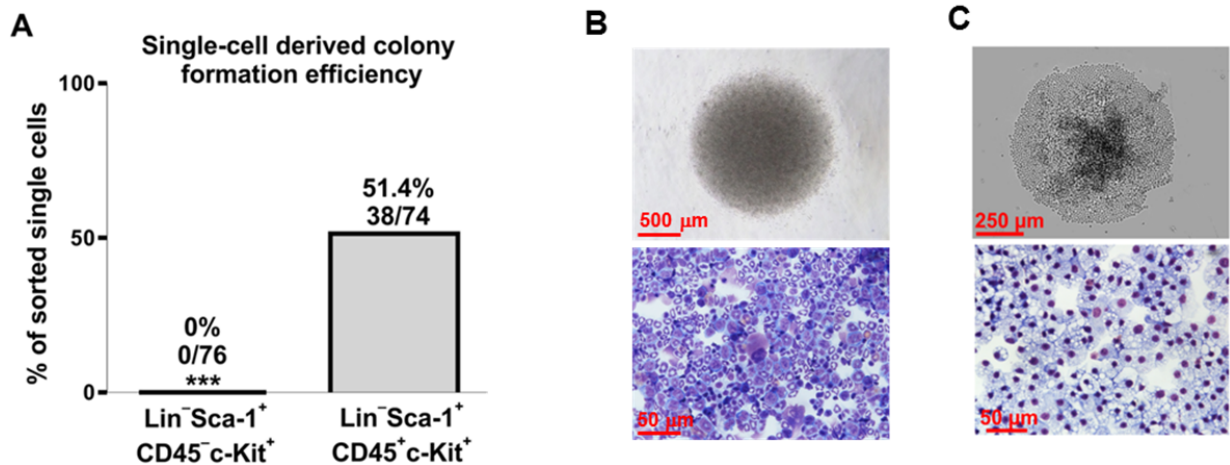
Fig. 3.5 *Verification of hematopoietic potential of Lin$^-$Sca-1$^+$CD45$^-$cKit$^+$ or Lin$^-$Sca-1$^+$CD45$^+$cKit$^+$ (positive control) cells by single cell-derived colony in-vitro assay. (A) Quantitative analysis of colony formation efficacy. (B,C) Examples of a colonies formed by Lin$^-$Sca-1$^+$CD45$^+$cKit$^+$ cells*

Conventional gating strategy for LKS CD34$^-$ cells [8, 22] revealed the presence of minor LKS CD45$^-$CD34$^-$ subpopulation in murine bone marrow (Fig. 3.6A). Moreover, we were able to distinguish population defined as KLS CD45$^-$CD105$^+$ (Fig. 3.6A), thus expressing the CD105 marker, shown to enrich for LT-HSC [12, 236]. Subsequent analyzes revealed that more than 70% of LKS CD45$^-$CD105$^+$ are CD34 negative (Fig. 3.6A) showing that SKL CD45$^-$CD34$^-$ and LKS CD45$^-$CD105$^+$ are highly overlapping. Consistently, both of these subpopulations showed FSC^{low} characteristics. The frequencies of cells defined as LKS CD45$^-$CD34$^-$ or LKS CD45$^-$CD105$^+$ in murine bone marrow measured by the flow cytometry were 0.0079% ± 0.0026% and 0.0057% ± 0.0023%, respectively (Fig. 3.6B), what is similar to the frequency of LT-HSC in mouse bone marrow demonstrated by the bone marrow transplant experiments [237, 238]. LKS CD45$^-$CD105$^+$ subsets substantially overlapped with Lin$^-$Sca-1$^+$CD45$^-$c-Kit$^+$FSC^{low} subpopulation, with more than 70% of Lin$^-$Sca-1$^+$CD45$^-$c-Kit$^+$FSC^{low} being CD105-positive.
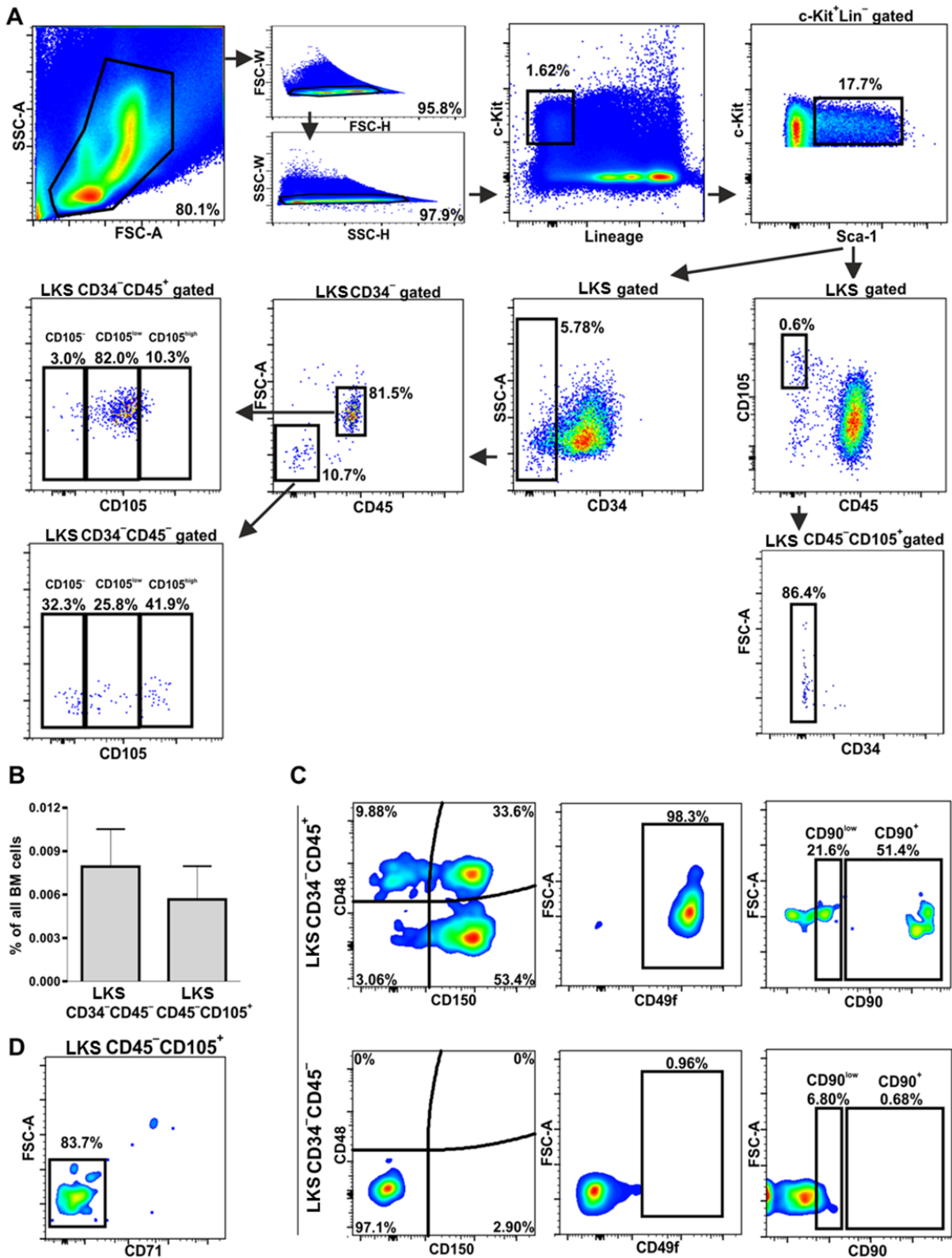
Fig. 3.6 (*A*) *Characterization of CD45⁻ subsets within classically defined LKS 34⁻ hematopoietic stem cells.* (*B*) *Quantitative analysis of SKL CD34⁻CD45⁻ and SKL CD45⁻CD105⁺ cells frequency in murine BM.* (*C,D*) *Evaluation of CD48, CD150, CD49f, CD90, CD71 expression on CD45⁻ fraction.*

Further phenotyping of LKS CD45$^-$CD34$^-$ and LKS CD45$^-$CD105$^+$ cells demonstrated that they do not share all characteristics of LT-HSC. Analysis of the signaling lymphocyte activating molecule (SLAM) markers [7], revealed that the LKS CD45$^-$CD34$^-$ were CD48$^-$CD150$^-$, in contrast to the LKS CD45$^+$CD34$^-$ cells, part of which displayed the CD48$^-$CD150$^+$ phenotype (Fig. 3.6C). Moreover, differently than LKS CD45$^+$CD34$^-$ population, the LKS CD45$^-$CD34$^-$ counterpart did not contain the CD49f-positive or CD90^{hi} cells and showed lower percentage of the CD90^{low} subset (Fig. 3.6C).

CD105 expression is not only a characteristic feature of LT-HSC cells [12, 236], but is also typical for erythroid precursors [239, 240], which additionally have downregulated CD45 level [241]. Therefore, expression of CD71, the erythroid marker [242], was evaluated on LKS CD45$^-$CD105$^+$ cells. As shown in Fig. 3.6D majority of LKS CD45$^-$CD105$^+$ cells did not have CD71, what suggested this population was distinct from CD71-positive early erythroid precursors.

Next we checked whether the Lin$^-$Sca-1$^+$CD45$^-$c-Kit$^+$CD105$^+$ cells display a clonogenic hematopoietic potential. The LKS CD45$^+$CD105^{dim} population was used in parallel as positive control (CD105 is expressed on LKS CD45$^+$ at lower level than on LKS CD45$^-$CD105$^+$, Fig. 3.7A). Again, in a single cell-derived hematopoietic colony *in vitro* assay the colonies were formed in 50% of wells (40/80) with single LKS CD45$^+$CD105^{dim} cells (Fig. 3.7A,B) and all of them contained progeny derived from different hematopoietic lineages (Fig. 3.7B). In contrast, only 1 out of 120 sorted single SKL CD45$^-$CD105$^+$cells (0.83%) gave rise to a colony (Fig. 3.7A). This efficacy did not overcome sorting purity limits, thus we conclude that SKL CD45$^-$CD105$^+$ subpopulation did not show hematopoietic stem cell activity in the performed assay.
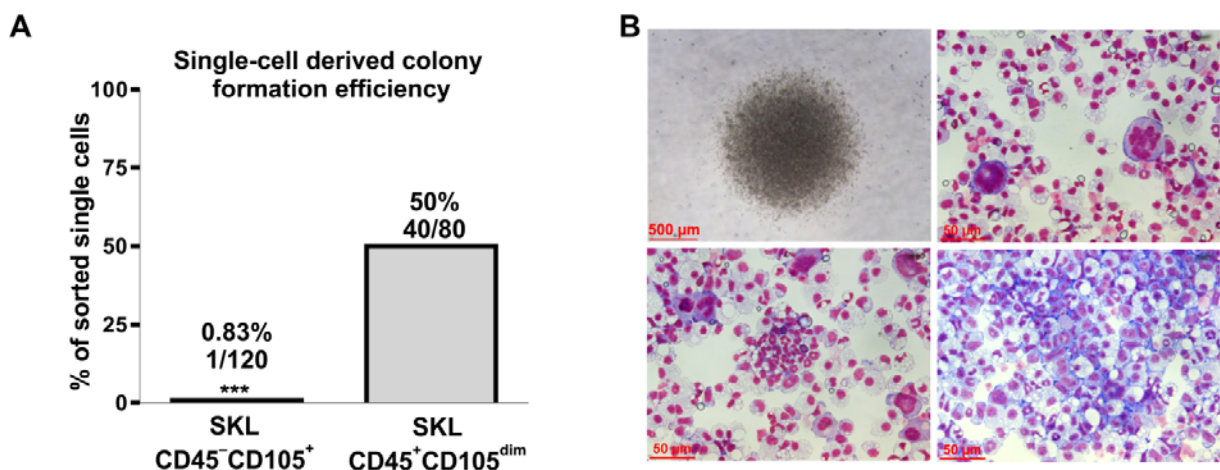
Fig. 3.7 (A) *Quantitative analysis of colony formation efficacy by LKS CD45$^-$CD105$^+$ and LKS CD45$^+$CD105^{dim} (positive control) cells in single cell-derived colony in vitro assay.* **(B)** *Representative colony formed by LKS Sca-1$^+$CD45$^+$CD105^{dim} cells.*

In the last step of analysis we verified if hematopoietic potential of any subpopulations within Lin⁻Sca-1⁺CD45⁻FSCˡᵒʷ fraction could be induced by co-culture with OP9 cells as suggested before [235]. To this aim, 1,000 Lin⁻Sca-1⁺CD45⁻FSCˡᵒʷ or Lin⁻Sca-1⁺CD45⁺c-Kit⁺ cells from BM of GFP⁺ mice were sorted onto well of 96-well plate with confluent OP9 culture. After 4 days of co-culture, the GFP⁺ cells from the co-culture were planned to be sorted for a single cell-derived hematopoietic colony assay as described above. However, Lin⁻Sca-1⁺CD45⁻FSCˡᵒʷ cells expressed GFP at lower levels than Lin⁻Sca-1⁺CD45⁺c-Kit⁺ counterparts during the sort for OP9 co-culture (Fig. 3.8A) and completely lost GFP expression after 4 days of co-culture with OP9 (Fig. 3.8B), what made testing their hematopoietic potential by single-cell method impossible. In contrast, the Lin⁻Sca-1⁺CD45⁺c-Kit⁺ population sustained high GFP expression after co-culture with OP9 (Fig. 3.8A,B), and 35.5% (38 of 107 sorted wells) of single sorted GFP⁺ cells formed hematopoietic colonies (Fig. 3.8C).

The observed decline of GFP expression in Lin⁻Sca-1⁺CD45⁻FSCˡᵒʷ fraction may be caused by death of the cells during co-culture with OP9 feeders or by deactivation of the promoter driving the GFP expression in Lin⁻Sca-1⁺CD45⁻FSCˡᵒʷ population. To exclude the latter possibility, we sorted from 100 to 1 Lin⁻Sca-1⁺CD45⁻FSCˡᵒʷ or Lin⁻Sca-1⁺CD45⁺c-Kit⁺ cells per well of 96-well plate with confluent OP9 culture and after 5 days all cells, including OP9 cells, were transferred to hematopoietic differentiation media. The limiting dilution analysis revealed that approximately 1 per 48 sorted Lin⁻Sca-1⁺CD45⁺c-Kit⁺ cells displayed the colony forming ability (Fig. 3.8D,E) while no colony growth was observed in Lin⁻Sca-1⁺CD45⁻FSCˡᵒʷ group (Fig. 3.8E). This indicates that Lin⁻Sca-1⁺CD45⁻FSCˡᵒʷ population did not possess hematopoietic cells with clonogenic potential even after priming with OP9 cells.

Lin⁻Sca-1⁺CD45⁻c-Kit⁺CD105⁺ population consists of early apoptotic cells

Lack of colony-forming capacities of the LKS CD45⁻CD105⁺ cells prompted us to more detailed investigation of their viability. Backgating has revealed that this population, despite being Annexin-V negative (Fig. 3.9A), was enriched in DAPI⁺ events, when compared with LKS CD45⁺ fraction. Nevertheless, most of these cells (>70%) were DAPI-negative, indicating an intact cell membrane (Fig. 3.9B). Moreover, DAPI⁺ cells were excluded during the single cell sorting and were not taken for hematopoietic assay. Interestingly, all LKS CD45⁻CD105⁺ cells stained highly with Hoechst 33343, with the signal over one order of magnitude higher than that

from LKS CD45$^+$ subset (Fig. 3.9C). This excluded a possibility that the difference resulted from a distinct cell cycle status. Instead, increased permeability for Hoechst may be one of early apoptosis symptoms [243]. Therefore, we sorted 50 cells on the slide glass and analyzed them using TUNEL assay [244] (Fig. 3.9D,E). It turned out that 83.3% of LKS CD45$^-$CD105$^+$ cells showed chromatin fragmentation, while all control LKS CD45$^+$ were TUNEL-negative.

Summing up, LKS CD45$^-$CD105$^+$ cells had intact cell membrane, did not bind annexin V, but showed increased permeability for Hoechst 33342 dye and displayed chromatin fragmentation, which altogether indicates that the population most possibly consisted of early apoptotic cells.
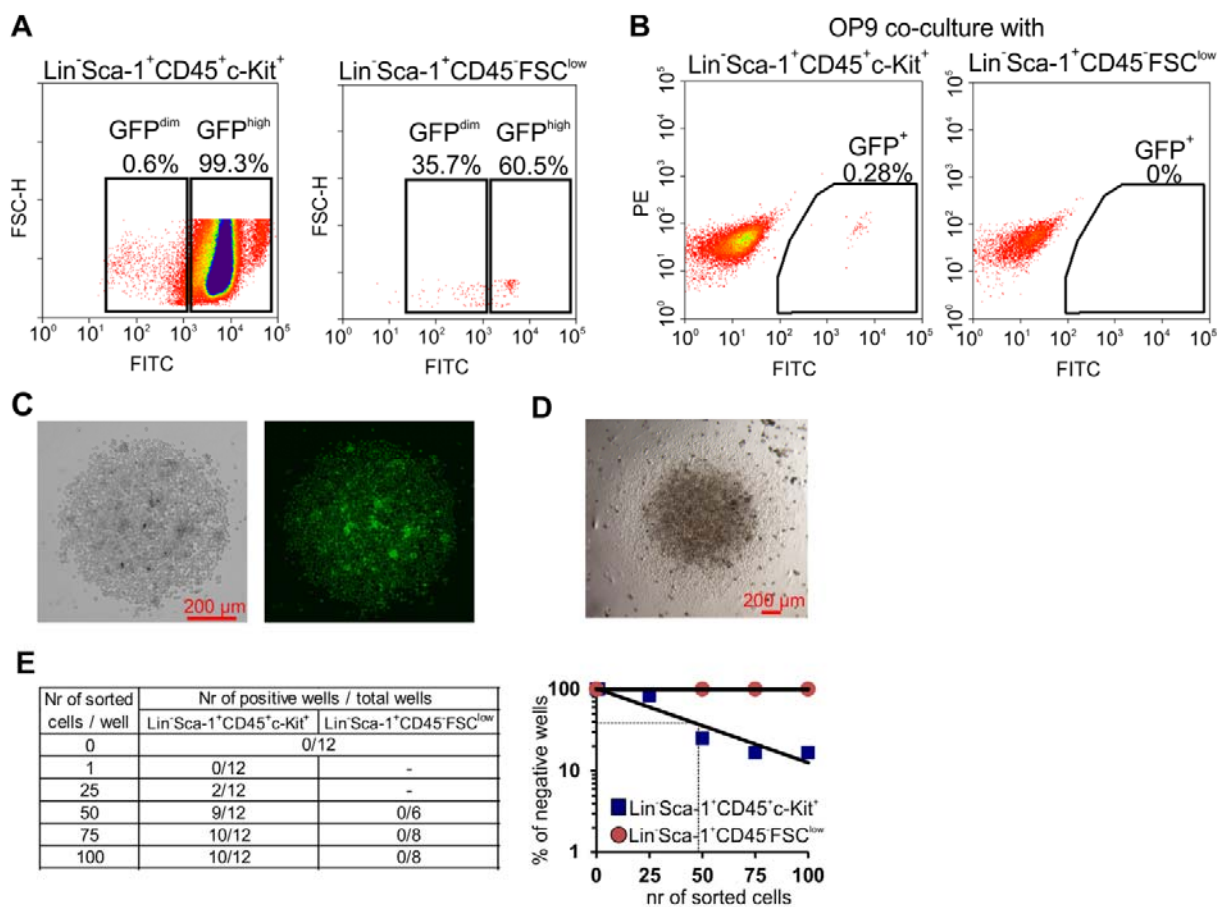
Fig. 3.8 *Hematopoietic differentiation after OP9 co-culture. (A) Expression of GFP among Lin$^-$ Sca-1$^+$ CD45$^-$FSC^{low} and Lin$^-$Sca-1$^+$CD45$^+$c-Kit$^+$ isolated from the BM of C57BL/6-Tg(UBC-GFP)30Scha/J mice (B) GFP expression after 4 days co-culture with OP9 cells. (C) Representative colony formed by single Lin$^-$Sca-1$^+$CD45$^+$c-Kit$^+$cell that was sorted from co-culture with OP9. (D) Representative colony formed by single Lin$^-$Sca-1$^+$CD45$^+$c-Kit$^+$ co-cultred with OP9 after transferring to hematopoietic differentiation media. (E) Limiting dilution analysis of colony forming cells co-cultured with OP9 cells.*
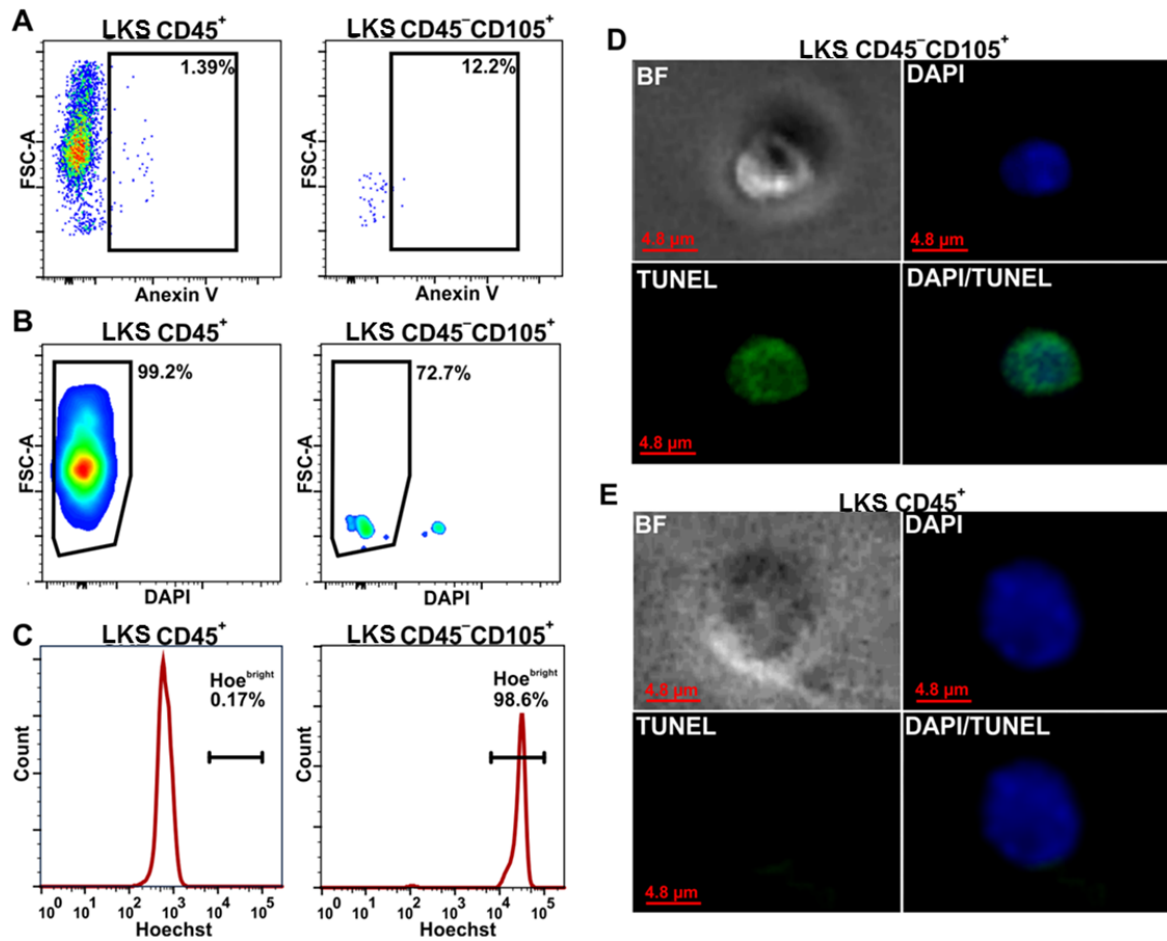
Fig. 3.9 *Viability of SKL CD45⁻CD105⁺ and SKL CD45⁺CD105^dim cells. assessed by (**A**) annexin V on cell surface,. (**B**) DAPI and (**C**) Hoechst 33342 staining. (**D,E**) TUNEL analysis of sorted subset revealed chromatin fragmentation in LKS CD45⁻CD105⁺ cells, but not in LKS CD45⁺ population.*

LKS CD45⁻CD105⁺ events in mouse BM may origin from nuclei expelled from erythroblasts

Given that Lin⁻Sca-1⁺CD45⁻c-Kit⁺CD105⁺ events seemed to be early apoptotic cells, we aimed to determine the possible ancestor population that they can derive from.

Features such as small size, high staining with nuclear dye and integral membrane resembles characteristics of nuclei expelled from erythroblasts during erythropoiesis (so called pyrenocytes) [216, 245]. Yet, there are no data indicating if the expelled nuclei could share LKS CD45⁻CD105⁺ marker profile. To verify if the origin of BM Lin⁻Sca-1⁺CD45⁻c-Kit⁺CD105⁺ cells can be associated with enucleation process, we sorted Ter119⁺CD45⁻ erythroblasts from a

bone marrow and incubated them *ex vivo* for 6 hours in 37°C to induce the enucleation process [216]. During time of incubation the kinetic of formation of small LKS CD45$^-$CD105$^+$ events, highly stained with Hoechst 33342, was evaluated (Fig. 3.10A).

All gates were set in the same manner as for the LKS CD45$^-$CD105$^+$ cells in whole bone marrow samples (Fig. 3.6, Fig. 3.10A). Immediately after erythroblast sorting the LKS CD45$^-$CD105$^+$ events were barely detectable. However, their number significantly increased with the incubation time (Fig. 3.10A). These data suggest that nuclei expelled from the erythroblasts can transiently present LKS CD45$^-$CD105$^+$ phenotype. Accordingly, we observed similar increase in a number of events defined as classic VSELs (Lin$^-$Sca-1$^+$CD45$^-$FSC^{low}) (Fig. 3.10B). Thus, it is likely that LKS CD45$^-$CD105$^+$ and Lin$^-$Sca-1$^+$CD45$^-$FSC^{low} populations isolated from the bone marrow can include the nuclei released during erythropoiesis.
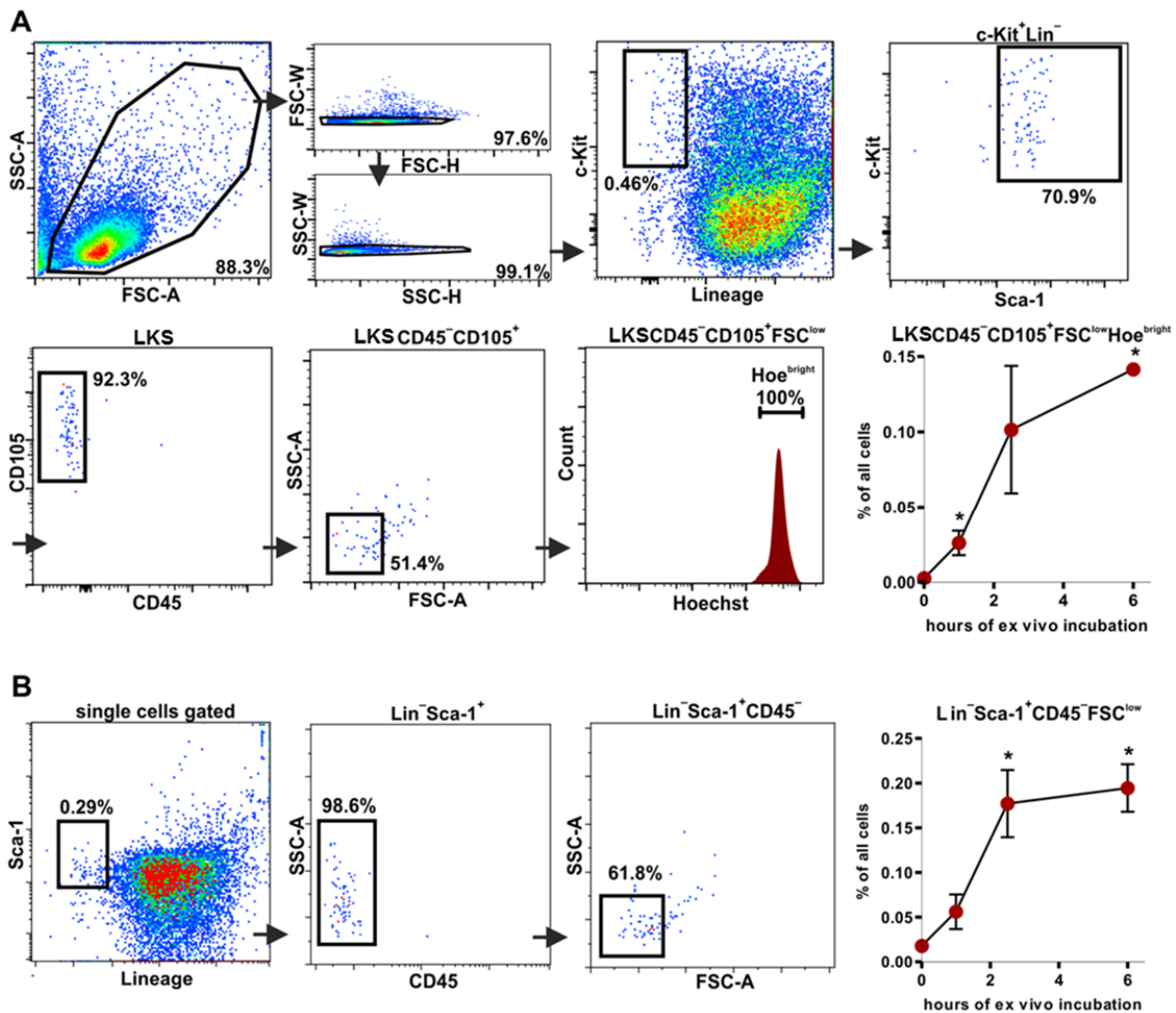
Fig. 3.10 *Phenotype of nuclei expelled from ex vivo cultured erythroblasts. (A,B) Gating strategy and analysis of number of events from tested populations during ex vivo enucleation process. .* - p<0.05 vs. t = 0 h.*

PART II – Verification if HO-1 protects HSC from premature aging

HO-1 deficiency disturbs blood cell counts

In the first step we checked how lack of HO-1 affects the complete blood cell count in young (3-month old) mice. We observed elevated white blood cell counts (WBC) in HO-1$^{-/-}$ mice. HO-1-deficiency caused global myeloid shift in blood composition: granulocytes and monocytes were more frequent while the lymphoid fraction was decreased (Fig. 3.11).

Other affected parameters regarded red blood cells (RBC). While total number of red blood cells was only slightly and not significantly decreased, the mean RBC hemoglobin (MCH) as well as mean RBC volume (MCV) were significantly lower in HO-1$^{-/-}$ mice (Fig 3.11). The affected RBC biology in HO-1$^{-/-}$ mice was also reflected by higher RBC width distribution (Fig. 3.11). Other blood cell counts were not affected (Fig 3.11).

Summing up, the HO-1 deficiency affected main blood cell parameters.

	HO-1$^{+/+}$ Mean ± SD	HO-1$^{-/-}$ Mean ± SD	p-value
HCT	51.5 ± 6.0	58.0 ± 7.1	0.18
HGB	14.8 ± 1.5	16.2 ± 1.9	0.26
MCHC	28.9 ± 0.9	27.9 ± 0.5	0.08
MPV	6.9 ± 0.5	3.0 ± 4.8	0.15
PLT	1027.8 ± 172.4	665.8 ± 549.3	0.25
RBC	11.9 ± 1.4	10.3 ± 1.2	0.10
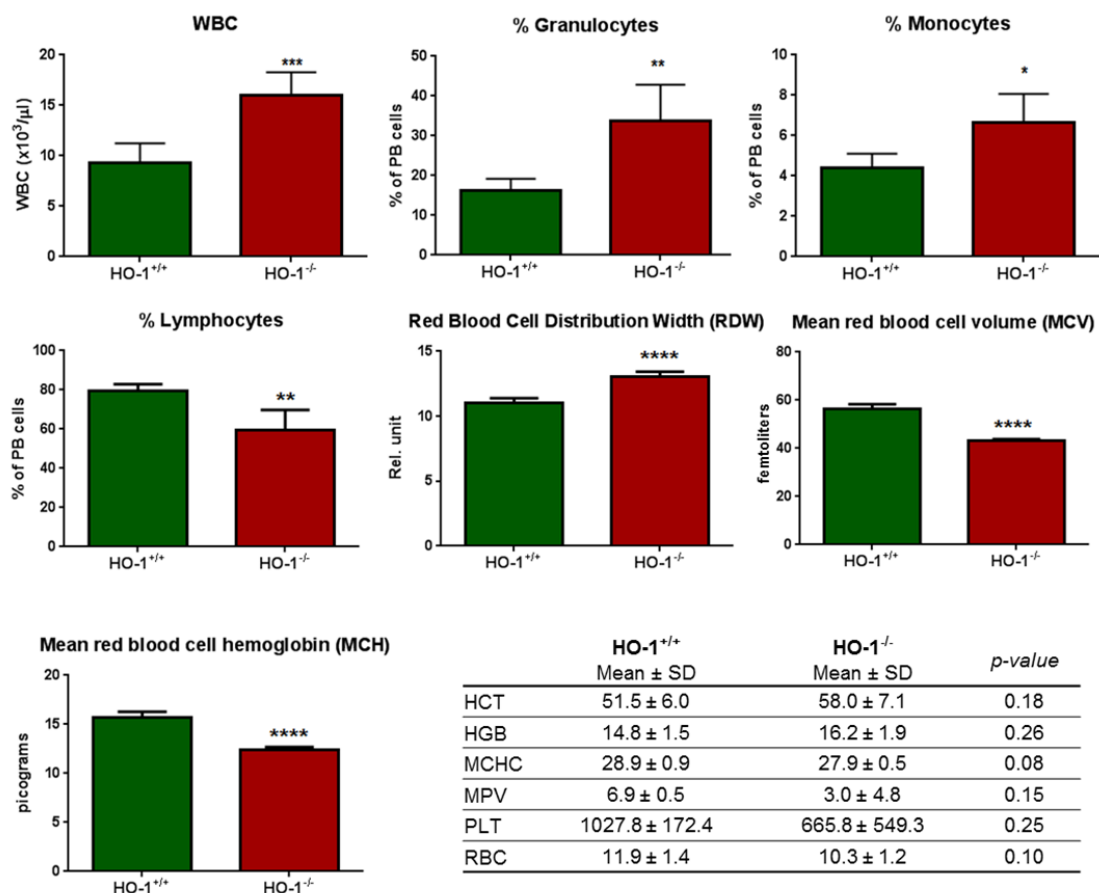
Fig. 3.11 *Complete blood cell counts in young (3 month -old) HO-1$^{-/-}$ mice. n = 6/group*

The pool of hematopoietic stem and progenitor cells is expanded in HO-1$^{-/-}$ mice

The myeloid shift (Fig 3.11) that characterized HO-1$^{-/-}$ mice is one of the main age-acquired declines of hematopoietic system originating already from HSC (see section *"Aging of HSC"* in *"Introduction"* chapter). Therefore, we checked if the HO-1 deficiency affects HSC pool, both in young (3-month old) and old mice (12-month old).

We observed increased frequency of long-term HSC (LT-HSC), short-term HSC (ST-HSC) and multipotent progenitors (MPP) in HO-1$^{-/-}$ mice in young mice (Fig 3.12). The total cellularity of bone marrow was not changed, thus the total numbers of hematopoietic stem and progenitor cells were also higher in HO-1$^{-/-}$ mice (Fig 3. 12).

The hematopoietic stem and progenitor cells were expanded in 12-month old animals (5.7 and 4.3 fold change of total number of HSC vs. young animals in HO-1$^{+/+}$ and HO-1$^{-/-}$ mice, respectively), but no changes between the genotypes were observed.

HSC from HO-1$^{-/-}$ mice lost quiescence

The LT-HSC cells were shown to be mainly in quiescent G0 cell cycle phase and do not actively proliferate (see section *"Different function of HSC and MPP: quiescence versus proliferation"* in *"Introduction"* chapter). Indeed, we observed that most young HO-1$^{+/+}$ LT-HSC exited cell cycle as only 11,5 ± 12.6 % of cells were in active G1 cell cycle phase and only 3.3 ± 2.9% proliferated (counted as cells in S/G2/M cell cycle phases) (Fig. 3.13). In contrast, significantly more young HO-1$^{-/-}$ LT-HSC were in G1 cell cycle (24.2 ± 10.7 %) and proliferated (9.1 ± 4.0 %) (Fig. 3.13). Oppositely to dormant LT-HSC, there were no changes between genotypes among MPP population (Fig. 3.13).

We checked also the cell cycle status in older (6-12 month old mice) LT-HSC and MPP. Still more LT-HSC from older HO-1$^{-/-}$ mice were in G1 cell cycle phase, but there was no differences in percentage of proliferating cells (Fig. 3.13). Similar to young mice, there were no differences in cell cycle status among MPP between genotype (Fig. 3.13).

Concluding, young HO-1$^{-/-}$ LT-HSC were in more activated and proliferative state, but during aging stopped the extensive proliferation. The observed alterations of cell cycle were unique to LT-HSC and were not observed in MPP.
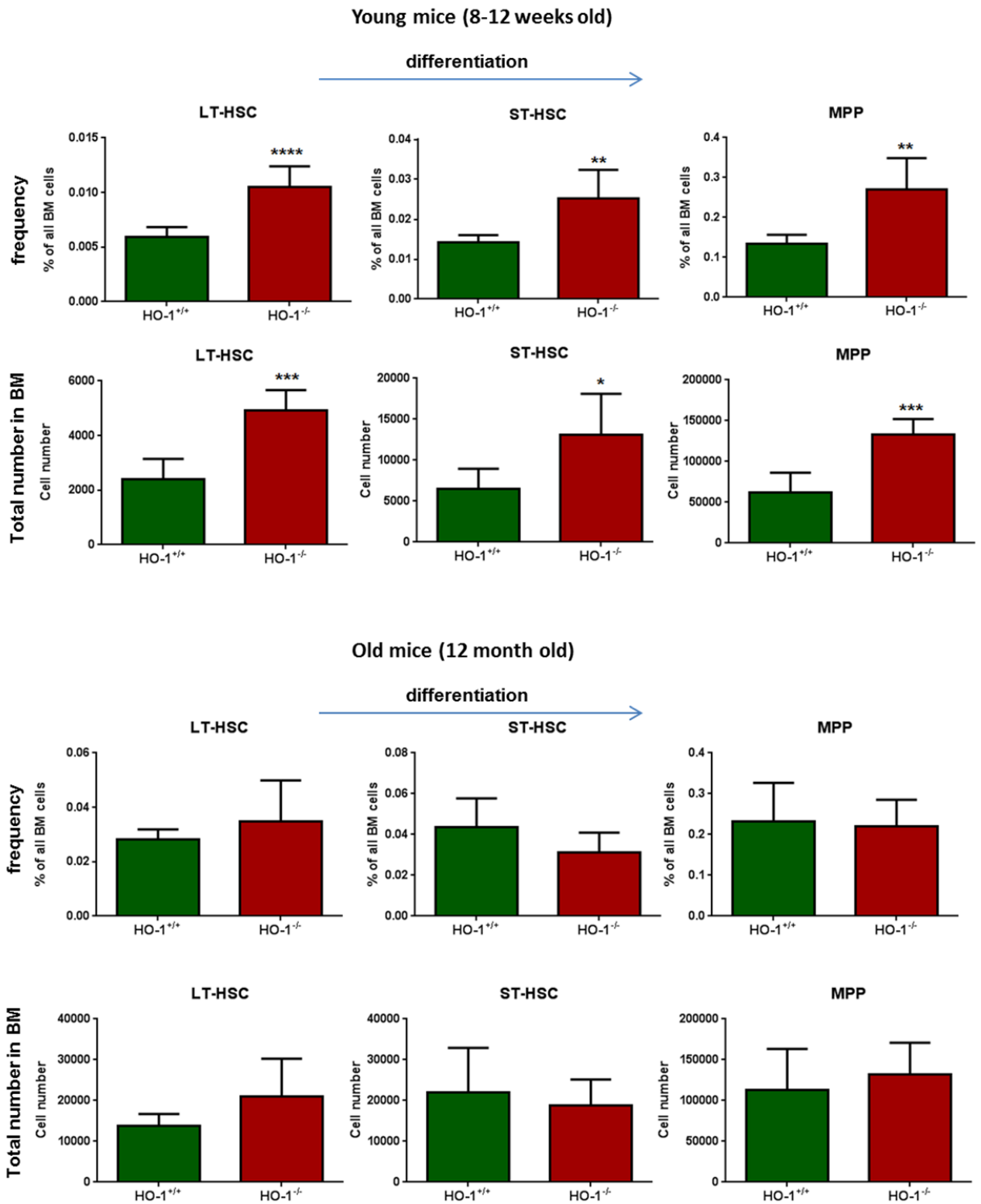
Fig. 3.12 *Frequency and total numbers of hematopoietic stem and progenitor cells in HO-1$^{-/-}$ mice. n = 4-8 group, shown 1-2 independent, representative experiments from several performed with similar results.*
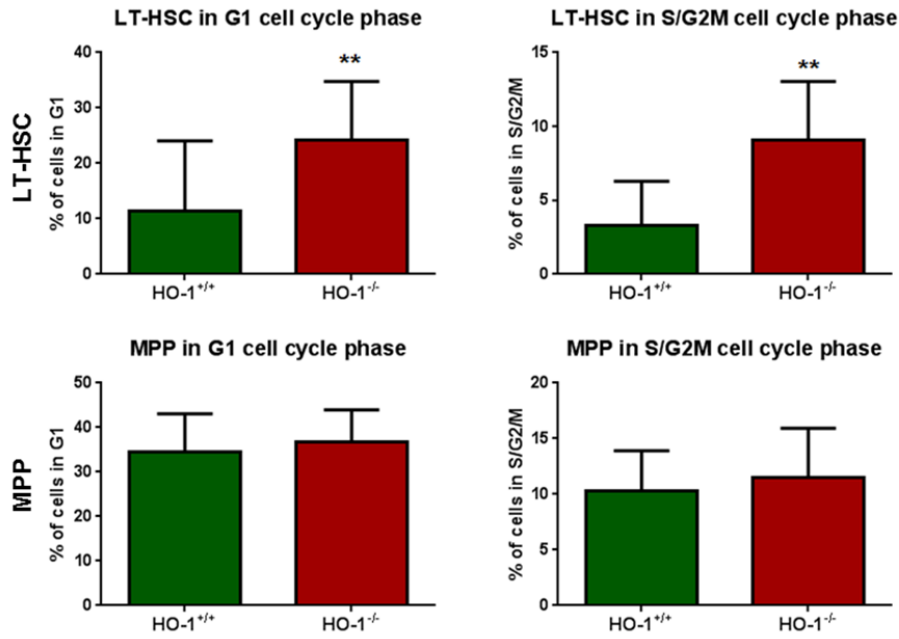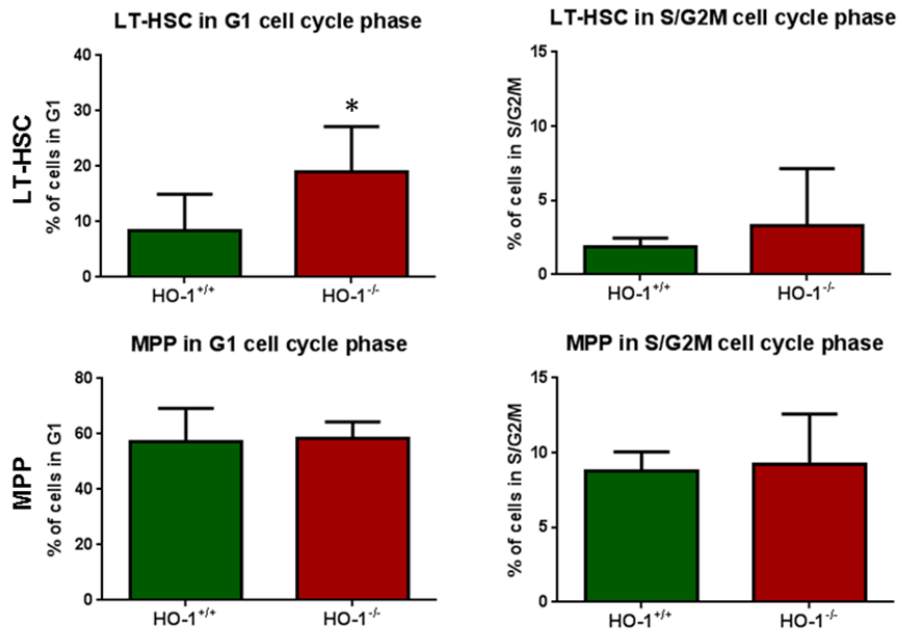
Fig. 3.13 *Cell cycle status of young and old LT-HSC and MPP isolated from HO-1$^{+/+}$ and HO-1$^{-/-}$ mice. LT-HSC defined as LKS CD150^{+}CD34^{-}, MPP as LKS CD150^{-}CD34^{+}. n = 8 – 17 group, results from 2-3 independent experiments.*

HO-1 deficiency is linked with DNA damage in LT-HSC and MPP

It is known that LT-HSC acquire DNA damage during aging [82]. Given that we observed aging features (myeloid bias and expansion of stem cell pool) already in young HO-1$^{-/-}$ mice, we evaluated DNA damage in young HO-1$^{+/+}$ and HO-1$^{-/-}$ hematopoietic stem and progenitor cells as next marker of LT-HSC aging. To estimate DNA damage we checked presence of γH2aX phosphorylated at serine 139 (pS139), which is involved in repair of double DNA breaks [246].

We observed more LT-HSC and MPP with high expression of pS139-γH2aX in HO-1$^{-/-}$ mice, indicating that the young HO-1-deficient LT-HSC and MPP possess more DNA damage (Fig. 3.14).
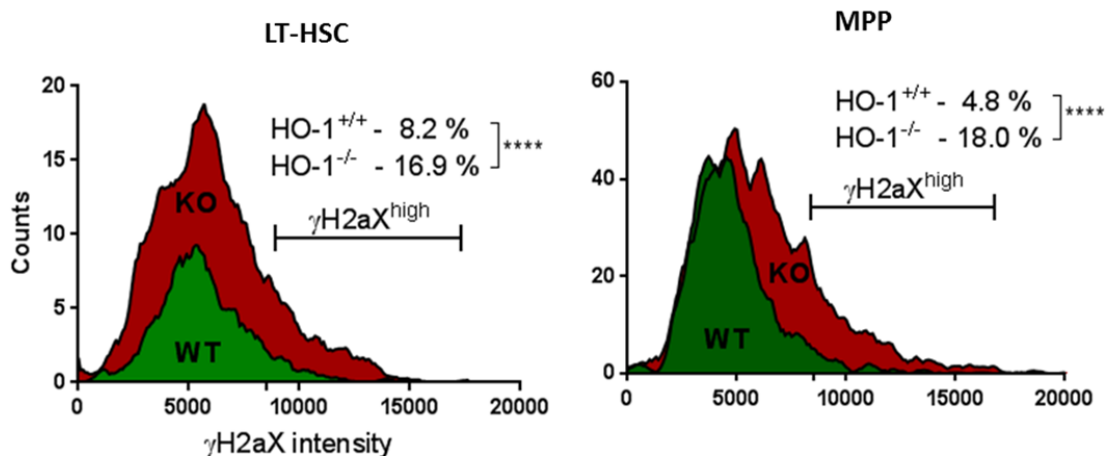
Fig. 3.14 *Evaluation of pS139-γH2aX expression in LT-HSC and MPP by flow cytometry. Shown total number of 371 – 2790 cells/group, isolated from 8 mice/group. The chi-square test with Yates' correction was used to test significance of γH2aX^{high} cells percentage in a given group.*

ATP content is lower in HO-1$^{-/-}$ hematopoietic stem and progenitor cells

To verify if HO-1 deficiency may potentially alter metabolism of hematopoietic stem and progenitor cells, we sorted LT-HSC, ST-HSC and MPP from HO-1$^{+/+}$ and HO-1$^{-/-}$ mice and check the cellular ATP levels. The lack of HO-1 significantly decreased ATP levels in ST-HSC and MPP and had similar trend in LT-HSC (p = 0.07) (Fig. 3.15).
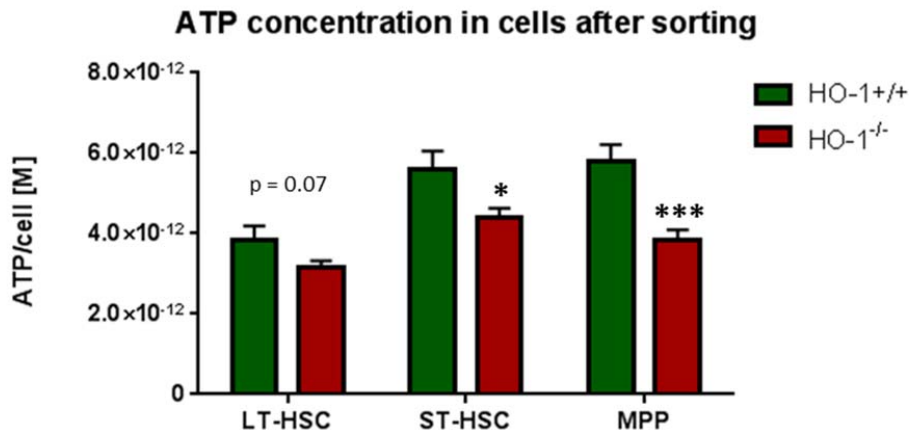
Fig. 3.15 *ATP levels in LT-HSC, ST-HSC and MPP from young HO-1$^{+/+}$ and HO-1$^{-/-}$ mice. n = 6-18/group, two independent experiments shown*.

LT-HSC from young HO-1$^{-/-}$ mice are functionally defective

We checked function of young HO-1$^{-/-}$ LT-HSC in a model of stem cell transplantation in competitive manner. Purified HO-1$^{-/-}$ LT-HSC reconstituted the myeloablated host worse than HO-1$^{+/+}$ LT-HSC (Fig. 3.16A). There was less HO-1$^{-/-}$ donor derived cells among all tested lineages: granulocytes, B-cells and T-cells (Fig. 3.16A). We did not observed myeloid-bias or preferential differentiation of HO-1$^{-/-}$ LT-HSC to any of tested lineages (Fig. 3.16B).

16 weeks after the first transplantation we sacrificed primary recipients, checked chimerism in BM and transplanted 1×10^6 donor derived GFP$^+$ only whole BM cells into secondary myeloablated hosts. We observed significantly lower donor-derived chimerism among ST-HSC and MPP and similar trend among LT-HSC (p = 0.07) in mice transplanted by HO-1$^{-/-}$ LT-HSC (Fig. 3.17A)

Till the date of writing this thesis, only short-term chimerism (4 weeks) after secondary transplantation was checked and no differences between groups were observed (Fig. 3.17B). As in the secondary transplant we did not transplanted purified LT-HSC, but whole BM, the function of LT-HSC is expected to be reflected by long-term chimerism. Therefore, the secondary recipients mice are kept in experiment to continue monitoring the chimerism.
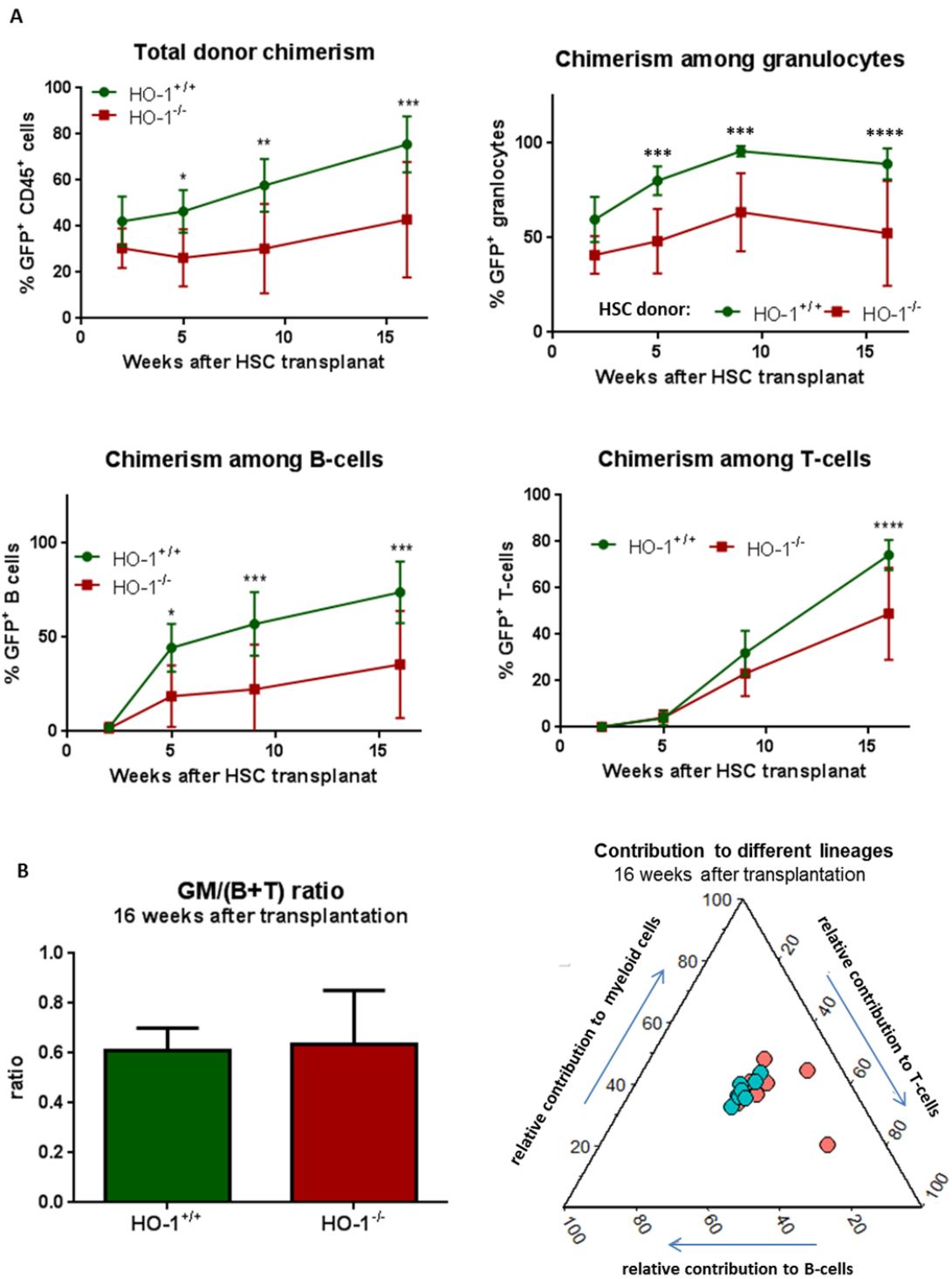
Fig. 3.16 *(A) Donor-derived blood cells after transplantation of HO-1$^{+/+}$ and HO-1$^{-/-}$ LT-HSC. n = 8/group (B) Differentiation of transplanted LT-HSC toward myeloid (granulocytes - GM) and lymphoid (B- and T-cells – B+T) lineages.*
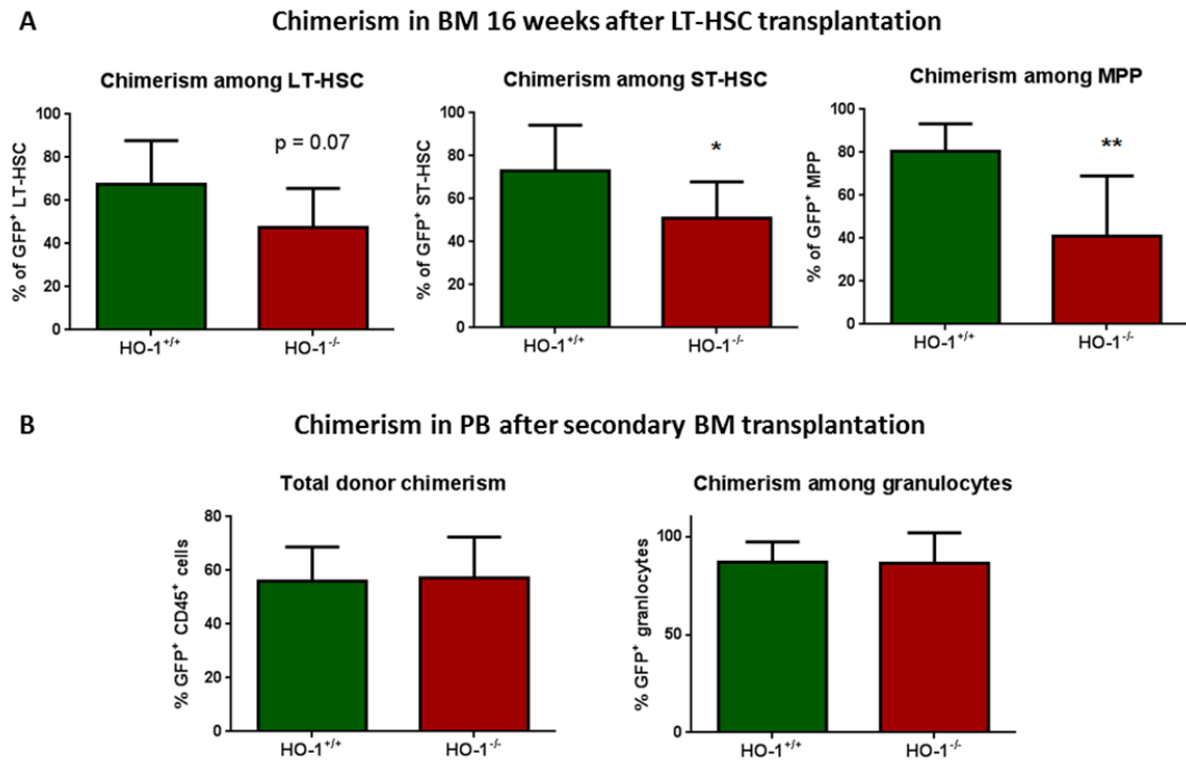
Fig. 3. 17 *(A) Chimerism in BM 16 weeks after transplantation of HO-1$^{+/+}$ HO-1$^{-/-}$ LT-HSC. (B) Chimerism in PB after secondarywhole donor-derived BM transplantation. Till the date only 4 week time point was measured. n = 7-8/group*

Transcriptome profiling of young and old LT-HSC from HO-1$^{+/+}$ and HO-1$^{-/-}$ mice

In aim to find molecular mechanisms underlying the functional defects and premature aging of HO-1$^{-/-}$ LT-HSC we analyzed transcriptome of young and old cells from both genotypes by next generation sequencing (NGS) applied to analyze RNA expression (RNA-seq).

The exploratory principal component analysis (PCA) revealed the transcriptome of young HO-1$^{-/-}$ LT-HSC was distinct from transcriptome of young HO-1$^{+/+}$ LT-HSC (Fig. 3.18). It is also visible that the principal component 2 (PC2) separated young HO-1$^{+/+}$ LT-HSC (bottom of the graph) and grouped young HO-1$^{-/-}$ LT-HSC together with old LT-HSC from both genotypes (upper region of the graph) (Fig. 3.18). This indicates that transcriptome of young HO-1$^{-/-}$ LT-HSC and transcriptome of old LT-HSC were at least partially similar.
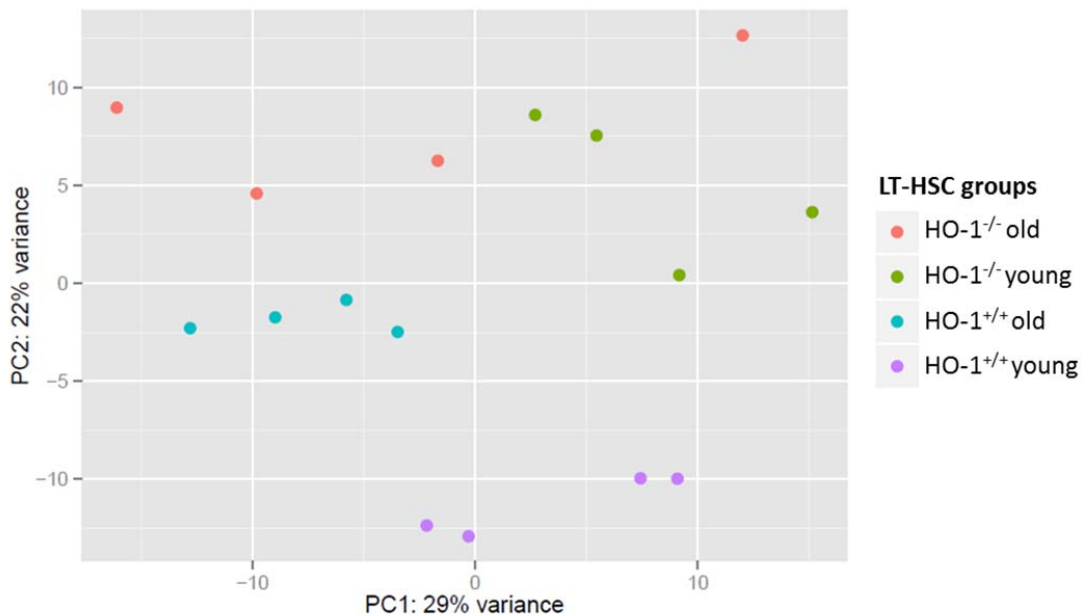
Fig 3.18 Principal component analysis of transcriptome of young and old LT-HSC from HO-1$^{+/+}$ and HO-1$^{-/-}$ mice.

The obtained results of genes expression were further processed by applying Gene Set Enrichment Analysis (GSEA) [247] (all genes and their fold change included in analysis) method and pathway enrichment analysis [223] (based on statistical testing of overrepresentation of selected number of genes revealed by NGS among given set of genes linked with biological process) based on Reactome, Gene Ontology (GO) and KEEG databases to reveal which biological processes are altered and may explain differences between HO-1$^{+/+}$ and HO-1$^{-/-}$ LT-HSC. All RNA-seq data including, expression of all detected genes, all altered pathways detected by GSEA and pathway enrichment using Reactome, GO (including Biological Processes (BP), Molecular Function (MF), cellular localization (CC) subbases), and KEEG databases are provided in supplementary results on attached DVD. The selected altered biological processes are presented at Table 3.1.

The enrichment map of altered pathways detected by GSEA showed that many of them are interdependent processes connected with disturbed cell cycle (Fig. 3.19). The expression of genes connected with cell cycle are presented on Fig. 3.20. The pathway enrichment analysis based on Reactome and GO databases pointed to similar gene sets and additionally revealed other altered processes, among them: signaling by TGFβ-receptor complex, canonical Wnt signaling, myeloid cell development, integrin and cell-matrix adhesion.

ReactomeID	Description	set size	enrichment score	p.adjust value	q values
5992043	G1/S-Specific Transcription	13	0.95	0.02	0.01
5992289	Condensation of Prometaphase Chromosomes	11	0.89	0.02	0.01
5991392	Inhibition of replication initiation of damaged DNA by RB1/E2F1	8	0.84	0.02	0.01
5991207	Chk1/Chk2(Cds1) mediated inactivation of Cyclin B:Cdk1 complex	12	0.80	0.02	0.01
5991393	E2F mediated regulation of DNA replication	28	0.80	0.02	0.01
5991563	Cyclin A/B1 associated events during G2/M transition	14	0.76	0.03	0.02
5991851	Mitotic Prometaphase	99	0.75	0.02	0.01
5991453	Mitotic Telophase/Cytokinesis	14	0.71	0.03	0.02
5991504	Extension of Telomeres	25	0.68	0.02	0.01
5991610	Telomere C-strand (Lagging Strand) Synthesis	23	0.68	0.02	0.01
5991020	G2/M DNA damage checkpoint	16	0.65	0.04	0.03
5991017	G2/M Checkpoints	51	0.65	0.02	0.01
5992050	Nucleosome assembly	40	0.64	0.02	0.01
5991016	Activation of ATR in response to replication stress	37	0.63	0.02	0.01
5991506	Chromosome Maintenance	72	0.63	0.02	0.01
5992122	Kinesins	22	0.62	0.04	0.03
5991502	Mitotic Metaphase and Anaphase	160	0.60	0.02	0.01
5991600	Mitotic Anaphase	159	0.60	0.02	0.01
5990990	G1/S Transition	100	0.58	0.02	0.01
5990991	Mitotic G1-G1/S phases	121	0.56	0.02	0.01
5990978	M/G1 Transition	78	0.56	0.02	0.01
5991578	Transcriptional activity of SMAD2/SMAD3:SMAD4 heterotrimer	38	0.56	0.03	0.02
5991454	M Phase	233	0.55	0.02	0.01
5990981	DNA Replication	99	0.55	0.02	0.01
5990988	S Phase	118	0.54	0.02	0.01
5990987	Synthesis of DNA	95	0.54	0.02	0.01
5991087	mRNA Splicing - Major Pathway	116	0.52	0.02	0.01
5990980	Cell Cycle	484	0.52	0.02	0.01
5991358	DNA Damage Bypass	43	0.51	0.04	0.03
5992067	Interferon Signaling	139	0.51	0.02	0.01
5990976	Assembly of the pre-replicative complex	64	0.50	0.02	0.01
5991009	Cell Cycle Checkpoints	122	0.50	0.02	0.01
5992066	Interferon gamma signaling	101	0.49	0.02	0.01
5991209	RHO GTPase Effectors	227	0.48	0.02	0.01
5991457	Mitotic G2-G2/M phases	99	0.46	0.03	0.02
5991449	APC/C-mediated degradation of cell cycle proteins	79	0.46	0.03	0.02
5991450	Regulation of mitotic cell cycle	79	0.46	0.03	0.02
5991456	G2/M Transition	97	0.46	0.03	0.02
5991094	RNA Polymerase II Transcription	104	0.44	0.04	0.03
5991416	Cell surface interactions at the vascular wall	92	0.43	0.03	0.02
5991124	DNA Repair	132	0.41	0.02	0.01
5991303	Cytokine Signaling in Immune system	264	0.40	0.02	0.01
5991095	Transcription	154	0.40	0.04	0.03
5991210	Signaling by Rho GTPases	338	0.39	0.02	0.01
5991411	Hemostasis	442	0.34	0.02	0.01
5991037	Gene Expression	777	0.32	0.02	0.01
5991024	Metabolism	1440	-0.19	0.03	0.02
5991146	Signalling by NGF	267	-0.26	0.02	0.01
5991979	Sphingolipid metabolism	64	-0.43	0.02	0.01
5991859	Nuclear Receptor transcription pathway	49	-0.49	0.02	0.01
5991935	Circadian Clock	25	-0.53	0.04	0.03
5992339	Ephrin signaling	16	-0.64	0.02	0.01
1368110	Bmal1:Clock,Npas2 activates circadian gene expression	15	-0.67	0.02	0.01
1368092	Rora activates gene expression	9	-0.77	0.02	0.01

Tab. 3.1 *The selected significantly altered (p.adj. < 0.05) gene sets detected by GSEA based on Reactome database.*
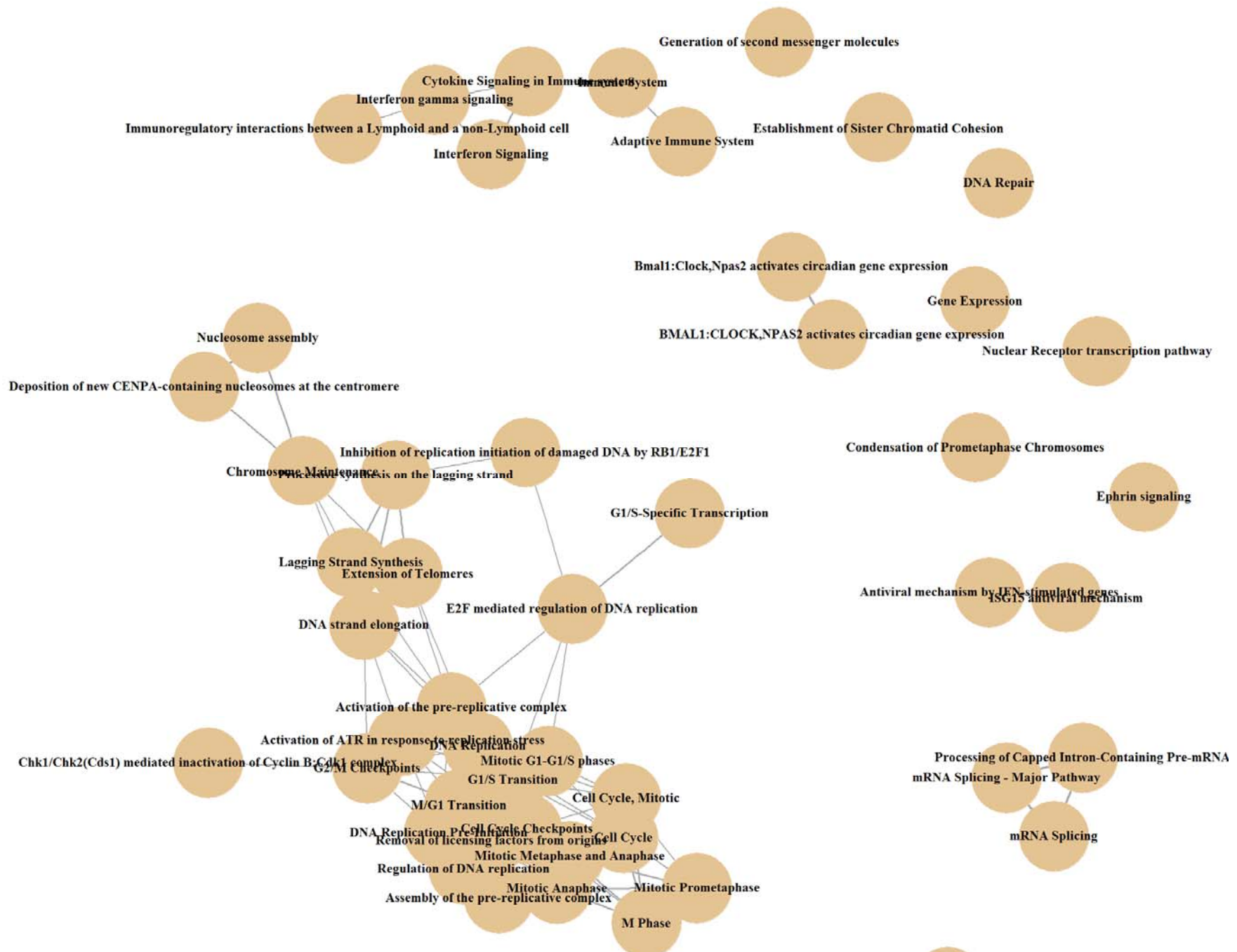
Fig. 3. 19 *A map showing the relations of enriched gene sets revealed by GSEA.*
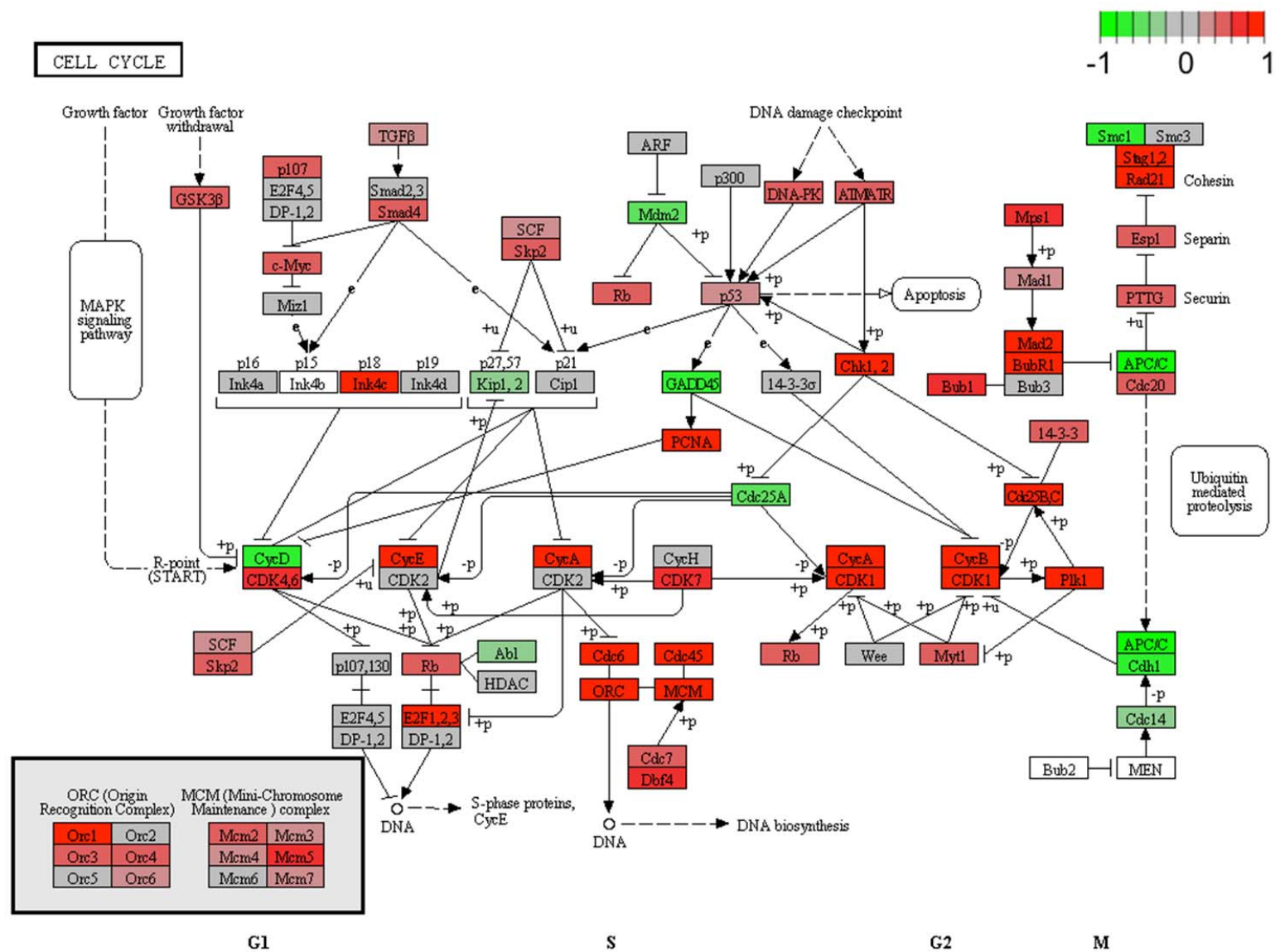
Fig. 3.20 *Altered expression of genes in HO-1^{-/-} LT-HSC involved in cell cycle regulation.*

GO ID	Description	Set size	Overlap	Odds Ratio	P-value
GO:0034340	response to type I interferon	21	7	10.5	0.00
GO:0042976	activation of Janus kinase activity	11	3	7.84	0.01
GO:0060337	type I interferon signaling pathway	17	4	6.43	0.01
GO:0060338	regulation of type I interferon-mediated signaling pathway	13	3	6.27	0.02
GO:0006925	inflammatory cell apoptotic process	18	3	4.18	0.05
GO:0016572	histone phosphorylation	25	4	3.99	0.03
GO:0001953	negative regulation of cell-matrix adhesion	27	4	3.64	0.03
GO:0090342	regulation of cell aging	28	4	3.48	0.04
GO:0033209	tumor necrosis factor-mediated signaling pathway	38	5	3.17	0.03
GO:0001952	regulation of cell-matrix adhesion	79	10	3.04	0.00
GO:0042771	intrinsic apoptotic signaling pathway in response to DNA damage by p53 class mediator	40	5	2.99	0.03
GO:0008631	intrinsic apoptotic signaling pathway in response to oxidative stress	42	5	2.83	0.04
GO:0033209	tumor necrosis factor-mediated signaling pathway	38	5	3.17	0.03
GO:0001952	regulation of cell-matrix adhesion	79	10	3.04	0.00
GO:0042771	intrinsic apoptotic signaling pathway in response to DNA damage by p53 class mediator	40	5	2.99	0.03
GO:0008631	intrinsic apoptotic signaling pathway in response to oxidative stress	42	5	2.83	0.04
GO:0090263	positive regulation of canonical Wnt signaling pathway	61	7	2.71	0.02
GO:0061515	myeloid cell development	44	5	2.69	0.05
GO:0042509	regulation of tyrosine phosphorylation of STAT protein	54	6	2.61	0.04
GO:0046427	positive regulation of JAK-STAT cascade	65	7	2.53	0.03
GO:0007569	cell aging	76	8	2.46	0.02
GO:0002573	myeloid leukocyte differentiation	178	18	2.37	0.00
GO:0030177	positive regulation of Wnt signaling pathway	93	9	2.24	0.03
GO:0032635	interleukin-6 production	97	9	2.14	0.03
GO:0044238	primary metabolic process	3742	175	1.24	0.01

Tab. 3.**2** *Selected gene sets that were altered in young HO-1$^{-/-}$ LT-HSC revealed by pathway enrichment analysis based on GO.BP database.*

Concluding, among changes revealed by transcriptome analysis of young HO-1$^{+/+}$ and HO-1$^{-/-}$ LT-HSC, we can list processes that might explain the altered function of HO-1-deficient LT-HSC: dysregulated cell cycle, altered DNA repair mechanisms, augmented type I interferon signaling, increased myeloid differentiation factors (eg. *Gata1*), altered TGFβ, Wnt signaling and differences in integrins expression. Profile of genes expression indicated that general metabolism was changed (Tab. 3.1 – decreased Reactome set "Metabolism" includes 1440 genes). In particular, we found changes in genes that promote direction of pyruvate toward mitochondrial oxidation instead of non-oxidative conversion toward lactate that characterizes quiescent LT-HSC [27] (Fig. 3.21A).

Additionally, we observed upregulation of *Cxcr4* (SDF-1α receptor) (Fig. 3.21B) - crucial receptor regulating HSC biology – what might indicate that SDF-1α signaling in HO-1$^{-/-}$ niche is altered.
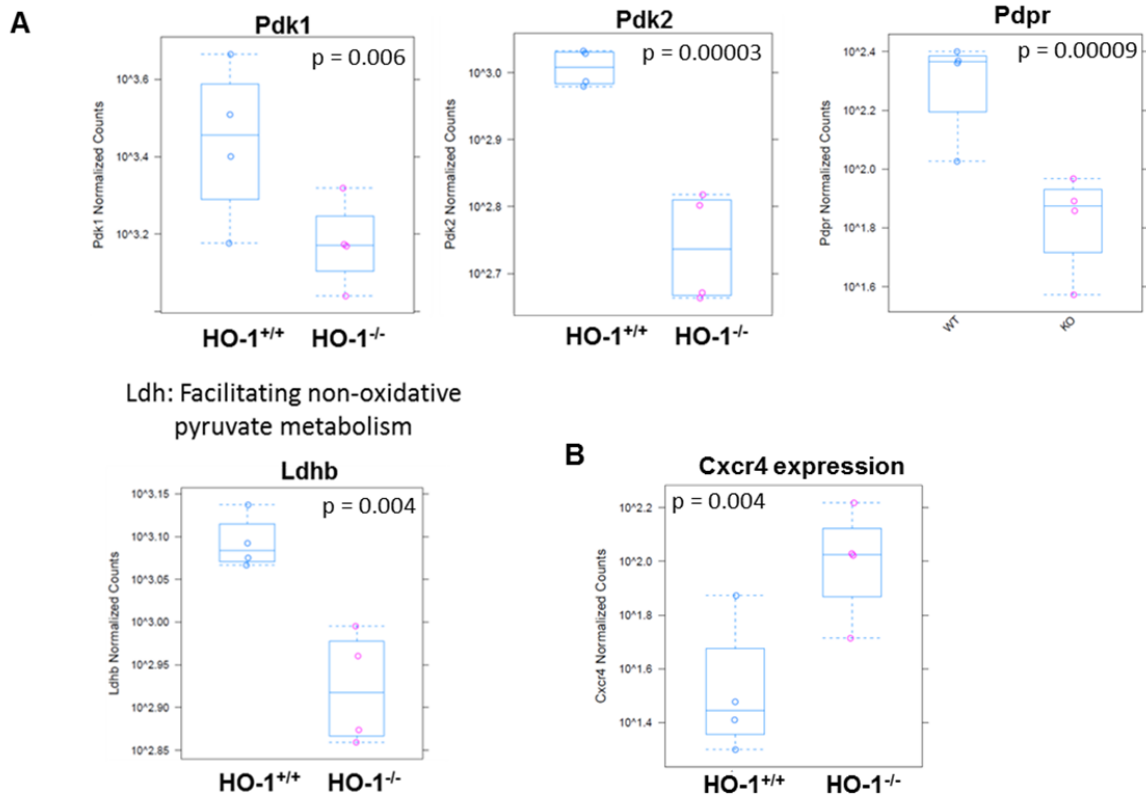
Fig. 3.21 *(A) Expression of genes regulating the metabolic fate of pyruvate and (B) expression of Cxcr4 (SDF-1α receptor) revealed by RNA-seq.*

The GSEA (Tab. 3.3) and pathway enrichment analysis (Tab 3.4) of transcriptome of old HO-1^{-/-} LT-HSC in comparison to old HO-1^{+/+} LT-HSC revealed even more altered set of genes than among young LT-HSC with different HO-1 genotype (322 hits in old vs. 99 hits in young, whole list in Supplementary Results). The main changes observed in young HO-1^{-/-} LT-HSC were also visible in old HO-1^{-/-} LT-HSC, including altered cell cycle, DNA repair processes, type I interferon, TGFβ and Wnt signaling as well as higher *Cxcr4* expression. Although, in contrast to young HO-1^{-/-} LT-HSC the *Ldhb*, *Pdk1*, *Pdk2* and *Pdpr* were not changed in old HO-1^{-/-} LT-HSC, but the whole pyruvate metabolism, citric acid and respiratory electron transport was altered what was also connected with increased mitochondrial translation and protein import (Tab. 3.3, 3.4). There were also changes in old HO-1^{-/-} LT-HSC that were not visible in young HO-1^{-/-} LT-HSC. These included increased signaling mediated by c-Kit and VEGFR2 receptors. We also found that expression of genes connected with Notch and retinoic acid signaling was decreased in old HO-1^{-/-} LT-HSC (Tab. 3.3)

ReactomeID	Description	set size	enrichment score	p.adjust value	qvalues
5991707	Metabolism of folate and pterines	8	0.72	0.03	0.02
5991572	Regulation of Glucokinase by Glucokinase Regulatory Protein	29	0.66	0.01	0.00
5991297	Signalling to p38 via RIT and RIN	15	0.66	0.03	0.02
5991830	p130Cas linkage to MAPK signaling for integrins	15	0.65	0.01	0.01
5991771	Regulation of KIT signaling	16	0.63	0.01	0.01
5991301	Interleukin-2 signaling	40	0.62	0.01	0.00
5991824	Integrin alphaIIb beta3 signaling	27	0.61	0.01	0.00
5991293	Prolonged ERK activation events	20	0.60	0.02	0.01
5992151	Mitochondrial protein import	28	0.59	0.01	0.00
5991310	Signaling by Leptin	21	0.58	0.01	0.01
5992365	Mitochondrial translation elongation	81	0.56	0.01	0.00
5992366	Mitochondrial translation termination	81	0.55	0.01	0.00
5992363	Mitochondrial translation	86	0.54	0.01	0.00
5992354	DNA methylation	32	0.54	0.01	0.00
5992362	Mitochondrial translation initiation	80	0.54	0.01	0.00
5991177	VEGFR2 mediated cell proliferation	27	0.53	0.02	0.01
5991602	SCF-beta-TrCP mediated degradation of Emi1	54	0.53	0.01	0.00
5991627	SCF(Skp2)-mediated degradation of p27/p21	52	0.51	0.01	0.00
5991797	PRC2 methylates histones and DNA	40	0.51	0.02	0.01
5991038	Glucose transport	39	0.46	0.04	0.03
5991206	Epigenetic regulation of gene expression	68	0.46	0.01	0.00
5991039	Hexose transport	41	0.45	0.03	0.02
5991560	beta-catenin independent WNT signaling	105	0.45	0.01	0.00
5991699	Degradation of beta-catenin by the destruction complex	66	0.44	0.01	0.01
5991507	Respiratory electron transport	65	0.43	0.01	0.01
5991078	Metabolism of nucleotides	77	0.43	0.01	0.01
5992197	PI Metabolism	49	0.43	0.04	0.03
5991508	Respiratory electron transport, ATP synthesis by chemiosmotic coupling, and heat production by uncoupling proteins.	86	0.42	0.01	0.00
5991178	VEGFA-VEGFR2 Pathway	92	0.41	0.01	0.01
5991179	Signaling by VEGF	100	0.40	0.01	0.01
5991046	The citric acid (TCA) cycle and respiratory electron transport	123	0.39	0.01	0.01
5991342	L1CAM interactions	77	0.37	0.04	0.03
5991242	Glycerophospholipid biosynthesis	88	0.37	0.03	0.02
5991129	Apoptosis	150	0.37	0.01	0.00
5991023	Metabolism of carbohydrates	244	0.31	0.02	0.01
5991561	Signaling by Wnt	231	0.30	0.02	0.01
5991414	Extracellular matrix organization	252	0.28	0.05	0.03
5991029	Biological oxidations	175	-0.34	0.01	0.01
5991688	Cell death signalling via NRAGE, NRIF and NADE	64	-0.38	0.05	0.03
5991734	Signaling by Retinoic Acid	53	-0.47	0.01	0.00
5991464	Activated NOTCH1 Transmits Signal to the Nucleus	26	-0.55	0.03	0.02
5991878	Regulation of Insulin-like Growth Factor (IGF) transport and uptake by Insulin-like Growth Factor Binding Proteins (IGFBPs)	30	-0.55	0.01	0.01
5992293	TRIF-mediated programmed cell death	10	-0.65	0.05	0.03
5991471	Signaling by NOTCH4	12	-0.66	0.04	0.02
5991469	NOTCH2 Activation and Transmission of Signal to the Nucleus	18	-0.66	0.02	0.01
5991468	Signaling by NOTCH3	12	-0.69	0.03	0.02
5991261	Synthesis of Prostaglandins (PG) and Thromboxanes (TX)	21	-0.70	0.01	0.00

Tab. 3.3 *Selected pathways altered in old HO-1^{-/-} LT-HSC that were not altered in young HO-1^{-/-} LT-HSC in GSEA analysis based on Reactome database.*

GO ID	Description	Set size	Overlap	Odds Ratio	P-value
GO:0060390	regulation of SMAD protein import into nucleus	14	3	5.74	0.02
GO:0006692	prostanoid metabolic process	28	5	4.58	0.01
GO:0070734	histone H3-K27 methylation	17	3	4.51	0.04
GO:0071353	cellular response to interleukin-4	25	4	4.01	0.03
GO:2000379	positive regulation of reactive oxygen species metabolic process	83	13	3.94	0.01
GO:0035924	cellular response to vascular endothelial growth factor stimulus	34	5	3.63	0.02
GO:0006801	superoxide metabolic process	48	7	3.6	0.01
GO:0071320	cellular response to cAMP	35	5	3.51	2.01
GO:1903428	positive regulation of reactive oxygen species biosynthetic process	43	6	3.42	0.01
GO:0032612	interleukin-1 production	51	7	3.36	0.01
GO:0045429	positive regulation of nitric oxide biosynthetic process	37	5	3.29	0.03
GO:0002763	positive regulation of myeloid leukocyte differentiation	53	7	3.21	0.01
GO:0006487	protein N-linked glycosylation	39	5	3.1	0.03
GO:0006090	pyruvate metabolic process	79	10	3.07	0.00
GO:0070301	cellular response to hydrogen peroxide	56	7	3.01	0.01
GO:0032655	regulation of interleukin-12 production	41	5	2.93	0.04
GO:0042993	positive regulation of transcription factor import into nucleus	42	5	2.85	0.04
GO:1900407	regulation of cellular response to oxidative stress	51	6	2.81	0.03
GO:0014068	positive regulation of phosphatidylinositol 3-kinase signaling	53	6	2.69	0.03
GO:0070374	positive regulation of ERK1 and ERK2 cascade	124	13	2.48	0.00
GO:0010827	regulation of glucose transport	67	7	2.46	0.03
GO:0001678	cellular glucose homeostasis	95	9	2.21	0.03
GO:1901568	fatty acid derivative metabolic process	108	10	2.16	0.03
GO:0046330	positive regulation of JNK cascade	103	9	2.02	0.04
GO:0071560	cellular response to transforming growth factor beta stimulus	154	13	1.95	0.02
GO:0071396	cellular response to lipid	359	27	1.73	0.01
GO:0008285	negative regulation of cell proliferation	439	31	1.63	0.01
GO:0006631	fatty acid metabolic process	342	23	1.53	0.04

Tab. 3.4 *Selected enriched sets of genes from GO BP database in old HO-1$^{-/-}$ LT-HSC*

The genes involved in apoptosis, epigenetic regulation of gene expression as well as biosynthesis and response to reactive oxygen species were also upregulated in old HO-1$^{-/-}$ LT-HSC, but not in young HO-1$^{-/-}$ LT-HSC (Tab. 3.3, 3.4).

HO-1 is highly expressed in a stem cell niche

Given that we used global HO-1 knockout mice model, the observed functional defects and associated changes in transcriptome may be the result of HO-1 intrinsic and/or extrinsic role in LT-HSC. In first step to verify these possibilities we compared the HO-1 expression in hematopoietic stem and progenitor cells with cells that compose the stem cell niche.

HO-1 immunohistochemistry of mouse tibia evidenced that HO-1 is highly expressed in cells with non-hematopoietic morphology (Fig. 3.22A). To further verify this observation we performed real time PCR analysis of HO-1 mRNA expression in sorted cell populations as well as flow cytometric evaluation of HO-1 protein levels (analyzed populations and gating scheme in Methods).

Indeed, the hematopoietic stem and progenitor cells expressed low levels of HO-1 mRNA (Fig. 3.22B). Higher HO-1 expression at RNA level was observed in macrophages and mesenchymal populations: PaS and CAR, while the highest HO-1 expression characterizes $CD31^{high}Sca-1^{+}$ endothelial cells (EC) (Fig. 3.22B). The high expression of HO-1 protein in mesenchymal and $CD31^{high}Sca-1^{+}$ endothelial cells (EC) was confirmed by flow cytometry (Fig. 3.22C). Notably, the protein levels of HO-1 was much higher in minor $CD31^{high}Sca-1^{+}$ fraction of EC in comparison to $CD31^{low}Sca-1^{-}$ fraction of EC, that prevails in bone marrow (Fig. 3.22C).

We also checked how lack of HO-1 affects the frequency of CAR and $CD31^{high}Sca-1^{+}$ EC in the bone marrow. There were more $CD31^{high}Sca-1^{+}$ EC in HO-1$^{-/-}$ animals, while the frequency of CAR was not changed (Fig. 3.22D).

Lack of extrinsic HO-1 impairs function of LT-HSC

As the highest expression of HO-1 characterizes cells that compose stem cell niche, we hypothesized that defective function of LT-HSC observed in HO-1$^{-/-}$ mice was caused by HO-1-deficiency in stem cell niche and not in LT-HSC itself. To verify this hypothesis we transplanted labeled HO-1$^{+/+}$ LT-HSC to HO-1$^{+/+}$ or HO-1$^{-/-}$ irradiated recipients and let them aging in HO-1 competent or deficient environment for 32 weeks (Fig. 3.23). We observed that LT-HSC transplanted into HO-1-deficient niche provided worse long-term chimerism than LT-HSC transplanted to HO-1-competent niche (Fig. 3.24A). We did not observed changes in differentiation preferences, as all transplanted LT-HSC were highly myeloid biased (Fig. 3.24C). After 32 weeks chimerism in BM among LT-HSC, ST-HSC and MPP tended to be lower in HO-1$^{-/-}$ recipients (Fig. 3.24B) what indicated that LT-HSC in HO-1 deficient environment exhausted faster and did not self-renew as well as in HO-1-competent environment,
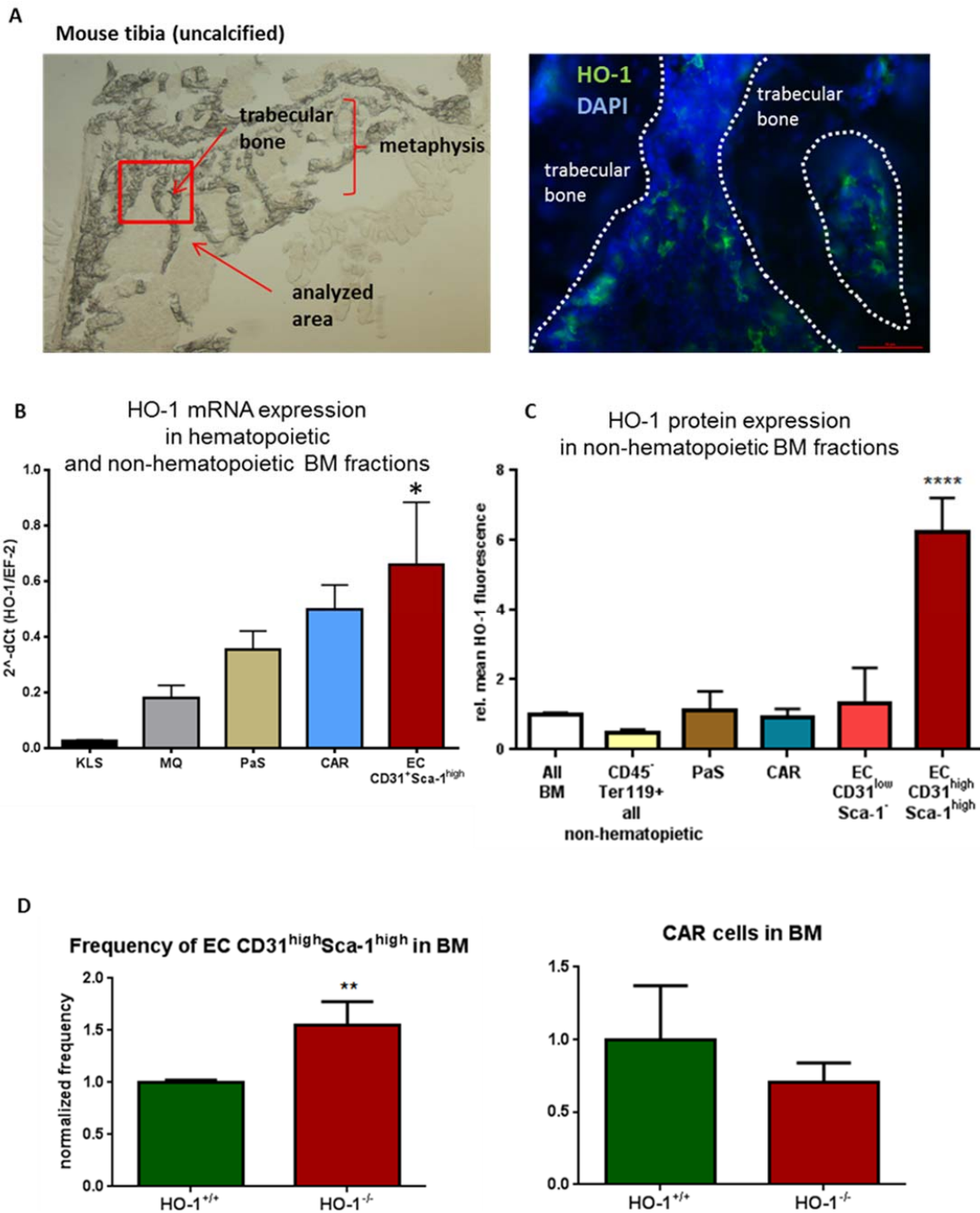
Fig. 3.22 (A) *The pattern of HO-1 expression in mouse tibia revealed by immunohistochemistry **(B)** Comparison of HO-1 mRNA expression in hematopoietic and non-hematopoietic BM fractions, n = 6 / group, shown two independent experiments **(C)** HO-1 protein expression in non-hematopoietic fractions of BM analyzed by flow cytometry. n = 3, shown one representative experiment from two performed **(D)** Frequency of CD31^high Sca-1^high EC and CAR cells in BM from HO-1^+/+ and HO-1^-/- mice. n = 8/ group, shown two independent experiments*
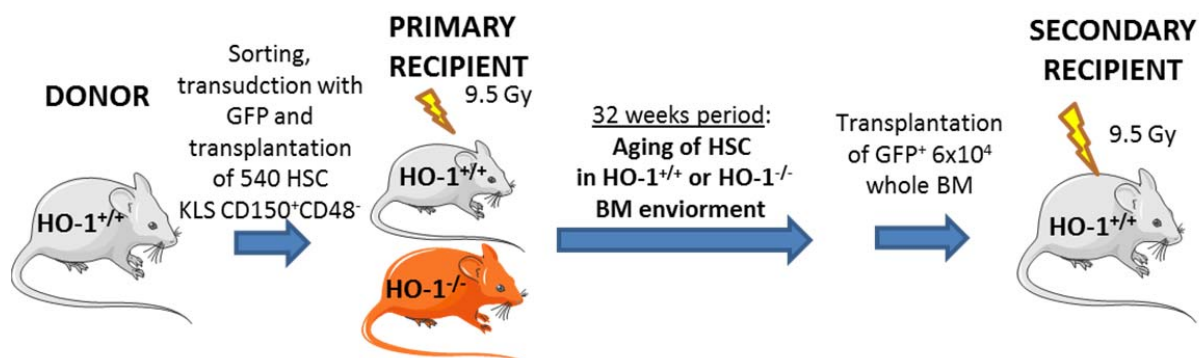
Fig. 3.23 *Outline of the experiment verifying the extrinsic role of HO-1 in maintenance of LT-HSC.*

Although the differences in chimersim among LT-HSC did not reach statistical significance, these conclusions were further functionally confirmed by transplanting the same number of donor-derived BM cells from primary HO-1$^{+/+}$ or HO-1$^{-/-}$ recipients to secondary young HO-1$^{+/+}$ recipients (Fig. 3.23). This scheme of experiment provided an experimental setting in which after secondary transplantation HO-1$^{+/+}$ LT-HSC resides in HO-1$^{+/+}$ environment. The only thing that differed the two compared groups was the previous period of 32 weeks when LT-HSC were aging in HO-1$^{+/+}$ or HO-1$^{-/-}$ environment.

In these secondary transplants, only the LT-HSC from HO-1$^{+/+}$ primary recipients gave reconstitution of hematopoietic system (Fig. 3.24D). There were no LT-HSC in BM of HO-1$^{-/-}$ primary recipients that were able to produced blood cells in the same conditions (Fig. 3.24D).

Concluding, the extrinsic HO-1 maintained the self-renewal of LT-HSC and protected them from premature exhaustion.

Transcriptome analysis of CAR and CD31^{+}Sca-1^{high} EC from HO-1$^{+/+}$ and HO-1$^{-/-}$ mice

To identify mechanism explaining indispensability of HO-1 in stem cell niche for protecting LT-HSC from premature aging we analyzed transcriptome of CAR and CD31^{+}Sca-1^{high} EC. These two populations were chosen as they are known to compose stem cell niche and showed high HO-1 expression.

GSEA and pathway enrichment analysis of obtained data (Tab. 3.5, 3.6) put our attention on two altered biological processes. Firstly, the production of several growth factors and cytokines that may regulate LT-HSC differs between HO-1$^{-/-}$ and HO-1$^{-/-}$ CD31^{+}Sca-1^{high} EC (Fig. 3.25).
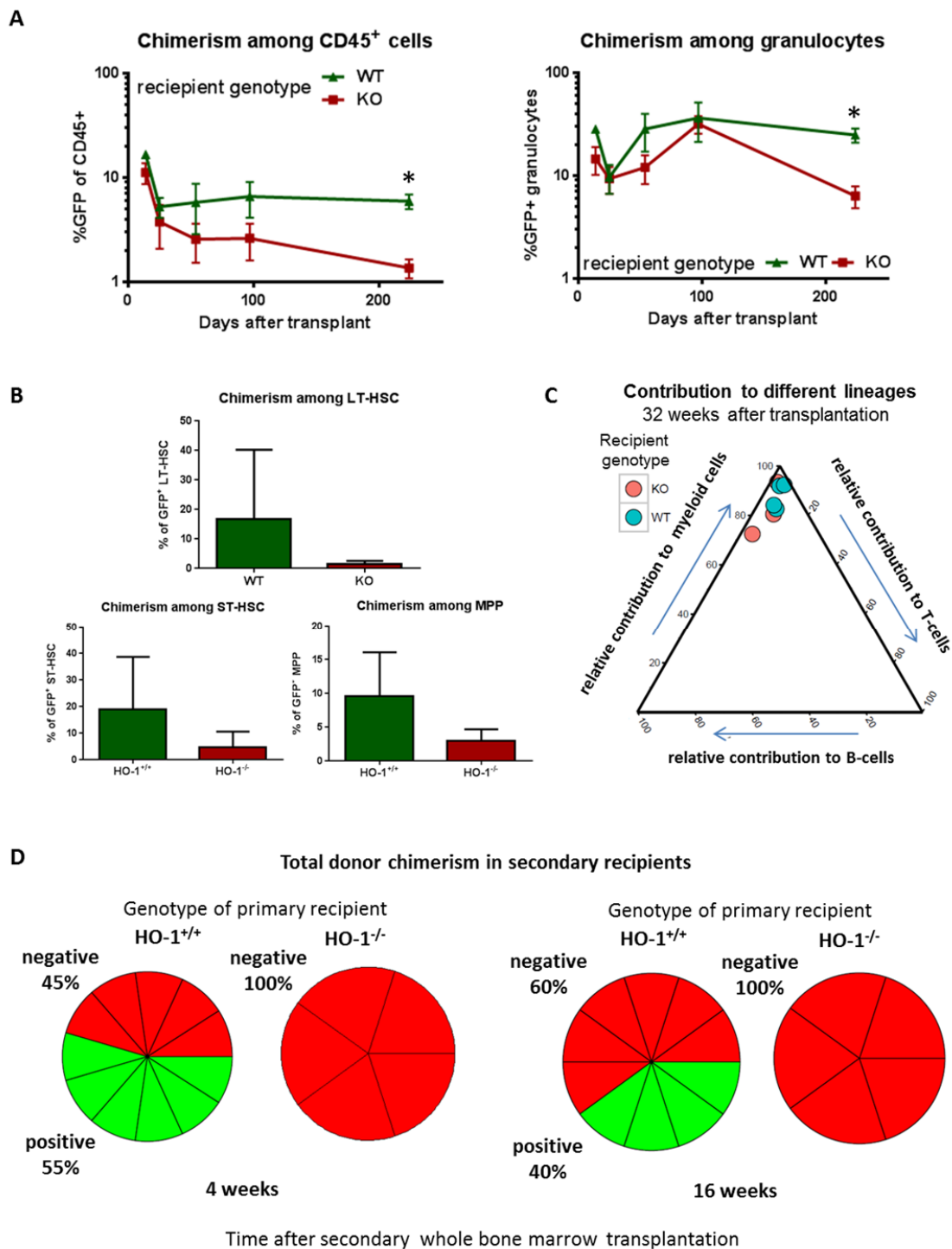
Fig. 3.24 *(A) PB chimerism after transplanting HO-1$^{+/+}$ LT-HSC into HO-1$^{+/+}$ or HO-1$^{-/-}$ mice. n = 3-4/group (B) Chimerism among BM hematopoietic stem and progenitor cells after 32 weeks n = 3-4/group (C) Relative contribution of transplanted LT-HSC to different lineages (D) Percentage of reconstituted secondary recipients n = 5-11/group*

Especially, we observed that CD31$^+$Sca-1^{high} EC expressed *Kitl* (known also as stem cell factor, SCF) and *Cxlc12* (SDF-1) – the known indispensable factors for LT-HSC function. The HO-1$^{-/-}$ CD31$^+$Sca-1^{high} EC expressed significantly less *Kitl* and tend (p = 0.06) also to express less *Cxlc12* (Fig. 3.26A). Lack of HO-1 in CD31$^+$Sca-1^{high} EC resulted also in lower expression of *Tgfb1*, which signaling pathway were affected in young and old LT-HSC from HO-1$^{-/-}$ mice (Fig. 3.26A).

ReactomeID	Description	set size	enrichment score	p.adjust value	qvalues
5991616	Packaging Of Telomere Ends	20	0.58	0.07	0.06
5992078	Meiotic recombination	46	0.56	0.05	0.04
5991973	SIRT1 negatively regulates rRNA Expression	35	0.55	0.05	0.04
5991710	CD28 co-stimulation	25	0.55	0.09	0.07
5991711	Costimulation by the CD28 family	45	0.53	0.07	0.06
5992274	Condensation of Prophase Chromosomes	27	0.51	0.10	0.09
5992354	DNA methylation	32	0.51	0.05	0.04
5991797	PRC2 methylates histones and DNA	40	0.49	0.05	0.04
5992219	Regulation of cholesterol biosynthesis by SREBP (SREBF)	36	0.48	0.07	0.06
5991172	Antigen activates B Cell Receptor (BCR) leading to generation of second messengers	32	0.48	0.09	0.07
5992217	Resolution of Sister Chromatid Cohesion	91	0.47	0.05	0.04
5991851	Mitotic Prometaphase	99	0.45	0.05	0.04
5992066	Interferon gamma signaling	98	0.45	0.05	0.04
5991757	RHO GTPases Activate Formins	101	0.43	0.05	0.04
5992197	PI Metabolism	49	0.43	0.10	0.09
5992079	Meiosis	74	0.43	0.07	0.06
5992067	Interferon Signaling	132	0.41	0.05	0.04
5991726	Immunoregulatory interactions between a Lymphoid and a non-Lymphoid cell	78	0.41	0.05	0.04
5992367	Transcriptional regulation by small RNAs	71	0.38	0.07	0.06
5991416	Cell surface interactions at the vascular wall	89	0.37	0.05	0.04
5991413	Integrin cell surface interactions	79	0.37	0.09	0.07
5991698	Rho GTPase cycle	120	0.37	0.10	0.09
5991124	DNA Repair	132	0.35	0.05	0.04
5991302	Signaling by Interleukins	102	0.35	0.09	0.07
5991210	Signaling by Rho GTPases	337	0.34	0.05	0.04
5992070	Factors involved in megakaryocyte development and platelet production	106	0.34	0.07	0.06
5990980	Cell Cycle	483	0.34	0.05	0.04
5990979	Cell Cycle, Mitotic	401	0.33	0.05	0.04
5991303	Cytokine Signaling in Immune system	253	0.32	0.05	0.04
5991209	RHO GTPase Effectors	226	0.32	0.05	0.04
5991454	M Phase	233	0.31	0.07	0.06
5991156	Immune System	874	0.27	0.05	0.04
5991174	Adaptive Immune System	414	0.27	0.05	0.04
5991411	Hemostasis	430	0.25	0.09	0.07
5991048	Metabolism of amino acids and derivatives	180	-0.30	0.09	0.07
5991029	Biological oxidations	173	-0.30	0.10	0.09
5991880	Olfactory Signaling Pathway	214	-0.31	0.07	0.06
5992206	Elastic fibre formation	37	-0.48	0.07	0.06
5992205	Molecules associated with elastic fibres	33	-0.52	0.05	0.04
5992266	Synthesis of epoxy (EET) and dihydroxyeicosatrienoic acids (DHET)	17	-0.61	0.10	0.09

Tab. 3.5 *Selected processes altered in HO-1$^{-/-}$ CD31$^+$Sca-1^{high} EC revealed by GSEA analysis*

GO ID	Description	Set Size	Overlap	Odds Ratio	P-value
GO:0033630	positive regulation of cell adhesion mediated by integrin	15	5	10.60	0.00
GO:0071850	mitotic cell cycle arrest	12	4	10.60	0.00
GO:0032727	positive regulation of interferon-alpha production	13	4	9.39	0.00
GO:0046459	short-chain fatty acid metabolic process	11	3	7.91	0.01
GO:0035458	cellular response to interferon-beta	26	7	7.80	0.00
GO:1903053	regulation of extracellular matrix organization	20	5	7.05	0.00
GO:0045078	positive regulation of interferon-gamma biosynthetic process	12	3	7.03	0.02
GO:0045351	type I interferon biosynthetic process	12	3	7.03	0.02
GO:0045414	regulation of interleukin-8 biosynthetic process	12	3	7.03	0.02
GO:0042228	interleukin-8 biosynthetic process	13	3	6.33	0.02
GO:0090330	regulation of platelet aggregation	13	3	6.33	0.02
GO:0032728	positive regulation of interferon-beta production	22	5	6.22	0.00
GO:0032753	positive regulation of interleukin-4 production	19	4	5.63	0.01
GO:0016577	histone demethylation	24	5	5.56	0.00
GO:0070076	histone lysine demethylation	21	4	4.97	0.01
GO:0044819	mitotic G1/S transition checkpoint	22	4	4.69	0.02
GO:0032479	regulation of type I interferon production	40	7	4.49	0.00
GO:0006925	inflammatory cell apoptotic process	18	3	4.22	0.05
GO:2000134	negative regulation of G1/S transition of mitotic cell cycle	49	8	4.13	0.00
GO:0042168	heme metabolic process	29	4	3.38	0.04
GO:0044773	mitotic DNA damage checkpoint	45	6	3.25	0.02
GO:0071158	positive regulation of cell cycle arrest	30	4	3.25	0.05
GO:0030330	DNA damage response, signal transduction by p53 class mediator	53	7	3.22	0.01
GO:0030199	collagen fibril organization	38	5	3.20	0.03
GO:0071346	cellular response to interferon-gamma	38	5	3.20	0.03
GO:0002040	sprouting angiogenesis	57	7	2.96	0.01
GO:2001238	positive regulation of extrinsic apoptotic signaling pathway	58	7	2.90	0.02
GO:0016525	negative regulation of angiogenesis	70	8	2.73	0.01
GO:0014068	positive regulation of phosphatidylinositol 3-kinase signaling	53	6	2.70	0.03
GO:0032200	telomere organization	53	6	2.70	0.03
GO:0014066	regulation of phosphatidylinositol 3-kinase signaling	71	8	2.69	0.01
GO:0071621	granulocyte chemotaxis	74	8	2.56	0.02
GO:0001936	regulation of endothelial cell proliferation	87	9	2.44	0.02
GO:0045765	regulation of angiogenesis	199	20	2.38	0.00
GO:0007229	integrin-mediated signaling pathway	73	7	2.24	0.05
GO:0007155	cell adhesion	355	32	2.19	0.00
GO:0042107	cytokine metabolic process	107	10	2.18	0.02
GO:0010594	regulation of endothelial cell migration	98	9	2.14	0.03
GO:0001525	angiogenesis	200	18	2.13	0.00
GO:0001935	endothelial cell proliferation	99	9	2.12	0.04
GO:0050727	regulation of inflammatory response	228	20	2.05	0.00
GO:0048762	mesenchymal cell differentiation	152	12	1.81	0.04
GO:0010564	regulation of cell cycle process	408	31	1.76	0.00
GO:0006974	cellular response to DNA damage stimulus	607	45	1.72	0.00
GO:1903706	regulation of hemopoiesis	313	21	1.53	0.05
GO:0006281	DNA repair	383	25	1.48	0.04
GO:0048534	hematopoietic or lymphoid organ development	802	51	1.45	0.01
GO:0044238	primary metabolic process	8366	440	1.32	0.00

Tab. 3.6 *Selected enriched pathways from GO BP database in HO-1$^{-/-}$ CD31^{+}Sca-1^{high} EC*
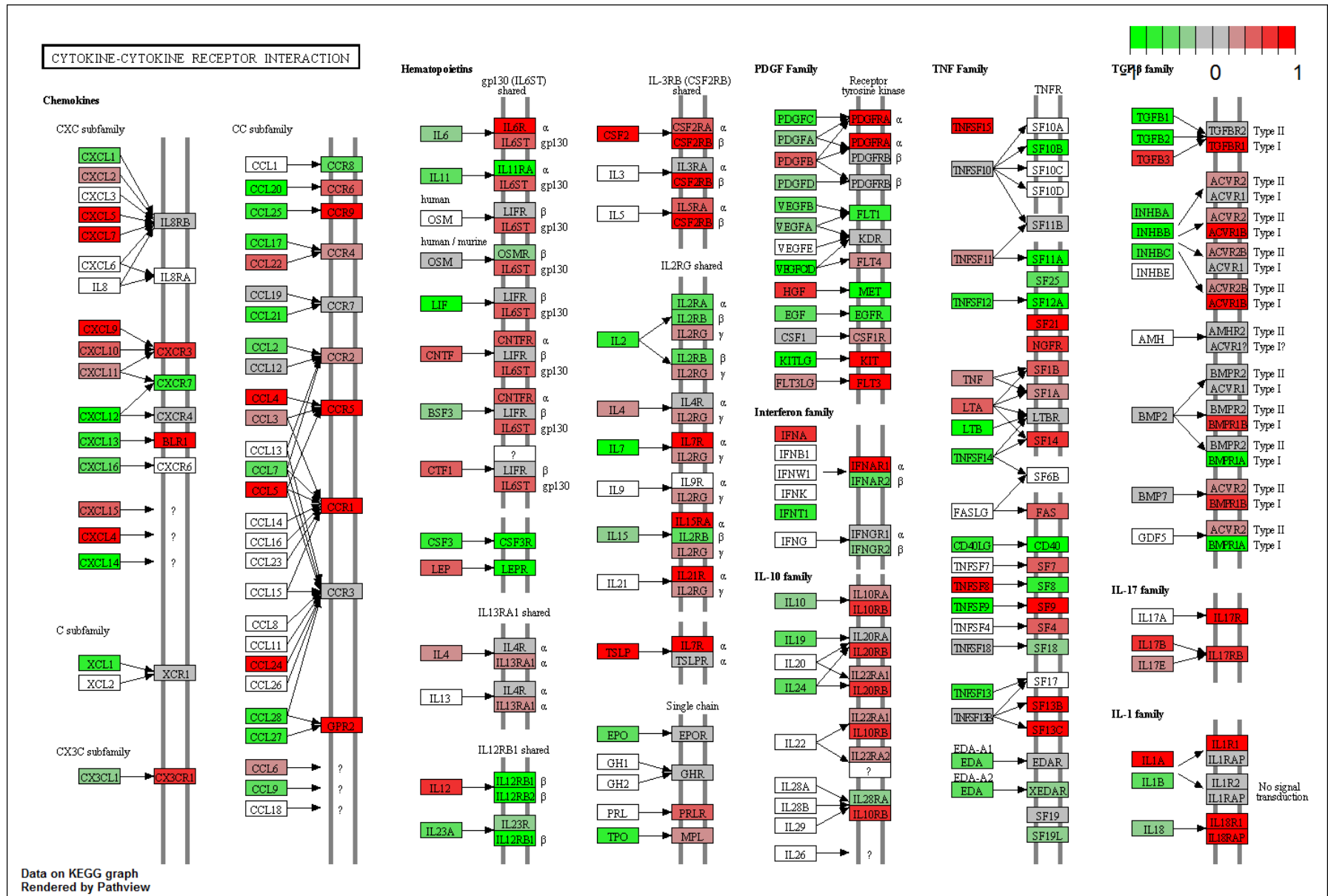
Fig. 3.25 *Diagram showing expression of selected cytokines and their receptors in HO-1$^{-/-}$ CD31$^+$Sca-1^{high} EC*

Second group of affected genes that are important for maintenance of LT-HSC are adhesion and cell surface molecules (Fig. 3.27). We identified two oppositely regulated integrins in HO-1$^{-/-}$ CD31$^+$Sca-1^{high} EC: integrinα4 (*Itga4*) and integrinα11 (*Itga11*) (Fig. 3.26B). Moreover, we found that CD31$^+$Sca-1^{high} EC highly expressed angiopoetin-like 4 (*Angptl4*) and its expression is lower in HO-1$^{-/-}$ EC (Fig. 3.26B).

Similarly to HO-1$^{-/-}$ LT-HSC, HO-1$^{-/-}$ CD31$^+$Sca-1^{high} EC showed altered expression profile of genes connected with cell cycle, DNA repair, metabolism and signaling pathway of interferons (Tab. 3.5, 3.6). However, the CD31$^+$Sca-1^{high} EC itself did not expressed considerable amounts of type I and II interferons (Supplementary Results).
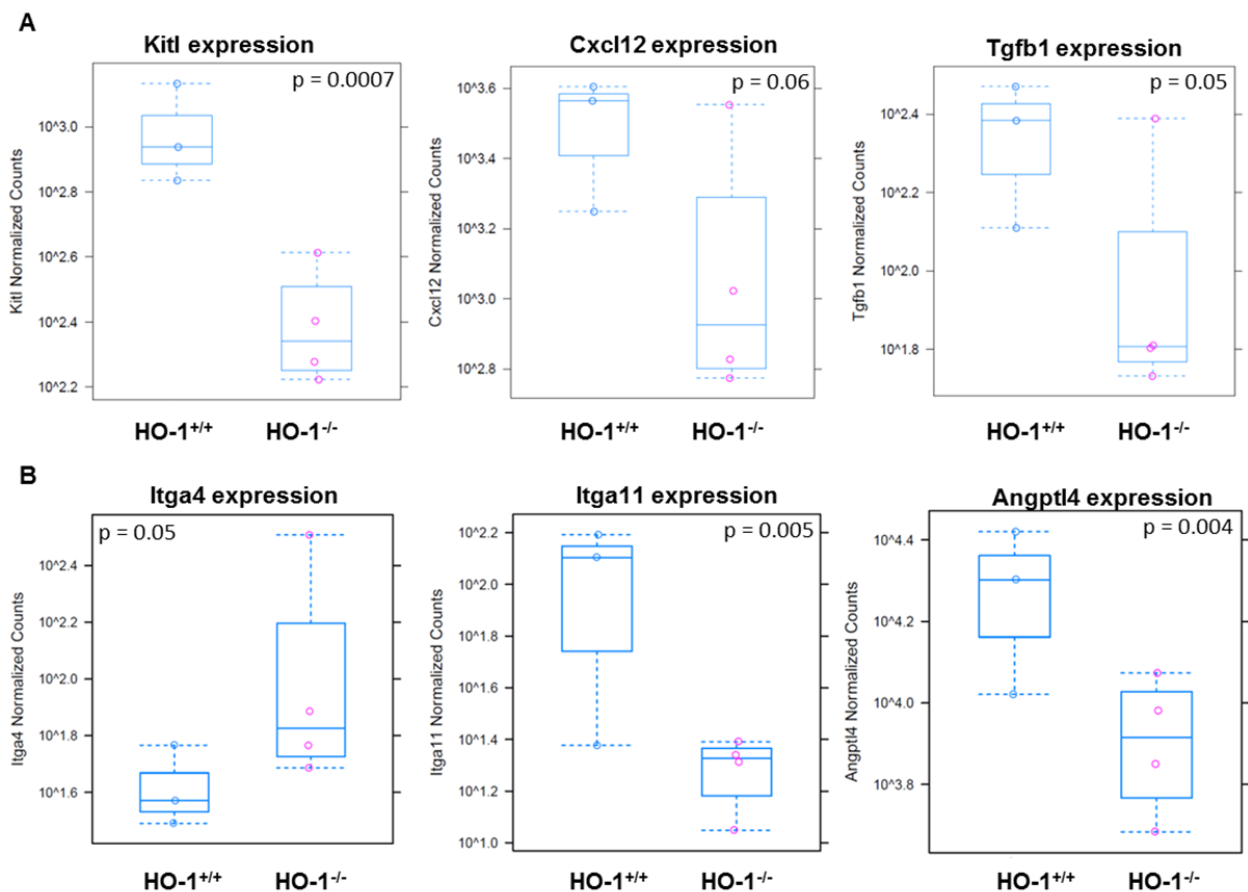
Fig. 3.26 *(A) Expression of selected crucial cytokines regulating LT-HSC function and quiescence produced by CD31$^+$Sca-1^{high} EC and (B) selected cell surface molecules with altered expression in HO-1$^{-/-}$ CD31$^+$Sca-1^{high} EC.*

The GSEA and enrichment analysis of CAR transcriptome of HO-1$^{+/+}$ and HO-1$^{-/-}$ mice also revealed alterations in expression of some hematopoietic cytokines and adhesion molecules (Tab 3.7, 3.8), however the overall changes were less pronounced than in CD31^{+}Sca-1^{high} EC cells (Fig. 3.28, 3.29). CAR cells highly expressed *Kitl* and *Cxcl12*, but lack of HO-1 only slightly tend to decrease their expression (Fig. 3.30A). The *Tgfb1* is also expressed by CAR cells, but oppositely to CD31^{+}Sca-1^{high} EC cell, HO-1-deficiency upregulate its expression in CAR cells (Fig. 3.30A). Among adhesion molecules we identified that HO-1-deficiency resulted in induction of *Itga2b* and *Cd34* expression (Fig. 3.30B). Similarly to CD31^{+}Sca-1^{high} EC cells CAR cells express *Angplt4* and lack of HO-1 also decreased its levels (Fig.3.30B).

The GSEA analysis revealed several other biological processes changed in HO-1$^{-/-}$ CAR cells that may be important in functioning of the LT-HSC niche (Tab. 3.7, 3.8). Firstly, the several genes regulating the angiogenesis and proliferation of endothelial cells were differentially regulated. Given that CAR and EC cells together compose the perivascular niche of LT-HSC, altered interaction between CAR and EC cells may affect the organization of niche and subsequently the LT-HSC. Secondly, expression of several genes involved in production of extracellular matrix were changed (Tab. 3.7, 3.8), what also may disturb architecture of the niche.

Finally, the transcriptome of HO-1$^{-/-}$ CAR cells indicated that they had upregulated oxidative metabolism and expressed more genes connected with metabolism of ROS. Consequently, the genes connected with "Oxidative Stress Induced Senescence" were upregulated (Tab. 3.7).

As in all other groups, the HO-1$^{-/-}$ CAR cells had altered interferons type I and II signaling pathways (Tab. 3.7), while did not produced interferons. Some of the cell cycle connected genes were also upregulated in HO-1$^{-/-}$ CAR cells (Tab. 3.7).

Fig. 3.27 *Diagram showing expression of cell adhesion molecules in HO-1$^{-/-}$ CD31^{+}Sca-1^{high} EC*

ReactomeID	Description	set size	enrichment score	pvalue	p.adjust
5991537	Initial triggering of complement	12	0.80	0.00	0.02
5991746	WNT mediated activation of DVL	8	0.73	0.02	0.11
5991126	Dimerization of procaspase-8	9	0.72	0.01	0.06
5992066	Interferon gamma signaling	101	0.70	0.00	0.02
5992328	CASP8 activity is inhibited	10	0.70	0.01	0.09
5992067	Interferon Signaling	140	0.66	0.00	0.02
5992086	TRAF3-dependent IRF activation pathway	14	0.65	0.00	0.06
5992064	The NLRP3 inflammasome	12	0.64	0.01	0.11
5992354	DNA methylation	32	0.62	0.00	0.02
5991797	PRC2 methylates histones and DNA	40	0.62	0.00	0.02
5992077	Interferon alpha/beta signaling	21	0.61	0.00	0.06
5992141	Antigen processing-Cross presentation	99	0.60	0.00	0.02
5992039	Interleukin receptor SHC signaling	26	0.58	0.01	0.07
5991616	Packaging Of Telomere Ends	20	0.55	0.02	0.12
5991303	Cytokine Signaling in Immune system	271	0.53	0.00	0.02
5991301	Interleukin-2 signaling	41	0.52	0.00	0.05
5992037	Interleukin-3, 5 and GM-CSF signaling	42	0.52	0.00	0.02
5991507	Respiratory electron transport	65	0.52	0.00	0.02
5991358	DNA Damage Bypass	43	0.49	0.00	0.03
5991206	Epigenetic regulation of gene expression	68	0.46	0.00	0.03
5991018	Oxidative Stress Induced Senescence	72	0.45	0.01	0.06
5992367	Transcriptional regulation by small RNAs	71	0.44	0.00	0.03
5991625	Senescence-Associated Secretory Phenotype (SASP)	62	0.44	0.01	0.06
5991547	RIG-I/MDA5 mediated induction of IFN-alpha/beta pathways	54	0.43	0.00	0.06
5991508	Respiratory electron transport, ATP synthesis by chemiosmotic coupling, and heat production by uncoupling proteins.	86	0.43	0.00	0.03
5991506	Chromosome Maintenance	72	0.40	0.01	0.10
5991342	L1CAM interactions	77	0.38	0.01	0.11
5992320	HATs acetylate histones	117	0.37	0.01	0.06
5991302	Signaling by Interleukins	104	0.37	0.00	0.04
5991011	Cellular Senescence	122	0.36	0.01	0.08
5991182	C-type lectin receptors (CLRs)	119	0.35	0.01	0.06
5990991	Mitotic G1-G1/S phases	122	0.34	0.01	0.09
5991210	Signaling by Rho GTPases	337	0.33	0.00	0.02
5990979	Cell Cycle, Mitotic	401	0.32	0.00	0.02
5991209	RHO GTPase Effectors	226	0.32	0.00	0.04
5990980	Cell Cycle	485	0.32	0.00	0.02
5992313	Chromatin modifying enzymes	209	0.31	0.01	0.08
5992314	Chromatin organization	209	0.31	0.01	0.08
5991100	Metabolism of proteins	556	0.28	0.00	0.02
5991024	Metabolism	1443	-0.27	0.00	0.02
5991148	Signaling by PDGF	167	-0.33	0.01	0.09
5991413	Integrin cell surface interactions	80	-0.39	0.01	0.10
5991956	Cell junction organization	66	-0.39	0.01	0.11
5992176	Degradation of the extracellular matrix	119	-0.40	0.00	0.04
5991633	Transport of glucose and other sugars, bile salts and organic acids, metal ions and amine compounds	93	-0.43	0.00	0.02
5991414	Extracellular matrix organization	253	-0.45	0.00	0.02
5992175	Collagen degradation	59	-0.46	0.00	0.04
5992282	ECM proteoglycans	63	-0.47	0.00	0.04
5992182	Collagen formation	68	-0.51	0.00	0.02
5992206	Elastic fibre formation	39	-0.52	0.00	0.02
5992205	Molecules associated with elastic fibres	35	-0.52	0.00	0.04
5992212	Collagen biosynthesis and modifying enzymes	57	-0.52	0.00	0.02
5991636	Iron uptake and transport	42	-0.52	0.00	0.02
5991935	Circadian Clock	26	-0.53	0.01	0.07
5992047	BMAL1:CLOCK,NPAS2 activates circadian gene expression	15	-0.68	0.00	0.05
5992277	NOTCH2 intracellular domain regulates transcription	10	-0.69	0.01	0.07
5991637	Heme biosynthesis	10	-0.73	0.01	0.07
5991478	Metabolism of porphyrins	17	-0.75	0.00	0.02
5991992	Passive transport by Aquaporins	11	-0.87	0.00	0.02
5992146	O2/CO2 exchange in erythrocytes	8	-0.92	0.00	0.02

Tab. 3.7 *Selected hits revealed by GSEA enrichment analysis of CAR transcriptome*

GO ID	Description	Set Size	Overlap	Odds Ratio	P-value
GO:0001886	endothelial cell morphogenesis	12	5	15.10	0.00
GO:0035455	response to interferon-alpha	15	6	14.10	0.00
GO:0034340	response to type I interferon	21	7	10.60	0.00
GO:0033690	positive regulation of osteoblast proliferation	11	3	7.89	0.01
GO:0033687	osteoblast proliferation	16	4	7.04	0.00
GO:0090025	regulation of monocyte chemotaxis	16	4	7.02	0.01
GO:0043518	negative regulation of DNA damage response, signal transduction by p53 class mediator	12	3	7.01	0.02
GO:1902165	regulation of intrinsic apoptotic signaling pathway in response to DNA damage by p53 class mediator	12	3	7.01	0.02
GO:0070098	chemokine-mediated signaling pathway	44	10	6.23	0.00
GO:0050873	brown fat cell differentiation	36	8	6.04	0.00
GO:0071425	hematopoietic stem cell proliferation	18	4	6.01	0.01
GO:0033622	integrin activation	16	3	4.85	0.03
GO:0001953	negative regulation of cell-matrix adhesion	27	5	4.79	0.01
GO:2000377	regulation of reactive oxygen species metabolic process	44	8	4.74	0.00
GO:0038066	p38MAPK cascade	17	3	4.51	0.04
GO:0042744	hydrogen peroxide catabolic process	17	3	4.51	0.04
GO:0036230	granulocyte activation	23	4	4.43	0.02
GO:0071634	regulation of transforming growth factor beta production	23	4	4.43	0.02
GO:0034341	response to interferon-gamma	18	3	4.24	0.05
GO:0001937	negative regulation of endothelial cell proliferation	30	5	4.21	0.01
GO:0043567	regulation of insulin-like growth factor receptor signaling pathway	24	4	4.21	0.02
GO:0051882	mitochondrial depolarization	18	3	4.21	0.05
GO:0071604	transforming growth factor beta production	24	4	4.21	0.02
GO:1901031	regulation of response to reactive oxygen species	30	5	4.21	0.01
GO:0032611	interleukin-1 beta production	43	7	4.10	0.00
GO:0016525	negative regulation of angiogenesis	70	11	3.95	0.00
GO:0060350	endochondral bone morphogenesis	52	8	3.84	0.00
GO:0048010	vascular endothelial growth factor receptor signaling pathway	42	6	3.51	0.01
GO:0002274	myeloid leukocyte activation	145	20	3.41	0.00
GO:0010712	regulation of collagen metabolic process	36	5	3.40	0.02
GO:0048146	positive regulation of fibroblast proliferation	51	7	3.35	0.01
GO:0032606	type I interferon production	45	6	3.24	0.02
GO:0032964	collagen biosynthetic process	38	5	3.19	0.03
GO:0045446	endothelial cell differentiation	77	10	3.15	0.00
GO:0046323	glucose import	63	7	2.63	0.02
GO:0045765	regulation of angiogenesis	129	14	2.60	0.00
GO:0046889	positive regulation of lipid biosynthetic process	67	7	2.46	0.03
GO:0034440	lipid oxidation	77	8	2.44	0.02
GO:0010906	regulation of glucose metabolic process	97	10	2.43	0.01
GO:0001935	endothelial cell proliferation	99	10	2.37	0.01
GO:0030099	myeloid cell differentiation	152	15	2.34	0.00
GO:0007229	integrin-mediated signaling pathway	73	7	2.23	0.05
GO:0030198	extracellular matrix organization	169	16	2.23	0.00
GO:0060348	bone development	168	16	2.23	0.00
GO:0001936	regulation of endothelial cell proliferation	87	8	2.13	0.04
GO:0043542	endothelial cell migration	132	12	2.11	0.02
GO:0070371	ERK1 and ERK2 cascade	200	18	2.10	0.00
GO:0045785	positive regulation of cell adhesion	303	27	2.08	0.00
GO:0001503	ossification	360	30	1.94	0.00
GO:0002244	hematopoietic progenitor cell differentiation	187	15	1.84	0.02
GO:0001666	response to hypoxia	165	13	1.81	0.04
GO:0097193	intrinsic apoptotic signaling pathway	259	20	1.77	0.02
GO:0080090	regulation of primary metabolic process	4640	243	1.21	0.01

Tab 3.8. *Selected hits revealed by GO BP database pathway enrichment analysis of CAR transcriptome*
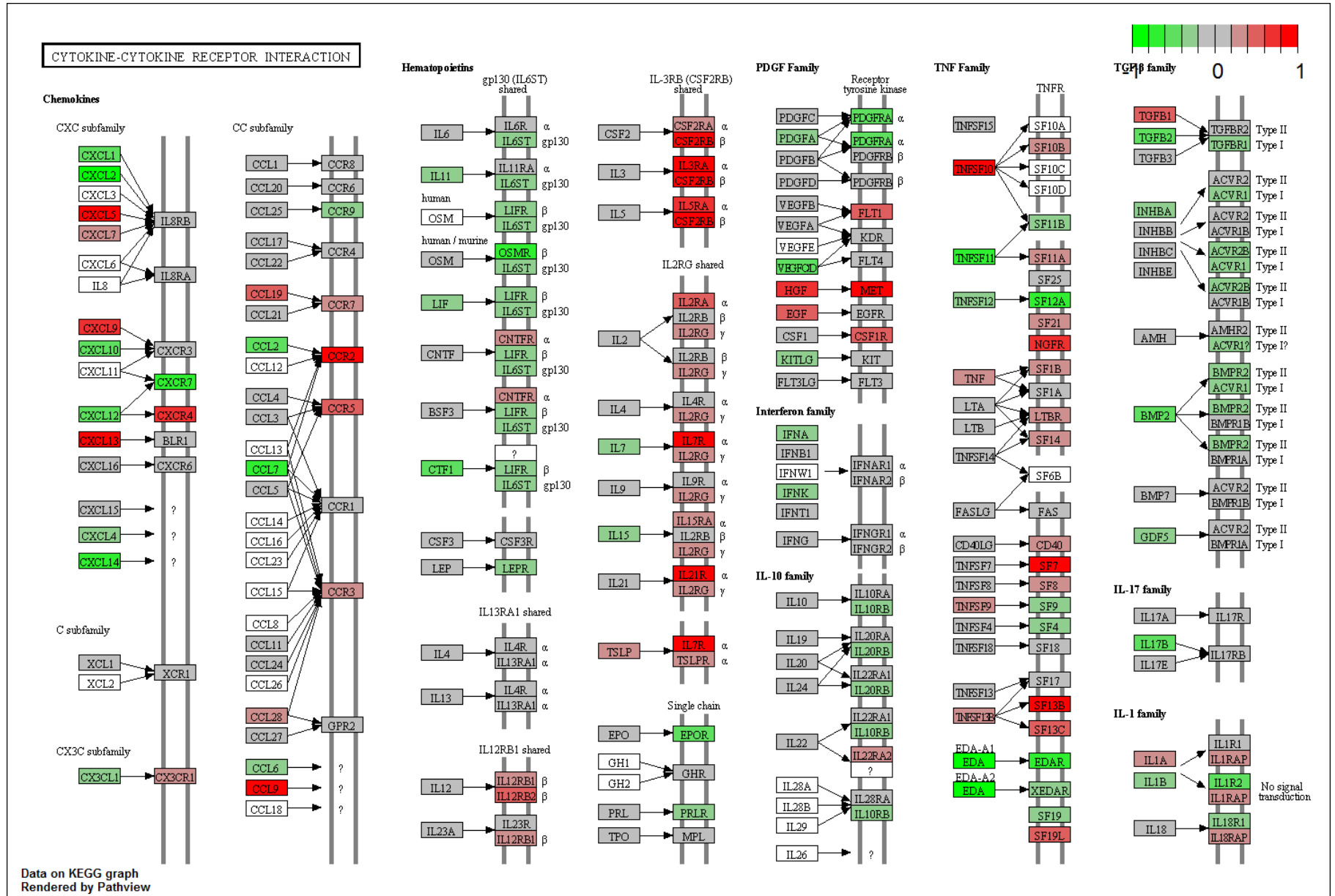
Fig. 3.28 Diagram showing expression of selected cytokines and their expression in HO-1$^{-/-}$ CD31^{+}Sca-1^{high} CAR
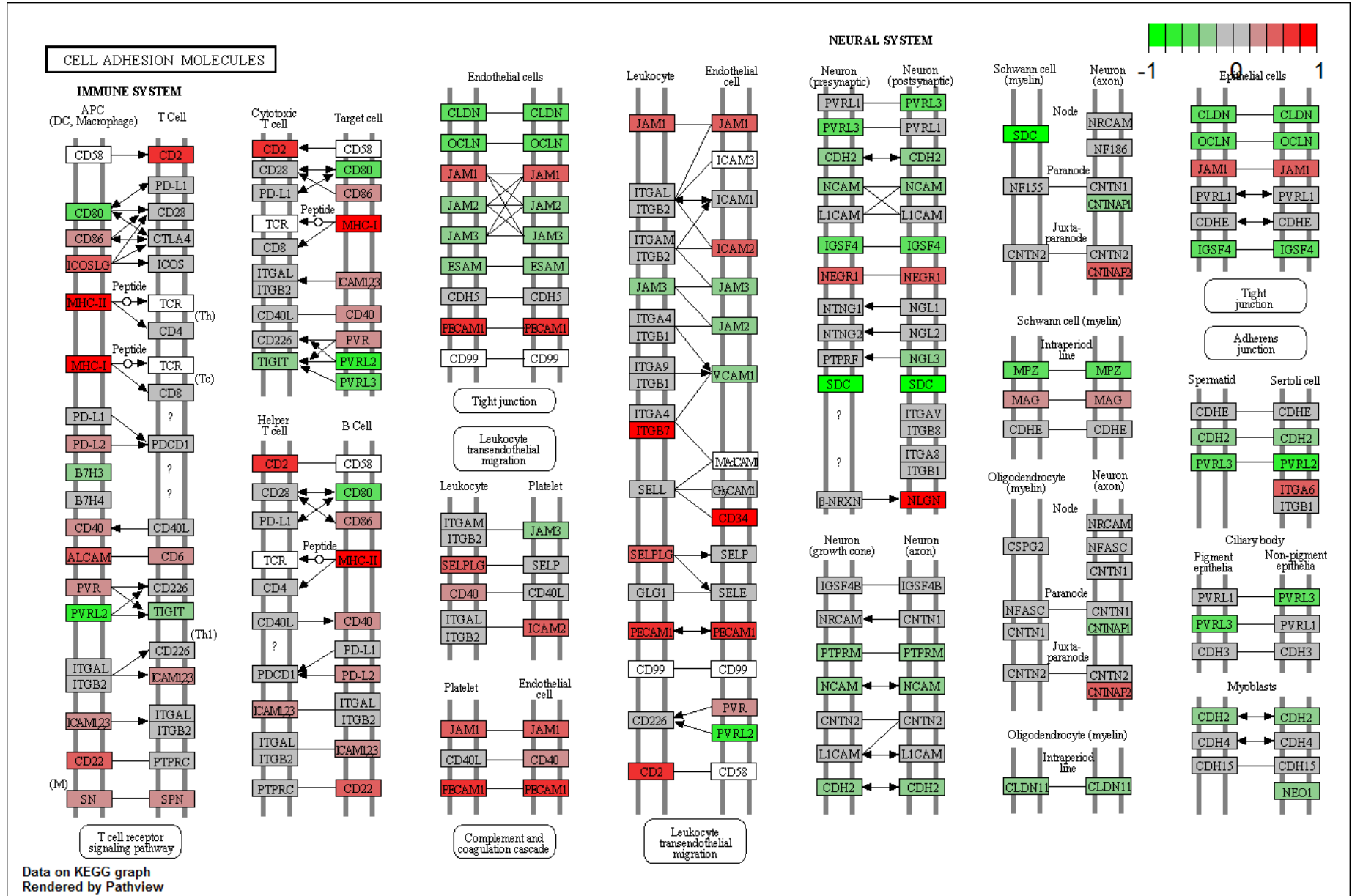
Fig. 3.29 Diagram showing expression of cell adhesion molecules in HO-1$^{-/-}$ CD31$^+$Sca-1^{high} CAR
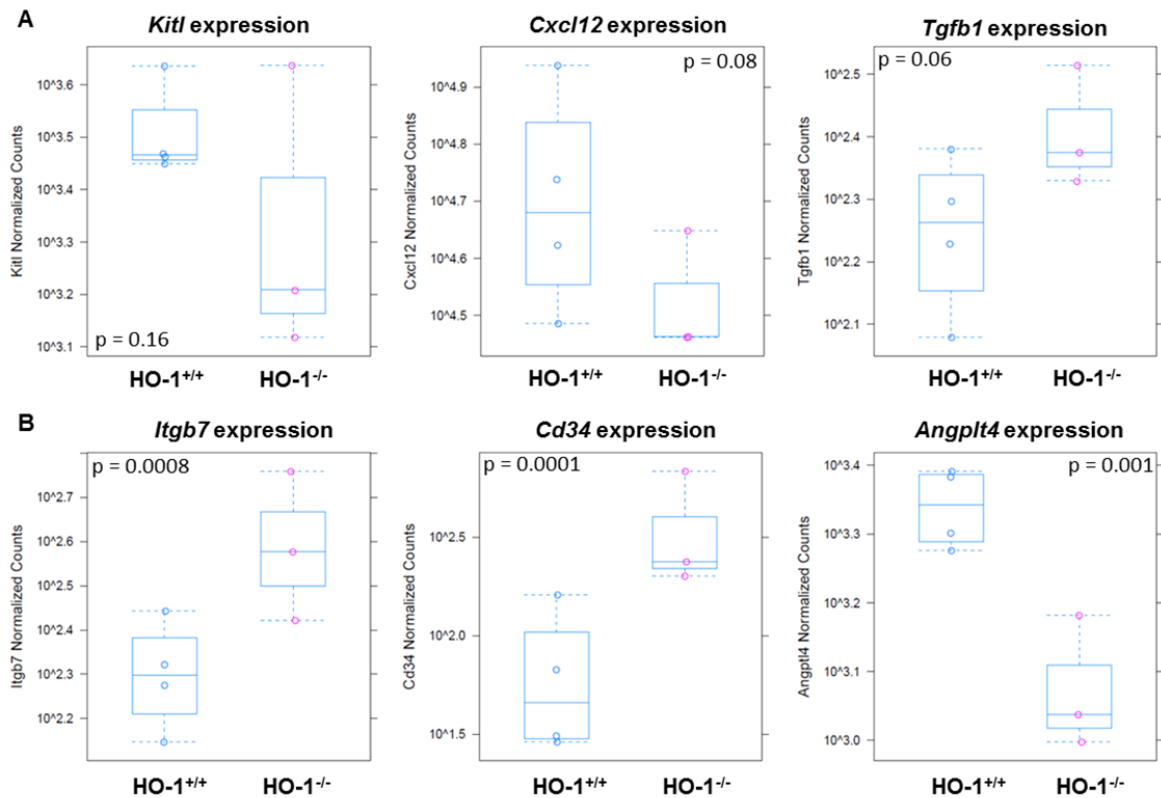
Fig. 3.30 (*A*) *Expression of selected crucial cytokines regulating LT-HSC function and quiescence produced by CAR and (**B**) selected cell surface molecules with altered expression in HO-1$^{-/-}$ CAR.*

The expression of HO-1 decreases with age

Our experiments on HO-1$^{-/-}$ mice model indicated that lack of HO-1 drives the premature aged-like phenotype of LT-HSC. However, if the expression of HO-1 is not decreased during aging, its physiological role in regulation of aging will not be justifiable. Therefore we checked how the age affects HO-1 expression in hematopoietic stem and progenitors as well as in CAR and CD31$^+$Sca-1^{high} EC.

Despite the general low expression of HO-1 in all hematopoietic stem and progenitor pool in comparison to non-hematopoietic niche cells (Fig. 3.22B), we observed that in young animals expression of HO-1 is increased during differentiation of LT-HCS toward ST-HSC and MPP (Fig. 3.31A). Oppositely, in old animals the HO-1 expression did not increase, but even decreased during the LT-HSC differentiation (Fig 3.31A).

In case of the HO-1 highly expressing CD31$^+$Sca-1^{high} EC and CAR cells we observed significantly decreased expression of HO-1 protein in old mice, with the biggest change in

CD31$^+$Sca-1^{high} EC (3.31B). In addition, the number of CD31$^+$Sca-1^{high} EC was also lower in old mice, what further decreased the total HO-1 expression in stem cell niche in elderly individuals (Fig. 3.31C). Concluding, in all tested populations, the HO-1 expression was lower in aged animals and thus it is likely that decreasing HO-1 expression in the stem cell niche may be one of the factors that drives age-related changes in LT-HSC.
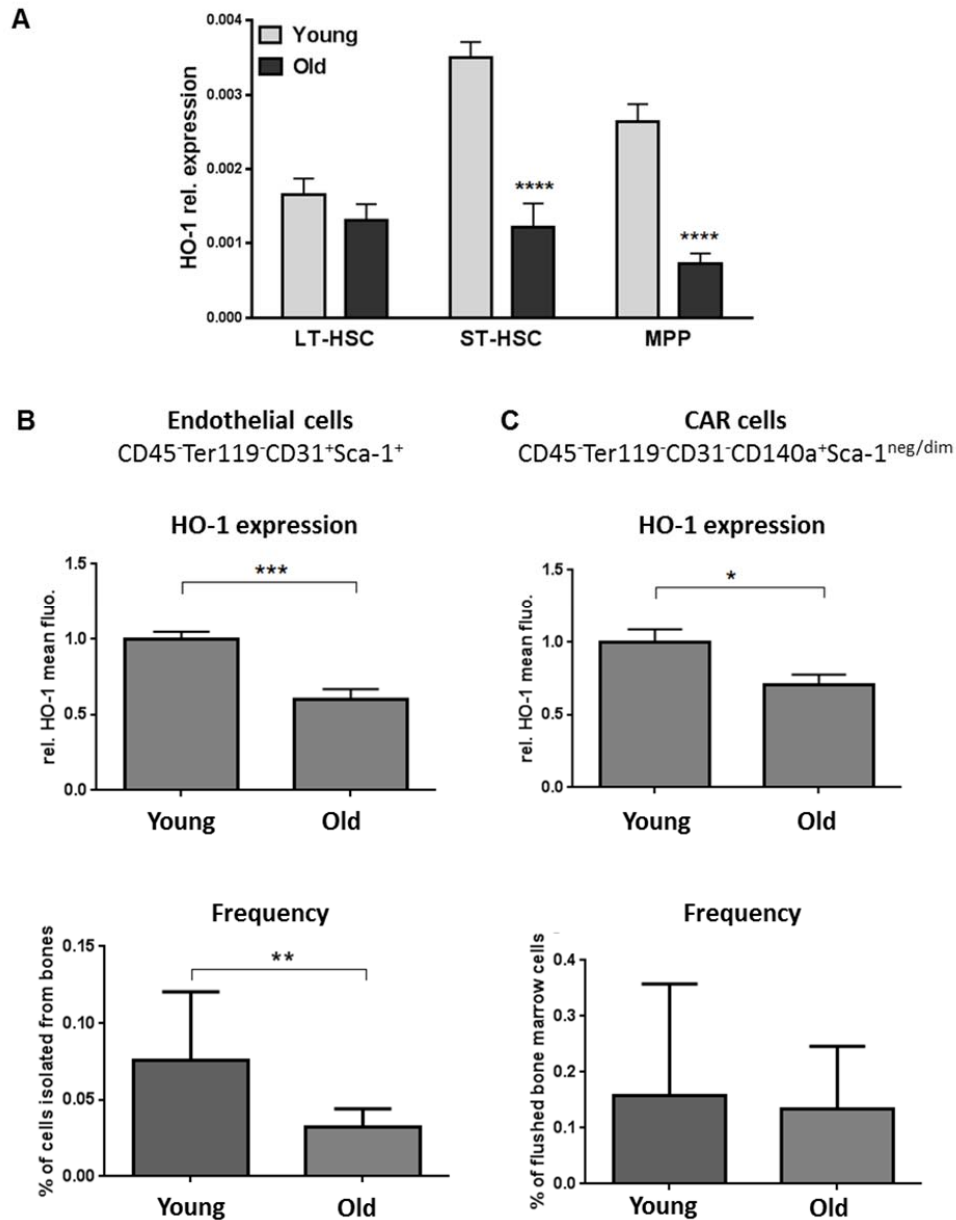
Fig. 3.31 *The changes of HO-1 expression with age in (**A**) hematopoietic stem and progenitor cells and (**B**) in CD31$^+$Sca-1^{high} EC and CAR cells. (**C**) The frequency of CD31$^+$Sca-1^{high} EC and CAR cells in young and old animals.*

Carbon monoxide is potential HO-1 dependent factor regulating LT-HSC

Not only the protein factors may explain the HO-1-dependent activity in the niche. We wanted to check if carbon monoxide (CO) - the gaseous product of HO-1 enzymatic reaction – mediates the HO-1 function in stem cell niche. Firstly, we observed moderately lower CO concertation in flushed BM in 3-month old or older mice. The CO concentration in BM did not decrease with age. Activity of heme oxygenases in flushed BM, measured as ability to produce CO in a given time after addition of substrate (NADPH), exhibited the same pattern.

However, the CO concentration in whole BM may not reflect the actual CO concentration in LT-HSC niche. To check if the CO is required for maintaining the LT-HSC function, we isolated LT-HSC and kept them ex-vivo for 36 hours in serum free medium with SCF and TPO in $3\%O_2$ atmosphere supplemented additionally with 250 ppm CO and then transplanted to irradiated recipients. Till the date of preparing the thesis, we analyzed only short-term chimerism (6 weeks after the transplant) and did not observed any differences between LT-HSC that were kept with or without CO supplementation. The transplanted mice are kept in the experiment to monitor long-term chimerism that will reflect function of the LT-HSC.
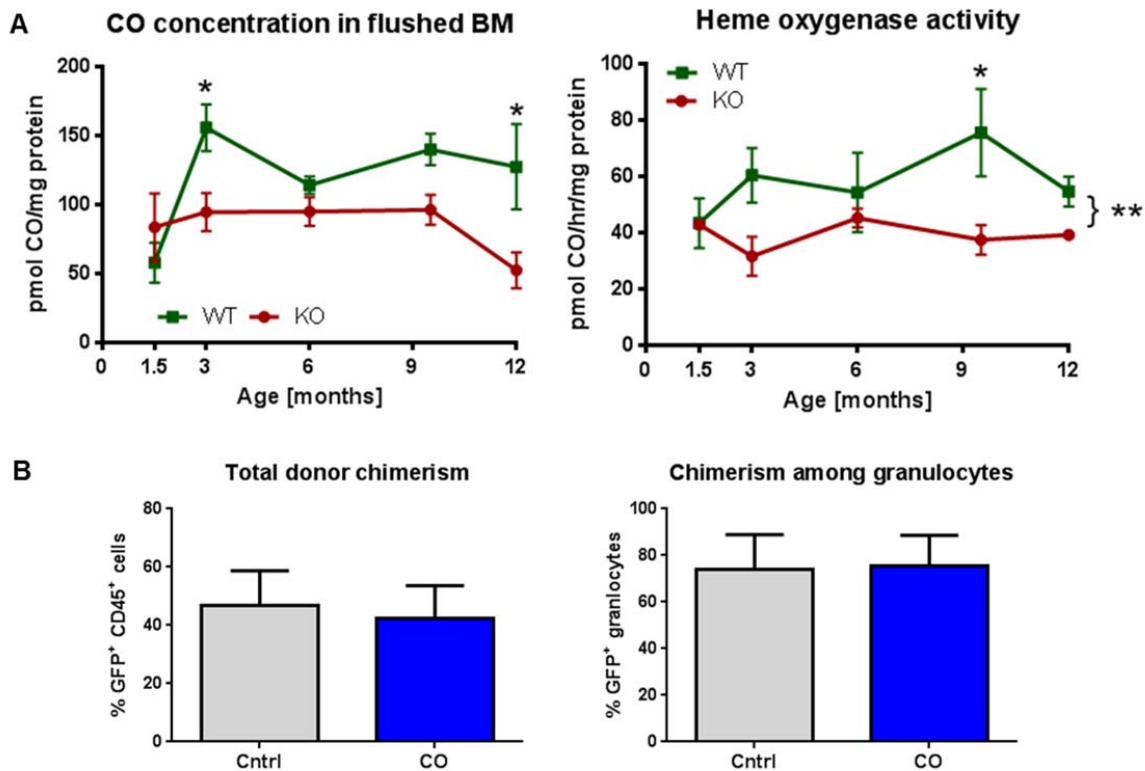
Fig. 3.32 (A) *Concentartion of CO and heme oxygenase activity in whole BM in HO-1$^{-/-}$ and HO-1$^{+/+}$ mice with age (**B**) Donor derived short-term chimerism (6 weeks) after transplanting LT-HSC kept in atmosphere with or without CO.*

DISCUSSION

PART I – Verification if the non-hematopoietic fraction of Lin⁻Sca-1⁺CD45⁻ from adult bone marrow give rise to blood cells

This part of discussion was already published in [228] and [248]:

Szade et al. Murine Bone Marrow Lin−Sca-1+CD45− Very Small Embryonic-Like (VSEL) Cells Are Heterogeneous Population Lacking Oct-4A Expression. (2013) **PLoS ONE** *8(5): e63329.*

Szade et al. *Comment on: The proper criteria for identification and sorting of very small embryonic-like stem cells, and some nomenclature issues. (2014)* **Stem Cells Dev**. *Apr 1;23(7):714-6.*

In the present study we investigated the mouse bone-marrow derived cells with Lin⁻Sca-1⁺CD45⁻ phenotype and small size. Such cells, named VSELs (very small embryonic-like cells), were described in 2006 by Kucia and colleagues as a homogenous population of pluripotent cells [56] or population enriched in pluripotent cells [231], expressing Oct-4 marker, and acting among others as precursors of long-term repopulating hematopoietic stem cells (LT-HSC) [235]. Our results indicate, however, that the mouse BM population defined as Lin⁻Sca-1⁺CD45⁻ FSC^{low} is heterogeneous and does not express Oct-4.

Using two more markers, c-Kit and KDR, we could distinguish three subsets within the Lin⁻Sca-1⁺CD45⁻ cells: c-Kit⁻KDR⁺, c-Kit⁻KDR⁻ , and c-Kit⁺KDR⁻. Events positive for both, c-Kit and KDR, detected in some samples, were too rare to allow reliable measurement by flow cytometry. Because c-Kit⁻KDR⁺ fraction consisted of cells with relatively big diameter, it did not fulfill VSEL size criterion and was excluded from further analysis. On the other hand, the entire c-Kit⁺KDR⁻ population and part of c-Kit⁻KDR⁻ subset contained far smaller cells, in compliance with definition of VSELs (Fig 3.1C,D, Fig. 2.4). Among them, c-Kit⁻KDR⁻ cells with lower FSC values were apoptotic, as they bound annexin V. We are aware that RBC-derived microvesicles (RMV) released during erythrocyte lysis may transfer phosphatidylserine (PS) to the surface of other cells, resulting in false-positivity for annexin V and erythrocyte marker glycophorin A [249]. However, it is not likely to be a case, as cells with erythrocyte marker Ter119⁺ (glycophorin A-associated protein) [250] were excluded from analysis together with lineage committed populations. Additionally, other subpopulations present in the same samples were annexin V negative and there are no data suggesting selective binding of RMV to Lin⁻Sca-

1$^+$CD45$^-$c-Kit$^-$KDR$^-$ cells. Thus is seems that Lin$^-$Sca-1$^+$CD45$^-$c-Kit$^-$KDR$^-$FSC^{low} cells were indeed apoptotic. Distinguishing a tentative stem cells fraction within this population, based on small size only, is not possible in reproducible way, unless discovery of next marker, better defining viable cells. Therefore, our further work was focused on Lin$^-$Sca-1$^+$CD45$^-$c-Kit$^+$KDR$^-$ subset.

The Lin$^-$Sca-1$^+$CD45$^-$c-Kit$^+$KDR$^-$ cells were annexin V negative, and showed homogeneity of the size distribution, with diameter of 6.8 ± 2.4 μm, which was similar to that of erythrocytes (6.2 ± 0.6 μm) and significantly smaller than in control Lin$^-$Sca-1$^+$CD45$^+$c-Kit$^+$ hematopoietic progenitors (11.4 ± 0.7 μm). Inconsistencies in description of the exact size of VSELs in previous reports make them difficult for a direct comparison with our data. Zuba-Surma and co-workers calculated the murine BM-derived VSEL size as 3.63 ± 0.27 μm and Lin$^-$Sca-1$^+$CD45$^+$ HSCs as 6.58 ± 1.09 μm [251]. Both these values are smaller than measured by us, although the HSC:VSEL size ratio is similar (1.8 versus 1.7 in previous and current report, respectively). In fact, in our hands the analysis of very small events (with diameter of 2-4 μm) using the ImageStream system (applied by Zuba-Surma and co-workers) did not allow for reliable detection of viable cells (Fig. 2.4B). Importantly, in another report by the same researchers, size of Lin$^-$Sca-1$^+$CD45$^-$ cells isolated from different organs varied profoundly ranging from 3.63 ± 0.27 μm for VSELs obtained from bone marrow to 6.81 ± 0.09 μm, 6.90 ± 0.29 μm, and 8.40 ± 0.17 μm for VSELs obtained from murine spleen, heart and liver, respectively [231].

As a principle for VSEL analysis, a population of events with diameter of 2-10 μm is used, based on the size calibration beads [231, 235, 252]. It also should be taken into consideration that fixation, and following preparation of cells for transmission electron microscopy or for intracellular staining, does affect cell size [253], what may explain a difference between our measurement (done on non-fixed cells) and earlier analyses performed on fixed cells [56, 231]. In addition, assessing the real diameter of cells using the synthetic beads as a size reference is of limited accuracy, as the light scattered along the laser axis (FSC) is not solely dependent on cell size, but also on the refractive index which can be different for cells and beads, and which can be affected by physiological state of a cell [254]. For example, dead cells typically have a lower refractive index due to leaky outer membranes, give lower FSC signals, and thus appear smaller than healthy cells. Concluding, it is highly probable that c-Kit$^+$KDR$^-$

subset of Lin⁻Sca-1⁺CD45⁻ cells with their relative small size, was included within VSELs population in previous studies.

Noteworthy, the heterogeneity of murine Lin⁻Sca-1⁺CD45⁻ cells was recently shown with respect to the expression of platelet-derived growth factor-α receptor (PDGFR-α), which is predominantly absent on LKS cells [255]. The PDGFR-α positive fraction was suggested as overlapping with CD105 positive multipotent mesenchymal precursors identified in murine bone marrow [256]. These cells, however, are different from our subpopulation, as they do not express c-Kit [256].

VSELs are described by their discoverers as the cells expressing Oct-4, what can be a feature characteristic for pluripotent cells [56, 231, 232, 235, 257–259]. Oct-4 transcription factor forms two splicing forms: whilst Oct-4A has been confirmed as the isoform responsible for maintaining the embryonic stem cell identity, Oct-4B localizes mainly in the cytoplasm of pluripotent cells, various non-pluripotent cells, and somatic cells, fails to confer ES cell self-renewal and pluripotency, and is thought to be involved in cell stress responses [260–262]. Recent study demonstrated that mouse Oct-4B can be translated into three distinct isoforms (Oct4B-247aa, Oct4B-190aa, and Oct4B-164aa) and, in contrast to Oct-4A, it is not a functional factor in process of reprogramming somatic cells to induced pluripotent stem cells (iPSC) [262]. Therefore, in research regarding pluripotency, it is necessary to distinguish Oct4A and Oct4B variants.

Importantly, using the primers recognizing specifically a functional Oct-4A [217] we were not able to detect the Oct-4A expression at mRNA level either in whole murine bone marrow or in sorted Lin⁻Sca-1⁺CD45⁻FSC^{low} cells. We applied both qRT-PCR in RNA isolated from sorted Lin⁻Sca-1⁺CD45⁻FSC^{low} subpopulation as well as qRT-PCR in the sorted single Lin⁻Sca-1⁺CD45⁻FSC^{low} cells, with the same outcome: no specific product for Oct-4A or Oct-4B was detected, despite strong specific signals from ESD3 murine embryonic cells used as a positive control. Our observation is consistent with studies showing the lack of Oct-4 expression in bone marrow of Oct-4-GFP transgenic mice [60], and with observation that genetic ablation of Oct-4 in several tissues did not affect homeostasis or regeneration capacity in adult mice [59].

We suppose that disparity between current and earlier analyzes of Oct-4 expression in VSELs can result from application of different primer sequences. False-positive findings caused by detection of Oct-4 pseudogenes with non-specific primers have already been evidenced [263–

265]. Here we demonstrated that primers used in the first paper by Kucia and co-workers [56] and then in the other reports [231, 232] may easily produce false positive results. Using them, we obtained an Oct-4 signal of expected length both in whole bone marrow and in sorted Lin⁻Sca-1⁺CD45⁻FSC^low VSELs, however, the product was transcribed from a pseudogene template. This false-positive reaction was not effectively prevented by DNase I treatment, what is in agreement with data described by Wang and Dai [266].

In several studies published by the same group, the Oct-4 expression in VSELs was demonstrated with additional methods – RT-PCR using re-designed primers [231, 235, 258], flow cytometry and immunohistochemistry for Oct-4 protein detection [231, 258] or analysis of Oct-4 promoter methylation [258]. Nevertheless, re-designed primers used in these studies [231, 235, 258] can still recognize both Oct-4A and Oct-4B isoforms [NM013633.3 and NM001252452.1] giving the products of the same length (51 bp). These primers allowed us to detect strong expression of Oct4 in iPSC but did not give a specific signal in our samples of total bone marrow or sorted Lin⁻Sca-1⁺CD45⁻FSC^low cells (data not shown). Similarly, Affymetrix microarrays used for global transcriptome profiling [259] is supposed to detect both Oct-4A and Oct-4B [264]. On the other hand, it is very difficult or even impossible to distinguish Oct-4A and Oct-4B proteins with antibodies currently available [264–267]. Although Oct-4A is present mostly in nucleus and Oct-4B preferentially localizes to cytoplasm, the localization itself cannot be treated as isoform marker, because Oct-4B can also display nuclear translocation [264, 266]. Interestingly, Oct-4 was found by another group in a low number of cells throughout the adult human pancreas [268]. The cells were very small (1.5 – 3 μm) and could be described as VSELs, but Oct-4 staining was visible only in cytoplasm [268]. Finally, analysis of methylation of Oct-4 promoter may indicate an active transcription of the gene but is not clear whether it can reveal the specific expression of Oct-4A. Altogether, it seems that the previous reports, which show Oct-4 in murine VSELs, cannot confirm the presence of Oct-4A isoform. Thus, the expression of functional Oct-4 in VSELs is still a matter of debate, while our results showed the absence of either Oct4A or Oct4B mRNA in murine bone marrow-derived Lin⁻Sca-1⁺CD45⁻FSC^low cells. Noteworthy, similar conclusion was driven recently from the study on human VSELs performed by Alt and co-workers [61]. The level of Oct4 signal, detected with Affymetix microarray probes (which bind both to functional gene and pseudogenes), was similar in VSELs and in B-cells used as negative control, and was significantly lower than in iPS or embryonic stem cells [61].

Lin$^-$Sca-1$^+$CD45$^-$c-Kit$^+$FSC^{low} subset of VSELs fulfills the LKS (Lin$^-$ c-Kit$^+$Sca-1$^+$) characteristics, so we tested whether it may contain cells with a hematopoietic stem cell potential. Single-cell assay performed in serum-free, chemically-defined medium showed that this subset, in contrast to Lin$^-$Sca-1$^+$CD45$^+$c-Kit$^+$ counterpart, did not give rise to hematopoietic colonies. This result confirms earlier observations, that freshly isolated Lin$^-$Sca-1$^+$CD45$^-$FSC^{low} VSELs do not show hematopoietic potential, but require co-culture with OP9 cells to acquire the HSC-like features [235]. However, it should be stressed that the colony growth observed after co-culture of VSELs with OP9 cells was not demonstrated for single cells, but for 10,000 cells seeded to each well [235]. As recently pointed out [61], the growth of hematopoietic colonies might result from inherited sorting impurities and potential presence of Lin$^-$Sca-1$^+$CD45$^+$ cells in the populations studied, especially when cells of different size (2-10 μm) [235] were harvested.

Therefore, we examined if Lin$^-$Sca-1$^+$CD45$^-$FSC^{low} fraction contains any cells with hematopoietic potential after priming with OP9 co-culture by applying experimental scheme that reduces risk of contamination caused by sorting impurities. However, Lin$^-$Sca-1$^+$CD45$^-$FCS^{low} cells isolated from GFP-expressing mice lost GFP expression after 4 days of co-culture with OP9 making single cell analysis impossible, in contrast to classical hematopoietic stem and progenitor cells population (Lin$^-$Sca-1$^+$CD45$^+$c-Kit$^+$). Next experiment that included higher number of cells and limiting dilution analysis also revealed no cell with clonogenic potential among aliquots of 100 Lin$^-$Sca-1$^+$CD45$^-$FCS^{low} cells.

These results suggest that murine Lin$^-$Sca-1$^+$CD45$^-$FSC^{low} VSEL population does not contain cells with hematopoietic potential. The same conclusion was drawn from the study, where human VSELs did not generate hematopoietic colonies either in stroma-supported or stroma-free cultures, and were described as dysfunctional cells with karyotypic abnormalities [61]. Although lack of proof is not a proof of absence, our results appear to support the recent papers questioning VSELs as pluripotent cells with hematopoietic potential [61, 255, 269].

In next step we examined if Lin$^-$Sca-1$^+$CD45$^-$c-Kit$^+$FSC^{low} cells can be included during regular gating scheme into the LT-HSC fraction [8, 22]. Noticeably, we found that among LKS CD34$^-$ subpopulation, the CD45-negative cells can be detected (LKS CD34$^-$CD45$^-$), but they did not accomplish all SLAM code criteria, established for LT-HSC [7]. Yet another marker defining the long-term repopulating stem cells, CD105 (endoglin) [12, 236], was highly expressed within SKL CD45$^-$CD34$^-$ fraction. Interestingly, although earlier reports on VSELs

indicated that these cells are CD105 negative [257] our analysis demonstrate that LKS CD45$^-$CD105$^+$ subpopulation, apart from showing some common antigens with LT-HSC, overlapped significantly with the Lin$^-$Sca-1$^+$CD45$^-$c-Kit$^+$FSC^{low} cells. Therefore we repeated the single-cells assay to check the hematopoietic potential of this fraction. Again, in contrast to the LKS CD45$^+$CD105^{dim} counterpart, the LKS CD45$^-$CD105$^+$ cells did not exhibit hematopoietic activity. Thorough analyzes of their viability revealed that LKS CD45$^-$CD105$^+$ cells display early apoptotic features, with still integral membrane (DAPI negative), without phosphatidylserine exposure (annexin V negative), but already with chromatin fragmentation process started (TUNEL positive), what explains negative results in the performed hematopoietic assays.

We noticed that several phenotypic features of SKL CD45$^-$CD105$^+$ events, namely the small size, high staining with nuclear dye, and integral membrane, can also characterize the nuclei expelled from erythroblasts [216]. What is more, due to differential protein sorting during erythroblast enucleation the Ter119 antigen is partitioned predominantly to the reticulocyte, and is barely detectable in extruded nuclei [270–273]. Similarly decreased expression was demonstrated for CD71 [273]. Our *ex vivo* analysis of the enucleation process of purified erythroblasts evidenced for the first time that some expelled nuclei possess, at least transiently, the LKS CD45$^-$CD105$^+$ or Lin$^-$Sca-1$^+$CD45$^-$FSC^{low} phenotypes. Obviously, nuclei expelled from erythroblasts are heterogenous and can be also annexin V positive, as was shown by Yoshida and co-workers in splenic erythroblasts [216]. For example, in the study on primitive erythropoiesis, the expelled nuclei presented mixed phenotype according to annexin V binding (49% 7AAD$^-$AnnexinV$^-$, 35% 7AAD$^-$AnnexinV$^+$) [245]. Keeping in mind that enucleation involves dynamic changes, resulting in heterogeneous phenotype of expelled nuclei [245], it is justifiable to suppose that expelled nuclei may only transiently show the SKL CD45$^-$CD105$^+$ or Lin$^-$Sca-1$^+$CD45$^-$ characteristics. Nevertheless, our results suggest that those populations isolated from the bone marrow may be contaminated with remnants of erythropoiesis.

VSELs were claimed to localize within side-population [56], what can support their viability and functional potential. However, in routine experiments they are identified by immunophenotyping only, as Lin$^-$Sca-1$^+$CD45$^-$FSC^{low} cells. In such analysis contamination of desired population with different events, is very possible. Moreover, equivalent phenotyping of human VSELs (Lin$^-$CXCR4$^+$CD45$^-$ FSC^{low}) gave a population containing the cells highly stained

with Hoechst 33342. This was interpreted as possible binuclearity, tetraploidy, or an unusual chromatin conformation in VSELs [61]. Our experiments suggest that similar effect might also result from contamination with pyrenocytes.

All our results showing lack of Oct-4 expression and hematopoietic potential of murine VSELs were independently confirmed, 3 months after publishing our study, by paper from Dr. Irving Weissman group [274]. They included additional, more stringent functional hematopoietic tests, including transplantation experiments and controls based on hematopoietic differentiation of embryonic stem cells [274].

Nevertheless, both studies were criticized by the Dr Ratajczak group [275]. The main argument was the supposed mistakes in gating caused VSELs to be excluded from the functional assays . Here, we discuss point-by-point these technical issues.

i) "Setting up an enlarged input gate on the FSC vs. SSC plot"[276]. It is well known that bone-marrow (BM) cells are extremely variable in size. In flow cytometry, FSC and SSC are rough parameters and the widely held notion that "forward scatter measures particle size" is oversimplified. Therefore, it is not possible to determine where the residual population of small cells clusters, based only on their FSC signal. Hence, first we gated all BM cells on the FSC/SSC plot, including events with low FSC and SSC signals, excluding only cellular debris. It is obvious that inclusion of larger objects does not exclude the smaller ones from analysis. In the next step, we selected cells fulfilling the immunophenotype criteria proposed for VSELs (Lin⁻ Sca-1⁺CD45⁻). Not mentioned in the comment by Suszynska et al., is the fact that in our analysis we backgated all potential subpopulations of VSELs on FSC *versus* SSC plot as a final step [228]. Only backgating allows determination of whether any cell subset separates into distinct cluster displaying low values of FSC and SSC. In summary, setting a larger FSC/SSC gate that includes all types of BM cells, especially when acquiring sufficient number of events to attain expected sensitivity, cannot exclude VSEL candidates from analysis.

ii) "additional loss of very small objects by their exclusion of VSELs by gating for singlets"[276]. As shown in Fig. 1B, we included analysis of pulse width for FSC and SSC parameters in our gating. Events with outstanding width signals represent doublets and cell debris with irregular shape. This strategy does not selectively exclude any small objects.

iii) "employing some selection markers that are unproven as VSEL markers (e.g., c-kit)"[276]. We showed that c-kit and KDR expression defined three distinct subpopulations among Lin⁻Sca-1⁺CD45⁻ phenotype that were proposed to identify VSELs [228]. However, we did not use c-kit and KDR to select VSELs in functional evaluations: Oct-4A expression and hematopoietic differentiation on OP9 cells [228]. For these assays we sorted events with general Lin⁻Sca-1⁺CD45⁻FSC^low phenotype [228] as proposed by the group that initially claimed to isolate VSELs [56]. Therefore, this argument cannot be used to explain the negative results obtained in the functional tests. Of note, the same group stated recently that "some murine VSELs express […] c-kit on their surface" [277].

iv) "focusing on some populations and discarding other fractions (potentially containing VSELs) based on results such as Annexin V binding"[276]. As explained above, in our experiments no potential VSEL fractions were discarded: functional tests were performed also on the whole, classically defined Lin⁻Sca-1⁺CD45⁻FSC^low population, without Annexin V staining [228]. We are aware that microvesicles released during erythrocyte lysis were suggested to transfer phosphatidylserine to the surface of other cells, resulting in a false-positivity for Annexin V and glycophorin A. However, cells with erythrocyte marker Ter119 (glycophorin A-associated protein) were excluded from our analysis together with lineage committed subsets. In fact, we showed a significant enrichment in the Annexin V⁺ cells among VSEL population when analyzing the heterogeneity of Lin⁻Sca-1⁺CD45⁻ phenotype [228]. Importantly, the Annexin V binding occurred selectively on Lin⁻Sca-1⁺CD45⁻cKit⁻KDR⁻ fraction, while almost no positive staining was detected on hematopoietic stem and progenitor cells that served as internal control [228]. There are no data suggesting a selective binding of erythrocyte-derived microvesicles to the surface of Lin-Sca-1+CD45-cKit-KDR- fraction.

v) "possibility of contamination by small CD45-negative erythroblasts"[276]. As far as we understand, Suszynska et al. suggest that we analyzed CD71⁺ erythroblast instead of VSELs due to our gating strategy. In fact, in our work we did show, that analyzed cells are mostly CD71 negative (Fig. 3.6D). Importantly, the CD71⁺ positive cells from the erythroid lineage, that exhibit lower Ter119 expression, are proerythroblasts – relatively large cells, displaying a high FSC signal, as described before [278]. Actually we demonstrated that nuclei expelled from erythroblasts during erythropoiesis exhibit a low FSC signal and may possess VSEL

immunophenotype [228]. Thus, we suggested that events attributed to a VSEL phenotype can be contaminated with these expelled nuclei.

In sum, we do not agree with objections raised by Suszynska et al. [276], and we maintain the conclusion that the hypothesis implying pluripotent features of VSELs in adult bone marrow has not been independently confirmed.

Altogether, our study does not support the hypothesis that cells of Lin$^-$Sca-1$^+$CD45$^-$ FSC^{low} phenotype represent a pluripotent population. In our hands these cells do not express pluripotent marker Oct-4A and do not show a hematopoietic potential in the single cell colony formation assay or after co-culture with OP9 cells. We found that Lin$^-$Sca-1$^+$CD45$^-$FSC^{low} population is heterogenous, enriched in early apoptotic cells, and can be potentially contaminated with the nuclei expelled from the erythroblasts. Thus, although this bone marrow-derived fraction potentially can include some multipotent cells, any definitive conclusions on their properties and potency require establishment of precise immonophenotyping, purification and propagation protocols.

PART II – Verification if HO-1 protects HSC from premature aging

HO-1 is widely recognized as cytoprotective enzyme [185]. In 1992 the first study done in animal model demonstrated the protective properties of HO-1 in model of acute stress caused by heme-protein overload [279]. Many following studies confirmed the beneficial role of HO-1 in different stress conditions in variety of tissues. Most of these studies concern the HO-1 function in cardiovascular bed [185], while the action of HO-1 in hematopoietic system was less intensively studied.

Nevertheless, some hematological disturbances in HO-1$^{-/-}$ mice were already described. The first report on HO-1$^{-/-}$ mice evidenced microcytic anemia caused by dysregulated iron homeostasis and elevated WBC levels [280]. Indeed, our analysis confirmed lower mean red blood cell volume (MCV) and mean red blood cell hemoglobin (MCH) – the symptoms of microcytic anemia (Fig. 3.11). Consequently we also detected the higher WBC levels (Fig. 3.11), suggesting the proinflammatory status of HO-1$^{-/-}$ mice. Previous studies linked this proinflammatory status with Th-1 shifted cytokine production [281]. Here, we showed that

despite the Th-1 proinflammatory profile, HO-1$^{-/-}$ mice are also characterized by expansion of myeloid fraction over the lymphoid fraction – the so called "myeloid bias".

Although, the HO-1 role was evidenced at several step of hematopoietic differentiation, such us erythropoiesis, thrombopoiesis and B-cells generation [182], till now only one study concerned HO-1 function in hematopoietic stem cell fraction . This study investigated HSC under actue heme stress in heterozygous HO-1$^{+/-}$ mice model and evidenced agumented HSC differentiation at cost of altered self-renewal, what resulted in faster HSC exhaustion [201]. Given that HO-1 is highly inducible and degrades highly proinflammatory free heme its role under acute heme overload is understandable. But despite earlier suggestion [282], there are no studies on potential importance of HO-1 in steady state conditions and aging of HSC. To our best knowledge this is the first study on HO-1 role in aging of LT-HSC in homeostatic conditions using the HO-1$^{-/-}$ mice model.

The primary finding of this study is the premature aging of young LT-HSC from HO-1$^{-/-}$ mice in steady state conditions. Young HO-1$^{-/-}$ LT-HSC showed several features of aged LT-HSC: expanded numbers, increased marker of DNA damage and general transcriptional profile resembling the old LT-HSC. Finally, similarly to aged LT-HSC, functional potential of young HO-1$^{-/-}$ LT-HSC was also decreased as shown by transplantation experiments (Fig. 3.16A).

LT-HSC reside in quiescent state and it is known that pushing them into proliferation, eg. by serial transplantation, causes their fast exhaustion [77]. Therefore, we checked the proliferation status of HO-1$^{-/-}$ LT-HSC and observed enhanced entrance into G1 cell cycle phase and increased proliferation rate (Fig. 3.13). These functional observations were further confirmed by transcriptome analysis evidencing dysregulation of genes controlling the cell cycle (Fig. 3.20). Thus, it is likely that permanent activation and proliferation in steady state conditions may be direct cause of premature aging of HO-1$^{-/-}$ LT-HSC (Fig. 4.1).

Apart from increased proliferation, the increased DNA repair markers (shown by γH2aX (Fig. 3.14) and transcriptome analysis (Tab. 3.1)) indicated DNA damage what also might be consider as potential factor inducing the premature aging. However, recent studies suggested that DNA damage is not likely to be driving force of LT-HSC aging, but rather the consequence of

intensive proliferation and loss of quiescence [82]. While the HO-1$^{-/-}$ LT-HSC extensively proliferate it is possible that DNA damage is the result of underwent cell divisions.
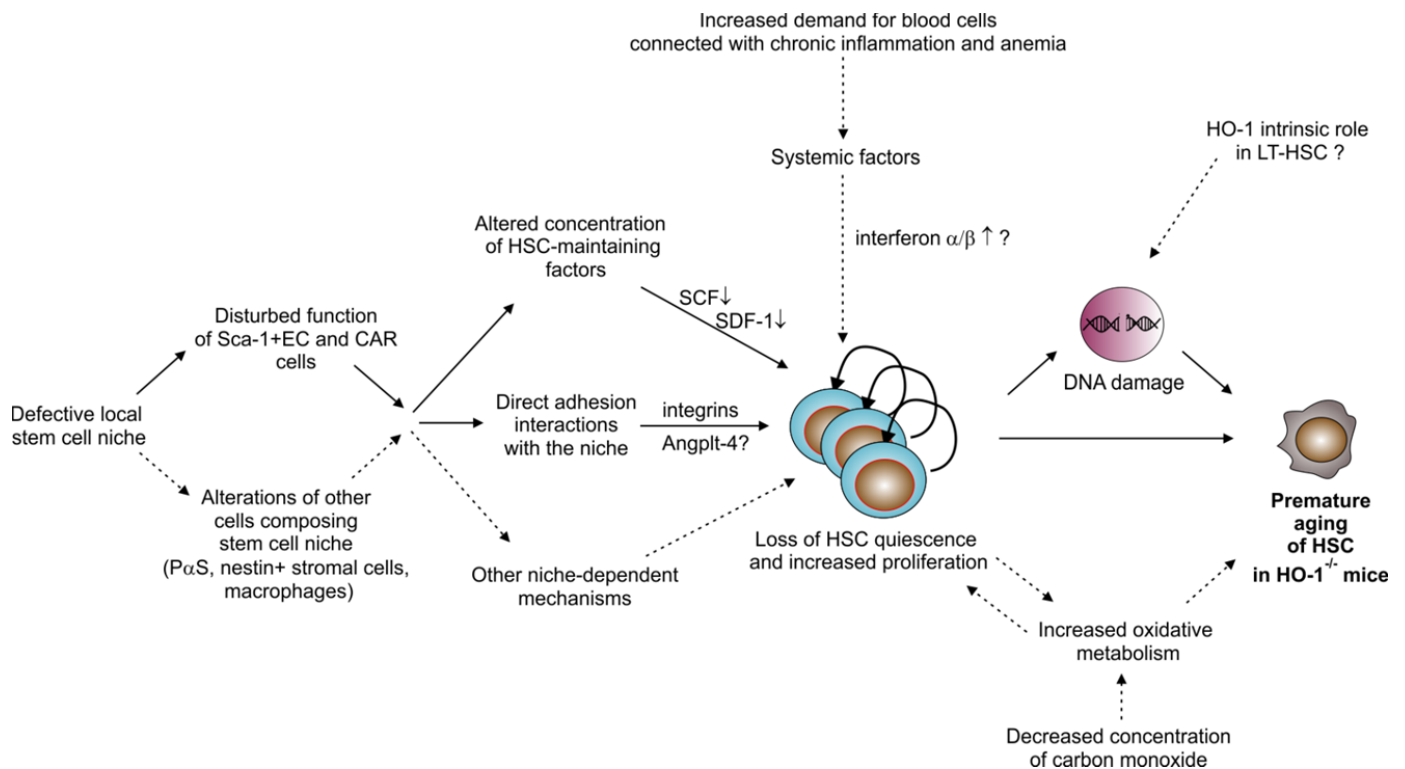
Fig. 4.1 *Proposed explanation of premature aging of LT-HSC in HO-1$^{-/-}$ mice. Solid lines represent mechanisms confirmed by obtained data. Dashed lines represent other hypothetical mechanisms indicated by obtained data and literatue.*

It is well evidenced that HO-1-deficiency was shown to be linked with increased ROS production [184]. Given that ROS can induce LT-HSC exhaustion as demonstrated previously [283], the increased oxidative stress could be other possible factor that causes the fast aging of HO-1$^{-/-}$ LT-HSC. Conversely, we did not observed increased expression of genes indicating increased oxidative stress in HO-1$^{-/-}$ LT-HSC, what makes hypothesis of ROS as causative factor of premature aging of young LT-HSC unlikely. But the role of HO-1 in ROS regulation may be more complex, as old HO-1$^{-/-}$ LT-HSC had increased expression of genes participating in response to oxidative stress (Tab. 3.3). Thus, even if ROS may not contribute to enhanced aging of young HO-1$^{-/-}$ LT-HSC, during aging they can facilitate acquiring elderly-associated changes.

120

Concluding the first part of the experiments, we think that the loss of quiescence and increased proliferation is possible direct reason of premature aging of HO-1$^{-/-}$ LT-HSC. In next steps of the study we aimed to identify what factors induce HO-1$^{-/-}$ LT-HSC proliferative status and elucidate the mechanism responsible for their premature aging.

In this study we used mice model in which HO-1 is non-selectively knockout from all tissues. Thus, the first question consider if the role of HO-1 is intrinsic or extrinsic to LT-HSC. The analysis of HO-1 expression in the bone marrow demonstrated that although HO-1 is expressed in LT-HSC as wells as in ST-HSC and MPP, the expression level in these cells was much lower than in macrophages and non-hematopoietic fraction (Fig. 3.22B). This suggested the extrinsic role of HO-1 in regulation of LT-HSC .

In this work we proposed experimental strategy which allowed verification of HO-1 extrinsic role in HSC aging. We transplanted HO-1$^{+/+}$ LT-HSC into HO-1$^{+/+}$ or HO-1$^{-/-}$ recipients and let them aging in HO-1-competent or HO-1-deficient environment. Not only we observed lower chimerism when LT-HSC were transplanted to HO-1$^{-/-}$ animals, but after the 32 weeks of aging in HO-1$^{-/-}$ environment, LT-HSC completely lost the ability to repopulate secondary HO-1$^{+/+}$ recipients (Fig. 3.24). This result strongly supports the notion about HO-1 extrinsic role in regulation of LT-HSC.

Although, this experiment demonstarted the LT-HSC-extrinsic role of HO-1, still there are several mechanisms that can potentially explain the observed phenomenon. Firstly, the HO-1 activity in the stem cell niche may guard the quiescence character and restricts the extensive proliferation of LT-HSC. We identified cells composing the stem cell niche that expressed HO-1. The relatively high HO-1 expression was detected in CAR cells and the highest expression was in minor CD31^{+}Sca1^{high} fraction of endothelial cells (Fig. 3.22B). Therefore we hypothesized that activity of HO-1 in CAR and CD31^{+}Sca-1^{high} EC may be crucial for regulating HSC and concentrated our research on these populations.

The main strategy to identify the possible molecular factors that mediates the role of HO-1 role in the niche was to analyze transcriptome of HO-1$^{-/-}$ CAR and CD31^{+}Sca-1^{high} EC cells. In the first step we checked the expression of several factors that were known to regulate LT-HSC. We focused on SCF and SDF-1 as these factors are produced by endothelial and stromal cells locally in the stem cell niche. The importance of restricted expression of SCF and SDF-1α in the

121

niche was well evidenced by elegant studies using conditional mice models [135, 136]. Additionally, we consider TGFβ as another potential mediator of HSC proliferation of LT-HSC in HO-1$^{-/-}$ mice as indicated by previous study [284].

We identified that CD31$^+$Sca1^{high} EC cells expressed *Kitl* (encodes SCF). Recently, the production of SCF by CD31$^+$Sca1^{high} EC fraction was confirmed by Ralf Adams group (personal communication). Notably, the HO-1-deficiency significantly decreased *Kitl* expression (Fig. 3.26A).

Lower *Kitl* expression in HO-1$^{-/-}$ CD31$^+$Sca-1^{high} EC may explain altered function of LT-HSC in HO-1$^{-/-}$ mice. This interpretation is supported by the previous study demonstrating that deletion of *Kitl* in Tie-2$^+$ endothelial cells disturbed the function of LT-HSC [135]. However, the difference between this study and our results is that the complete deletion of *Kitl* from Tie-2$^+$ EC cells [135] or even temporary blockage of c-Kit signaling [285] caused loss of HSC, while we observed expansion of stem cell pool in young HO-1$^{-/-}$ mice [Fig. 3.12]. The possible explanation of these dissimilarities may be connected with the level of *Kitl* downregulation. It cannot be excluded that total deletion/blockage of SCF signaling depletes LT-HSC, while partial decrease of its level observed in HO-1$^{-/-}$ CD31$^+$Sca-1^{high} EC cells has other effects, eg. loss of quiescence and expansion. Other possible reason is the existence of different splicing isoforms of *Kitl* transcript. The shorter isoform encodes the soluble SCF and the longer isoform encodes the membrane-bound form. The potential difference between function of these isoforms might clarify the discussed inconsistencies.

CD31$^+$Sca-1^{high} EC expressed also considerable amounts of *Cxcl12,* and its expression also tend to be lower, with borderline statistics (p = 0.06). Similarly to *Kitl*, deletion of *Cxcl12* in Tie-2$^+$ endothelial cells also depletes HSC, however to lesser extent than deletion of *Kitl* [136].

TGF-β is another factor that regulates quiescence and proliferation of LT-HSC [284]. We observed tendency (p = 0.05) to decreased counts number of *Tgfb1* transcripts in HO-1$^{-/-}$ CD31$^+$Sca-1^{high} EC.

All these three factors were also produced by CAR cells. HO-1 deficiency resulted in similar tendencies to downregulate expression of *Kitl* and *Cxcl12* in CAR cells, however the differences were less pronounced and did not reach statistical significance (p = 0.16 and p = 0.08). Production of these factors by CAR cells is also important for maintenance of LT-

HSC, as shown by *Kitl* and *Cxcl12* conditional knockout mice models [135, 136]. Knocking out the *Kitl* gene from leptin receptor-expressing (*Lepr*^{+}) cells depleted HSC [135]. The results of *Cxcl12* deletion depended on the genetic promotor used for the gene knockout. Depletion of *Cxcl12* in stromal cells using paired related homeobox 1 (*Prx*) promotor also depleted HSC and in the same time increased their cycling [136]. But the depletion of *Cxcl12* using *Osterix* (*Osx*) promotor did not altered LT-HSC [136]. In our study the CAR cells, sorted as CD45^{-}Ter119^{-}CD31^{-}Sca-1^{-}PDGFRα^{+}, expressed both *Prx* and *Osx,* thus making interpretation of our data in the light of the discussed papers difficult.

The role of TGFβ as potential mediator of altered function of the niche in HO-1^{-/-} mice is not clear. The HO-1^{-/-} CAR cells expressed higher levels of *Tgfb* what is in contrast to HO-1^{-/-} CD31^{+}Sca-1^{high} EC which showed downregulation of *Tgfb* in comparison to HO-1^{+/+} group. Thus, the local concentration of TGFβ in the niche is not likely to mediate HO-1 deficiency effects on LT-HSC.

Not only the transcriptome analysis allows investigating the genes that were already known to be crucial for HSC, but also gives opportunity to identify novel factors produced by the of CD31^{+}Sca-1^{high} EC and CAR that may regulates LT-HSC. We observed that expression of several adhesion and extracellular matrix molecules differed between HO-1^{+/+} and HO-1^{-/-} CAR and EC cells (Fig. 3.27, 3.29). We identified dysregulated integrins: *Itga4*, *Itga11* and *Itgb7* (Fig. 3.26B, 3.30B)*. Itga4* was already investigated in the context of HSC [148], but there are no reports on *Itga11* and *Itgb7* role in stem cell niche. Other interesting surface protein highlighted by the transcriptome analysis is angiopoietin-like protein 4 (*Angplt4*). It is highly expressed by CAR and CD31^{+}Sca-1^{high} EC cells, but is downregulated in both populations in HO-1^{-/-} mice (Fig. 3.26B, 3.30B). While angiopoietin like proteins are known as extrinsic factors that support HSC, previous studies concentrated on *Angplt2, Angplt3* and *Angplt5* [286]. Our work suggested that *Angplt4* may also be important member of angiopoietin like proteins expressed by niche cells and potentially might contribute to the altered LT-HSC phenotype in HO-1^{-/-} mice.

These potentially novel niche factors described above are few examples from larger group of genes that may explain the decline of LT-HSC in HO-1^{-/-} mice. It is worth mentioning, that due to character and costs of next generation sequencing we were limited to only 4 samples per group (additionally 1 sample from CAR and 1 sample from CD31^{+}Sca-1^{high} EC did not pass the quality check after sequencing). This number is too small to obtain definitive statistical

conclusions. Moreover, isolation of CAR and CD31$^+$Sca-1^{high} EC includes bone crushing and enzymatic digestion. These methods introduce additional noise to analyzed data and changes among many of the observed genes reached only border line statistical significance. Therefore, this data could be treated as screening for the factors, which significance of selected ones can be verified on larger group of animals and in functional experiments elucidating their role in niche-dependent regulation of HSC.

Nevertheless, the global transcriptome analysis showed that HO-1 deficiency altered several processes in CAR and CD31$^+$Sca-1^{high} EC cells. GSEA and pathway enrichment analysis pointed to several basic biological processes like altered expression of genes linked with cell cycle, DNA repair, inflammatory cell apoptosis or angiogenesis in case of CD31$^+$Sca-1^{high} EC (Tab. 3.5, 3.6) and epigenetic regulation of gene expression, increased oxidative phosphorylation, cellular senescence, collagen formation/degradation and response to ROS in case of CAR cells (Tab. 3.7, 3.8). We think that such global biological alterations in these niche populations are likely to have an impact on their function to support LT-HSC (Fig. 4.1).

But there are also possible mechanisms, other than alteration of stem cell niche, that can mediate the HO-1 extrinsic role in regulating LT-HSC. Given the chronic inflammatory state and anemia in HO-1$^{-/-}$ mice the basal production of blood cells has to be increased. Therefore, it is possible that some systemic factor pass the information concerning demand for increased blood cell production to HSC and induce their proliferation (Fig. 4.1). It known that M-CSF [287], interferon α [288] and interferon γ [289] are systemic factors that activates HSC during the infection or injury.

Indeed, performed transcriptome analysis indicated activation of interferon α and interferon γ signaling pathways in both young and old LT-HSC in HO-1$^{-/-}$ (Tab. 3.1, 3.3). The same was observed in CD31$^+$Sca-1^{high} EC and CAR cells. While CAR and CD31$^+$Sca-1^{high} EC cells did not express *Ifna1* and *Ifng* (supplementary results with expression data), it raises possibility that both types of interferon are systemically upregulated. However, as studied by our group, the interferon γ in not elevated in serum or bone marrow of HO-1$^{-/-}$ mice (shown in PhD thesis of Agata Szade). At the moment we do not have data concerning concentration of interferon α in plasma and bone marrow of HO-1$^{-/-}$ mice and its possible role will be addressed in next research.

It also should be considered that activation of interferons signaling in LT-HSC and niche cells may not be necessarily caused by increased global concentration of interferons in peripheral blood. Oppositely, other cells present in the stem cell niche, which were not analyzed in this study, eg. macrophages, may produce interferons and thus increase its concertation locally in stem cell niche.

Regarding the possible role of M-CSF, our group reported its significantly higher concentration in serum of HO-1$^{-/-}$ mice (2.7±0.8 pg/ml in HO-1$^{+/+}$ vs. 9.2±8.5 pg/ml in HO-1$^{-/-}$, p < 0.01, shown in PhD thesis of Agata Szade). However, other results questioned M-CSF as systematic factor that activates LT-HSC in HO-1$^{-/-}$ mice. Firstly, it was shown that M-CSF activates LT-HSC by upregulating expression of PU.1 transcription factor (*Spi1*), what was not observed in HO-1$^{-/-}$ LT-HSC (analysis of transcriptome of young LT-HSC, Supplementary Results). Secondly, in our analysis the expression of M-CSF receptor (*Csf1r*) in HO-1$^{+/+}$ and HO-1$^{-/-}$ is very low (analysis of transcriptome, Supplementary Results). Finally, the concentration of M-CSF in whole bone marrow is not changed in HO-1$^{-/-}$ animals. Altogether, is seems that upregulation of M-CSF at levels observed in HO-1$^{-/-}$ mice did not cause the observed activation and exhaustion of LT-HSC.

As discussed before, we interpreted the higher frequency of myeloid over lymphoid peripheral blood cells in HO-1$^{-/-}$ mice – the so called myeloid-bias – as one of the possible signs of premature aging of LT-HSC. However, when we transplanted HO-1$^{-/-}$ LT-HSC to HO-1$^{+/+}$ recipients we did not observe any myeloid-biased differentiation of transplanted LT-HSC. This may suggest that HO-1$^{-/-}$ LT-HSC transplanted to the HO-1$^{+/+}$ environment had restored balanced differentiation potential and their myeloid-bias was erased. If so, it should be the HO-1 extrinsic role that skews the LT-HSC fate toward myeloid lineage.

To verify this hypothesis we monitored the differentiation fate of HO-1$^{+/+}$ LT-HSC transplanted into HO-1$^{-/-}$ mice. However, the applied experimental scheme made this analysis difficult. This experiment involved ex-vivo transduction of LT-HSC with lentiviral vectors to stably overexpress GFP (the HO-1$^{-/-}$ are on mixed genetic background and at time of the experiment we did not have access to GFP^{+} mice on this mixed background). It was shown that maintaining LT-HSC in ex-vivo conditions can alter its differentiation potential [30]. Indeed, the ex vivo transduction of LT-HSC itself strongly shifted differentiation toward myeloid cells, as majority (87.8±5.1%) of HO-1$^{+/+}$ LT-HSC transplanted to HO-1$^{+/+}$ mice give rise mainly to
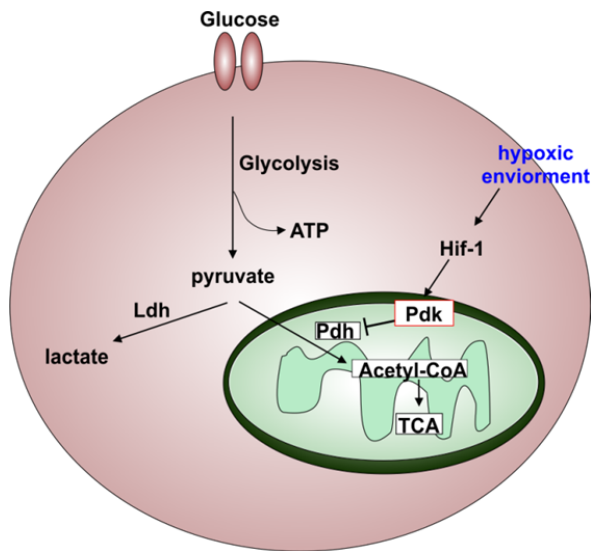
Fig. 4.2 *Role of Pdk in regulation of metabolic fate of pyruvate*.

Gr-1^{+} cells. Thus, it was not likely that in this experimental model we would observed any stronger myeloid shift when HO-1^{+/+} LT-HSC were transplanted to HO-1^{-/-} mice. To investigate the potential extrinsic role of HO-1 in skewing the LT-HSC differentiation, we need to repeat this experiment with transplantation scheme that will not involve their ex-vivo manipulation.

The transcriptome analysis put also our attention on many differentially regulated genes linked with metabolic pathways in tested HO-1^{-/-} populations (Tab. 3.1, 3.3, 3.5, 3.7). Firstly, we observed that young HO-1^{-/-} LT-HSC presented changed expression of genes connected with pyruvate conversion (Fig. 3.21A). Importantly, the fate of pyruvate conversion was demonstrated to be crucial for general non-oxidative metabolic profile of LT-HSC and its linked with their quiescence [27]. The pyruvate can be metabolized by mitochondrial enzyme pyruvate dehydrogenase (*Pdh*) into acetyl coenzyme A (acetyl-CoA), which then can be introduced in tricarboxylic acid cycle (TCA) and subsequent oxidative phosphorylation (Fig. 4.2). The Pdh could be inhibited by phosphorylation mediated by pyruvate dehydrogenase kinases (*Pdk*). The transition of non-active phosphorylated Pdh back to active non-phosphorylated state is catalyzed by pyruvate dehydrogenase phosphatase regulatory subunit (*Pdpr*). It was shown that high expression of Pdk isofroms in LT-HSC, driven by HIF-1α, reduce the oxidative metabolism of pyruvate and facilitate its non-oxidative conversion to lactate catalyzed by lactate dehydrogenase (Ldh) [27]. Genetic deletion of two isoforms of Pdks (Pdk2, Pdk4) in LT-HSC resulted in loss of quiescence and reconstitution potential [27]. Importantly, the deletion of Pdks resulted in decreased concentration of ATP in these cells.

In the young HO-1^{-/-} LT-HSC two *Pdk* isoforms (*Pdk1*, *Pdk2*) and *Pdpr* were downregulated what indicates possible higher activity of Pdh and mitochondrial oxidative metabolism of pyruvate (Fig. 3.21A). Consistently, the *Ldhb* isoform is also downregulated suggesting reduced non-oxidative conversion of pyruvate (Fig. 3.21A). Finally, we demonstrated that HO-1^{-/-}

hematopoietic stem and progenitor cells possessed reduced ATP levels (Fig. 3.15) and lost quiescence (Fig. 3.13) – the effects reported previously to be a result of Pdks deletion [27].

Concluding, lower ATP content and expression levels pf *Pdk1*, *Pdk2*, *Pdpr*, *Ldhb* indicates that the crucial regulation point of LT-HSC metabolism – the choice between oxidative and non-oxidative pyruvate utilization is shifted toward oxidative pathway in HO-1^{-/-} mice. However, it is hard to state if this phenomenon is a trigger of increased activation and proliferation of HO-1^{-/-} LT-HSC or rather their consequence (Fig. 4.1). It is also possible that lower ATP levels are result of other processes than oxidative metabolic shift, eg. increased apoptosis or ATP consumption.

Among the old HO-1^{-/-} LT-HSC we observed similar pattern of metabolic profile. The GSEA and pathway enrichment analysis indicted that expression of whole set of genes involved in pyruvate metabolism was changed (Tab. 3.3). This was linked with increased expression of genes responsible for respiratory chain electron transport, ATP synthesis and TCA cycle (Tab. 3.3). In relation to increased mitochondrial oxidation, we observed upregulated expression of genes linked with mitochondrial translation (Tab. 3.3).

Similarly to old HO-1^{-/-} LT-HSC, CAR cells from HO-1^{-/-} mice also showed enriched set of genes controlling the respiratory electron transport (Tab. 3.7). All these observations led us to search for a common factor that can trigger the increase oxidative metabolism in different populations in HO-1^{-/-} mice. Recent studies indicated that carbon monoxide (CO) – the enzymatic product of heme degradation – possess ability to modulate cell metabolism [290]. Firstly, CO regulates the pentose phosphate metabolism [291]. Furthermore, it was proposed that CO decrease ROS production by mild uncoupling of mitochondrial respiration. Consistently with this hypothesis, we observed that the Reactome gene set "Respiratory electron transfer, ATP synthesis and heat production by uncoupling proteins" was one of the most significantly enriched hits revealed by GSEA in HO-1^{-/-} old LT-HSC (Tab. 3.3) and in HO-1^{-/-} CAR cells (Tab. 3.7).

Therefore we tried to verify if the decreased concentration of CO mediates at least some of the alterations observed in HO-1^{-/-} mice. Nonetheless, investigating the role of carbon monoxide in the bone marrow remains technically difficult. It is possible to measure the carbon monoxide by gas chromatography, but only in whole flushed BM. We (in cooperation with Dr Lucie Muchova, Charles Unversity, Prague) analyzed how the CO is changing with age in the bone marrow and observed moderate decrease in HO-1^{-/-} mice. The lower CO concentration was

visible only in mice older than 1.5-month old, reached statistically significant difference already in 3-month old mice, but then did not significantly decrease with age (Fig. 3.32A). The question appears what is the source of relatively high CO concentration in bone marrow of HO-1$^{-/-}$. The possible answer is the CO is produced by heme oxygenase 2 (HO-2) – the non-inducible, ubiquitously expressed isoform. However, in this study we did not checked the expression of HO-2 in bone marrow or use the HO-2 knockout mouse model, therefore we cannot state to what extend HO-2 compensate CO concentration in bone marrow of HO-1$^{-/-}$ mice. It remains important task to be addressed by next studies, to consider potential role of CO as a mediator of HO-1 activity in bone marrow.

Other limitation is that till now there is no methodology allowing evaluation of CO concentration locally in the stem cell niche. We cannot exclude that concentration of CO across bone marrow is not equal and that it is different locally in stem cell niche. Therefore, if the CO concentration in stem cell niche is different, than values measured in whole bone marrow by gas chromatography are misleading for investigating the biology of LT-HSC.

Nevertheless, to address a direct role of LT-HSC function we designed an experiment in which the HO-1$^{+/+}$ LT-HSC were kept ex-vivo in serum free medium with minimal cytokine supplement and low O$_2$ concentration to resemble the conditions of stem cell niche. We checked if the addition of 250 ppm CO in such conditions will have any functional benefit for HSC upon transplantation. While at the moment of writing the thesis we are waiting for the results of long-term chimerism (short-term chimerism reflecting the function of progenitors did not show any differences (Fig. 3.32B) we are aware that the proposed experimental scheme possesses drawbacks. First, we do not know if the used concertation of CO reflects the physiological concentration of CO in stem cell niche. Secondly we had to keep HSC in artificial ex-vivo conditions, what is known to alter their function. Nevertheless, we are not able to propose any better research strategy to investigate CO influence on LT-HSC at the moment.

Although, the presented experiments point to the possible mechanisms explaining premature aging of LT-HSC in young HO-1$^{-/-}$ mice (Fig. 4.1), this study possesses limitations that disable us to fully distinguish reasons of this phenomena. Even though we demonstrated that dysfunction of the stem cell niche likely contributed to the premature aging of LT-HSC, this was not shown with conditional HO-1 knockout mice models with Cre-LoxP system and tissue specific gene promotors. Deleting the HO-1 gene only in selected populations composing stem

cell niche would allow investigating the role of HO-1 in the niche independently of other extrinsic mechanism, such us discussed influence of systemic factors.

Moreover, we were focused on two selected populations composing stem cell niche. There are several other kinds of cells building the niche, like macrophages, nestin$^+$ stromal cells or PαS, in which HO-1 may play a role. Furthermore, we proposed several factors that can mediate impact of niche dysfunction on LT-HSC, but till now we did not prove their role in functional manner (Fig. 4.1). The elegant way to confirm a role of a given factor would be the ability to reverse effect of HO-1 deficiency upon its complementation. On the other hand, it is possible that the phenomena of the observed premature aging is a complex output of several factors and reversal of selected one or few of them would not reverse the effects of HO-1 deficiency on LT-HSC aging. .

Finally, although HO-1 is expressed at low levels in LT-HSC, its intrinsic role in LT-HSC cannot be excluded. There are studies suggesting the potential role of nuclear HO-1 in DNA repair. Indeed, our RNA-seq analysis as well γH2aX staining demonstrated alteration in DNA repair machinery in HO-1$^{-/-}$ mice. This could be the result of accelerated proliferation of HO-1$^{-/-}$ cells, but potentially might be also linked with postulated role of nuclear HO-1 in DNA repair.

SUMMARY

In the presented study we tried to verify two hypotheses. The main conclusions of performed experiments are as follows:

<u>Hypothesis 1</u>: **The non-hematopoietic fraction of Lin⁻Sca-1⁺CD45⁻ give rise to blood cells**

- Lin⁻Sca-1⁺CD45⁻FSC^{low} population is heterogenous, enriched in early apoptotic cells
- Lin⁻Sca-1⁺CD45⁻FSC^{low} do not express pluripotent marker Oct-4A
- Lin⁻Sca-1⁺CD45⁻FSC^{low} did not showed hematopoietic potential in the single cell colony formation assay or after co-culture with OP9 cells
- Lin⁻Sca-1⁺CD45⁻FSC^{low} can be potentially contaminated with the nuclei expelled from the erythroblasts.

Summing up, we did not confirm the hematopoietic potential of Lin⁻Sca-1⁺CD45⁻ fraction from adult murine bone marrow.

<u>Hypothesis 2</u>: **HO-1 protects HSC from premature aging**

- HO-1$^{-/-}$ mice possess LT-HSC that show signs of premature aging.
- LT-HSC from HO-1$^{-/-}$ mice lost quiescence and intensively proliferate
- HO-1-deficiency resulted in gene expression profile connected with increased oxidative metabolism
- HO-1 is highly expressed in a stem cell niche and is decreasing during aging
- HO-1-defiency in CD31⁺Sca-1^{high} EC cells decreased expression of *Kitl*
- Lack of extrinsic HO-1 impairs function of LT-HSC

Concluding, we confirmed hypothesis concerning protective role of HO-1 in aging of LT-HSC. Our experiments demonstrated the extrinsic role of HO-1 in maintaining LT-HSC. We showed that lack HO-1 affected the selected populations composing stem cell niche: CAR and CD31⁺Sca-1^{high} EC cells. Finally, we proposed several potential factors that may be involved in HO-1-depedent protection of LT-HSC from premature aging.

SUPPLEMENTARY METHODS AND RESULTS

The additional materials are attached on DVD. These materials included description of supplementary methods (R-scripts written to analyze the RNA-seq data) and supplementary results (data obtained from RNA-seq). The supplementary results are divided in four folders: comparison of young HSC, old HSC, CAR and EC between HO-1$^{+/+}$ and HO-1$^{-/-}$ genotypes. Within each comparison there are: a Excel file with differential expression analysis of all genes, a Excel files with all significantly changed gen sets revealed by GSEA and pathway enrichment analysis, graphic files representing the affected pathways revealed by KEEG database and enrichment maps based on GSEA analysis. Additionally, in subfolder called "reports" there are *.html* files directing to web browser-based interface for easier searching, sorting and visualization on graphs the differential expression of most significantly affected genes as well as processes indicated by analysis based on Gene Ontology (GO) databases: molecular function (MF), biological processes (BP) and cellular compartment (CC).

REFERENCES

1. Bryder D, Rossi DJ, Weissman IL: **Hematopoietic stem cells: the paradigmatic tissue-specific stem cell**. *Am J Pathol* 2006, **169**:338–346.

2. TILL JE, McCULLOCH EA: **A direct measurement of the radiation sensitivity of normal mouse bone marrow cells**. *Radiat Res* 1961, **14**:213–222.

3. SIMINOVITCH L, MCCULLOCH EA, TILL JE: **The distribution of colony-forming cells among spleen colonies**. *J Cell Physiol* 1963, **62**:327–336.

4. Spangrude GJ, Heimfeld S, Weissman IL: **Purification and characterization of mouse hematopoietic stem cells**. *Science* 1988, **241**:58–62.

5. Weissman IL, Shizuru JA: **The origins of the identification and isolation of hematopoietic stem cells, and their capability to induce donor-specific transplantation tolerance and treat autoimmune diseases**. *Blood* 2008, **112**:3543–3553.

6. Morrison SJ, Weissman IL: **The long-term repopulating subset of hematopoietic stem cells is deterministic and isolatable by phenotype**. *Immunity* 1994, **1**:661–673.

7. Kiel MJ, Yilmaz OH, Iwashita T, Yilmaz OH, Terhorst C, Morrison SJ: **SLAM family receptors distinguish hematopoietic stem and progenitor cells and reveal endothelial niches for stem cells**. *Cell* 2005, **121**:1109–1121.

8. Osawa M, Hanada K, Hamada H, Nakauchi H: **Long-term lymphohematopoietic reconstitution by a single CD34-low/negative hematopoietic stem cell**. *Science* 1996, **273**:242–245.

9. Christensen JL, Weissman IL: **Flk-2 is a marker in hematopoietic stem cell differentiation: a simple method to isolate long-term stem cells**. *Proc Natl Acad Sci U S A* 2001, **98**:14541–14546.

10. Balazs AB, Fabian AJ, Esmon CT, Mulligan RC: **Endothelial protein C receptor (CD201) explicitly identifies hematopoietic stem cells in murine bone marrow**. *Blood* 2006, **107**:2317–2321.

11. Arai F, Hirao A, Ohmura M, Sato H, Matsuoka S, Takubo K, Ito K, Koh GY, Suda T: **Tie2/angiopoietin-1 signaling regulates hematopoietic stem cell quiescence in the bone marrow niche**. *Cell* 2004, **118**:149–161.

12. Chen C-Z, Li L, Li M, Lodish HF: **The endoglin(positive) sca-1(positive) rhodamine(low) phenotype defines a near-homogeneous population of long-term repopulating hematopoietic stem cells**. *Immunity* 2003, **19**:525–533.

13. Akashi K, Traver D, Miyamoto T, Weissman IL: **A clonogenic common myeloid progenitor that gives rise to all myeloid lineages**. *Nature* 2000, **404**:193–197.

14. Kondo M, Weissman IL, Akashi K: **Identification of clonogenic common lymphoid progenitors in mouse bone marrow**. *Cell* 1997, **91**:661–672.

15. Goodell MA, Brose K, Paradis G, Conner AS, Mulligan RC: **Isolation and functional properties of murine hematopoietic stem cells that are replicating in vivo**. *J Exp Med* 1996, **183**:1797–1806.

16. Zhou S, Schuetz JD, Bunting KD, Colapietro AM, Sampath J, Morris JJ, Lagutina I, Grosveld GC, Osawa M, Nakauchi H, Sorrentino BP: **The ABC transporter Bcrp1/ABCG2 is expressed in a wide variety of stem cells and is a molecular determinant of the side-population phenotype**. *Nat Med* 2001, **7**:1028–1034.

17. Weksberg DC, Chambers SM, Boles NC, Goodell MA: **CD150- side population cells represent a functionally distinct population of long-term hematopoietic stem cells**. *Blood* 2008, **111**:2444–2451.

18. Kiel MJ, Yilmaz OH, Morrison SJ: **CD150- cells are transiently reconstituting multipotent progenitors with little or no stem cell activity**. *Blood* 2008, **111**:4413–4414; author reply 4414–4415.

19. Baum CM, Weissman IL, Tsukamoto AS, Buckle AM, Peault B: **Isolation of a candidate human hematopoietic stem-cell population**. *Proc Natl Acad Sci* 1992, **89**:2804–2808.

20. Notta F, Doulatov S, Laurenti E, Poeppl A, Jurisica I, Dick JE: **Isolation of single human hematopoietic stem cells capable of long-term multilineage engraftment**. *Science* 2011, **333**:218–221.

21. Smith LG, Weissman IL, Heimfeld S: **Clonal analysis of hematopoietic stem-cell differentiation in vivo**. *Proc Natl Acad Sci U S A* 1991, **88**:2788–2792.

22. Ema H, Morita Y, Yamazaki S, Matsubara A, Seita J, Tadokoro Y, Kondo H, Takano H, Nakauchi H: **Adult mouse hematopoietic stem cells: purification and single-cell assays**. *Nat Protoc* 2007, **1**:2979–2987.

23. Purton LE, Scadden DT: **Limiting factors in murine hematopoietic stem cell assays**. *Cell Stem Cell* 2007, **1**:263–270.

24. Weissman IL: **Stem cells: units of development, units of regeneration, and units in evolution**. *Cell* 2000, **100**:157–168.

25. Wilson A, Laurenti E, Oser G, van der Wath RC, Blanco-Bose W, Jaworski M, Offner S, Dunant CF, Eshkind L, Bockamp E, Lió P, Macdonald HR, Trumpp A: **Hematopoietic stem cells reversibly switch from dormancy to self-renewal during homeostasis and repair**. *Cell* 2008, **135**:1118–1129.

26. Suda T, Takubo K, Semenza GL: **Metabolic regulation of hematopoietic stem cells in the hypoxic niche**. *Cell Stem Cell* 2011, **9**:298–310.

27. Takubo K, Nagamatsu G, Kobayashi CI, Nakamura-Ishizu A, Kobayashi H, Ikeda E, Goda N, Rahimi Y, Johnson RS, Soga T, Hirao A, Suematsu M, Suda T: **Regulation of glycolysis by Pdk functions as a metabolic checkpoint for cell cycle quiescence in hematopoietic stem cells**. *Cell Stem Cell* 2013, **12**:49–61.

28. Reya T, Morrison SJ, Clarke MF, Weissman IL: **Stem cells, cancer, and cancer stem cells**. *Nature* 2001, **414**:105–111.

29. Copley MR, Beer PA, Eaves CJ: **Hematopoietic Stem Cell Heterogeneity Takes Center Stage**. *Cell Stem Cell* 2012, **10**:690–697.

30. Dykstra B, Kent D, Bowie M, McCaffrey L, Hamilton M, Lyons K, Lee S-J, Brinkman R, Eaves C: **Long-term propagation of distinct hematopoietic differentiation programs in vivo**. *Cell Stem Cell* 2007, **1**:218–229.

31. Sanjuan-Pla A, Macaulay IC, Jensen CT, Woll PS, Luis TC, Mead A, Moore S, Carella C, Matsuoka S, Bouriez Jones T, Chowdhury O, Stenson L, Lutteropp M, Green JCA, Facchini R, Boukarabila H, Grover A, Gambardella A, Thongjuea S, Carrelha J, Tarrant P, Atkinson D, Clark S-A, Nerlov C, Jacobsen SEW: **Platelet-biased stem cells reside at the apex of the haematopoietic stem-cell hierarchy**. *Nature* 2013, **502**:232–236.

32. Lu R, Neff NF, Quake SR, Weissman IL: **Tracking single hematopoietic stem cells in vivo using high-throughput sequencing in conjunction with viral genetic barcoding**. *Nat Biotechnol* 2011, **29**:928–933.

33. Müller-Sieburg CE, Cho RH, Thoman M, Adkins B, Sieburg HB: **Deterministic regulation of hematopoietic stem cell self-renewal and differentiation**. *Blood* 2002, **100**:1302–1309.

34. Orkin SH, Zon LI: **Hematopoiesis: An Evolving Paradigm for Stem Cell Biology**. *Cell* 2008, **132**:631–644.

35. Wechsler J, Greene M, McDevitt MA, Anastasi J, Karp JE, Le Beau MM, Crispino JD: **Acquired mutations in GATA1 in the megakaryoblastic leukemia of Down syndrome**. *Nat Genet* 2002, **32**:148–152.

36. Pabst T, Mueller BU, Zhang P, Radomska HS, Narravula S, Schnittger S, Behre G, Hiddemann W, Tenen DG: **Dominant-negative mutations of CEBPA, encoding CCAAT/enhancer binding protein-alpha (C/EBPalpha), in acute myeloid leukemia**. *Nat Genet* 2001, **27**:263–270.

37. Mueller BU, Pabst T, Osato M, Asou N, Johansen LM, Minden MD, Behre G, Hiddemann W, Ito Y, Tenen DG: **Heterozygous PU.1 mutations are associated with acute myeloid leukemia**. *Blood* 2002, **100**:998–1007.

38. Mulligan CG, Goorha S, Radtke I, Miller CB, Coustan-Smith E, Dalton JD, Girtman K, Mathew S, Ma J, Pounds SB, Su X, Pui C-H, Relling MV, Evans WE, Shurtleff SA, Downing

JR: **Genome-wide analysis of genetic alterations in acute lymphoblastic leukaemia**. *Nature* 2007, **446**:758–764.

39. Moignard V, Macaulay IC, Swiers G, Buettner F, Schütte J, Calero-Nieto FJ, Kinston S, Joshi A, Hannah R, Theis FJ, Jacobsen SE, de Bruijn MF, Göttgens B: **Characterization of transcriptional networks in blood stem and progenitor cells using high-throughput single-cell gene expression analysis**. *Nat Cell Biol* 2013, **15**:363–372.

40. Arinobu Y, Mizuno S, Chong Y, Shigematsu H, Iino T, Iwasaki H, Graf T, Mayfield R, Chan S, Kastner P, Akashi K: **Reciprocal activation of GATA-1 and PU.1 marks initial specification of hematopoietic stem cells into myeloerythroid and myelolymphoid lineages**. *Cell Stem Cell* 2007, **1**:416–427.

41. Starck J, Cohet N, Gonnet C, Sarrazin S, Doubeikovskaia Z, Doubeikovski A, Verger A, Duterque-Coquillaud M, Morle F: **Functional cross-antagonism between transcription factors FLI-1 and EKLF**. *Mol Cell Biol* 2003, **23**:1390–1402.

42. Usui T, Preiss JC, Kanno Y, Yao ZJ, Bream JH, O'Shea JJ, Strober W: **T-bet regulates Th1 responses through essential effects on GATA-3 function rather than on IFNG gene acetylation and transcription**. *J Exp Med* 2006, **203**:755–766.

43. Ye M, Iwasaki H, Laiosa CV, Stadtfeld M, Xie H, Heck S, Clausen B, Akashi K, Graf T: **Hematopoietic stem cells expressing the myeloid lysozyme gene retain long-term, multilineage repopulation potential**. *Immunity* 2003, **19**:689–699.

44. Orkin SH: **Priming the hematopoietic pump**. *Immunity* 2003, **19**:633–634.

45. Hu M, Krause D, Greaves M, Sharkis S, Dexter M, Heyworth C, Enver T: **Multilineage gene expression precedes commitment in the hemopoietic system.** *Genes Dev* 1997, **11**:774–785.

46. Duran-Struuck R, Dysko RC: **Principles of Bone Marrow Transplantation (BMT): Providing Optimal Veterinary and Husbandry Care to Irradiated Mice in BMT Studies**. *J Am Assoc Lab Anim Sci JAALAS* 2009, **48**:11–22.

47. Yeager AM, Shinn C, Shinohara M, Pardoll DM: **Hematopoietic cell transplantation in the twitcher mouse. The effects of pretransplant conditioning with graded doses of busulfan**. *Transplantation* 1993, **56**:185–190.

48. Czechowicz A, Kraft D, Weissman IL, Bhattacharya D: **Efficient Transplantation via Antibody-based Clearance of Hematopoietic Stem Cell Niches**. *Science* 2007, **318**:1296–1299.

49. Maris M, Storb R: **The transplantation of hematopoietic stem cells after non-myeloablative conditioning**. *Immunol Res* 2003, **28**:13–24.

50. Sun J, Ramos A, Chapman B, Johnnidis JB, Le L, Ho Y-J, Klein A, Hofmann O, Camargo FD: **Clonal dynamics of native haematopoiesis**. *Nature* 2014, **514**:322–327.

51. Busch K, Klapproth K, Barile M, Flossdorf M, Holland-Letz T, Schlenner SM, Reth M, Höfer T, Rodewald H-R: **Fundamental properties of unperturbed haematopoiesis from stem cells in vivo**. *Nature* 2015, **518**:542–546.

52. Jiang Y, Jahagirdar BN, Reinhardt RL, Schwartz RE, Keene CD, Ortiz-Gonzalez XR, Reyes M, Lenvik T, Lund T, Blackstad M, Du J, Aldrich S, Lisberg A, Low WC, Largaespada DA, Verfaillie CM: **Pluripotency of mesenchymal stem cells derived from adult marrow**. *Nature* 2002, **418**:41–49.

53. Check E: **Stem cells: the hard copy**. *Nature* 2007, **446**:485–486.

54. Dulak J, Szade K, Szade A, Nowak W, Józkowicz A: **Adult stem cells: hopes and hypes of regenerative medicine**. *Acta Biochim Pol* 2015.

55. Serafini M, Dylla SJ, Oki M, Heremans Y, Tolar J, Jiang Y, Buckley SM, Pelacho B, Burns TC, Frommer S, Rossi DJ, Bryder D, Panoskaltsis-Mortari A, O'Shaughnessy MJ, Nelson-Holte M, Fine GC, Weissman IL, Blazar BR, Verfaillie CM: **Hematopoietic reconstitution by multipotent adult progenitor cells: precursors to long-term hematopoietic stem cells**. *J Exp Med* 2007, **204**:1729–1729.

56. Kucia M, Reca R, Campbell FR, Zuba-Surma E, Majka M, Ratajczak J, Ratajczak MZ: **A population of very small embryonic-like (VSEL) CXCR4(+)SSEA-1(+)Oct-4+ stem cells identified in adult bone marrow**. *Leukemia* 2006, **20**:857–869.

57. Ratajczak MZ, Zuba-Surma EK, Wysoczynski M, Ratajczak J, Kucia M: **Very small embryonic-like stem cells: characterization, developmental origin, and biological significance**. *Exp Hematol* 2008, **36**:742–751.

58. Ratajczak J, Wysoczynski M, Zuba-Surma E, Wan W, Kucia M, Yoder MC, Ratajczak MZ: **Adult murine bone marrow-derived very small embryonic-like stem cells differentiate into the hematopoietic lineage after coculture over OP9 stromal cells**. *Exp Hematol* 2011, **39**:225–237.

59. Lengner CJ, Camargo FD, Hochedlinger K, Welstead GG, Zaidi S, Gokhale S, Scholer HR, Tomilin A, Jaenisch R: **Oct4 expression is not required for mouse somatic stem cell self-renewal**. *Cell Stem Cell* 2007, **1**:403–415.

60. Lengner CJ, Welstead GG, Jaenisch R: **The pluripotency regulator Oct4**. *Cell Cycle* 2008, **7**:725–728.

61. Danova-Alt R, Heider A, Egger D, Cross M, Alt R: **Very small embryonic-like stem cells purified from umbilical cord blood lack stem cell characteristics**. *PloS One* 2012, **7**:e34899.

62. Snoeck H-W: **Aging of the hematopoietic system**. *Curr Opin Hematol* 2013, **20**:355–361.

63. Rossi DJ, Bryder D, Zahn JM, Ahlenius H, Sonu R, Wagers AJ, Weissman IL: **Cell intrinsic alterations underlie hematopoietic stem cell aging**. *Proc Natl Acad Sci U S A* 2005, **102**:9194–9199.

64. Gibson KL, Wu Y-C, Barnett Y, Duggan O, Vaughan R, Kondeatis E, Nilsson B-O, Wikby A, Kipling D, Dunn-Walters DK: **B-cell diversity decreases in old age and is correlated with poor health status**. *Aging Cell* 2009, **8**:18–25.

65. Naylor K, Li G, Vallejo AN, Lee W-W, Koetz K, Bryl E, Witkowski J, Fulbright J, Weyand CM, Goronzy JJ: **The influence of age on T cell generation and TCR diversity**. *J Immunol Baltim Md 1950* 2005, **174**:7446–7452.

66. Linton PJ, Dorshkind K: **Age-related changes in lymphocyte development and function**. *Nat Immunol* 2004, **5**:133–139.

67. Kogut I, Scholz JL, Cancro MP, Cambier JC: **B cell maintenance and function in aging**. *Semin Immunol* 2012, **24**:342–349.

68. Goronzy JJ, Weyand CM: **T cell development and receptor diversity during aging**. *Curr Opin Immunol* 2005, **17**:468–475.

69. Carmel R: **Anemia and aging: an overview of clinical, diagnostic and biological issues**. *Blood Rev* 2001, **15**:9–18.

70. Labrie JE, Sah AP, Allman DM, Cancro MP, Gerstein RM: **Bone marrow microenvironmental changes underlie reduced RAG-mediated recombination and B cell generation in aged mice**. *J Exp Med* 2004, **200**:411–423.

71. Domínguez-Gerpe L, Rey-Méndez M: **Evolution of the thymus size in response to physiological and random events throughout life**. *Microsc Res Tech* 2003, **62**:464–476.

72. Rossi DJ, Jamieson CHM, Weissman IL: **Stems Cells and the Pathways to Aging and Cancer**. *Cell* 2008, **132**:681–696.

73. Guerrettaz LM, Johnson SA, Cambier JC: **Acquired hematopoietic stem cell defects determine B-cell repertoire changes associated with aging**. *Proc Natl Acad Sci U S A* 2008, **105**:11898–11902.

74. Pang WW, Price EA, Sahoo D, Beerman I, Maloney WJ, Rossi DJ, Schrier SL, Weissman IL: **Human bone marrow hematopoietic stem cells are increased in frequency and myeloid-biased with age**. *Proc Natl Acad Sci U S A* 2011, **108**:20012–20017.

75. Kikushige Y, Ishikawa F, Miyamoto T, Shima T, Urata S, Yoshimoto G, Mori Y, Iino T, Yamauchi T, Eto T, Niiro H, Iwasaki H, Takenaka K, Akashi K: **Self-renewing hematopoietic stem cell is the primary target in pathogenesis of human chronic lymphocytic leukemia**. *Cancer Cell* 2011, **20**:246–259.

76. Morrison SJ, Wandycz AM, Akashi K, Globerson A, Weissman IL: **The aging of hematopoietic stem cells**. *Nat Med* 1996, **2**:1011–1016.

77. Dykstra B, Olthof S, Schreuder J, Ritsema M, de Haan G: **Clonal analysis reveals multiple functional defects of aged murine hematopoietic stem cells**. *J Exp Med* 2011, **208**:2691–2703.

78. Geiger H, de Haan G, Florian MC: **The ageing haematopoietic stem cell compartment**. *Nat Rev Immunol* 2013, **13**:376–389.

79. Kollman C, Howe CW, Anasetti C, Antin JH, Davies SM, Filipovich AH, Hegland J, Kamani N, Kernan NA, King R, Ratanatharathorn V, Weisdorf D, Confer DL: **Donor characteristics as risk factors in recipients after transplantation of bone marrow from unrelated donors: the effect of donor age**. *Blood* 2001, **98**:2043–2051.

80. Finke J, Schmoor C, Bethge WA, Ottinger HD, Stelljes M, Zander AR, Volin L, Heim DA, Schwerdtfeger R, Kolbe K, Mayer J, Maertens JA, Linkesch W, Holler E, Koza V, Bornhäuser M, Einsele H, Bertz H, Grishina O, Socié G, ATG-Fresenius Trial Group: **Prognostic factors affecting outcome after allogeneic transplantation for hematological malignancies from unrelated donors: results from a randomized trial**. *Biol Blood Marrow Transplant J Am Soc Blood Marrow Transplant* 2012, **18**:1716–1726.

81. Heining C, Spyridonidis A, Bernhardt E, Schulte-Mönting J, Behringer D, Grüllich C, Jakob A, Bertz H, Finke J: **Lymphocyte reconstitution following allogeneic hematopoietic stem cell transplantation: a retrospective study including 148 patients**. *Bone Marrow Transplant* 2007, **39**:613–622.

82. Wahlestedt M, Pronk CJ, Bryder D: **Concise review: hematopoietic stem cell aging and the prospects for rejuvenation**. *Stem Cells Transl Med* 2015, **4**:186–194.

83. Beerman I, Bhattacharya D, Zandi S, Sigvardsson M, Weissman IL, Bryder D, Rossi DJ: **Functionally distinct hematopoietic stem cells modulate hematopoietic lineage potential during aging by a mechanism of clonal expansion**. *Proc Natl Acad Sci U S A* 2010, **107**:5465–5470.

84. Holstege H, Pfeiffer W, Sie D, Hulsman M, Nicholas TJ, Lee CC, Ross T, Lin J, Miller MA, Ylstra B, Meijers-Heijboer H, Brugman MH, Staal FJT, Holstege G, Reinders MJT, Harkins TT, Levy S, Sistermans EA: **Somatic mutations found in the healthy blood compartment of a 115-yr-old woman demonstrate oligoclonal hematopoiesis**. *Genome Res* 2014, **24**:733–742.

85. Beerman I, Bock C, Garrison BS, Smith ZD, Gu H, Meissner A, Rossi DJ: **Proliferation-dependent alterations of the DNA methylation landscape underlie hematopoietic stem cell aging**. *Cell Stem Cell* 2013, **12**:413–425.

86. Foudi A, Hochedlinger K, Van Buren D, Schindler JW, Jaenisch R, Carey V, Hock H: **Analysis of histone 2B-GFP retention reveals slowly cycling hematopoietic stem cells**. *Nat Biotechnol* 2009, **27**:84–90.

87. Schaniel C, Moore KA: **Genetic models to study quiescent stem cells and their niches**. *Ann N Y Acad Sci* 2009, **1176**:26–35.

88. Qiu J, Papatsenko D, Niu X, Schaniel C, Moore K: **Divisional History and Hematopoietic Stem Cell Function during Homeostasis**. *Stem Cell Rep* 2014, **2**:473–490.

89. Rossi DJ, Bryder D, Seita J, Nussenzweig A, Hoeijmakers J, Weissman IL: **Deficiencies in DNA damage repair limit the function of haematopoietic stem cells with age**. *Nature* 2007, **447**:725–729.

90. Rübe CE, Fricke A, Widmann TA, Fürst T, Madry H, Pfreundschuh M, Rübe C: **Accumulation of DNA damage in hematopoietic stem and progenitor cells during human aging**. *PloS One* 2011, **6**:e17487.

91. Chambers SM, Shaw CA, Gatza C, Fisk CJ, Donehower LA, Goodell MA: **Aging hematopoietic stem cells decline in function and exhibit epigenetic dysregulation**. *PLoS Biol* 2007, **5**:e201.

92. Beerman I, Seita J, Inlay MA, Weissman IL, Rossi DJ: **Quiescent hematopoietic stem cells accumulate DNA damage during aging that is repaired upon entry into cell cycle**. *Cell Stem Cell* 2014, **15**:37–50.

93. Janzen V, Forkert R, Fleming HE, Saito Y, Waring MT, Dombkowski DM, Cheng T, DePinho RA, Sharpless NE, Scadden DT: **Stem-cell ageing modified by the cyclin-dependent kinase inhibitor p16INK4a**. *Nature* 2006, **443**:421–426.

94. Donehower LA: **Using mice to examine p53 functions in cancer, aging, and longevity**. *Cold Spring Harb Perspect Biol* 2009, **1**:a001081.

95. Attema JL, Pronk CJH, Norddahl GL, Nygren JM, Bryder D: **Hematopoietic stem cell ageing is uncoupled from p16INK4A-mediated senescence**. *Oncogene* 2009, **28**:2238–2243.

96. Allsopp RC, Cheshier S, Weissman IL: **Telomere Shortening Accompanies Increased Cell Cycle Activity during Serial Transplantation of Hematopoietic Stem Cells**. *J Exp Med* 2001, **193**:917–924.

97. Allsopp RC, Morin GB, Horner JW, DePinho R, Harley CB, Weissman IL: **Effect of TERT over-expression on the long-term transplantation capacity of hematopoietic stem cells**. *Nat Med* 2003, **9**:369–371.

98. Wahlestedt M, Norddahl GL, Sten G, Ugale A, Frisk M-AM, Mattsson R, Deierborg T, Sigvardsson M, Bryder D: **An epigenetic component of hematopoietic stem cell aging amenable to reprogramming into a young state**. *Blood* 2013, **121**:4257–4264.

99. Reik W: **Stability and flexibility of epigenetic gene regulation in mammalian development**. *Nature* 2007, **447**:425–432.

100. Challen GA, Sun D, Mayle A, Jeong M, Luo M, Rodriguez B, Mallaney C, Celik H, Yang L, Xia Z, Cullen S, Berg J, Zheng Y, Darlington GJ, Li W, Goodell MA: **Dnmt3a and Dnmt3b Have Overlapping and Distinct Functions in Hematopoietic Stem Cells**. *Cell Stem Cell* 2014, **15**:350–364.

101. Sun D, Luo M, Jeong M, Rodriguez B, Xia Z, Hannah R, Wang H, Le T, Faull KF, Chen R, Gu H, Bock C, Meissner A, Göttgens B, Darlington GJ, Li W, Goodell MA: **Epigenomic Profiling of Young and Aged HSCs Reveals Concerted Changes during Aging that Reinforce Self-Renewal**. *Cell Stem Cell* 2014, **14**:673–688.

102. Brown K, Xie S, Qiu X, Mohrin M, Shin J, Liu Y, Zhang D, Scadden DT, Chen D: **SIRT3 Reverses Aging-Associated Degeneration**. *Cell Rep* 2013, **3**:319–327.

103. Schwartz YB, Pirrotta V: **Polycomb silencing mechanisms and the management of genomic programmes**. *Nat Rev Genet* 2007, **8**:9–22.

104. Florian MC, Dörr K, Niebel A, Daria D, Schrezenmeier H, Rojewski M, Filippi M-D, Hasenberg A, Gunzer M, Scharffetter-Kochanek K, Zheng Y, Geiger H: **Cdc42 activity regulates hematopoietic stem cell aging and rejuvenation**. *Cell Stem Cell* 2012, **10**:520–530.

105. Satoh Y, Yokota T, Sudo T, Kondo M, Lai A, Kincade PW, Kouro T, Iida R, Kokame K, Miyata T, Habuchi Y, Matsui K, Tanaka H, Matsumura I, Oritani K, Kohwi-Shigematsu T, Kanakura Y: **The Satb1 protein directs hematopoietic stem cell differentiation toward lymphoid lineages**. *Immunity* 2013, **38**:1105–1115.

106. Johnson SC, Rabinovitch PS, Kaeberlein M: **mTOR is a key modulator of ageing and age-related disease**. *Nature* 2013, **493**:338–345.

107. Chen C, Liu Y, Liu Y, Zheng P: **mTOR regulation and therapeutic rejuvenation of aging hematopoietic stem cells**. *Sci Signal* 2009, **2**:ra75.

108. Ergen AV, Boles NC, Goodell MA: **Rantes/Ccl5 influences hematopoietic stem cell subtypes and causes myeloid skewing**. *Blood* 2012, **119**:2500–2509.

109. Tuljapurkar SR, McGuire TR, Brusnahan SK, Jackson JD, Garvin KL, Kessinger MA, Lane JT, O' Kane BJ, Sharp JG: **Changes in human bone marrow fat content associated with changes in hematopoietic stem cell numbers and cytokine levels with aging**. *J Anat* 2011, **219**:574–581.

110. Cancelas JA, Koevoet WL, de Koning AE, Mayen AE, Rombouts EJ, Ploemacher RE: **Connexin-43 gap junctions are involved in multiconnexin-expressing stromal support of hemopoietic progenitors and stem cells**. *Blood* 2000, **96**:498–505.

111. Taniguchi Ishikawa E, Gonzalez-Nieto D, Ghiaur G, Dunn SK, Ficker AM, Murali B, Madhu M, Gutstein DE, Fishman GI, Barrio LC, Cancelas JA: **Connexin-43 prevents hematopoietic stem cell senescence through transfer of reactive oxygen species to bone marrow stromal cells**. *Proc Natl Acad Sci U S A* 2012, **109**:9071–9076.

112. Wagner W, Horn P, Bork S, Ho AD: **Aging of hematopoietic stem cells is regulated by the stem cell niche**. *Exp Gerontol* 2008, **43**:974–980.

113. Bellantuono I, Aldahmash A, Kassem M: **Aging of marrow stromal (skeletal) stem cells and their contribution to age-related bone loss**. *Biochim Biophys Acta* 2009, **1792**:364–370.

114. Freemont AJ, Hoyland JA: **Morphology, mechanisms and pathology of musculoskeletal ageing**. *J Pathol* 2007, **211**:252–259.

115. Bianco P: **Bone and the hematopoietic niche: a tale of two stem cells**. *Blood* 2011, **117**:5281–5288.

116. Morrison SJ, Scadden DT: **The bone marrow niche for haematopoietic stem cells**. *Nature* 2014, **505**:327–334.

117. Schofield R: **The relationship between the spleen colony-forming cell and the haemopoietic stem cell**. *Blood Cells* 1978, **4**:7–25.

118. Dexter TM, Allen TD, Lajtha LG: **Conditions controlling the proliferation of haemopoietic stem cells in vitro**. *J Cell Physiol* 1977, **91**:335–344.

119. Calvi LM, Adams GB, Weibrecht KW, Weber JM, Olson DP, Knight MC, Martin RP, Schipani E, Divieti P, Bringhurst FR, Milner LA, Kronenberg HM, Scadden DT: **Osteoblastic cells regulate the haematopoietic stem cell niche**. *Nature* 2003, **425**:841–846.

120. Zhang J, Niu C, Ye L, Huang H, He X, Tong W-G, Ross J, Haug J, Johnson T, Feng JQ, Harris S, Wiedemann LM, Mishina Y, Li L: **Identification of the haematopoietic stem cell niche and control of the niche size**. *Nature* 2003, **425**:836–841.

121. Kiel MJ, Radice GL, Morrison SJ: **Lack of evidence that hematopoietic stem cells depend on N-cadherin-mediated adhesion to osteoblasts for their maintenance**. *Cell Stem Cell* 2007, **1**:204–217.

122. Nombela-Arrieta C, Pivarnik G, Winkel B, Canty KJ, Harley B, Mahoney JE, Park S-Y, Lu J, Protopopov A, Silberstein LE: **Quantitative Imaging of Hematopoietic Stem and Progenitor Cell localization and hypoxic status in the Bone Marrow microenvironment**. *Nat Cell Biol* 2013, **15**:533–543.

123. Lo Celso C, Fleming HE, Wu JW, Zhao CX, Miake-Lye S, Fujisaki J, Côté D, Rowe DW, Lin CP, Scadden DT: **Live-animal tracking of individual haematopoietic stem/progenitor cells in their niche**. *Nature* 2009, **457**:92–96.

124. Sipkins DA, Wei X, Wu JW, Runnels JM, Côté D, Means TK, Luster AD, Scadden DT, Lin CP: **In vivo imaging of specialized bone marrow endothelial microdomains for tumour engraftment**. *Nature* 2005, **435**:969–973.

125. Bourke VA, Watchman CJ, Reith JD, Jorgensen ML, Dieudonnè A, Bolch WE: **Spatial gradients of blood vessels and hematopoietic stem and progenitor cells within the marrow cavities of the human skeleton**. *Blood* 2009, **114**:4077–4080.

126. Ehninger A, Trumpp A: **The bone marrow stem cell niche grows up: mesenchymal stem cells and macrophages move in**. *J Exp Med* 2011, **208**:421–428.

127. Sacchetti B, Funari A, Michienzi S, Di Cesare S, Piersanti S, Saggio I, Tagliafico E, Ferrari S, Robey PG, Riminucci M, Bianco P: **Self-renewing osteoprogenitors in bone marrow sinusoids can organize a hematopoietic microenvironment**. *Cell* 2007, **131**:324–336.

128. Kusumbe AP, Ramasamy SK, Adams RH: **Coupling of angiogenesis and osteogenesis by a specific vessel subtype in bone**. *Nature* 2014, **507**:323–328.

129. Kunisaki Y, Bruns I, Scheiermann C, Ahmed J, Pinho S, Zhang D, Mizoguchi T, Wei Q, Lucas D, Ito K, Mar JC, Bergman A, Frenette PS: **Arteriolar niches maintain haematopoietic stem cell quiescence**. *Nature* 2013, **502**:637-43

130. Weiss L: **The hematopoietic microenvironment of the bone marrow: An ultrastructural study of the stroma in rats**. *Anat Rec* 1976, **186**:161–184.

131. Bianco P, Cao X, Frenette PS, Mao JJ, Robey PG, Simmons PJ, Wang C-Y: **The meaning, the sense and the significance: translating the science of mesenchymal stem cells into medicine**. *Nat Med* 2013, **19**:35–42.

132. Bianco P: **"Mesenchymal" Stem Cells**. *Annu Rev Cell Dev Biol* 2014, **30**:677–704.

133. Houlihan DD, Mabuchi Y, Morikawa S, Niibe K, Araki D, Suzuki S, Okano H, Matsuzaki Y: **Isolation of mouse mesenchymal stem cells on the basis of expression of Sca-1 and PDGFR-α**. *Nat Protoc* 2012, **7**:2103–2111.

134. Méndez-Ferrer S, Michurina TV, Ferraro F, Mazloom AR, Macarthur BD, Lira SA, Scadden DT, Ma'ayan A, Enikolopov GN, Frenette PS: **Mesenchymal and haematopoietic stem cells form a unique bone marrow niche**. *Nature* 2010, **466**:829–834.

135. Ding L, Saunders TL, Enikolopov G, Morrison SJ: **Endothelial and perivascular cells maintain haematopoietic stem cells**. *Nature* 2012, **481**:457–462.

136. Greenbaum A, Hsu Y-MS, Day RB, Schuettpelz LG, Christopher MJ, Borgerding JN, Nagasawa T, Link DC: **CXCL12 in early mesenchymal progenitors is required for haematopoietic stem-cell maintenance**. *Nature* 2013, **495**:227–230.

137. Chan CKF, Seo EY, Chen JY, Lo D, McArdle A, Sinha R, Tevlin R, Seita J, Vincent-Tompkins J, Wearda T, Lu W-J, Senarath-Yapa K, Chung MT, Marecic O, Tran M, Yan KS, Upton R, Walmsley GG, Lee AS, Sahoo D, Kuo CJ, Weissman IL, Longaker MT: **Identification and specification of the mouse skeletal stem cell**. *Cell* 2015, **160**:285–298.

138. Worthley DL, Churchill M, Compton JT, Tailor Y, Rao M, Si Y, Levin D, Schwartz MG, Uygur A, Hayakawa Y, Gross S, Renz BW, Setlik W, Martinez AN, Chen X, Nizami S, Lee HG, Kang HP, Caldwell J-M, Asfaha S, Westphalen CB, Graham T, Jin G, Nagar K, Wang H, Kheirbek MA, Kolhe A, Carpenter J, Glaire M, Nair A, et al.: **Gremlin 1 identifies a skeletal stem cell with bone, cartilage, and reticular stromal potential**. *Cell* 2015, **160**:269–284.

139. Katayama Y, Battista M, Kao W-M, Hidalgo A, Peired AJ, Thomas SA, Frenette PS: **Signals from the sympathetic nervous system regulate hematopoietic stem cell egress from bone marrow**. *Cell* 2006, **124**:407–421.

140. Méndez-Ferrer S, Lucas D, Battista M, Frenette PS: **Haematopoietic stem cell release is regulated by circadian oscillations**. *Nature* 2008, **452**:442–447.

141. Yamazaki S, Ema H, Karlsson G, Yamaguchi T, Miyoshi H, Shioda S, Taketo MM, Karlsson S, Iwama A, Nakauchi H: **Nonmyelinating Schwann cells maintain hematopoietic stem cell hibernation in the bone marrow niche**. *Cell* 2011, **147**:1146–1158.

142. Chow A, Lucas D, Hidalgo A, Mendez-Ferrer S, Hashimoto D, Scheiermann C, Battista M, Leboeuf M, Prophete C, van Rooijen N, Tanaka M, Merad M, Frenette PS: **Bone marrow CD169+ macrophages promote the retention of hematopoietic stem and progenitor cells in the mesenchymal stem cell niche**. *J Exp Med* 2011, **208**:261–271.

143. Kollet O, Dar A, Shivtiel S, Kalinkovich A, Lapid K, Sztainberg Y, Tesio M, Samstein RM, Goichberg P, Spiegel A, Elson A, Lapidot T: **Osteoclasts degrade endosteal components and promote mobilization of hematopoietic progenitor cells**. *Nat Med* 2006, **12**:657–664.

144. Winkler IG, Sims NA, Pettit AR, Barbier V, Nowlan B, Helwani F, Poulton IJ, van Rooijen N, Alexander KA, Raggatt LJ, Lévesque J-P: **Bone marrow macrophages maintain hematopoietic stem cell (HSC) niches and their depletion mobilizes HSCs**. *Blood* 2010, **116**:4815–4828.

145. Bruns I, Lucas D, Pinho S, Ahmed J, Lambert MP, Kunisaki Y, Scheiermann C, Schiff L, Poncz M, Bergman A, Frenette PS: **Megakaryocytes regulate hematopoietic stem cell quiescence through CXCL4 secretion**. *Nat Med* 2014, **20**:1315–1320.

146. Zhao M, Perry JM, Marshall H, Venkatraman A, Qian P, He XC, Ahamed J, Li L: **Megakaryocytes maintain homeostatic quiescence and promote post-injury regeneration of hematopoietic stem cells**. *Nat Med* 2014, **20**:1321–1326.

147. Fujisaki J, Wu J, Carlson AL, Silberstein L, Putheti P, Larocca R, Gao W, Saito TI, Lo Celso C, Tsuyuzaki H, Sato T, Côté D, Sykes M, Strom TB, Scadden DT, Lin CP: **In vivo imaging of Treg cells providing immune privilege to the haematopoietic stem-cell niche**. *Nature* 2011, **474**:216–219.

148. Celso CL, Scadden DT: **The haematopoietic stem cell niche at a glance**. *J Cell Sci* 2011, **124**:3529–3535.

149. Mendelson A, Frenette PS: **Hematopoietic stem cell niche maintenance during homeostasis and regeneration**. *Nat Med* 2014, **20**:833–846.

150. Barker JE: **Sl/Sld hematopoietic progenitors are deficient in situ**. *Exp Hematol* 1994, **22**:174–177.

151. Sugiyama T, Kohara H, Noda M, Nagasawa T: **Maintenance of the hematopoietic stem cell pool by CXCL12-CXCR4 chemokine signaling in bone marrow stromal cell niches**. *Immunity* 2006, **25**:977–988.

152. Huang E, Nocka K, Beier DR, Chu TY, Buck J, Lahm HW, Wellner D, Leder P, Besmer P: **The hematopoietic growth factor KL is encoded by the Sl locus and is the ligand of the c-kit receptor, the gene product of the W locus**. *Cell* 1990, **63**:225–233.

153. Zsebo KM, Williams DA, Geissler EN, Broudy VC, Martin FH, Atkins HL, Hsu RY, Birkett NC, Okino KH, Murdock DC: **Stem cell factor is encoded at the Sl locus of the mouse and is the ligand for the c-kit tyrosine kinase receptor**. *Cell* 1990, **63**:213–224.

154. Shiohara M, Koike K, Kubo T, Amano Y, Takagi M, Muraoka K, Nakao J, Nakahata T, Komiyama A: **Possible role of stem cell factor as a serum factor: monoclonal anti-c-kit antibody abrogates interleukin-6-dependent colony growth in serum-containing culture**. *Exp Hematol* 1993, **21**:907–912.

155. Bosbach B, Deshpande S, Rossi F, Shieh J-H, Sommer G, Stanchina E de, Veach DR, Scandura JM, Manova-Todorova K, Moore MAS, Antonescu CR, Besmer P: **Imatinib resistance and microcytic erythrocytosis in a KitV558Δ;T669I/+ gatekeeper-mutant mouse model of gastrointestinal stromal tumor**. *Proc Natl Acad Sci* 2012, **109**:E2276–E2283.

156. Zheng J, Huynh H, Umikawa M, Silvany R, Zhang CC: **Angiopoietin-like protein 3 supports the activity of hematopoietic stem cells in the bone marrow niche**. *Blood* 2011, **117**:470–479.

157. Fleming HE, Janzen V, Celso CL, Guo J, Leahy KM, Kronenberg HM, Scadden DT: **Wnt signaling in the niche enforces hematopoietic stem cell quiescence and is necessary to preserve self-renewal in vivo**. *Cell Stem Cell* 2008, **2**:274–283.

158. Renström J, Istvanffy R, Gauthier K, Shimono A, Mages J, Jardon-Alvarez A, Kröger M, Schiemann M, Busch DH, Esposito I, Lang R, Peschel C, Oostendorp RAJ: **Secreted frizzled-related protein 1 extrinsically regulates cycling activity and maintenance of hematopoietic stem cells**. *Cell Stem Cell* 2009, **5**:157–167.

159. Kieslinger M, Hiechinger S, Dobreva G, Consalez GG, Grosschedl R: **Early B Cell Factor 2 Regulates Hematopoietic Stem Cell Homeostasis in a Cell-Nonautonomous Manner**. *Cell Stem Cell* 2010, **7**:496–507.

160. Koch U, Wilson A, Cobas M, Kemler R, Macdonald HR, Radtke F: **Simultaneous loss of beta- and gamma-catenin does not perturb hematopoiesis or lymphopoiesis**. *Blood* 2008, **111**:160–164.

161. Jeannet G, Scheller M, Scarpellino L, Duboux S, Gardiol N, Back J, Kuttler F, Malanchi I, Birchmeier W, Leutz A, Huelsken J, Held W: **Long-term, multilineage hematopoiesis occurs in the combined absence of beta-catenin and gamma-catenin**. *Blood* 2008, **111**:142–149.

162. Nemeth MJ, Topol L, Anderson SM, Yang Y, Bodine DM: **Wnt5a inhibits canonical Wnt signaling in hematopoietic stem cells and enhances repopulation**. *Proc Natl Acad Sci* 2007, **104**:15436–15441.

163. Povinelli BJ, Nemeth MJ: **Wnt5a regulates hematopoietic stem cell proliferation and repopulation through the Ryk receptor**. *Stem Cells Dayt Ohio* 2014, **32**:105–115.

164. Sugimura R, He XC, Venkatraman A, Arai F, Box A, Semerad C, Haug JS, Peng L, Zhong X-B, Suda T, Li L: **Noncanonical Wnt signaling maintains hematopoietic stem cells in the niche**. *Cell* 2012, **150**:351–365.

165. Luis TC, Naber BAE, Roozen PPC, Brugman MH, de Haas EFE, Ghazvini M, Fibbe WE, van Dongen JJM, Fodde R, Staal FJT: **Canonical wnt signaling regulates hematopoiesis in a dosage-dependent fashion**. *Cell Stem Cell* 2011, **9**:345–356.

166. Poulos MG, Guo P, Kofler NM, Pinho S, Gutkin MC, Tikhonova A, Aifantis I, Frenette PS, Kitajewski J, Rafii S, Butler JM: **Endothelial Jagged-1 is necessary for homeostatic and regenerative hematopoiesis**. *Cell Rep* 2013, **4**:1022–1034.

167. Shalaby F, Rossant J, Yamaguchi TP, Gertsenstein M, Wu XF, Breitman ML, Schuh AC: **Failure of blood-island formation and vasculogenesis in Flk-1-deficient mice**. *Nature* 1995, **376**:62–66.

168. Maillard I, Koch U, Dumortier A, Shestova O, Xu L, Sai H, Pross SE, Aster JC, Bhandoola A, Radtke F, Pear WS: **Canonical notch signaling is dispensable for the maintenance of adult hematopoietic stem cells**. *Cell Stem Cell* 2008, **2**:356–366.

169. Priestley GV, Scott LM, Ulyanova T, Papayannopoulou T: **Lack of α4 integrin expression in stem cells restricts competitive function and self-renewal activity**. *Blood* 2006, **107**:2959–2967.

170. Ulyanova T, Priestley GV, Nakamoto B, Jiang Y, Papayannopoulou T: **VCAM-1 ABLATION IN NON-HEMATOPOIETIC CELLS IN MxCre+ VCAM-1f/f MICE IS VARIABLE AND DICTATES THEIR PHENOTYPE**. *Exp Hematol* 2007, **35**:565–571.

171. Jiang Y, Bonig H, Ulyanova T, Chang K, Papayannopoulou T: **On the adaptation of endosteal stem cell niche function in response to stress**. *Blood* 2009, **114**:3773–3782.

172. Nilsson SK, Johnston HM, Whitty GA, Williams B, Webb RJ, Denhardt DT, Bertoncello I, Bendall LJ, Simmons PJ, Haylock DN: **Osteopontin, a key component of the hematopoietic stem cell niche and regulator of primitive hematopoietic progenitor cells**. *Blood* 2005, **106**:1232–1239.

173. Weber GF, Ashkar S, Glimcher MJ, Cantor H: **Receptor-ligand interaction between CD44 and osteopontin (Eta-1)**. *Science* 1996, **271**:509–512.

174. Smith-Berdan S, Nguyen A, Hassanein D, Zimmer M, Ugarte F, Ciriza J, Li D, García-Ojeda ME, Hinck L, Forsberg EC: **Robo4 cooperates with CXCR4 to specify hematopoietic stem cell localization to bone marrow niches**. *Cell Stem Cell* 2011, **8**:72–83.

175. Lévesque J-P, Helwani FM, Winkler IG: **The endosteal "osteoblastic" niche and its role in hematopoietic stem cell homing and mobilization**. *Leukemia* 2010, **24**:1979–1992.

176. Adams GB, Chabner KT, Alley IR, Olson DP, Szczepiorkowski ZM, Poznansky MC, Kos CH, Pollak MR, Brown EM, Scadden DT: **Stem cell engraftment at the endosteal niche is specified by the calcium-sensing receptor**. *Nature* 2006, **439**:599–603.

177. Mohyeldin A, Garzón-Muvdi T, Quiñones-Hinojosa A: **Oxygen in stem cell biology: a critical component of the stem cell niche**. *Cell Stem Cell* 2010, **7**:150–161.

178. Spencer JA, Ferraro F, Roussakis E, Klein A, Wu J, Runnels JM, Zaher W, Mortensen LJ, Alt C, Turcotte R, Yusuf R, Côté D, Vinogradov SA, Scadden DT, Lin CP: **Direct measurement of local oxygen concentration in the bone marrow of live animals**. *Nature* 2014, **advance online publication**.

179. Takubo K, Goda N, Yamada W, Iriuchishima H, Ikeda E, Kubota Y, Shima H, Johnson RS, Hirao A, Suematsu M, Suda T: **Regulation of the HIF-1alpha level is essential for hematopoietic stem cells**. *Cell Stem Cell* 2010, **7**:391–402.

180. Winkler IG, Barbier V, Wadley R, Zannettino A, Williams S, Lévesque J-P: **Positioning of bone marrow hematopoietic and stromal cells relative to blood flow in vivo: Serially reconstituting hematopoietic stem cells reside in distinct non-perfused niches**. *Blood* 2010.

181. Parmar K, Mauch P, Vergilio J-A, Sackstein R, Down JD: **Distribution of hematopoietic stem cells in the bone marrow according to regional hypoxia**. *Proc Natl Acad Sci* 2007, **104**:5431–5436.

182. Kozakowska M, Szade K, Dulak J, Jozkowicz A: **Role of Heme Oxygenase-1 in Postnatal Differentiation of Stem Cells: A Possible Cross-Talk with MicroRNAs**. *Antioxid Redox Signal* 2013, **20**:1827–1850.

183. Tenhunen R, Marver HS, Schmid R: **The enzymatic conversion of heme to bilirubin by microsomal heme oxygenase**. *Proc Natl Acad Sci U S A* 1968, **61**:748–755.

184. Ryter SW, Alam J, Choi AMK: **Heme oxygenase-1/carbon monoxide: from basic science to therapeutic applications**. *Physiol Rev* 2006, **86**:583–650.

185. Dulak J, Deshane J, Jozkowicz A, Agarwal A: **Heme Oxygenase-1 and Carbon Monoxide in Vascular Pathobiology Focus on Angiogenesis**. *Circulation* 2008, **117**:231–241.

186. Sikorski EM, Hock T, Hill-Kapturczak N, Agarwal A: **The story so far: Molecular regulation of the heme oxygenase-1 gene in renal injury**. *Am J Physiol Renal Physiol* 2004, **286**:F425–441.

187. Ewing JF, Maines MD: **Distribution of constitutive (HO-2) and heat-inducible (HO-1) heme oxygenase isozymes in rat testes: HO-2 displays stage-specific expression in germ cells**. *Endocrinology* 1995, **136**:2294–2302.

188. Dulak J, Józkowicz A, Foresti R, Kasza A, Frick M, Huk I, Green CJ, Pachinger O, Weidinger F, Motterlini R: **Heme oxygenase activity modulates vascular endothelial growth factor synthesis in vascular smooth muscle cells**. *Antioxid Redox Signal* 2002, **4**:229–40.

189. Bussolati B, Ahmed A, Pemberton H, Landis RC, Carlo FD, Haskard DO, Mason JC: **Bifunctional role for VEGF-induced heme oxygenase-1 in vivo: induction of angiogenesis and inhibition of leukocytic infiltration**. *Blood* 2004, **103**:761–766.

190. Dulak J, Łoboda A, Zagórska A, Józkowicz A: **Complex role of heme oxygenase-1 in angiogenesis**. *Antioxid Redox Signal* 2004, **6**:858–866.

191. Deshane J, Chen S, Caballero S, Grochot-Przeczek A, Was H, Li Calzi S, Lach R, Hock TD, Chen B, Hill-Kapturczak N, Siegal GP, Dulak J, Jozkowicz A, Grant MB, Agarwal A: **Stromal cell-derived factor 1 promotes angiogenesis via a heme oxygenase 1-dependent mechanism**. *J Exp Med* 2007, **204**:605–618.

192. Suzuki M, Iso-o N, Takeshita S, Tsukamoto K, Mori I, Sato T, Ohno M, Nagai R, Ishizaka N: **Facilitated angiogenesis induced by heme oxygenase-1 gene transfer in a rat model of hindlimb ischemia**. *Biochem Biophys Res Commun* 2003, **302**:138–143.

193. Kong D, Melo LG, Mangi AA, Zhang L, Lopez-Ilasaca M, Perrella MA, Liew CC, Pratt RE, Dzau VJ: **Enhanced inhibition of neointimal hyperplasia by genetically engineered endothelial progenitor cells**. *Circulation* 2004, **109**:1769–1775.

194. Tang YL, Tang Y, Zhang YC, Qian K, Shen L, Phillips MI: **Improved graft mesenchymal stem cell survival in ischemic heart with a hypoxia-regulated heme oxygenase-1 vector**. *J Am Coll Cardiol* 2005, **46**:1339–1350.

195. Blancou P, Tardif V, Simon T, Rémy S, Carreño L, Kalergis A, Anegon I: **Immunoregulatory properties of heme oxygenase-1**. *Methods Mol Biol Clifton NJ* 2011, **677**:247–268.

196. Jozkowicz A, Was H, Dulak J: **Heme Oxygenase-1 in Tumors: Is It a False Friend?** *Antioxid Redox Signal* 2007, **9**:2099–2118.

197. Lin Q, Weis S, Yang G, Weng Y-H, Helston R, Rish K, Smith A, Bordner J, Polte T, Gaunitz F, Dennery PA: **Heme Oxygenase-1 Protein Localizes to the Nucleus and Activates Transcription Factors Important in Oxidative Stress**. *J Biol Chem* 2007, **282**:20621–20633.

198. Linnenbaum M, Busker M, Kraehling JR, Behrends S: **Heme oxygenase isoforms differ in their subcellular trafficking during hypoxia and are differentially modulated by cytochrome P450 reductase**. *PloS One* 2012, **7**:e35483.

199. Hori R, Kashiba M, Toma T, Yachie A, Goda N, Makino N, Soejima A, Nagasawa T, Nakabayashi K, Suematsu M: **Gene Transfection of H25A Mutant Heme Oxygenase-1 Protects Cells against Hydroperoxide-induced Cytotoxicity**. *J Biol Chem* 2002, **277**:10712–10718.

200. Dennery PA: **Signaling function of heme oxygenase proteins**. *Antioxid Redox Signal* 2013.

201. Cao Y-A, Wagers AJ, Karsunky H, Zhao H, Reeves R, Wong RJ, Stevenson DK, Weissman IL, Contag CH: **Heme oxygenase-1 deficiency leads to disrupted response to acute stress in stem cells and progenitors**. *Blood* 2008, **112**:4494–4502.

202. Merchant AA, Singh A, Matsui W, Biswal S: **The redox-sensitive transcription factor Nrf2 regulates murine hematopoietic stem cell survival independently of ROS levels**. *Blood* 2011, **118**:6572–6579.

203. Tsai JJ, Dudakov JA, Takahashi K, Shieh J-H, Velardi E, Holland AM, Singer NV, West ML, Smith OM, Young LF, Shono Y, Ghosh A, Hanash AM, Tran HT, Moore MAS, van den Brink MRM: **Nrf2 regulates haematopoietic stem cell function**. *Nat Cell Biol* 2013, **15**:309–316.

204. So AY-L, Garcia-Flores Y, Minisandram A, Martin A, Taganov K, Boldin M, Baltimore D: **Regulation of APC development, immune response, and autoimmunity by Bach1/HO-1 pathway in mice**. *Blood* 2012, **120**:2428–2437.

205. Ozono R: **New Biotechnological Methods to Reduce Oxidative Stress in the Cardiovascular System: Focusing on the Bach1/Heme Oxygenase-1 Pathway**. *Curr Pharm Biotechnol* 2006, **7**:87–93.

206. Watanabe-Matsui M, Muto A, Matsui T, Itoh-Nakadai A, Nakajima O, Murayama K, Yamamoto M, Ikeda-Saito M, Igarashi K: **Heme regulates B-cell differentiation, antibody class switch, and heme oxygenase-1 expression in B cells as a ligand of Bach2**. *Blood* 2011, **117**:5438–5448.

207. Ibrahim NG, Lutton JD, Levere RD: **The role of haem biosynthetic and degradative enzymes in erythroid colony development: the effect of haemin**. *Br J Haematol* 1982, **50**:17–28.

208. Abraham NG, Levere RD, Lutton JD: **Eclectic mechanisms of heme regulation of hematopoiesis**. *Int J Cell Cloning* 1991, **9**:185–210.

209. BESSIS M: **[Erythroblastic island, functional unity of bone marrow]**. *Rev Hématologie* 1958, **13**:8–11.

210. Chasis JA, Mohandas N: **Erythroblastic islands: niches for erythropoiesis**. *Blood* 2008, **112**:470–478.

211. Alves LR, Costa ES, Sorgine MHF, Nascimento-Silva MCL, Teodosio C, Bárcena P, Castro-Faria-Neto HC, Bozza PT, Orfao A, Oliveira PL, Maya-Monteiro CM: **Heme-oxygenases during erythropoiesis in K562 and human bone marrow cells**. *PloS One* 2011, **6**:e21358.

212. Toobiak S, Shaklai M, Shaklai N: **Carbon monoxide induced erythroid differentiation of K562 cells mimics the central macrophage milieu in erythroblastic islands**. *PloS One* 2012, **7**:e33940.

213. Cao Y-A, Kusy S, Luong R, Wong RJ, Stevenson DK, Contag CH: **Heme oxygenase-1 deletion affects stress erythropoiesis**. *PloS One* 2011, **6**:e20634.

214. O'Brien JJ, Baglole CJ, Garcia-Bates TM, Blumberg N, Francis CW, Phipps RP: **15-deoxy-Delta12,14 prostaglandin J2-induced heme oxygenase-1 in megakaryocytes regulates thrombopoiesis**. *J Thromb Haemost JTH* 2009, **7**:182–189.

215. Motohashi H, Kimura M, Fujita R, Inoue A, Pan X, Takayama M, Katsuoka F, Aburatani H, Bresnick EH, Yamamoto M: **NF-E2 domination over Nrf2 promotes ROS accumulation and megakaryocytic maturation**. *Blood* 2010, **115**:677–686.

216. Yoshida H, Kawane K, Koike M, Mori Y, Uchiyama Y, Nagata S: **Phosphatidylserine-dependent engulfment by macrophages of nuclei from erythroid precursor cells**. *Nature* 2005, **437**:754–758.

217. Mizuno N, Kosaka M: **Novel variants of Oct-3/4 gene expressed in mouse somatic cells**. *J Biol Chem* 2008, **283**:30997–31004.

218. Picelli S, Faridani OR, Björklund ÅK, Winberg G, Sagasser S, Sandberg R: **Full-length RNA-seq from single cells using Smart-seq2**. *Nat Protoc* 2014, **9**:171–181.

219. Li H, Durbin R: **Fast and accurate short read alignment with Burrows–Wheeler transform**. *Bioinformatics* 2009, **25**:1754–1760.

220. Love MI, Huber W, Anders S: **Moderated estimation of fold change and dispersion for RNA-seq data with DESeq2**. *Genome Biol* 2014, **15**:550.

221. Croft D, Mundo AF, Haw R, Milacic M, Weiser J, Wu G, Caudy M, Garapati P, Gillespie M, Kamdar MR, Jassal B, Jupe S, Matthews L, May B, Palatnik S, Rothfels K, Shamovsky V, Song H, Williams M, Birney E, Hermjakob H, Stein L, D'Eustachio P: **The Reactome pathway knowledgebase**. *Nucleic Acids Res* 2014, **42**(Database issue):D472–D477.

222. Ashburner M, Ball CA, Blake JA, Botstein D, Butler H, Cherry JM, Davis AP, Dolinski K, Dwight SS, Eppig JT, Harris MA, Hill DP, Issel-Tarver L, Kasarskis A, Lewis S, Matese JC, Richardson JE, Ringwald M, Rubin GM, Sherlock G: **Gene ontology: tool for the unification of biology. The Gene Ontology Consortium**. *Nat Genet* 2000, **25**:25–29.

223. Falcon S, Gentleman R: **Using GOstats to test gene lists for GO term association**. *Bioinforma Oxf Engl* 2007, **23**:257–258.

224. Kanehisa M, Goto S: **KEGG: kyoto encyclopedia of genes and genomes**. *Nucleic Acids Res* 2000, **28**:27–30.

225. Luo W, Friedman MS, Shedden K, Hankenson KD, Woolf PJ: **GAGE: generally applicable gene set enrichment for pathway analysis**. *BMC Bioinformatics* 2009, **10**:161.

226. Weber K, Bartsch U, Stocking C, Fehse B: **A Multicolor Panel of Novel Lentiviral "Gene Ontology" (LeGO) Vectors for Functional Gene Analysis**. *Mol Ther* 2008, **16**:698–706.

227. Mostoslavsky G, Kotton DN, Fabian AJ, Gray JT, Lee J-S, Mulligan RC: **Efficiency of transduction of highly purified murine hematopoietic stem cells by lentiviral and oncoretroviral vectors under conditions of minimal in vitro manipulation**. *Mol Ther J Am Soc Gene Ther* 2005, **11**:932–940.

228. Szade K, Bukowska-Strakova K, Nowak WN, Szade A, Kachamakova-Trojanowska N, Zukowska M, Jozkowicz A, Dulak J: **Murine bone marrow Lin⁻Sca⁻1⁺CD45⁻ very small embryonic-like (VSEL) cells are heterogeneous population lacking Oct-4A expression**. *PloS One* 2013, **8**:e63329.

229. Zuba-Surma EK, Kucia M, Abdel-Latif A, Dawn B, Hall B, Singh R, Lillard JW, Ratajczak MZ: **Morphological characterization of very small embryonic-like stem cells (VSELs) by ImageStream system analysis**. *J Cell Mol Med* 2007, **12**:292–303.

230. Wlodkowic D, Telford W, Skommer J, Darzynkiewicz Z: **Apoptosis and beyond: cytometry in studies of programmed cell death**. *Methods Cell Biol* 2011, **103**:55–98.

231. Zuba-Surma EK, Kucia M, Wu W, Klich I, Lillard JW, Ratajczak J, Ratajczak MZ: **Very Small Embryonic- Like stem cells (VSELs) are present in adult murine organs: ImageStream based morphological analysis and distribution studies**. *Cytom Part J Int Soc Anal Cytol* 2008, **73A**:1116–1127.

232. Zuba-Surma EK, Kucia M, Rui L, Shin D-M, Wojakowski W, Ratajczak J, Ratajczak MZ: **Fetal liver very small embryonic/epiblast like stem cells follow developmental migratory pathway of hematopoietic stem cells**. *Ann N Y Acad Sci* 2009, **1176**:205–218.

233. Ye J, Coulouris G, Zaretskaya I, Cutcutache I, Rozen S, Madden TL: **Primer-BLAST: A tool to design target-specific primers for polymerase chain reaction**. *BMC Bioinformatics* 2012, **13**:134.

234. Siracusa LD, Rosner MH, Vigano MA, Gilbert DJ, Staudt LM, Copeland NG, Jenkins NA: **Chromosomal location of the octamer transcription factors, Otf-1, Otf-2, and Otf-3, defines multiple Otf-3-related sequences dispersed in the mouse genome**. *Genomics* 1991, **10**:313–326.

235. Ratajczak J, Wysoczynski M, Zuba-Surma E, Wan W, Kucia M, Yoder MC, Ratajczak MZ: **Adult murine bone marrow-derived very small embryonic-like stem cells differentiate into the hematopoietic lineage after coculture over OP9 stromal cells**. *Exp Hematol* 2011, **39**:225–237.

236. Chen CZ, Li M, De Graaf D, Monti S, Göttgens B, Sanchez MJ, Lander ES, Golub TR, Green AR, Lodish HF: **Identification of endoglin as a functional marker that defines long-term repopulating hematopoietic stem cells**. *Proc Natl Acad Sci* 2002, **99**:15468.

237. Szilvassy SJ, Humphries RK, Lansdorp PM, Eaves AC, Eaves CJ: **Quantitative assay for totipotent reconstituting hematopoietic stem cells by a competitive repopulation strategy.** *Proc Natl Acad Sci U S A* 1990, **87**:8736–8740.

238. Harrison DE, Jordan CT, Zhong RK, Astle CM: **Primitive hemopoietic stem cells: direct assay of most productive populations by competitive repopulation with simple binomial, correlation and covariance calculations**. *Exp Hematol* 1993, **21**:206–219.

239. Moody JL, Singbrant S, Karlsson G, Blank U, Aspling M, Flygare J, Bryder D, Karlsson S: **Endoglin Is Not Critical for Hematopoietic Stem Cell Engraftment and Reconstitution but Regulates Adult Erythroid Development**. *STEM CELLS* 2007, **25**:2809–2819.

240. Cho SK, Bourdeau A, Letarte M, Zúñiga-Pflücker JC: **Expression and function of CD105 during the onset of hematopoiesis from Flk1+ precursors**. *Blood* 2001, **98**:3635–3642.

241. Voura EB, Billia F, Iscove NN, Hawley RG: **Expression mapping of adhesion receptor genes during differentiation of individual hematopoietic precursors**. *Exp Hematol* 1997, **25**:1172–1179.

242. Lesley J, Hyman R, Schulte R, Trotter J: **Expression of transferrin receptor on murine hematopoietic progenitors**. *Cell Immunol* 1984, **83**:14–25.

243. Schmid I, Uittenbogaart C, Jamieson BD: **Live-cell assay for detection of apoptosis by dual-laser flow cytometry using Hoechst 33342 and 7-amino-actinomycin D**. *Nat Protoc* 2007, **1**:187–190.

244. Gavrieli Y, Sherman Y, Ben-Sasson SA: **Identification of programmed cell death in situ via specific labeling of nuclear DNA fragmentation**. *J Cell Biol* 1992, **119**:493–501.

245. McGrath KE, Kingsley PD, Koniski AD, Porter RL, Bushnell TP, Palis J: **Enucleation of primitive erythroid cells generates a transient population of "pyrenocytes" in the mammalian fetus**. *Blood* 2007, **111**:2409–2417.

246. Paull TT, Rogakou EP, Yamazaki V, Kirchgessner CU, Gellert M, Bonner WM: **A critical role for histone H2AX in recruitment of repair factors to nuclear foci after DNA damage**. *Curr Biol CB* 2000, **10**:886–895.

247. Subramanian A, Tamayo P, Mootha VK, Mukherjee S, Ebert BL, Gillette MA, Paulovich A, Pomeroy SL, Golub TR, Lander ES, Mesirov JP: **Gene set enrichment analysis: A knowledge-based approach for interpreting genome-wide expression profiles**. *Proc Natl Acad Sci* 2005, **102**:15545–15550.

248. Szade K, Bukowska-Strakova K, Nowak WN, Jozkowicz A, Dulak J: **Comment on: The proper criteria for identification and sorting of very small embryonic-like stem cells, and some nomenclature issues**. *Stem Cells Dev* 2014, **23**:714–716.

249. Liu R, Klich I, Ratajczak J, Ratajczak MZ, Zuba-Surma EK: **Erythrocyte-derived microvesicles may transfer phosphatidylserine to the surface of nucleated cells and falsely "mark" them as apoptotic**. *Eur J Haematol* 2009, **83**:220–229.

250. Kina T, Ikuta K, Takayama E, Wada K, Majumdar AS, Weissman IL, Katsura Y: **The monoclonal antibody TER-119 recognizes a molecule associated with glycophorin A and specifically marks the late stages of murine erythroid lineage**. *Br J Haematol* 2000, **109**:280–287.

251. Zuba-Surma EK, Kucia M, Ratajczak J, Ratajczak MZ: **"Small Stem Cells" in Adult Tissues: Very Small Embryonic-Like Stem Cells (VSELs) Stand Up!** *Cytom Part J Int Soc Anal Cytol* 2009, **75**:4–13.

252. Ratajczak MZ, Kucia M, Ratajczak J, Zuba-Surma EK: **A multi-instrumental approach to identify and purify very small embryonic like stem cells (VSELs) from adult tissues**. *Micron Oxf Engl 1993* 2009, **40**:386–393.

253. Cui Y-X, Johnson T, Baumbach A, Reeves BC, Rogers CA, Angelini GD, Marsden D, Madeddu P: **Stepwise optimization of the procedure for assessment of circulating progenitor cells in patients with myocardial infarction**. *PloS One* 2012, **7**:e30389.

254. Shapiro HM: **Forward Light Scattering and Cell Size**. In *In: Practical Flow Cytometry 4th Edition*. John Wiley & Sons; 2003:275–276.

255. Heider A, Danova-Alt R, Egger D, Cross M, Alt R: **Murine and human very small embryonic-like cells: A perspective**. *Cytom Part J Int Soc Anal Cytol* 2012.

256. Morikawa S, Mabuchi Y, Kubota Y, Nagai Y, Niibe K, Hiratsu E, Suzuki S, Miyauchi-Hara C, Nagoshi N, Sunabori T, Shimmura S, Miyawaki A, Nakagawa T, Suda T, Okano H, Matsuzaki Y: **Prospective identification, isolation, and systemic transplantation of multipotent mesenchymal stem cells in murine bone marrow**. *J Exp Med* 2009, **206**:2483–2496.

257. Zuba-Surma EK, Wu W, Ratajczak J, Kucia M, Ratajczak MZ: **Very small embryonic-like stem cells in adult tissues-potential implications for aging**. *Mech Ageing Dev* 2009, **130**:58–66.

258. Shin DM, Zuba-Surma EK, Wu W, Ratajczak J, Wysoczynski M, Ratajczak MZ, Kucia M: **Novel epigenetic mechanisms that control pluripotency and quiescence of adult**

bone marrow-derived Oct4(+) very small embryonic-like stem cells. *Leuk Off J Leuk Soc Am Leuk Res Fund UK* 2009, **23**:2042–2051.

259. Shin D-M, Liu R, Wu W, Waigel SJ, Zacharias W, Ratajczak MZ, Kucia M: **Global gene expression analysis of very small embryonic-like stem cells reveals that the Ezh2-dependent bivalent domain mechanism contributes to their pluripotent state**. *Stem Cells Dev* 2012, **21**:1639–1652.

260. Lee J, Kim HK, Rho J-Y, Han Y-M, Kim J: **The human OCT-4 isoforms differ in their ability to confer self-renewal**. *J Biol Chem* 2006, **281**:33554–33565.

261. Atlasi Y, Mowla SJ, Ziaee SAM, Gokhale PJ, Andrews PW: **OCT4 spliced variants are differentially expressed in human pluripotent and nonpluripotent cells**. *Stem Cells Dayt Ohio* 2008, **26**:3068–3074.

262. Guo C, Liu L, Jia Y, Zhao X, Zhou Q, Wang L: **A novel variant of Oct3/4 gene in mouse embryonic stem cells**. *Stem Cell Res* 2012, **9**:69–76.

263. Liedtke S, Enczmann J, Waclawczyk S, Wernet P, Kögler G: **Oct4 and its pseudogenes confuse stem cell research**. *Cell Stem Cell* 2007, **1**:364–366.

264. Ryan JM, Pettit AR, Guillot PV, Chan JKY, Fisk NM: **Unravelling the Pluripotency Paradox in Fetal and Placental Mesenchymal Stem Cells: Oct-4 Expression and the Case of the Emperor's New Clothes**. *Stem Cell Rev* 2011.

265. Warthemann R, Eildermann K, Debowski K, Behr R: **False-positive antibody signals for the pluripotency factor OCT4A (POU5F1) in testis-derived cells may lead to erroneous data and misinterpretations**. *Mol Hum Reprod* 2012, **18**:605–612.

266. Wang X, Dai J: **Concise review: isoforms of OCT4 contribute to the confusing diversity in stem cell biology**. *Stem Cells Dayt Ohio* 2010, **28**:885–893.

267. Kotoula V, Papamichos SI, Lambropoulos AF: **Revisiting OCT4 expression in peripheral blood mononuclear cells**. *Stem Cells Dayt Ohio* 2008, **26**:290–291.

268. White MG, Al-Turaifi HR, Holliman GN, Aldibbiat A, Mahmoud A, Shaw JAM: **Pluripotency-associated stem cell marker expression in proliferative cell cultures derived from adult human pancreas**. *J Endocrinol* 2011, **211**:169–176.

269. Ivanovic Z: **Human Umbilical Cord Blood-Derived Very-Small-Embryonic-Like Stem Cells with Maximum Regenerative Potential?** *Stem Cells Dev* 2012:120417095046005.

270. Lee JC-M, Gimm JA, Lo AJ, Koury MJ, Krauss SW, Mohandas N, Chasis JA: **Mechanism of protein sorting during erythroblast enucleation: role of cytoskeletal connectivity**. *Blood* 2004, **103**:1912–1919.

271. Salomao M, Chen K, Villalobos J, Mohandas N, An X, Chasis JA: **Hereditary spherocytosis and hereditary elliptocytosis: aberrant protein sorting during erythroblast enucleation**. *Blood* 2010, **116**:267–269.

272. Keerthivasan G, Wickrema A, Crispino JD: **Erythroblast Enucleation**. *Stem Cells Int* 2011, **2011**:1–9.

273. Ji P, Yeh V, Ramirez T, Murata-Hori M, Lodish HF: **Histone deacetylase 2 is required for chromatin condensation and subsequent enucleation of cultured mouse fetal erythroblasts**. *Haematologica* 2010, **95**:2013–2021.

274. Miyanishi M, Mori Y, Seita J, Chen JY, Karten S, Chan CKF, Nakauchi H, Weissman IL: **Do pluripotent stem cells exist in adult mice as very small embryonic stem cells?** *Stem Cell Rep* 2013, **1**:198–208.

275. Suszynska M, Zuba-Surma EK, Maj M, Mierzejewska K, Ratajczak J, Kucia M, Ratajczak MZ: **The proper criteria for identification and sorting of very small embryonic-like stem cells, and some nomenclature issues**. *Stem Cells Dev* 2014, **23**:702–713.

276. Suszynska M, Zuba-Surma E, Maj M, Mierzejewska K, Ratajczak J, Kucia M, Ratajczak MZ: **The proper criteria for identification and sorting of very small embryonic-like stem cells (VSELs), and some nomenclature issues**. *Stem Cells Dev* 2013.

277. Shin D-M, Suszynska M, Mierzejewska K, Ratajczak J, Ratajczak MZ: **Very small embryonic-like stem-cell optimization of isolation protocols: an update of molecular signatures and a review of current in vivo applications**. *Exp Mol Med* 2013, **45**:e56.

278. Liu J, Zhang J, Ginzburg Y, Li H, Xue F, De Franceschi L, Chasis JA, Mohandas N, An X: **Quantitative analysis of murine terminal erythroid differentiation in vivo: novel method to study normal and disordered erythropoiesis**. *Blood* 2013, **121**:e43–49.

279. Nath KA, Balla G, Vercellotti GM, Balla J, Jacob HS, Levitt MD, Rosenberg ME: **Induction of heme oxygenase is a rapid, protective response in rhabdomyolysis in the rat**. *J Clin Invest* 1992, **90**:267–270.

280. Poss KD, Tonegawa S: **Heme oxygenase 1 is required for mammalian iron reutilization**. *Proc Natl Acad Sci U S A* 1997, **94**:10919–10924.

281. Kapturczak MH, Wasserfall C, Brusko T, Campbell-Thompson M, Ellis TM, Atkinson MA, Agarwal A: **Heme Oxygenase-1 Modulates Early Inflammatory Responses**. *Am J Pathol* 2004, **165**:1045–1053.

282. Cornall RJ: **HO-1 extends to stem cells**. *Blood* 2008, **112**:4363–4364.

283. Ito K, Hirao A, Arai F, Takubo K, Matsuoka S, Miyamoto K, Ohmura M, Naka K, Hosokawa K, Ikeda Y, Suda T: **Reactive oxygen species act through p38 MAPK to limit the lifespan of hematopoietic stem cells**. *Nat Med* 2006, **12**:446–451.

284. Challen GA, Boles NC, Chambers SM, Goodell MA: **Distinct Hematopoietic Stem Cell Subtypes Are Differentially Regulated by TGFβ1**. *Cell Stem Cell* 2010, **6**:265–278.

285. Czechowicz A, Kraft D, Weissman IL, Bhattacharya D: **Efficient Transplantation via Antibody-based Clearance of Hematopoietic Stem Cell Niches**. *Science* 2007, **318**:1296–1299.

286. Walasek MA, van Os R, de Haan G: **Hematopoietic stem cell expansion: challenges and opportunities**. *Ann N Y Acad Sci* 2012, **1266**:138–150.

287. Mossadegh-Keller N, Sarrazin S, Kandalla PK, Espinosa L, Stanley ER, Nutt SL, Moore J, Sieweke MH: **M-CSF instructs myeloid lineage fate in single haematopoietic stem cells**. *Nature* 2013, **497**:239–243.

288. Essers MAG, Offner S, Blanco-Bose WE, Waibler Z, Kalinke U, Duchosal MA, Trumpp A: **IFNalpha activates dormant haematopoietic stem cells in vivo**. *Nature* 2009, **458**:904–908.

289. Baldridge MT, King KY, Boles NC, Weksberg DC, Goodell MA: **Quiescent haematopoietic stem cells are activated by IFN-γ in response to chronic infection**. *Nature* 2010, **465**:793–797.

290. Queiroga CSF, Almeida AS, Vieira HLA, Queiroga CSF, Almeida AS, Vieira HLA: **Carbon Monoxide Targeting Mitochondria, Carbon Monoxide Targeting Mitochondria**. *Biochem Res Int Biochem Res Int* 2012, **2012, 2012**:e749845.

291. Yamamoto T, Takano N, Ishiwata K, Ohmura M, Nagahata Y, Matsuura T, Kamata A, Sakamoto K, Nakanishi T, Kubo A, Hishiki T, Suematsu M: **Reduced methylation of PFKFB3 in cancer cells shunts glucose towards the pentose phosphate pathway**. *Nat Commun* 2014, **5**:3480.